N69-38617

(ACCESSION NUMBER) (THRU)

363 1

(PAGES) (CODE)

NASA-CR-101930 28

(NASA CR OR TMX OR AD NUMBER) (CATEGORY)

FACILITY FORM 602

:ribed above may be processed by Code UST in accordance with the ab

[illegible] and Office Code D

CHNICAL MONITOR

REVERSE SIDE OF GREEN COPY FOR GENERAL POLICY REGARDING

UST USE ONLY

101930 NASA - TMX Number

NASA CR 101750

THE Marquardt CORPORATION VAN NUYS, CALIFORNIA

A-1080

FINAL REPORT

VOLUME 2

APOLLO SM-LM RCS ENGINE DEVELOPMENT PROGRAM SUMMARY REPORT

Contract NAS 9-7281

EDITED BY:

J. F. Foote
Project Engineer

APPROVED BY:

D. C. Sund
Senior Project Engineer

L. R. Bell, Jr.
Chief Engineer

C. A. Kerner
Program Manager

TABLE OF CONTENTS

VOLUME 1

Preface

Chapter 1 Marquardt R-4D Engine Development

VOLUME 2

Chapter 2 Thermal Management

Chapter 3 Space Ignition Characteristics

Chapter 4 Gas Pressurization Effects

Chapter 5 Contamination Control

Chapter 6 System Dynamic Effects

VOLUME 3

Chapter 7 Structural Design

Chapter 8 Material Selection

Chapter 9 Propellant Valve Design

Chapter 10 Injector Design

Chapter 11 Thrust Chamber Design

VOLUME 4

Chapter 12 Test Facilities and Instrumentation

Chapter 13 Test Data Analysis

Chapter 14 Flight Test Experience

Chapter 15 Reliability

CHAPTER 2

THERMAL MANAGEMENT

BY

C. S. HILL
and
R. C. STECHMAN

TABLE OF CONTENTS

SECTION		PAGE
I.	INTRODUCTION	2-1
II.	ENGINE DESCRIPTION	2-2
III.	ANALYSIS TECHNIQUES	2-4
	A. Energy Balance	2-4
	B. Marquardt's Thermal Analyzer Computer Program	2-6
	C. Analysis Results	2-18
IV.	THERMAL DEVELOPMENT HISTORY	2-23
	A. Increase Performance	2-23
	B. Excessive Injector Head Temperature	2-25
	C. Hot Phasing	2-26
	D. Ignition Overpressures	2-37
	E. Preigniter Effects	2-37
V.	SUPPORTING PROGRAMS	2-38
	A. Columbium Alloy Combustion Chamber	2-38
	B. Moog Valves	2-40
	C. Passive Thermal Management Program	2-40
	D. Lunar Orbiter	
	REFERENCES	2-50

LIST OF ILLUSTRATIONS

FIGURE NO.		PAGE NO.
1	R-4D Rocket Engine	2-3
2	Heat Transfer Paths	2-5
3	R-A 100-Lb. Thrust Engine Thermal Network	2-8
4	Effective Gas Temperature for Heat Transfer	2-12
5	Convective Heat Transfer Coefficient	2-14
6	Emittance of Solar Absorbtivity of Columbium	2-15
7	Thermal Conductivity of Columbium	2-16
8	Specific Heat of Alloys	2-17
9	Temperature vs. Time	2-19
10	Temperature Characteristics of R-4B	2-20
11	Power Requirements for R-4D	2-22
12	Hot Phasing Data Trace	2-27
13	Hot Phasing Data Trace	2-28
14	Hot Phasing Photo	2-30
15	T-10060 and Preigniter Injectors	2-33
16	Chamber Flange Temperature vs. Mixture Ratio	2-34
17	Molybdenum Flange Temperature Time History	2-35
18	Specific Impulse vs. Throat Temperature	2-36
19	Thermal Resistance Test Setup	2-45
20	Combustor-Injector Seat Thermal Hardware	2-46
21	Seal Thermal Resistance Test Results	2-47

LIST OF TABLES

TABLE NO.		PAGE
I	R-4D Component Temperatures	2-18
II	Development History	2-33
III	Columbium Chamber Temperature Summary	2-39
IV	Material Properties	2-42

THERMAL MANAGEMENT HISTORY OF THE MARQUARDT R-4D ROCKET ENGINE

I. INTRODUCTION

The successful application of Marquardt precision control rocket engines in space vehicles is partially due to thermal management techniques which were developed in conjunction with the Apollo Service Module Reaction Control Engine Program. During this program, thermal analysis techniques were developed which provided rapid and accurate evaluation of proposed engine designs. Analytical predictions that were made were verified by thermal testing of the Marquardt R-4D 100 pound thrust rocket engine in simulated space environments which provided pressure and radiation backgrounds approximating space flight conditions. These analytical techniques contributed significantly to the successful performance of this engine on the Apollo Service Module, the Lunar Module, and the Lunar Orbiter Spacecraft. During the development tests and space flights of these engines, more than one million altitude ignitions and 500,000 seconds of firing were successfully accomplished.

The thermal management techniques used in the design of the R-4D engine include (1) the use of fuel film cooling of the engine walls, (2) minimization of heat conduction through the use of seals and minimum area conduction paths, and (3) the use of heaters to control the engine temperature during long off times in space. The thermal management techniques have resulted in a rocket engine whose component temperatures are well below the structural design limits of the constituent materials.

In the following report, analysis techniques used in the design and analysis of the R-4D 100 pound thrust rocket engine are described. The evolution of the R-4D design in terms of its thermal characteristics is described and the results of various programs in which the basic thermal design of the engine was modified are presented.

II. ENGINE DESCRIPTION

The Marquardt R-4D precision control rocket engine consists of two high response integral solenoid operated valves, an injector assembly, and a two-piece thrust chamber (Figure 1).

The radiation and film cooled combustion chamber is made of forged molybdenum and coated with molybdenum disilicide to provide oxidation protection from the combustion gases formed by the nitrogen tetroxide oxidizer and hydrazine type fuels. The radiation cooled Model R-4D nozzle is also made of coated molybdenum to an expansion ratio of 6.8:1 at which point a light weight, thin walled, bell shaped L-605 cobalt base alloy expansion bell is attached. The present expansion ratio is 40:1, but due to the two-piece construction, a variety of expansion ratios are obtainable. The injector head contains four concentric rings of equally spaced injector orifices and a preigniter to provide smooth ignition. The rings consist of eight injector orifices for wall fuel cooling, eight injector orifices for preigniter wall fuel cooling, and eight like on unlike propellant injector doublets.

The preigniter chamber is a tubular chamber extending from the face of the injector head assembly and contains two propellant injection orifices. The preigniter chamber is designed to mix and ignite a small quantity of propellants within the preigniter chamber prior to ignition of the main combustion chamber. Ignition of the preigniter chamber pre-pressurizes the main combustion chamber, minimizing ignition delays of the main propellant streams.

Propellant valving is provided by two normally closed, dual coil, solenoid actuated coaxial flow poppet-type valves with an integral propellant flow regulation orifice. Integral fixed orifices are incorporated into each valve to provide the correct propellant pressure drops at the design inlet pressure to obtain the required O/F and thrust level.

REPRODUCIBILITY OF THE ORIGINAL PAGE IS POOR.

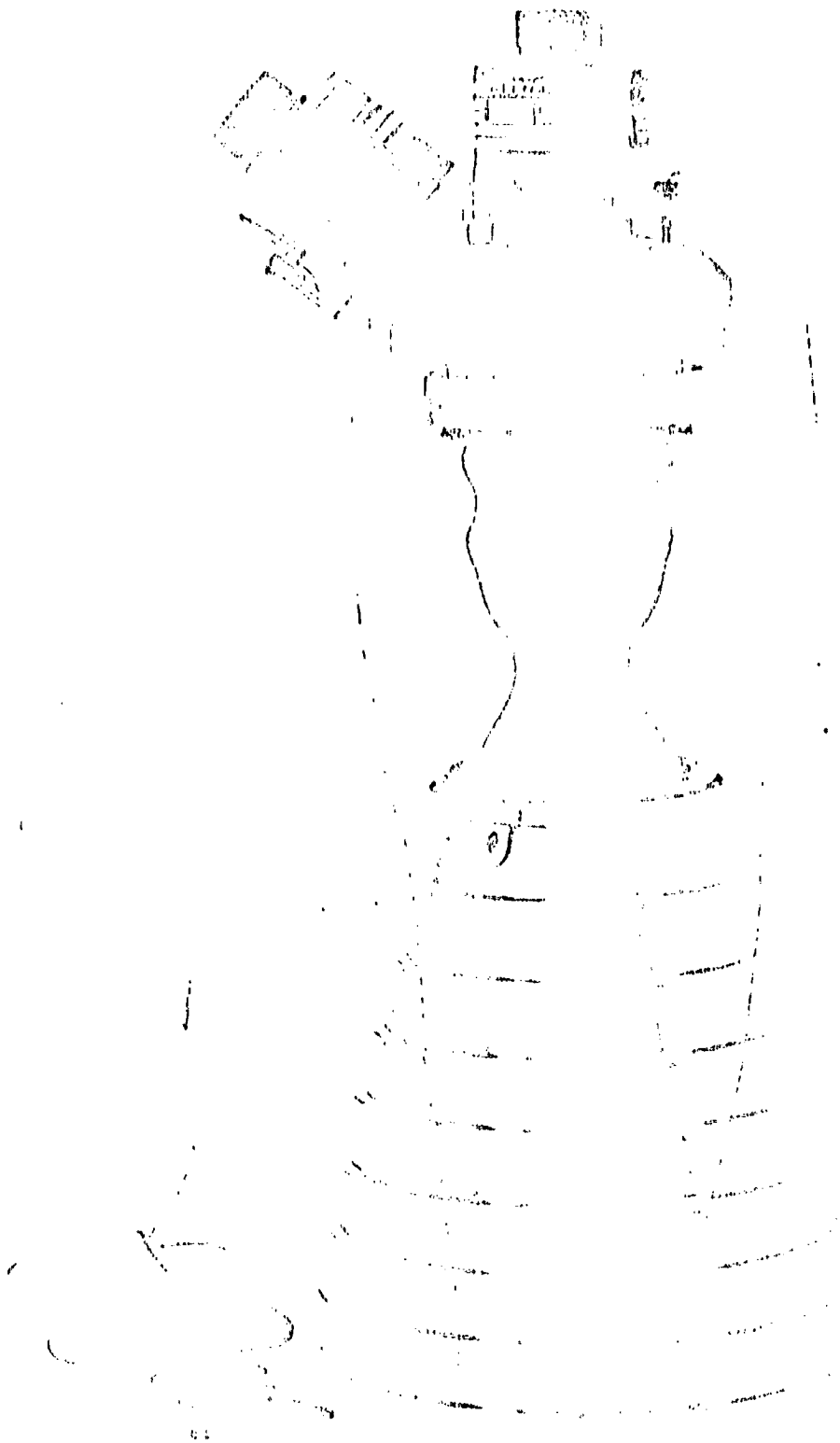

NEG. CA6839-3

R-4D Rocket Engine

Figure 1

III. ANALYSIS TECHNIQUES

The analysis of the thermal characteristics of the R-4D engine system encompassed many facets of analysis; these techniques and procedures are described in the following section.

A. Energy Balance

The R-4D rocket engine attains a steady state thermal condition approximately 50-100 seconds after ignition. After shutdown, the energy stored in the chamber is transferred to the surroundings by radiation and by conduction to the injector, valves, and spacecraft structure.

It was necessary to evaluate the engine system, both during the heating and during the nonfiring cases, to determine the engine characteristics as a function of duty cycles. This requirement meant that the heat transfer paths throughout the engine must be accurately defined in order to determine the energy transfer. In the establishment of the energy balance through the system, the heat transfer paths can be classified into either convection, conduction, or radiation transfer paths. Figure 2 shows the heat transfer paths for a sample block model of the R-4D engine, where Q_r is radiation, Q_c is convection, Q_{cd} is conduction, and Q_p is power generation.

A simplified energy balance for the system is:

$$Q_r + Q_c + Q_{cd} = Q_p = C \frac{dt}{d\theta}$$

$C \frac{dt}{d\theta}$ is the transient term to complete the equation. During steady state the equation reduced to

$$Q_r + Q_c + Q_{cd} + Q_p = 0$$

During the nonfiring conditions, the convection terms are zero and the addition of a power source at the injector is required if active methods of heating the engine, such as a heater, are used.

HEAT TRANSFER PATHS

SAMPLE BLOCK: MODEL R-4D ENGINE

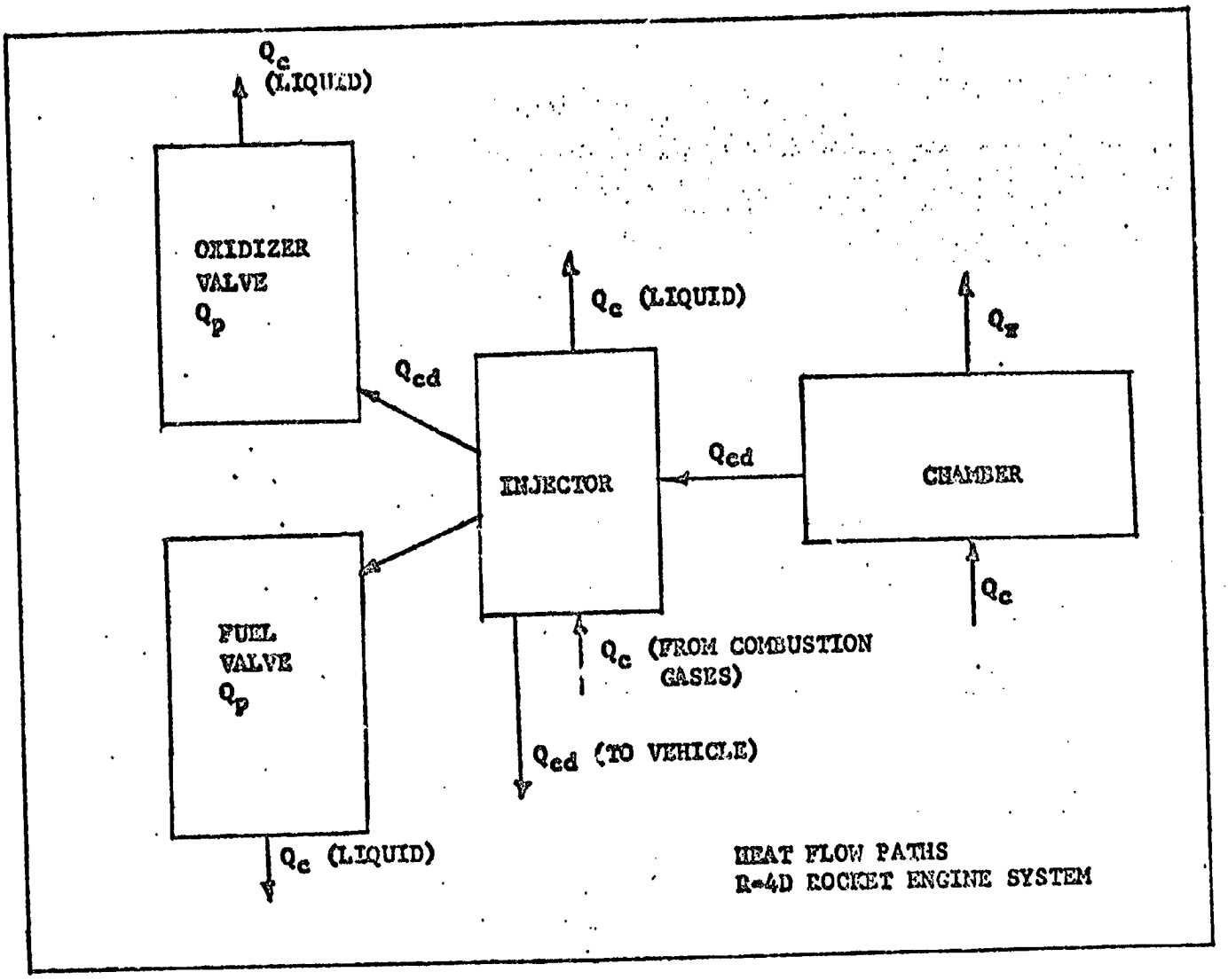

Figure 2

B. Marquardt's Thermal Analyzer Computer Program

The thermal characteristics of the R-4D rocket engine were calculated, using the Marquardt Thermal Analyzer program (Reference 1). The Thermal Analyzer computer program solves the pertinent heat transfer equations at each specified location (node) in the engine by a finite difference method. The procedure can be visualized by using the analogy between heat transfer and electrical circuits.

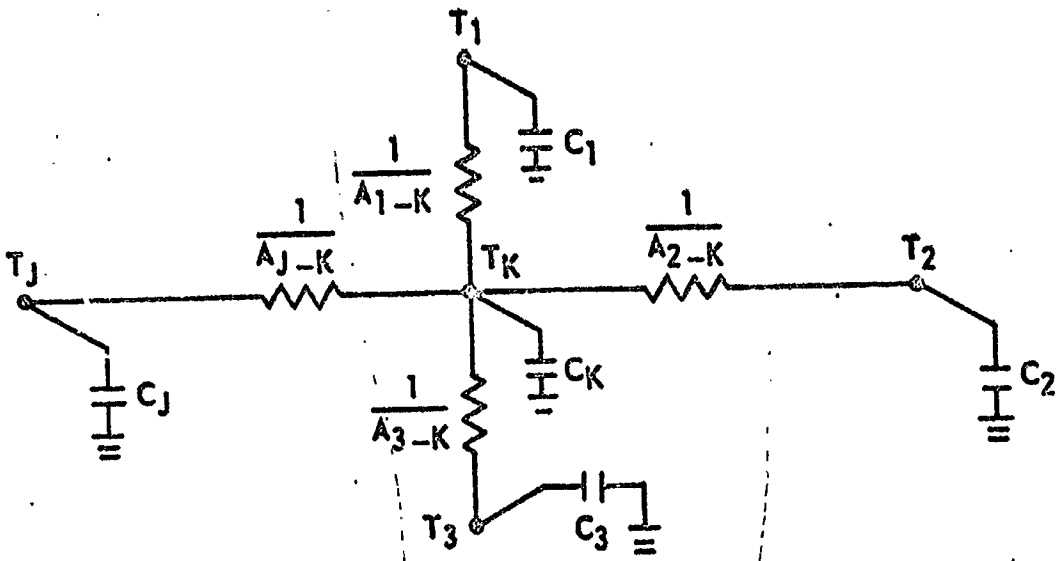

Typical Heat Transfer Network
Electrical Analogy

From an energy balance at each node

$$C\frac{dT}{d\theta} = \sum_{J=1}^{\eta} T_J A_{J-K} - T_K \sum_{J=1}^{\eta} A_{J-K}$$

or expressed in finite difference notation

$$\frac{T_{\theta+\Delta\theta}}{\Delta\theta} = \frac{1}{C}\left\{\sum_{j=1}^{n} T_j A_{j-K} - T_K \sum_{j=1}^{n} A_{j-K}\right\}$$

where

C	thermal capacity of specified material lump or node
T_θ	initial temperature at time θ, ^oF
$T_{\theta+\Delta\theta}$	temperature after a time interval $\Delta\theta$
A_{j-k}	reciprocal of thermal resistance, for conduction, convection, or radiation between nodes

An application of the R-C network approach to the Marquardt R-4D rocket is shown in Figure 3.

In order to use the Thermal Analyzer computer program, the various data describing the heat transfer processes and rates must be determined. These data include:

1. The convective heat transfer coefficients from the combustion gases to the walls of the combustor and nozzle.

2. Combustor and nozzle wall temperatures with film cooling.

3. Heat transfer coefficients from the propellants flowing in the injector and valves.

4. Thermal characteristics of the materials.

5. Environmental characteristics and resultant electrical energy inputs required from heater and valves.

R-4 100 POUND THRUST ENGINE THERMAL NETWORK

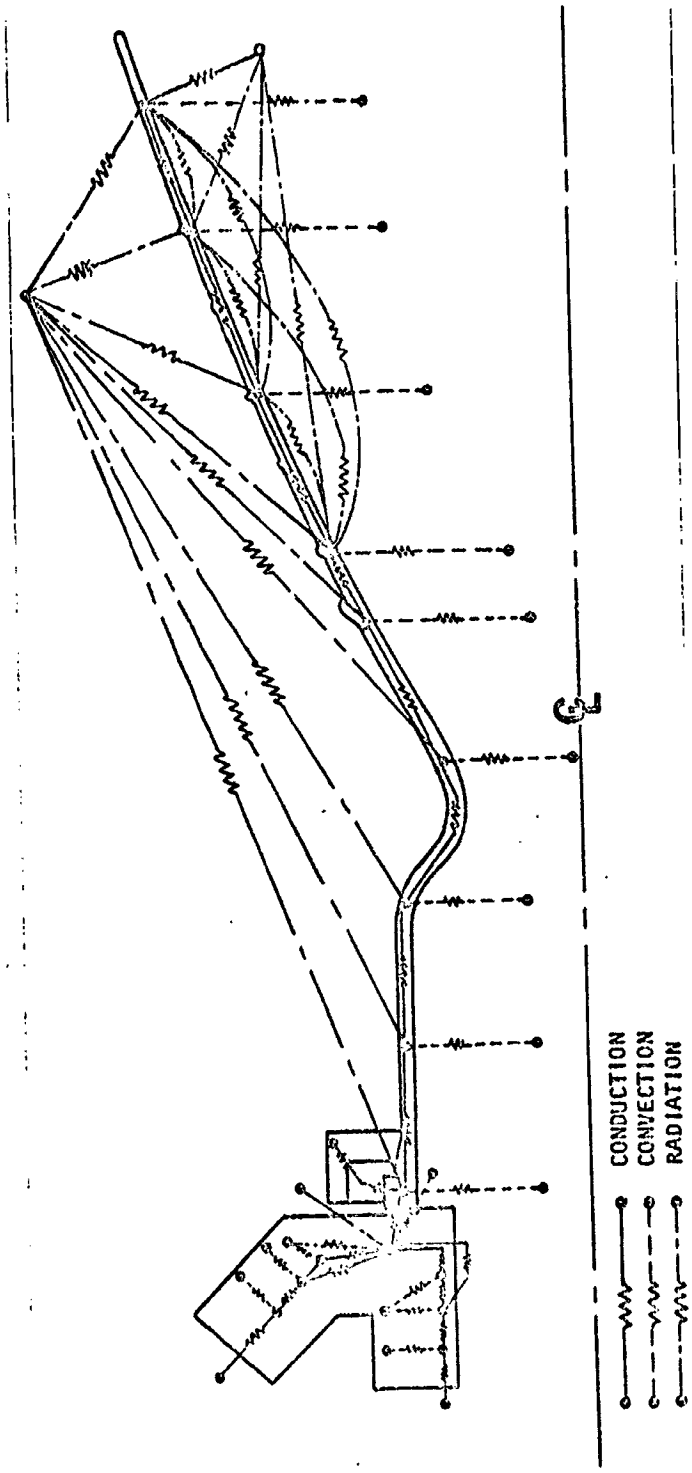

Figure 3

The evaluation of these properties used in conjunction with the Thermal Analyzer program then portrayed a thermal history of the engine during all phases of operation.

1. Coefficients of Convective Gas Heat Transfer

During the last ten years many equations and correlations have been derived to predict the coefficients of convective heat transfer from the combustion gases to the engine combustor and nozzle walls. An evaluation of some of these equations was made during the program and a correlation which provided an adequate representation of the heat transfer process due to forced convection in the engine reported by D. R. Bartz (Reference 2). This simplified method of determining the coefficient of heat transfer due to forced convection provided an adequate simulation of the actual process. During the program, modifications of this equation were made to include the effect due to liquid and gaseous film cooling. The resulting equation is:

$$h_{cg} = \frac{0.026}{D_*^{0.2}} \frac{\mu_f^{0.2}}{Pr_f^{0.6}} \left(\frac{W}{A_*}\right)^{0.8} \left(\frac{A_*}{A}\right)^{0.9} \left(\frac{H_R - H_W}{T_R - T_W}\right) \sigma$$

where

h_{cg}	heat transfer coefficient
D	diameter
Pr	Prandtl No.
μ	viscosity
W	propellant flow rate
A	flow area
σ	correction factor
H	enthalpy of gas
T	temperature

Subscript

*	throat conditions
f	film temperature
R	recovery temperature
W	wall temperature

2. Combustor and Nozzle Wall Temperatures with Film Cooling

An extensive background in thrust chamber cooling, both analytical and experimental, was developed during many of the NASA and Air Force contracts on cooling techniques. Investigations included evaluation of propulsion performance penalties due to film cooling. The design criteria generated by these contracts was verified during tests conducted in the Apollo SM/RCE Program. The engine was successfully film cooled using both monomethylhydrazine and a mixture of hydrazine and UDMH in 50/50 wt portions. The radiation cooled refractory concept of the R-4D engine has been used with varying amounts of film cooling ranging from 0% to 40%. The amount of fuel coolant used on the present engine configuration is approximately 25%. This results in a maximum wall temperature of approximately 2000°F, using MMH fuel and a maximum wall temperature of ~ 2400°F using the 50/50 mixture. The principal reason for this difference has not been established, but indications are that the hotter temperature is the result of the two-phase properties of the coolant (hydrazine and UDMH) and the slightly higher reaction rate of propellant combination, which results in a higher gas temperature.

Film Cooling Analysis Methods

Extensive analysis and experimental data have been generated in the liquid and gaseous film cooling regions and these correlations have been described in detail in Reference 6.

The evaporative film cooling correlations described have been derived for the simplified physical model employing a simplified liquid/vapor diffusion model which assumes that after the total liquid heat capacity and heat of vaporization of the fuel is exceeded, the resultant vapor is allowed to diffuse away from the wall at a finite rate. The equation for the length of the liquid portion of the film coolant is

$$L_1 = \left[\frac{W_{fc}\, Cp_\ell\, (T_s - T_i)}{P\, hc_g\, (T_r - T_s)} + \frac{W_{fc}\, \lambda}{P\, hc_g\, (T_r - T_s)} \right]$$

The first term on the right hand side of this equation represents the distance from the injection point required to change the film temperature from its initial injection temperature to its saturated liquid temperature. The second term represents the distance over which the effective gas temperature is constant and equal to the film coolant saturation temperature.

At L_1 the liquid film coolant is vaporized and is assumed to be saturated vapor. The equations used to predict the effective gas temperature in the gaseous region are shown below.

$$\frac{T_r - T_w}{T_r - T_s} = \exp\left(-\frac{h_{c_g} A}{\phi\, C_{p_{fc}} W_{fc}}\right)$$

$$\frac{1}{\phi} = \left(\frac{S\, V_g}{\alpha_c}\right)^{1/8} f\left(\frac{V_g}{V_c}\right)$$

$$\frac{V_g}{V_c} \leq 1.0 \qquad f\left(\frac{V_g}{V_c}\right) = \left(\frac{V_c}{V_g}\right)^{1.5\left(\frac{V_c}{V_g} - 1\right)}$$

$$\frac{V_g}{V_c} > 1.0 \qquad f\left(\frac{V_g}{V_c}\right) = 1 + 0.4\, \mathrm{TAN}^{-1}\left(\frac{V_g}{V_c} - 1\right)$$

These equations have been programmed on the IBM 360/40 to predict the effective gas temperature vs. distance from the injector face. Typical results for the R-4D engine are shown in Figure 4. It can be seen that the latent heat of vaporization of the fuel maintains a relatively cool wall temperature at considerable distances from the injection point. Once the fuel has vaporized the effective gas temperature increases rapidly, approaching at the limit, the combustion gas recovery temperature.

The equations for prediction of these lengths of the liquid film and the gas temperature at the edge of the boundary layer have been verified by test data obtained from tests conducted on the R-4D engine, and is shown in the Analysis Results section of this report.

EFFECTIVE GAS TEMPERATURE FOR HEAT TRANSFER DUE TO COMBUSTION GAS CONVECTION

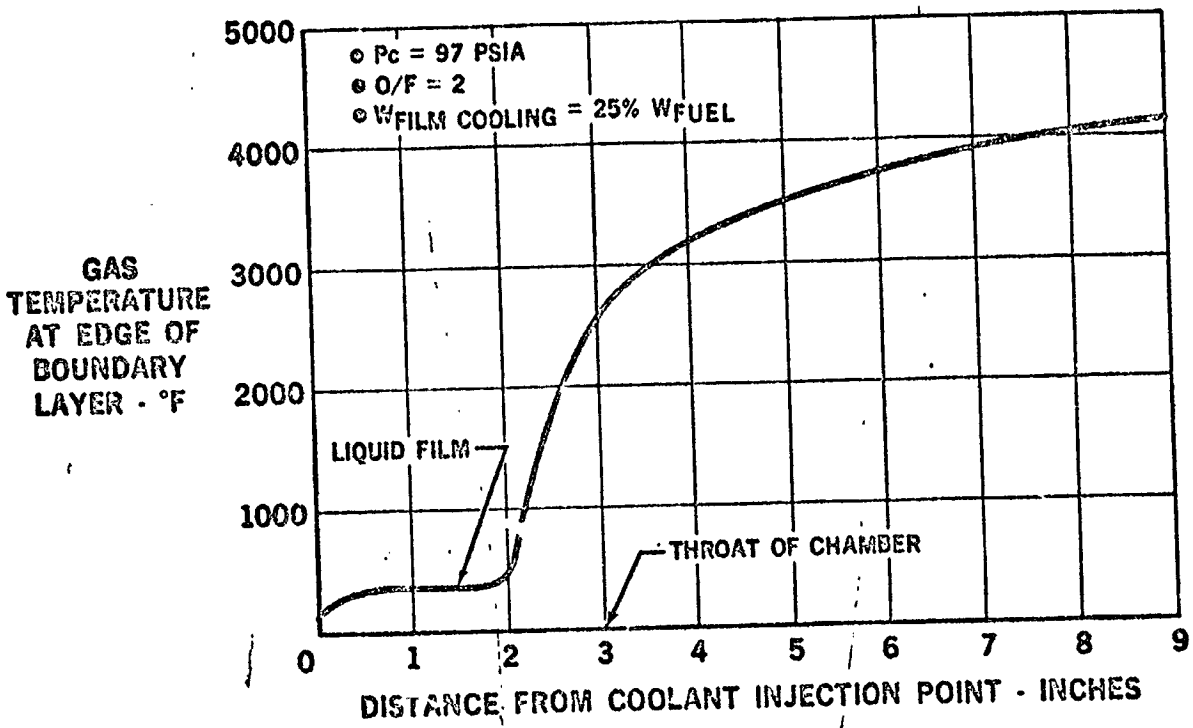

Figure 4

3. Convective Heat Transfer Coefficients for Propellant Flow Through Valve and Injector Passages

Convective heat transfer coefficients for the heat exchange between the propellants and the injector and valve passages was determined by using the equation in Reference 3,

$$\frac{hD}{K} = 0.23\ RE^{0.8}\ PR^{0.4}$$

in the region of turbulent flow.

When the fuel and oxidizer flow in the passages was in the laminar and transition regions, the convective heat transfer coefficients were determined by using the data from Reference 4, Figure 5.

4. Engine Material Thermal Characteristics

During the development of the R-4D engine, many materials were incorporated into the construction. These materials included the refractory metals, molybdenum and columbium, L-605 cobalt alloy, A286 alloys, 321 stainless, Rene' 41, and aluminum. Each of these materials has varying thermal property characteristics which would affect the thermal analysis. The properties which were required for use on the program were:

a. Density
b. Specific heat
c. Thermal conductivity
d. Emittance (total and spectral)
e. Solar absorbtivity.

A majority of the properties were known from literature, but in some cases it was necessary to evaluate the properties of the materials. Two such cases were the determination of the emittance of molybdenum and columbium, and the thermal conductivity and specific heat of C-103 columbium. These properties were obtained from tests at Marquardt and various outside sources. Figures 6, 7, and 8 show typical data for these materials.

RECOMMENDED CURVES

FOR

DETERMINING HEAT TRANSFER COEFFICIENT

IN THE

TRANSITION REGIME

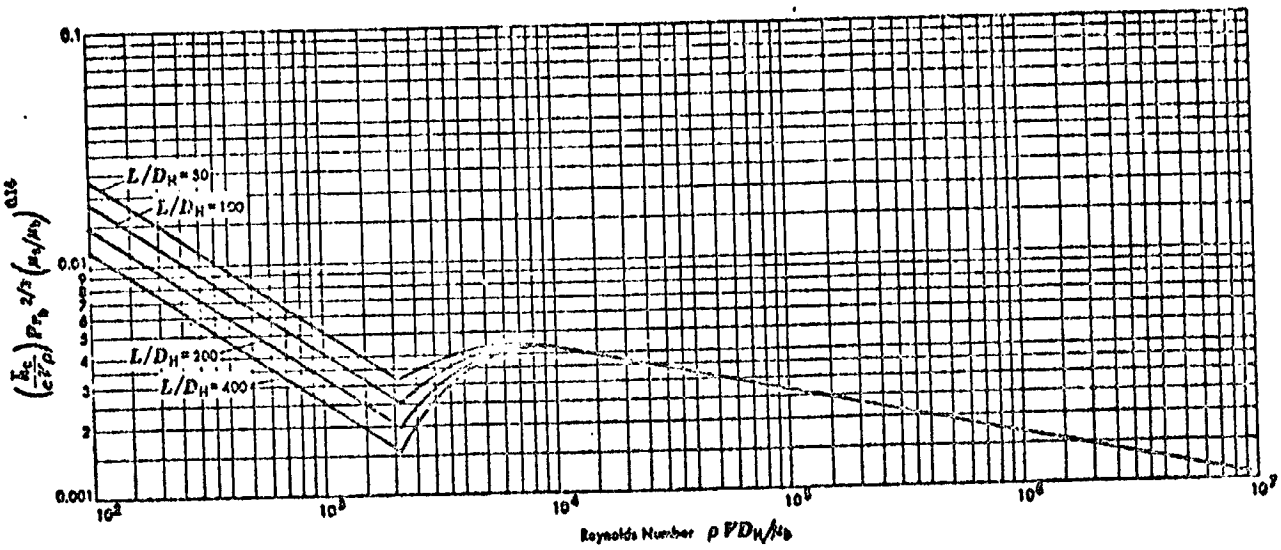

Figure 5

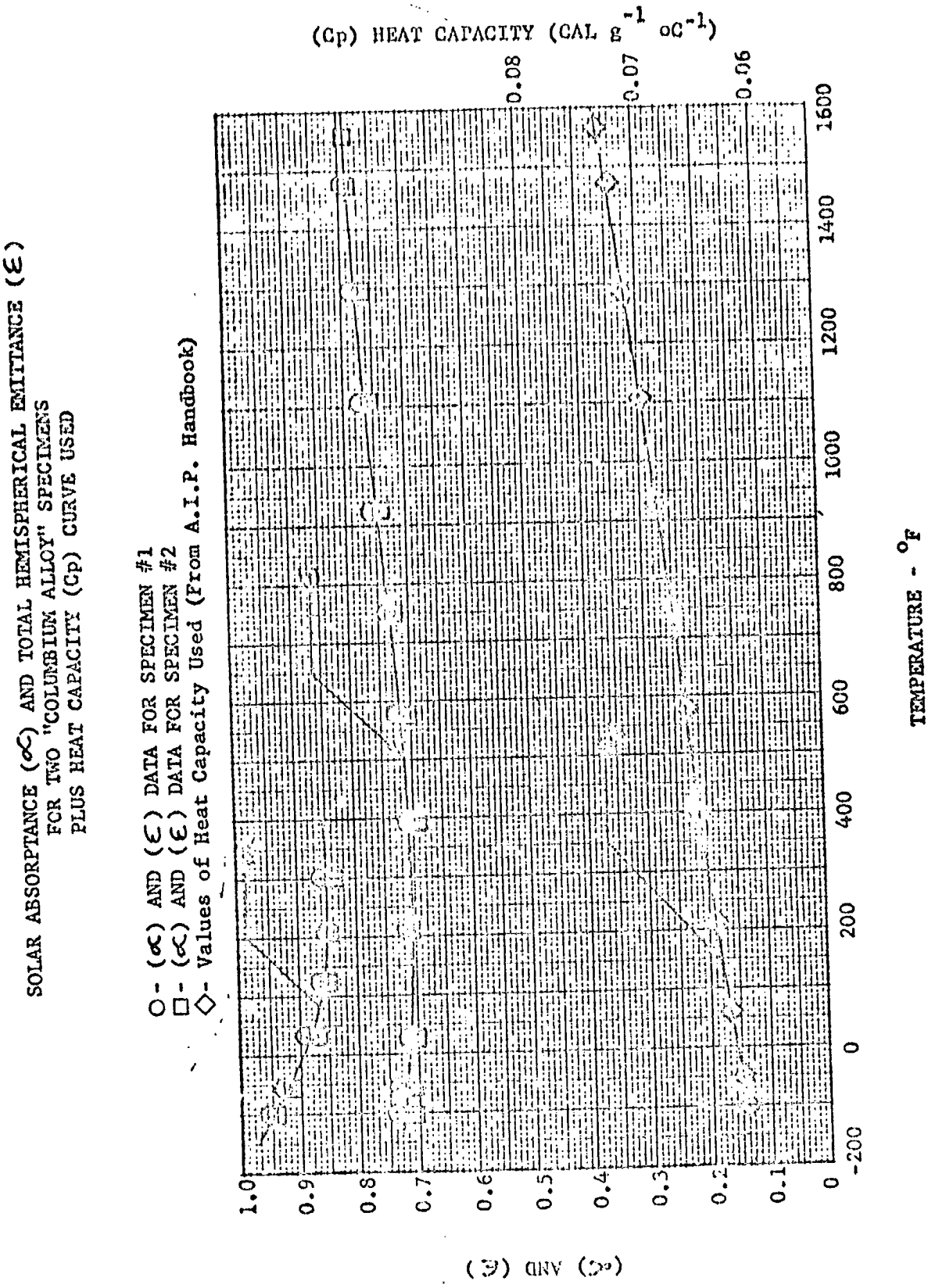
SOLAR ABSORPTANCE (α) AND TOTAL HEMISPHERICAL EMITTANCE (ε)
FOR TWO "COLUMBIUM ALLOY" SPECIMENS
PLUS HEAT CAPACITY (Cp) CURVE USED
○ - (α) AND (ε) DATA FOR SPECIMEN #1
□ - (α) AND (ε) DATA FOR SPECIMEN #2
◇ - Values of Heat Capacity Used (From A.I.P. Handbook)
(Cp) HEAT CAPACITY (CAL g-1 oC-1)
0.08
0.07
0.06
1.0
0.9
0.8
0.7
0.6
0.5
0.4
0.3
0.2
0.1
0
-200
0
200
400
600
800
1000
1200
1400
1600
TEMPERATURE - °F
(α) AND (ε)

Figure 6

THERMAL CONDUCTIVITY VS TEMPERATURE

C-103 COLUMBIUM ALLOY

Cb-10Hf-1Ti

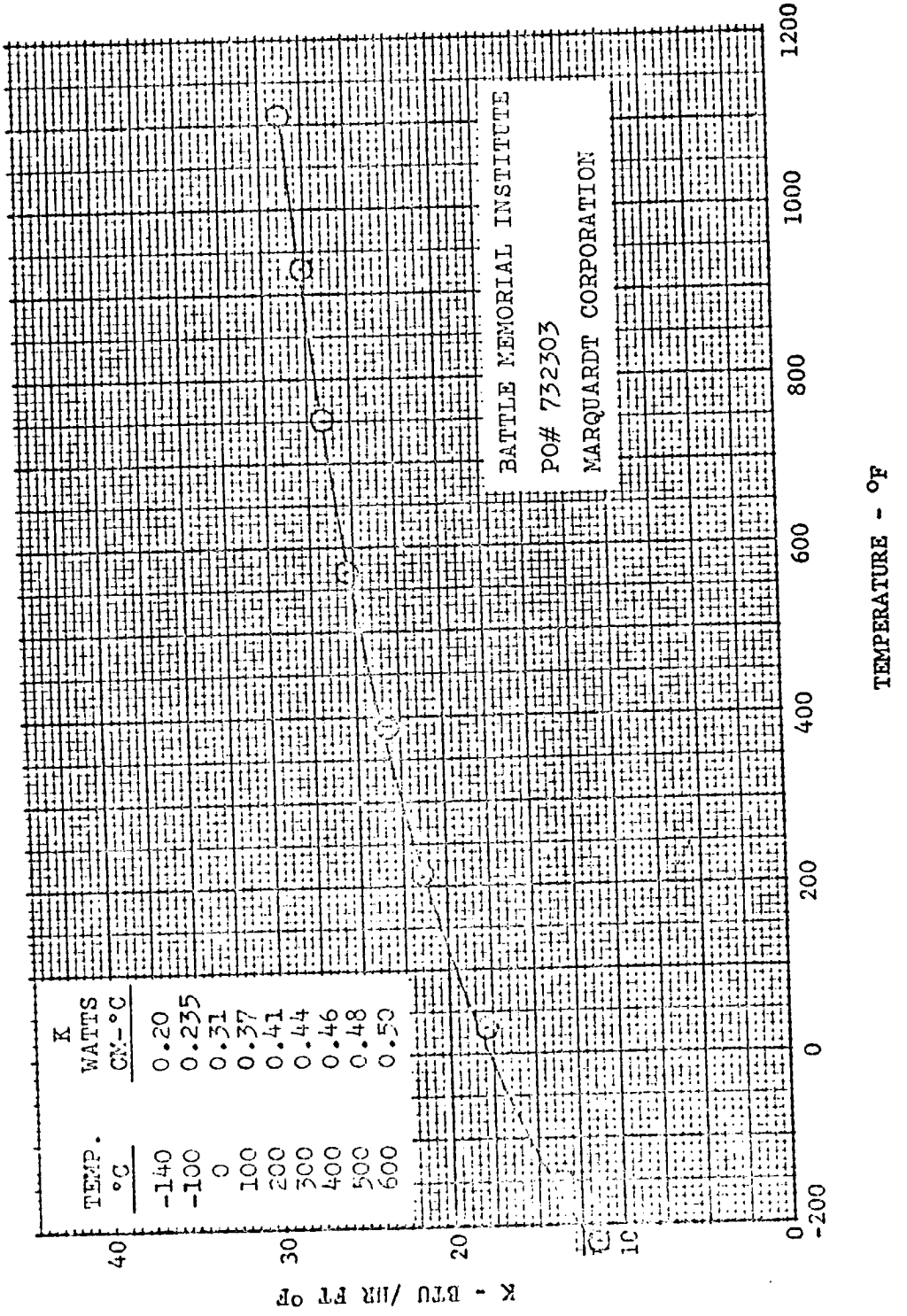

Figure 7

SPECIFIC HEAT ALLOYS AND PURE METALS

(1) Handbook of thermophysical Properties
(2) ASD-TDR-63-597
(3) THIS REPORT

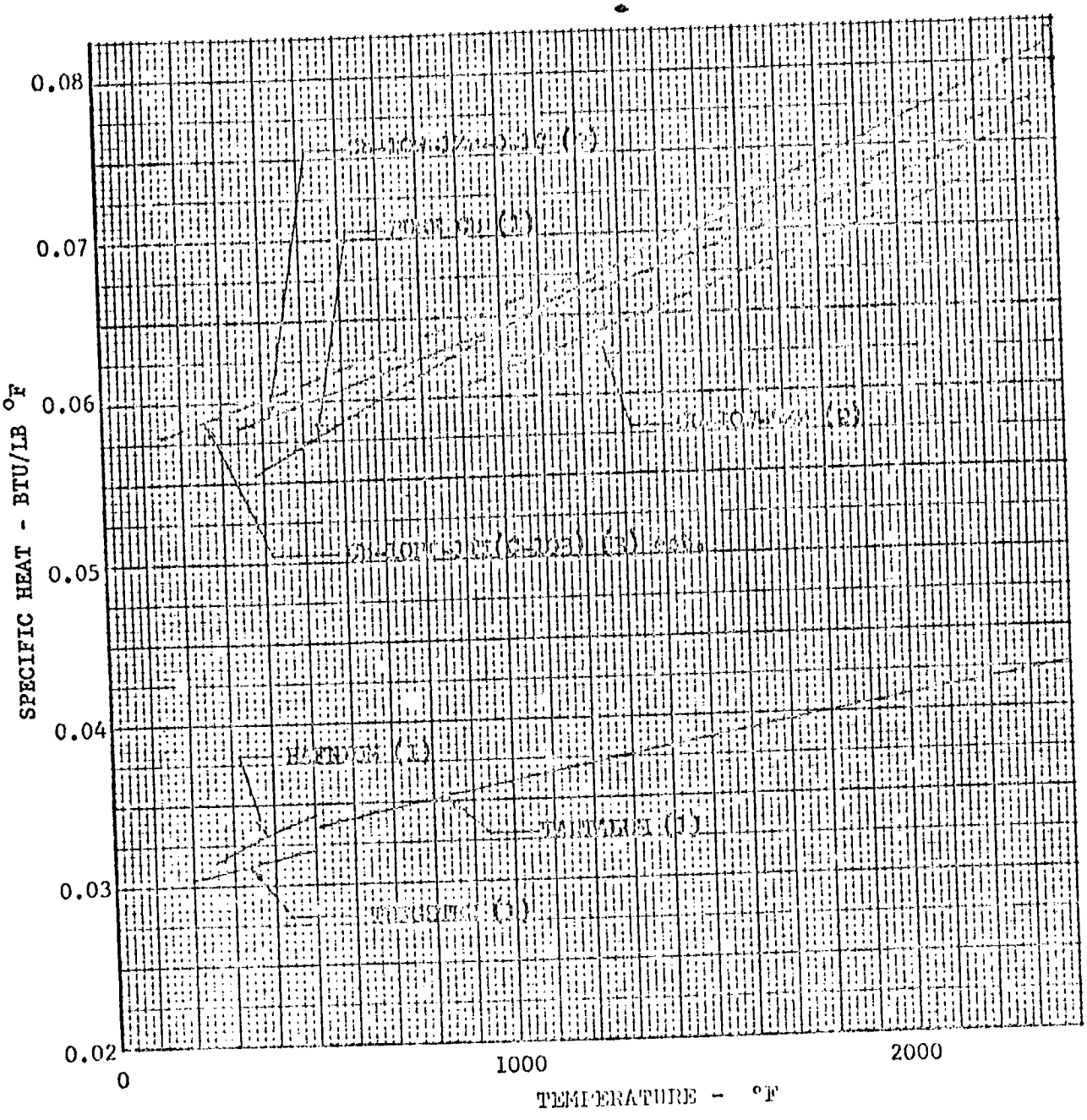

Figure 8

C. Analysis Results

The appropriate values for the heat transfer coefficients, effective gas temperature, and the various material properties as a function of temperature, were input to the Thermal Analyzer program. The output from the Thermal Analyzer program was plotted on an automatic plotter for rapid evaluation. Figure 9 shows the comparison between the theoretical temperatures obtained from the Thermal Analyzer computer program and temperatures recorded during a test firing of the R-4D engine; Figure 10 shows the steady state results for an engine using a higher performance 8-on-8 injector as another comparison. The comparison for both engines is well within the accuracy required and shows the effectiveness of using the film cooling design techniques described.

Table I shows the experimental temperatures obtained from hot firing tests, and the temperatures resulting from the analysis techniques described for the engine operating at a mixture ratio of 2, using nitrogen tetroxide oxidizer and 50% b. w. N_2H_4/50% b.w. UDMH.

TABLE I

R-4D COMPONENT TEMPERATURES

	THEORETICAL	EXPERIMENTAL
COMBUSTION CHAMBER A. FLANGE 1. STEADY STATE 2. SOAKBACK	 330°F 440°F	 270 – 330°F 400 – 460°F
B. THROAT 1. THERMOSCOPE 2. XR FILM	2150°F	1900 – 2200°F 2200°F
C. BELL NUT	1800°F	1800°F
INJECTOR 1. STEADY STATE 2. SOAKBACK	188°F 326°F	165 – 185°F 300 – 330°F
VALVES 1. OXIDIZER VALVE SOAKBACK	144°F	140°F

TEMPERATURE VS TIME
MARQUARDT 100 LB. THRUST ROCKET ENGINE
O/F = 2 200 SEC. FIRING

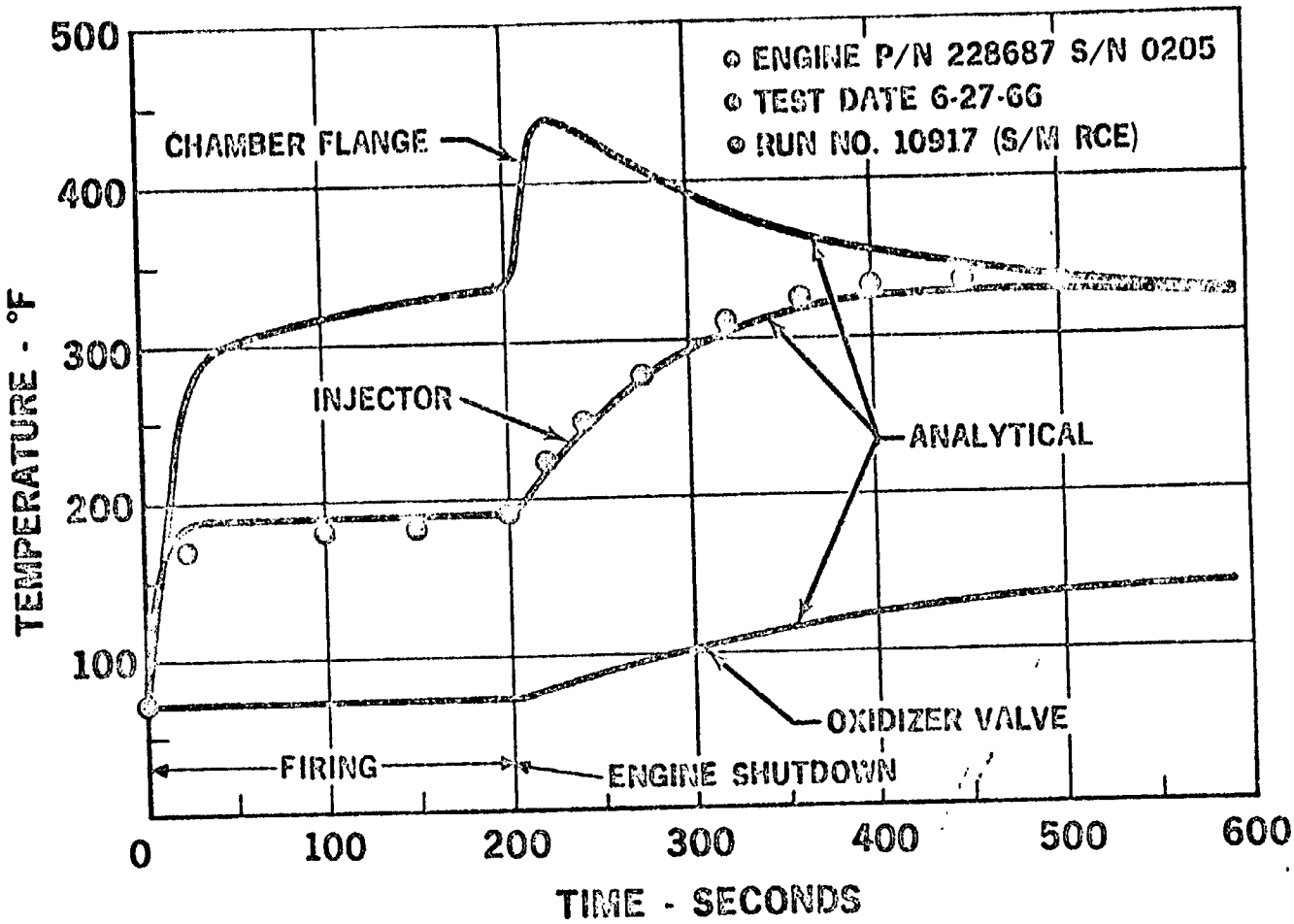

Figure 9

100 POUND THRUST RADIATION COOLED ENGINE TEMPERATURE CHARACTERISTICS

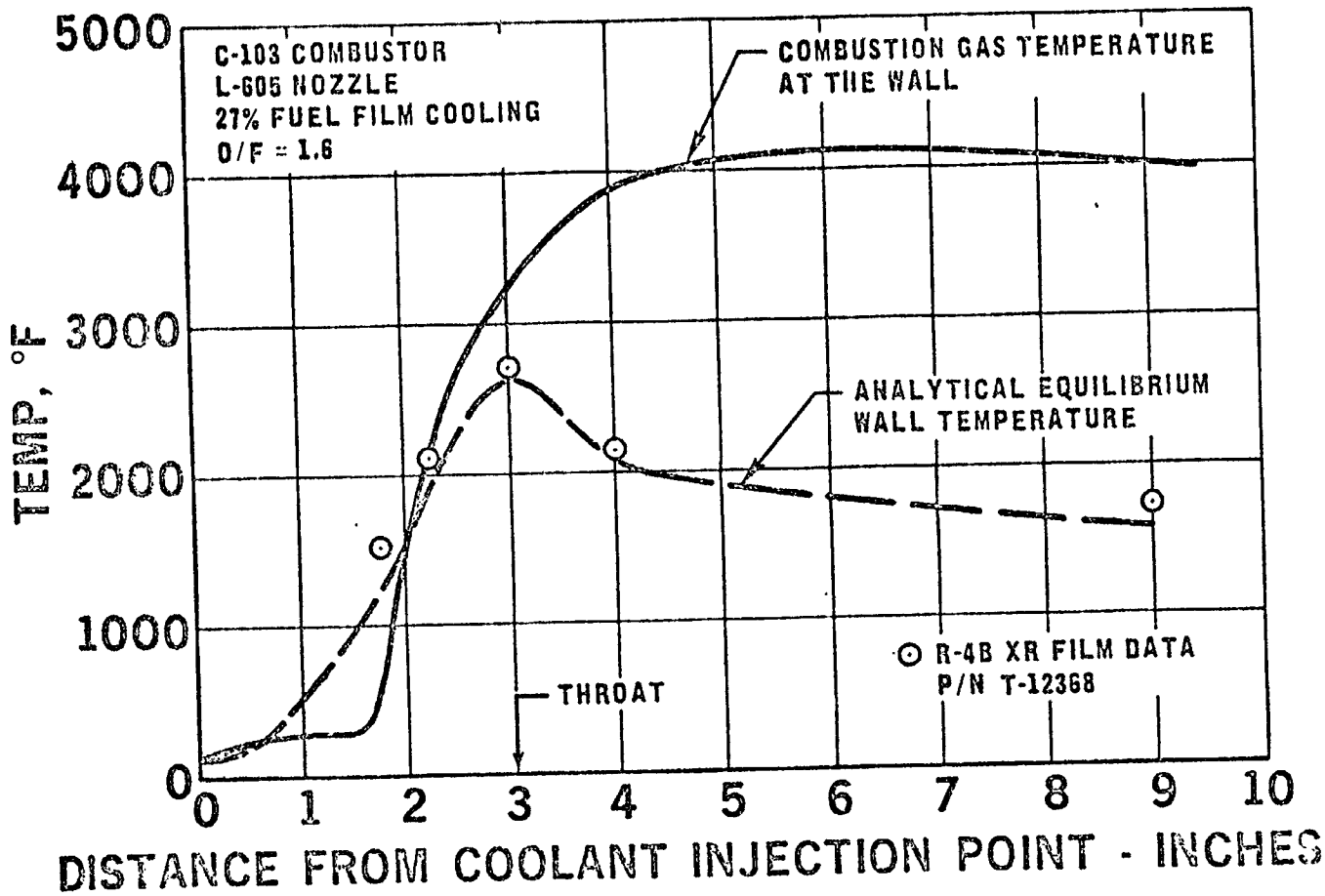

Figure 10

In addition to the hot firing tests which were conducted during the development program, a series of tests were conducted to determine the engine characteristics during cold soak (radiation to deep space) operation. During space operation the engine usually radiates to space vacuum (-460°F), but during ground tests the engine was tested in vacuum test cells where the surroundings were ambient (70°F). Since the temperature of the combustor is in the 1000-3000°F range, the effect due to the temperature difference of the surroundings is negligible. During the time when the engine is not operating, i.e., cold soak, and the engine must be maintained at temperatures above the freezing point of the propellants, it was necessary to simulate the space environment. This was accomplished by locating the engine in the test cell where the surrounding test cell walls are cooled with liquid nitrogen. The engine was then heated by a resistance heater and the power required to maintain the engine at various temperature levels was obtained. These data were then compared to the thermal model results. Figure 11 shows the power requirements for the R-4D engine vs. injector temperature based on the experimental results and the analytical model.

The data show that the analytical methods used to calculate the thermal characteristics of the R-4D engine can adequately predict the actual temperature during both hot firings and cold soak conditions. As will be shown later, the analytical methods which evolved from this program were used in successful supplementary programs to provide the necessary thermal design criteria.

POWER REQUIREMENTS
RADIATION TO DEEP SPACE
R-4D 100 LB. THRUST ROCKET ENGINE

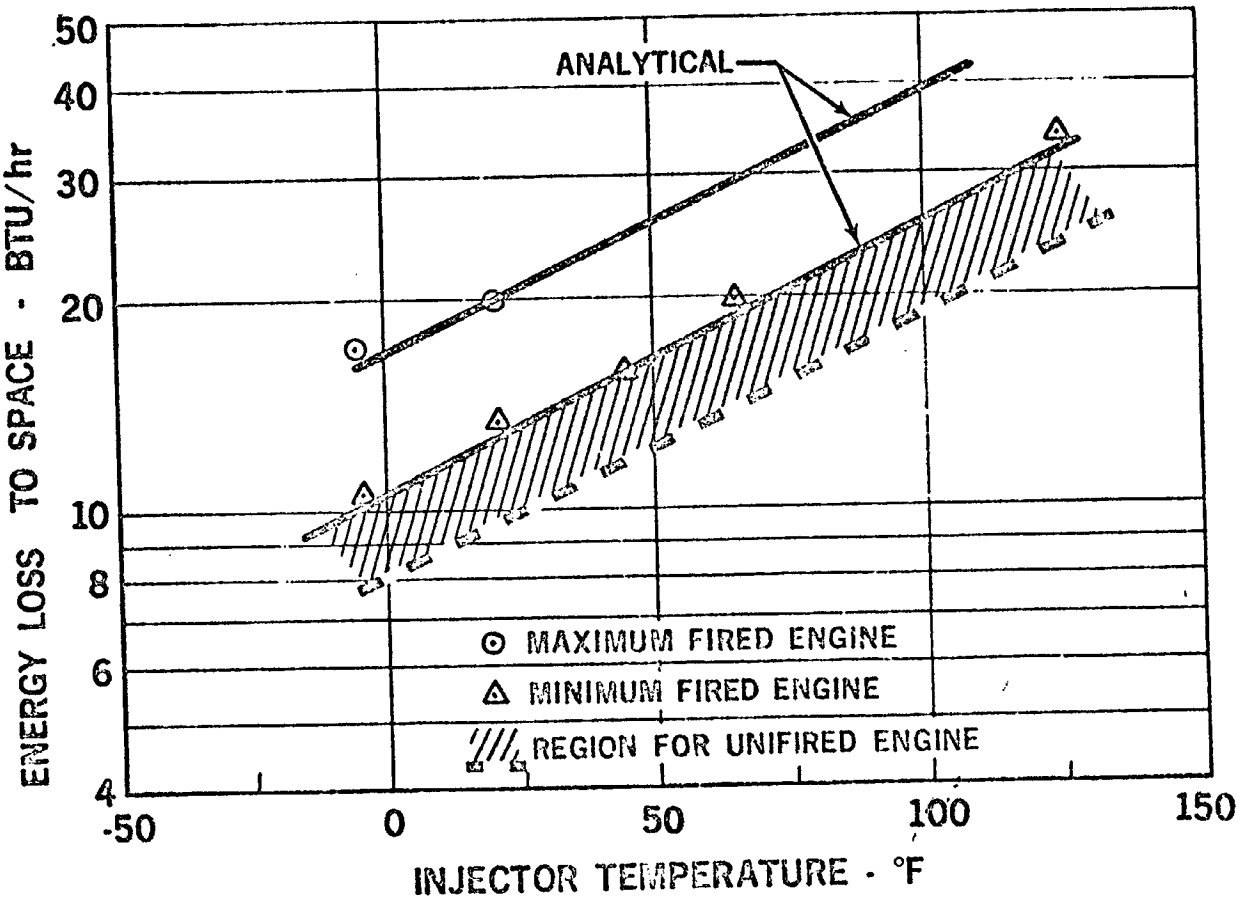

Figure 11

IV. THERMAL DEVELOPMENT HISTORY

The development of the Marquardt R-4D engine can be discussed chronologically, using the time periods required to accomplish major areas of engine development. The approximate time periods and areas of development effort are listed in Table II.

TABLE II

Areas of Development Effort	Time Period	Solutions Investigated
A. Increase performance	Sept. 62 to Dec. 62	Use multiple doublet to improve propellant mixing.
B. Reduce injector thermal soakback temperature	January 63 to June 63	Use higher resistance "K" seal and add fuel cooling annulus downstream of valve seat.
C. Eliminate "hot phasing" of propellants	July 63 to Jan. 64	Isolate oxidizer propellant passage. Use oxidizer valve standoff. Remove oxidizer flow paths from head "spider." Add film cooling.
D. Eliminate ignition over-pressures	June 63 to July 64	Change injector design to 12-on-12 pattern Use stronger chamber. Add preigniter.

Each effort was inter-related with others and the engine design evolved as a compromise which could satisfy the technical requirements within the constraints of cost and schedule.

A. Increase Performance

The minimum specific impulse requirement at the initiation of the development program was 300 $\frac{lb_f}{lb_m}$/second: The initial design concept, a single doublet, was selected due to ease of manufacture, simplicity of design, and high pulse performance, however, the steady state performance

was below 300 seconds. Several design and development studies were made which attempted to reach 300 seconds specific impulse. Various single doublet configurations were used which incorporated splash plates, pre-mixing cups, and various combinations of oxidizer and fuel injection velocities and impingement angles. The best results obtained were 270-280 seconds I_{sp}, which was below the minimum specification requirement.

A multiple doublet injector was tested to increase mixing efficiency and to provide a more uniform chamber temperature. Several combinations were tested:

Multiple Doublet Configuration Tested	Results
4 on 4	Improvement over single doublet
6 on 6	Greater improvement, but still not sufficient.
8 on 8	This injector met the 300 second minimum and was eventually selected as the candidate design. Several iterations upon the doublet configuration were made to optimize performance.
12 on 12	This injector further improved the performance and the temperature distribution. It was selected as the backup design to the 8 on 8 since it was harder to manufacture than the 8 on 8 and resulted in lower life capability due to higher chamber temperature.
24 on 24	One injector of this design was tested but provided no significant improvement in performance. Greatly increased manufacturing difficulty for this design precluded further consideration.

The 8 on 8 configuration delivered the required specific impulse, but the steady state injector temperature and thermal soakback were greater than the limits set for some portions of the engine. It was selected for further development, based on the performance improvement.

The pre-prototype engine configuration consisted of (1) chamber, all molybdenum ".040" wall thickness bolted directly to the head, (2) valves, fuel and oxidizer seated directly on the aluminum head, and (3) head, 8 on 8 injector.

B. Excessive Injector Head Temperature

The 8 on 8 injector design resulted in high performance and a high chamber temperature--typical throat temperatures of 2800°F and chamber flange temperatures of 1500°F. This flange temperature resulted in a large amount of conductive heat transfer to the head. This heat was not adequately removed by the propellants, thus, some mode of thermal management was required to minimize the heat transfer from the combustor.

1. Higher Resistance "K" Seal

To lower the amount of heat conducted into the head from the chamber, a steel bearing ring was added to the "K" seal. This configuration was known as the "wide flange K seal." This change did lower head temperatures significantly; however, the flange temperature increased to 2000°F, which caused the seal to fail. No performance degradation was measurable, nor was there any evident physical damage to the engine. However, effects of the leakage of the combustion products through the seal to the vehicle were unknown and therefore not desirable. Several changes to the seal configuration were made in an attempt to solve the problem, including some attempts to change the heat release pattern by changing the injection momentum angle. This problem was finally resolved by using fuel film cooling which lowered the flange temperature to less than 400°F. Concurrently, the seal joint was designed for 2000°F by using a flat labyrinth L-605 seal. Both film cooling and the high temperature flat chamber seal were incorporated at about the same time.

Two attempts were made to reduce the heat input to the injector head by convection from the combustion gases. The approach used was to install a convective barrier across the portion of the injector face which was outside the doublet impingement diameter. A stainless steel barrier was used and a thermally insulated phenolic washer was attempted. Both attempts resulted in very little head temperature difference and the concept was dropped.

2. Fuel Cooled Head

A two-pass fuel cooling annulus was added to the basic 8 on 8 injector in an attempt to lower the running temperature of the injector head and, consequently, the maximum soakback temperature. The fuel entered a cooling passage downstream of the valve seat, made one complete circle, passed into a lower cooling path, circled the head again, then entered the fuel distribution manifold. These cooling annuluses were small diameter passages for high efficiency cooling and minimum dribble

volume. They were very effective and lowered the heat temperature steady state head temperatures to 150°F as opposed to 350°F without the cooling path.

One detrimental effect was anticipated, i.e., the effect of the large dribble volume on pulse performance. During testing to verify this effect, the chamber was destroyed by an ignition overpressure. This was the first time this had occurred at TMC without a questionable facility malfunction (a prior chamber failure during Advent development was caused by a plugged chamber, due to faulty purging techniques). The injector head was refitted with a new chamber and the test series repeated. The second chamber was also destroyed.

Analyses of this phenomena lead to the conclusion that the oxidizer lead and large fuel dribble volume was the basic cause and the fuel cooled injector head idea was scrapped. A fuel cooling loop located upstream of the valve seat was thought to be unusable as the fuel would vaporize during soakback from the long run.

Because of the destroyed chamber, the backup design 12 on 12 design was pressed into service and the prototype testing was started. The 12 on 12 injector design had a larger impingement diameter, therefore, a larger diameter fuel metering annulus. This larger annulus provided much more head cooling and the injector head temperature was lower than the 8 on 8. The higher performance resulted in a higher chamber temperature of 2900-3000°F. This temperature approaches the upper limit of the molybdenum disilicide coating but the life capability was still considerably beyond the mission requirements.

C. Hot Phasing (Reference 5)

The mission duty cycle simulation tests of the injector design required an engine start and operation from high temperature soakback conditions. It was known as "Maneuver No. 1" and consisted of:

10 seconds on, 30 seconds off,
3 seconds on, 360 seconds off,
10 seconds on.

During execution of the above cycle, a peculiar behavior of the thrust and chamber pressure, and an extremely rapid heating of the chamber was observed. Typical data traces are shown in Figures 12 and 13.

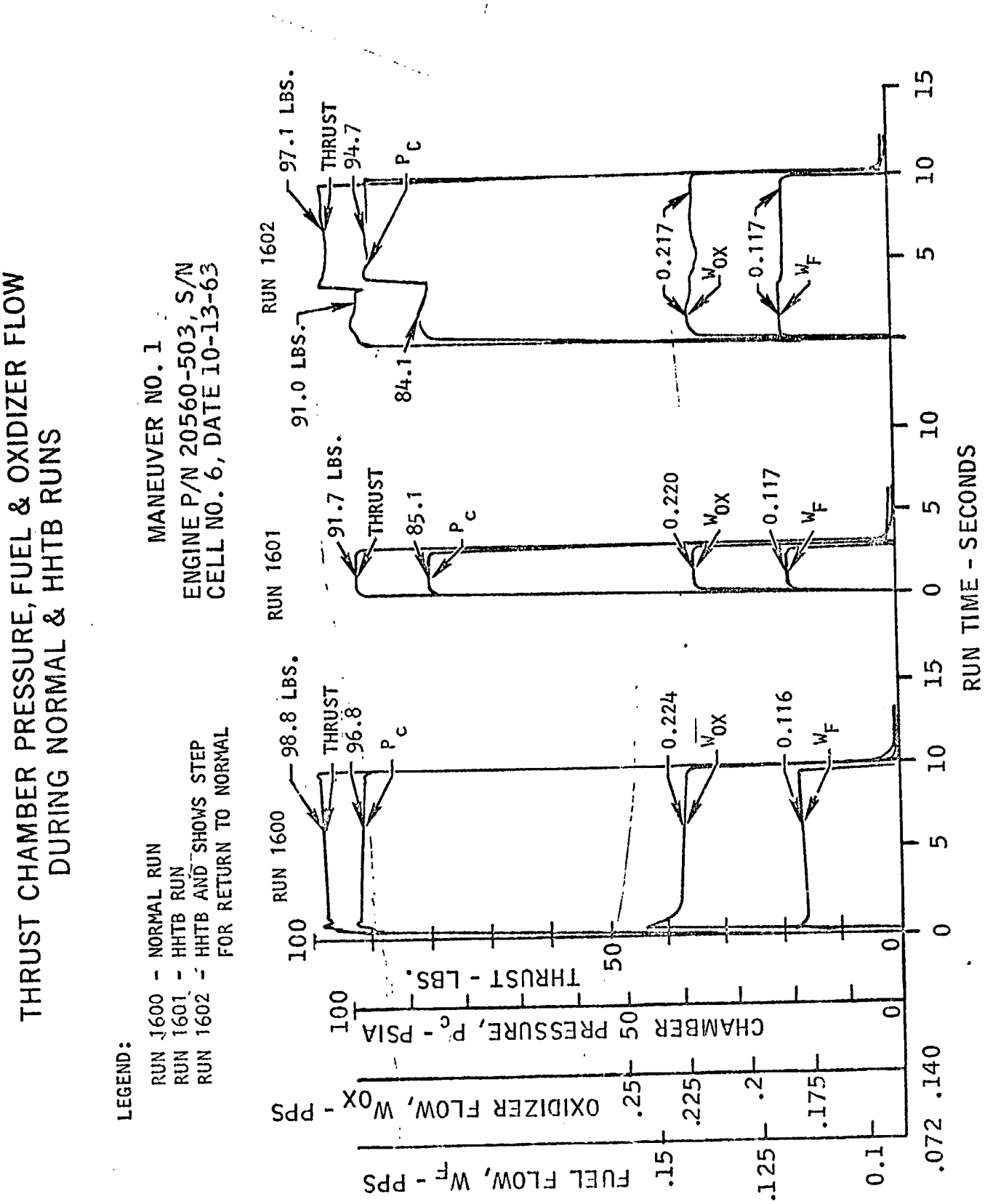
THRUST CHAMBER PRESSURE, FUEL & OXIDIZER FLOW
DURING NORMAL & HHTB RUNS
MANEUVER NO. 1
ENGINE P/N 20560-503, S/N
CELL NO. 6, DATE 10-13-63
LEGEND:
RUN 1600 - NORMAL RUN
RUN 1601 - HHTB RUN
RUN 1602 - HHTB AND SHOWS STEP FOR RETURN TO NORMAL
RUN 1600
98.8 LBS.
THRUST
96.8
P_c
0.224
W_{OX}
0.116
W_F
RUN 1601
91.7 LBS.
THRUST
85.1
P_c
0.220
W_{OX}
0.117
W_F
RUN 1602
97.1 LBS.
THRUST
94.7
P_c
91.0 LBS.
84.1
0.217
W_{OX}
0.117
W_F
THRUST - LBS.
100
50
0
CHAMBER PRESSURE, P_c - PSIA
100
50
0
OXIDIZER FLOW, W_{OX} - PPS
.25
.225
.2
.175
.140
FUEL FLOW, W_F - PPS
.15
.125
0.1
.072
0
5
10
15
RUN TIME - SECONDS

Figure 12

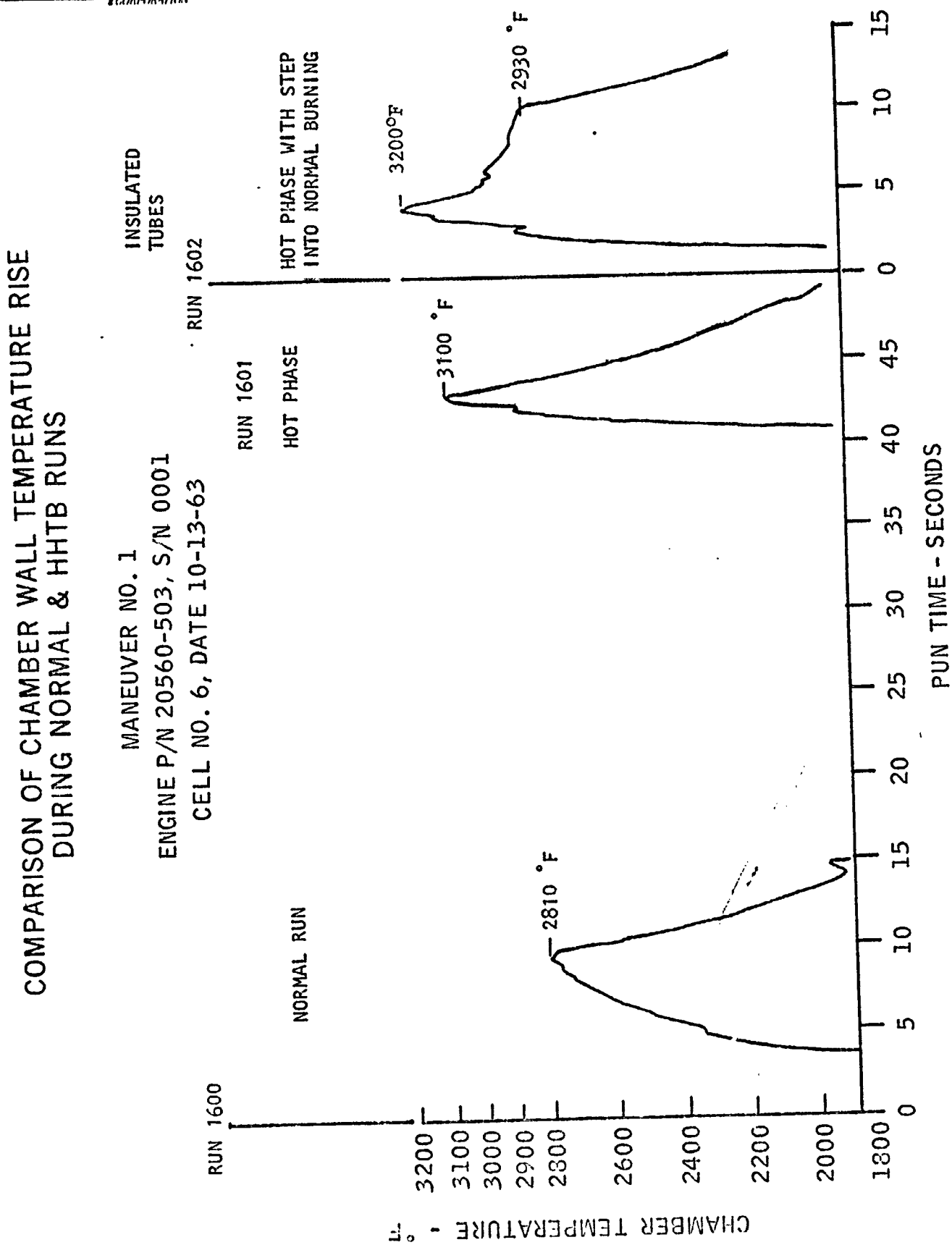
COMPARISON OF CHAMBER WALL TEMPERATURE RISE
DURING NORMAL & HHTB RUNS
MANEUVER NO. 1
ENGINE P/N 20560-503, S/N 0001
CELL NO. 6, DATE 10-13-63
INSULATED TUBES
RUN 1602
HOT PHASE WITH STEP INTO NORMAL BURNING
3200°F
2930 °F
RUN 1601
HOT PHASE
3100 °F
NORMAL RUN
2810 °F
RUN 1600
CHAMBER TEMPERATURE - °F
3200
3100
3000
2900
2800
2600
2400
2200
2000
1800
0
5
10
15
20
25
30
35
40
45
0
5
10
15
PUN TIME - SECONDS

Figure 13

A photograph showing the exterior of the chamber under a normal burning condition is shown in Figure 14 upper. A photograph of similar type during high heat transfer burning is shown in Figure 14 lower. This phenomena was given the coined name of "Hot Phase", although the official name was HHTB (High Heat Transfer Burning).

Several chambers were burned out at the area just above the throat during the time of experimentation with this type of burning. The heating rate was exceptionally impressive. A normal start shows dull red streaks starting, then slowly reaches full cherry redness within about ten seconds after "engine on." Observations showed that HHTB burning was like having a light bulb turned on in the cell. The chamber was almost instantly and rather uniformly "white" hot from the flange to the throat.

The rate increase of chamber temperature was faster than the Bristol response of the thermoscope and reached failure temperatures of 3300°F within two to three seconds.

When the "step" occurred, i.e., changed from HHTB to normal burning, the engine reverted to normal operation and the chamber temperature cooled to standard 2700-2800°F steady state operation. This reversion was an abrupt, almost instantaneous event. Thrust and chamber pressure increased by about seven percent, causing a step in the instrument traces (hence its name, "step").

Since the Hot Phase occurred only when the engine was started from high temperatures, it was believed that the cause was a two-phasing effect on combustion due to boiling of the propellant as it passed through the manifolds. Since the oxidizer has a much lower boiling temperature at these pressures, development effort was concentrated in this area. A fair correlation was observed between a propellant temperature within the oxidizer valve of 145°F and the occurrence of the step. The Hot Phase burning presented no difficulty unless it continued for more than two seconds; therefore, thermal isolation was attempted to lower the maximum temperature of the oxidizer valve upon soakback and to minimize the time required to cool the oxidizer flow passages.

Two methods were used to lower the maximum temperature of the oxidizer valve upon soakback: (1) use of an oxidizer valve standoff, and (2) film cooling.

(1) Oxidizer Valve Standoff

An oxidizer standoff was designed using stainless steel A-286. This is a steel tube of minimum cross section which is used as

CHAMBER APPEARANCE DURING NORMAL & HIGH HEAT TRANSFER BURNING

NEG. CT3106-123CN

NEG. CT3106-124CN

Figure 14

the propellant passage between the valve and the head. The thermal resistance between the injector and the oxidizer valve was increased by using long stainless steel bolts. A phenolic insulator was installed to absorb the transverse loads.

Initially the standoff was a removable part with omniseals at each end for propellant sealing. This was changed to a pressed-in A-286 insert to eliminate sealing and installation difficulties experienced with the omniseal injector interface.

Alternate approaches were tried to reduce the cooldown time of the oxidizer propellant passages: (a) use of pressed-in steel lines into the oxidizer distribution manifold, and (b) a "spider" design using individual stainless steel tubes as propellant passages.

(a) Pressed-in Steel Lines

In this approach, steel lines were pressed directly into the oxidizer distribution manifold. This design proved difficult to fabricate and provided no observable benefits.

(b) Spider Design

A radical departure from the central standoff and the propellant distribution manifold was made in the spider design. It carried the concept of thermal isolation of the oxidizer valve and the rapid cooling of the propellant passages to the ultimate extreme. In this design, the valve loading was structurally reacted by the bolts and head. The propellant was injected into the chamber by individual stainless steel tubes. This allowed maximum isolation of the oxidizer valve from the head and provided low heat capability propellant passages.

The individual tubes were slip fitted into the injector to allow for thermal expansion and to minimize the stresses. The difficulty of fabrication techniques was the major reason that the design was not more readily accepted. Leakage of combustion products through the slip fit joints, with possible accumulation of propellants, also presented difficulty. Assembly and fabrication techniques have advanced tremendously in the past five years, and this design may now be feasible. It could be considered for thermal isolation of advanced injector designs.

(2) Film Cooling

The chamber flange temperature was too high to allow effective sealing of the injector head interface and too much heat was conducted into the head. An idea was presented to spray a small quantity of fuel

(fuel film cooling) onto the chamber flange to cool it. The results were phenomenal. In one stroke the high temperature flange seal problem and the hot phase burning were eliminated. In addition, the chamber temperature was reduced to such a low level that the R-4D chamber has almost unlimited operational life.

Various amounts of fuel were used in an attempt to optimize the film cooling relative to the I_{sp} performance degradation and run time.

The chamber flange temperature for the film cooled engine design had two separate operating characteristics, one at 500°F or less and the second at 1600-1800°F. This change in temperature is caused by a shift from nucleate to film boiling of the fuel cooling streams. The higher flange temperatures are undesirable because of the increased heat stored in the flange and chamber which must be absorbed by the head and valves during soakback. The soakback temperatures also become higher as the thickness of the chamber is increased.

Every test of a film cooled engine starts with nucleate boiling heat transfer of the coolant on the wall. The abrupt transition to film boiling and its corresponding high chamber wall temperature is a function of O/F ratio, percent fuel cooling, and time. The time to transition increases as the O/F and percent cooling are increased.

The T-10060 (Figure 15) injector, with 12 to 13% fuel cooling, shifts to film boiling when the O/F ratio is 1.8. At an O/F ratio greater than 1.85, the flange temperature is low, i.e., 500°F or less. Figure 16 shows chamber flange temperature versus O/F for most engine configurations through T-10060. Figure 17 shows the effect of O/F ratio upon the length of run time until the transition to film boiling and its associated high temperature occurs.

The fuel cooled injector design did not have the same performance as a non-film cooled injector of the same hole size, because the doublet O/F is not optimum. The cooling fuel is included in the engine O/F ratio but does not react as efficiently as if mixed in a doublet. A good correlation was made of engine temperature vs. I_{sp} for various amounts of cooling. This data indicates that engine chamber temperature is a direct function of performance within relatively narrow limits. Figure 18 shows throat temperature vs. I_{sp} for engines with fuel cooling from 9 to 12% and data from an engine with film cooling of 19.5%. At the 300 second performance level, the additional film cooling had decreased the throat temperature by 300°F.

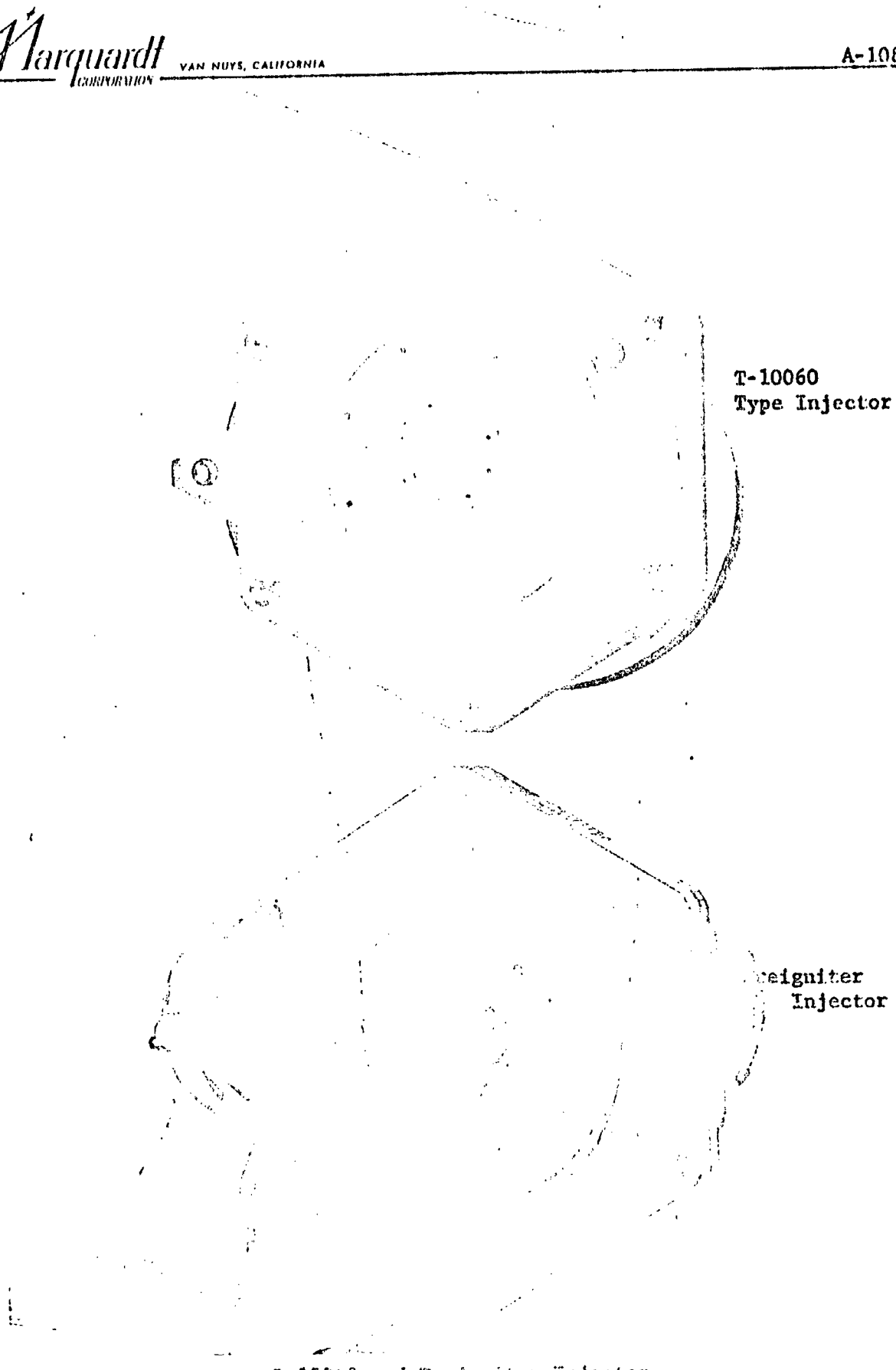

T-10060 and Freiguiter Injector

Figure 15

CHAMBER FLANGE TEMPERATURE VS MIXTURE RATIO

DATA TAKEN AT 60 OR 90 SECOND POINT

SYMBOL	ENGINE P/N	S/N	RUNS	CELL	RUN DATE	% BLEED
○	T-10020	0001	3060-3134	6	3-03-64	10.7
△	T-10020	0001	471-518	1	2-22-64	10.7
□	T-10020	0001-2	819 886	1	3-12-64	19.4
◇	T-10050	0002	3386-3474	6	3-24 TO 3-27-64	12.9
◺	T-9730	0001	625-711	1	2-29 TO 3-04-64	21.5
▢	T-10100	0001-2	3861-3876	6	5-06-64	10.6
⬯	T-10060	0003-3	3877-3907	6	5-15-64	12.92
◊	T-10010	0001	386-432	1	2-17-64	11.4
◺	T-10030	0002-1	3135-3231	6	3-04 TO 3-06-64	8.9

SOLID SYMBOLS: DATA NOT STEADY STATE AS RUN WAS CUT IN TRANSIENT FROM NUCLEATE TO FILM BOILING.

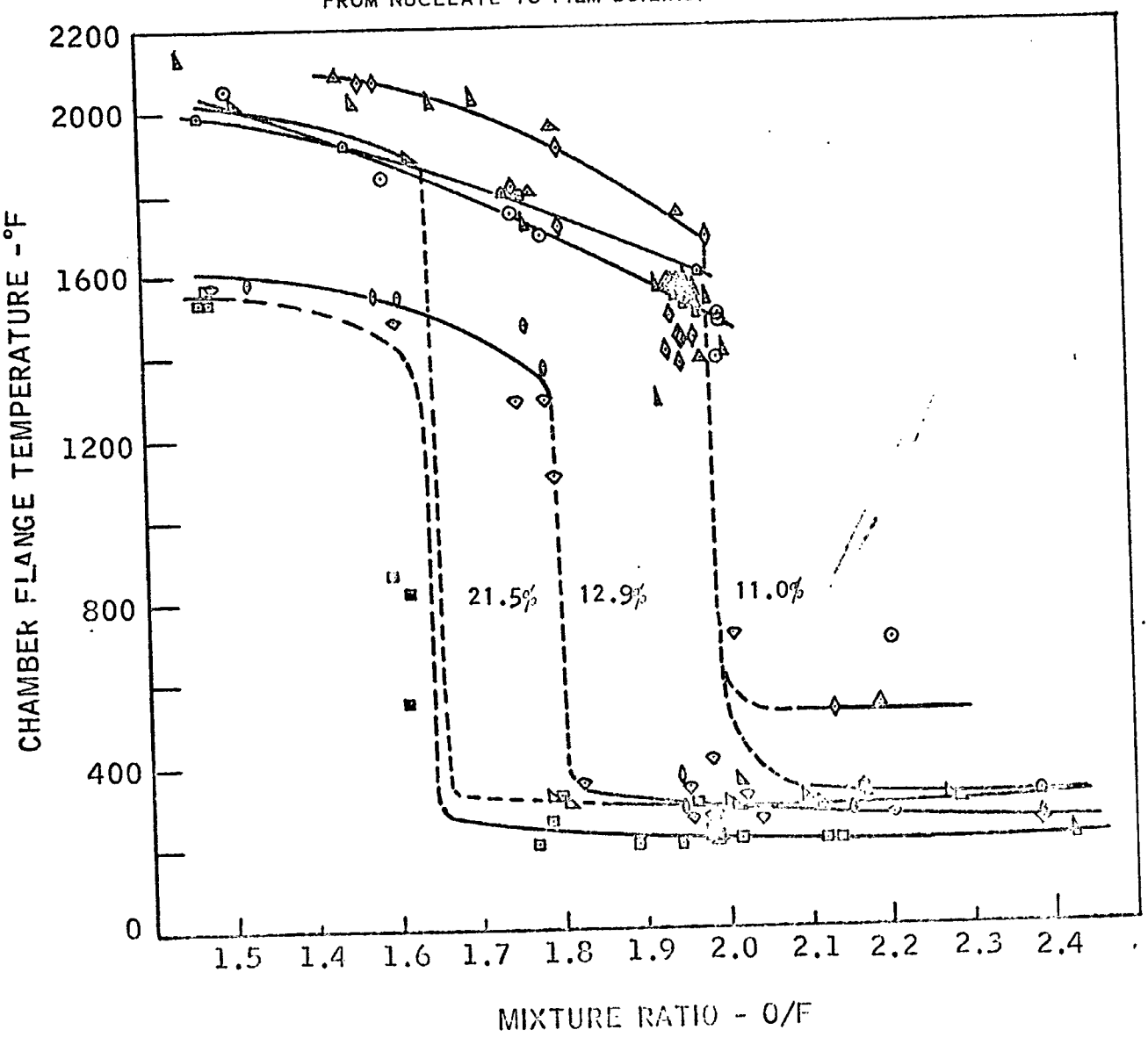

Figure 16

MOLYBDENUM FLANGE TEMPERATURE TIME HISTORY

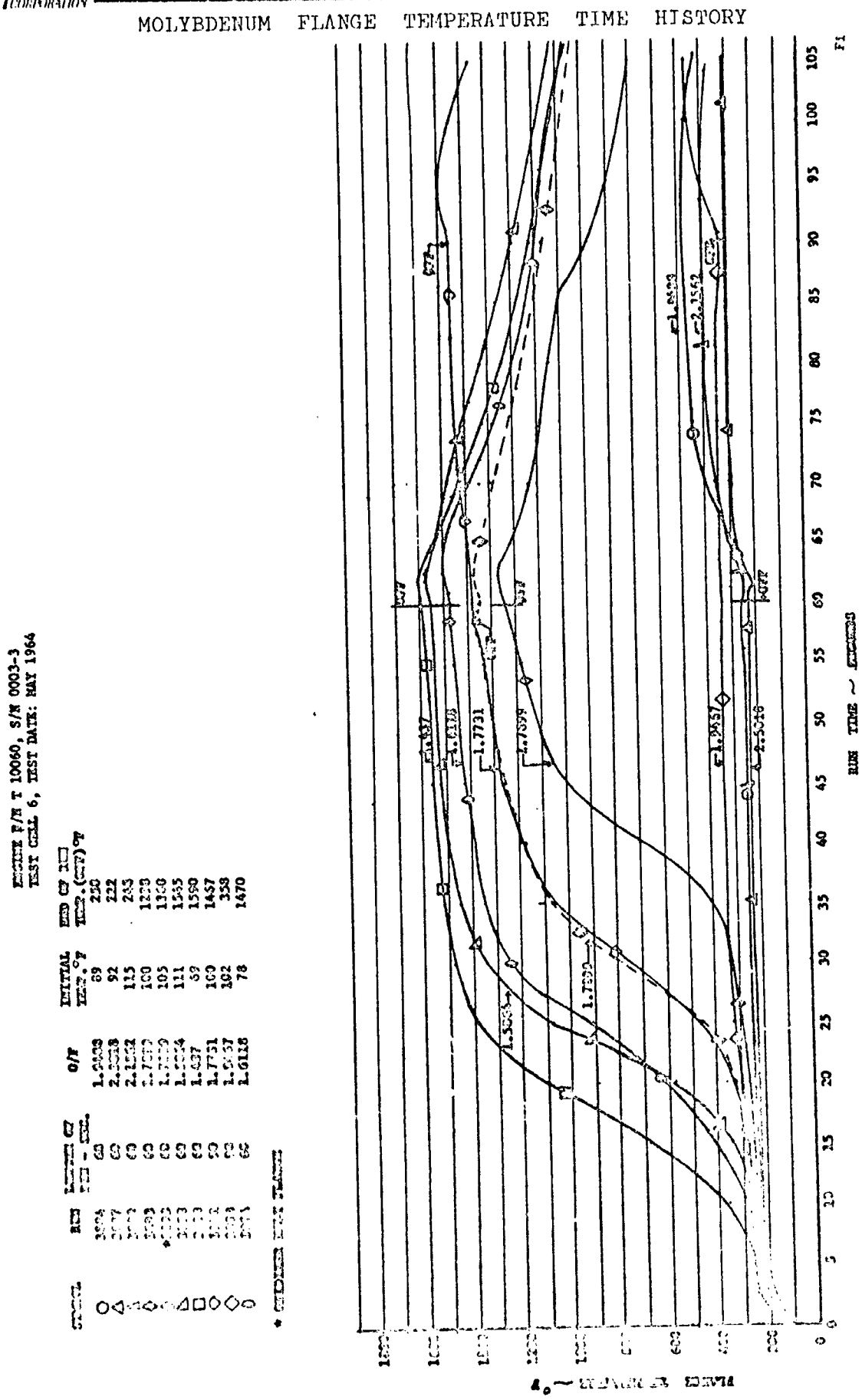

SPECIFIC IMPULSE VS THROAT TEMPERATURE

KEY:

SYMBOL	ENGINE	% BLEED	O/F
△		0	1.4
○		"	1.6
△		"	1.8
□		"	2.0
◊		"	2.2
○	T-10020	10.7	
○	T-10020	19.5	
●	T-10030	8.9	
◐	T-10050	12.0	
----		19.5	

NOTES:
ALL TEMPERATURES TAKEN AT THE THROAT BY THERMOSCOPE

ALL CHAMBERS RIBBED AND GRIT-BLASTED

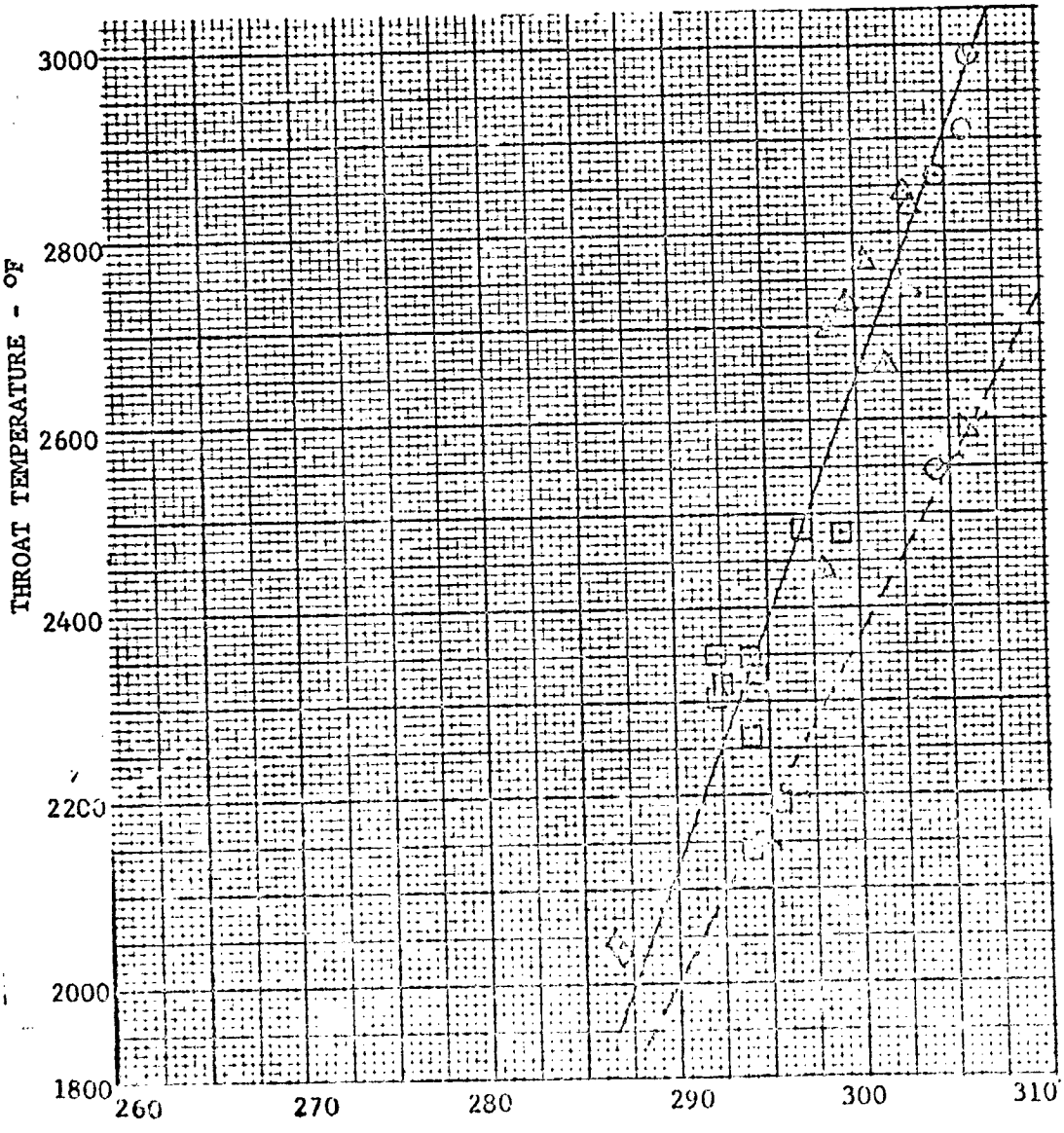

Figure 18

D. Ignition Overpressures

In August, 1963, a 12-on-12 engine was destroyed by an ignition overpressure. This placed great emphasis on understanding how, what, and why an ignition transient pressure would sometimes shatter a chamber. A two-prong engineering development effort was launched to examine ignition phenomena and combustion characteristics in detail. The injector combinations which were built and tested were dash numbers of Drawing VX20560 (-501 through -533). These engines were tested for thermal characteristics and ignition pressure levels.

The most successful 12 on 12 configuration for thermal considerations was the -511. It always "stepped" out of hot phase operation in less than 0.5 second and delivered specific impulse in excess of 295 seconds. It had a hot chamber temperature of 2900-3000°F but was the best candidate for a successful engine. Unfortunately, a second injector of this configuration (S/N 002) would not behave in the same manner as S/N 001. After several tests to verify that S/N 002 was different from S/N 001, the 12 on 12 injector design was dropped.

An injector design selection was also being made on the basis of ignition spike testing. This testing indicated the 8 on 8 had lower pressure transients and the program eventually selected the -525 engine as the injector design to be developed.

E. Pre-Igniter Effects

The T-10060 fuel cooled engine had demonstrated the most successful engine design. Its steady state chamber temperature was 2200°F and the maximum head temperature was less than 350°F and was thermally acceptable for the Apollo Mission. It was not acceptable from the standpoint of ignition transient pressures that it generated. The pre-igniter was introduced to reduce or eliminate these overpressures (Figure 15).

The pre-igniter had an adverse effect on the engine's thermal characteristics. The percentage of fuel film cooling had to be increased from 13% on the chamber wall to 22-23% on the wall to obtain the same chamber wall temperature and to allow runs of infinite length without a shift to film boiling.

Additional fuel cooling was required on the pre-igniter itself to prevent burnout of the steel (A286) wall. The effect of this large amount of fuel, which was not mixed in the main doublet, was a lowering of performance. This can be attributed to a very high doublet O/F ratio and poor mixing of the fuel used for film cooling.

V. SUPPORTING PROGRAMS

During the Apollo program, additional programs were conducted to determine the characteristics and performance of the engine due to various design changes. These programs included:

A. NAS-9-6003, Columbium Alloy Combustion Chamber

B. NAS-9-5626, Apollo S/M RCS Engine Modification for Moog Valve.

C. M4J7XA-406013 NAA, Thermal Management of Apollo SM/RCS.

D. TBC P.O. N-672458 7674, Lunar Orbiter Velocity Control Engine

A. Columbium Alloy Combustion Chamber

The Columbium Alloy Combustion Chamber development program, funded by NASA-MSC under Contract NAS-9-6003, was conducted to develop a coated columbium alloy combustion chamber suitable for incorporation into the Apollo LM/SM RCS engine. Heat transfer analysis of the engine system was conducted to predict the various structural temperatures during and after an engine hot firing (Reference 6). The engine combustor was composed of a C-103 columbium alloy. The component and columbium structural temperatures predicted by the analysis and the actual temperature measured during test firings of the engine are listed on Table III for the R-4D engine. In summary, the valves, injector head, and combustor flange temperatures were lower with the columbium alloy than the corresponding temperatures with a similar molybdenum alloy chamber. The maximum combustion chamber temperature, using the columbium alloy, is approximately 100° hotter than with a similar molybdenum chamber. The principal reason for this difference is due to the lower thermal conductivity of the columbium. This lower thermal conductivity results in less conduction heat transfer along the chamber wall.

Since the thermal conductivity and emittance of the C-103 columbium alloy was not known at the start of the program, a determination of these properties was made by Marquardt, Battelle Memorial Institute, and the U. S. Naval Radiological Defense Laboratory. The results of these tests are shown on Figures 6 and 7,

The results of the tests indicated that columbium could be successfully incorporated into the R-4D engine. The majority of the structural portion of the engine would be operated at or near the operating temperatures of a molybdenum combustor engine system, while the columbium alloy combustor would run up to 100°F hotter than a similar

TABLE III

SUMMARY OF S/M RCS TEMPERATURES
STEADY STATE AND SOAKBACK

	MOLYBDENUM		COLUMBIUM	
	Theoretical	Experimental	Theoretical	Experimental
I. COMBUSTION CHAMBER A. Flange 1. Steady State 2. Soakback	329 440	270-330 400-460	288 295	230-280 300-330
B. Throat 1. Thermoscope 2. XR Film	2150	1900-2100 2165	2230	1900-2300 2200
C. Ball Nut	1800	1800	1800	1750-1800
II. INJECTOR 1. Steady State 2. Soakback	185 328	165-185 300-330	187 255	170-190 250-270
III. VALVES A. Oxidizer Valve Seat 1. Soakback	145	140	120	N.A.
B. Fuel Valve Seat 1. Soakback	156	155	132	N.A.

P_c = 97 psia Fuel N_2H_4/UDMH or MMH

O/F = 2.0 200 seconds/soakback

Propellant Temperature = 70°F

molybdenum combustor. Tests of the oxidation resistant coating on the columbium combustor indicate a maximum safe temperature above 2800-3000°F, which is well above the operating temperature of the engine.

B. Moog Valves

NASA Contract NAS-9-5626, "Apollo Service Module Reaction Control System Engine Modification for the Moog Valve" was conducted to provide an engine which uses the Moog bipropellant valve, but retains the combustion characteristic of the R-4D engine. A heat transfer analysis was conducted to determine the design requirements when the Moog valve (which is a bipropellant valve) is used instead of the twin coaxial valves.

The heat transfer analysis of the engine using a Moog valve was conducted using the thermal analyzer program for a majority of the study. This was required because of the thermal resistance change between the injector and the valve. The design of the Moog valve required redesign of the injector to minimize the heat transfer to the valve. The analyses and data generated in the test program (Reference 7) indicated that the injector and combustor temperatures are approximately the same as for the R-4D engine, with coaxial valves, and that the Moog valve temperatures are higher than for the coaxial valves during soakback from a steady state run. The temperatures are well below the valve upper temperature limit. The approximate temperature of the valve seat of the Moog valve was 200-210°F at soakback, compared with 160-180°F for the coaxial valve configuration.

C. Passive Thermal Management Program

The major objectives of this program, funded by NASA-MSC under Contract NAS-9-5026, were to,

1. Establish minimum and maximum operational temperatures for the engine.

2. Determine radiation properties of the combustion chamber and of possible alternate materials.

3. Verify major thermal characteristics of the engine.

4. Evaluate potential changes to the engine design which would improve thermal characteristics and recommend an engine configuration for optimum thermal performance.

Results

1. The minimum operational temperature was determined to be -30°F head temperature. This limit was established by pulse performance degradation for short pulse widths. The residue of propellant in the dribble volume froze due to evaporative expansion and plugged the flow passages for subsequent pulses. The minimum head temperature was lowered to -90°F for runs long enough to raise the head temperature high enough to evaporate all the propellant in the dribble volume.

2. The thermal radiation characteristics were determined by lab measurement at Hughes Aircraft and Grumman Aircraft Engineering Corporation. Table 4 lists the emissivity and solar absorbtivity of the probable material combinations for the Apollo engine.

3. The thermal characteristics of the nonpassive thermal design engine were analyzed and a computer thermal model prepared using the radiation properties determined. The primary features of this design were an oxidizer standoff and flat L-605 seal. The fuel valve injector joint was a ball seat directly in the aluminum head. The model used lumped mass nodes connected by thermal resistances. This model was used to evaluate the effects of various thermal properties and engine designs. The model and temperature time transients are presented in the final report of the thermal management study program (Reference 8).

4. The culmination of the study effort was that the engine could be significantly improved relative to thermal power losses and solar soak time limit by relatively minor design changes such as,

a. Fuel valve standoff to increase the time required to reach the limiting valve temperature.

b. High resistance chamber head seal to reduce the heat loss from the chamber.

c. Changes to the chamber bell to reduce solar absorbtivity and emissivity. These recommended changes did not consider any peripheral effects such as lower chamber and head temperatures upon the start pressure transients.

A direct result of the thermal management study was a directive from NAA to implement 1) a fuel valve standoff with a thermal resistance of 44,000 $\frac{sec-°F}{btu}$, 2) a head chamber seal resistance of the maximum possible as a retrofit into the present design.

TABLE IV

RADIATION DATA

Sample	Test Facility	ϵ (2) -100	0	+100	+200	α_s
1. L-605 as fabricated	HAC GAEC	.18 .13	.18 .14	.18 .15	.19	.46 .49
2. L-605 as fabricated and then oxidized at 1800° F and .05 psia for 1 minute	HAC GAEC	.29	.30	.34	.37	.83
3. L-605 as fabricated, oxidized at 1800°F and .05 psia for one minute, and exposed to a vacuum of 10^{-6} torr for 8 hours at room temperature	HAC GAEC	.30	.31	.35	.37	.79 .79
4. L-605 polished and then oxidized at 1800°F and .9 .05 psia for 1 minute	HAC GAEC	.18 .13	.19 .14	.20 .16	.21	.74
5. L-605 polished, oxidized at. 1800°F and .05 psia for 1 minute and exposed to a vacuum of 10^{-6} torr for 8 hours at room temperature	HAC GAEC	.19	.26	.27	.28	.74
6. TZM nongrit-blasted, coated with disilicide and smoke checked (1)	HAC GAEC	.21 .13	.23 .14	.24 .16	.26	.84 .85
7. TZM grit-blasted, coated with disilicide and smoke checked(1)	HAC GAEC	.23 .16	.24 .18	.26 .21	.27	.84 .87
8. TZM nongrit-blasted, coated with disilicide, smoke checked (1) and vacuum treated	GAEC	.11	.12	.13		.86
9. Moly nongrit-blasted, coated with disilicide, and smoke checked (1)	NR GAEC	.07	.07	.20 .09	.11	.82 .785
10. Moly grit-blasted, coated with disilicide and smoke checked(1)	NR GAEC	.37	.40	.43(3) .43	.45	.90 .86
11. L-605 polished	GAEC			.11		.31

(1) Two cycles of heating to 2000°F and holding for 5 minutes in air
(2) GAEC ϵ is normal; HAC ϵ is total hemispherical
(3) Not smoke checked

1) Fuel Valve Standoff

The standoff design was a straightforward extension of the principle used for the already existing ox valve standoff. Since extended length of the bolts was not possible due to the injector configuration, good thermal isolation and stress relief for thermal expansion was provided by using long titanium bolts with titanium standoffs under the bolt heads between the valve cap. The primary difficulty was encountered in provin that an overall resistance of 44,000 $\frac{sec\,^{o}F}{Btu}$ was obtained.

Several attempts were made to measure the thermal resistance by conductive cooling of the head and measuring a known heat input. These attempts were unsuccessful due to excessive uncontrollable heat leaks in the setup. These heat leaks were not repeatable and led to several erroneous conclusions about possible problems of unrepeatable valve seat joint thermal resistance.

A radiation space cold soak test vacuum chamber was assembled to verify the actual overall valve head thermal resistance. This test facility proved the overall resistance to be 47,000 $\frac{sec\,^{o}F}{Btu}$ for the ox valve and 55,000 $\frac{sec\,^{o}F}{Btu}$ for the fuel valve. These resistances were very close to the analytical evaluation and were proven to be repeatable.

D. High Resistance Chamber Head Seal (Reference 9)

The high resistance seal program objective was to design, fabricate, and functionally test a chamber head seal which had a thermal resistance 5.0 $\frac{hr\text{-}^{o}F}{Btu}$. The seal was to be interchangeable with the standard Apollo seal. A seal design was built and tested which would furnish a thermal resistance of 5 $\frac{hr\text{-}^{o}F}{Btu}$ but would require slight modification to the head-seal cavity. A seal with a thermal resistance $\approx$ 3.0 $\frac{hr\text{-}^{o}F}{Btu}$ was designed for the existing cavity. The latter seal has almost as effective as a 5.0 $\frac{hr\text{-}^{o}F}{Btu}$ resistance seal in reducing the heat loss and would have considerably smaller impact upon the Apollo program.

To provide thermal data for structural analysis, a thermal model of the R-4D engine under soakback from firing and cold soak conditions of the engine was made. Good agreement with temperature results from firing tests were obtained. The model gave temperature profiles which were within 15° of the actual test data. Accurate soakback temperature predictions enabled a good structural evaluation to be made.

Detailed thermal evaluation of candidate seal designs was made by comparative calculation of thermal resistance from maximum and minimum dimensions. Practical seal design configurations were selected, fabricated, and tested for verification of the analysis.

Test Methods

The test method used for verification of the thermal resistance calculations was a direct measurement of the heat loss across the seal under actual heating rates and thermal load conditions.

Simulated heads were heated by small electrical resistance heaters. An actual chamber was attached to the head, using the seal and attach hardware. The power input to head was measured and used with the measured temperature difference across the seal to calculate the thermal resistance of the seal. Figure 19 is a schematic of the experimental test setup. Figure 20 shows the actual test hardware. The heat input was calculated from current and voltage measurements. All heat generated was assumed to go across the seal. Convective losses were negligible at low pressure $p \leq 10^{-5}$ mmHg. Radiative losses were made approximately zero by controlling the boundary temperature to the same temperature as the simulated head.

The temperature difference resulting between simulated head and the chamber flange was measured and used to calculate the seal thermal resistance,

$$R_s = \frac{T_h - T_f}{Q_{in}} \quad \frac{Hr\text{-}^{o}F}{Btu}$$

The excellent agreement with calculated value and high degree of repeatability indicate all assumptions were justified. Figure 21 compares the test results and calculated thermal resistance.

REPRODUCIBILITY OF THE ORIGINAL PAGE IS POOR.

THERMAL RESISTANCE TEST SETUP

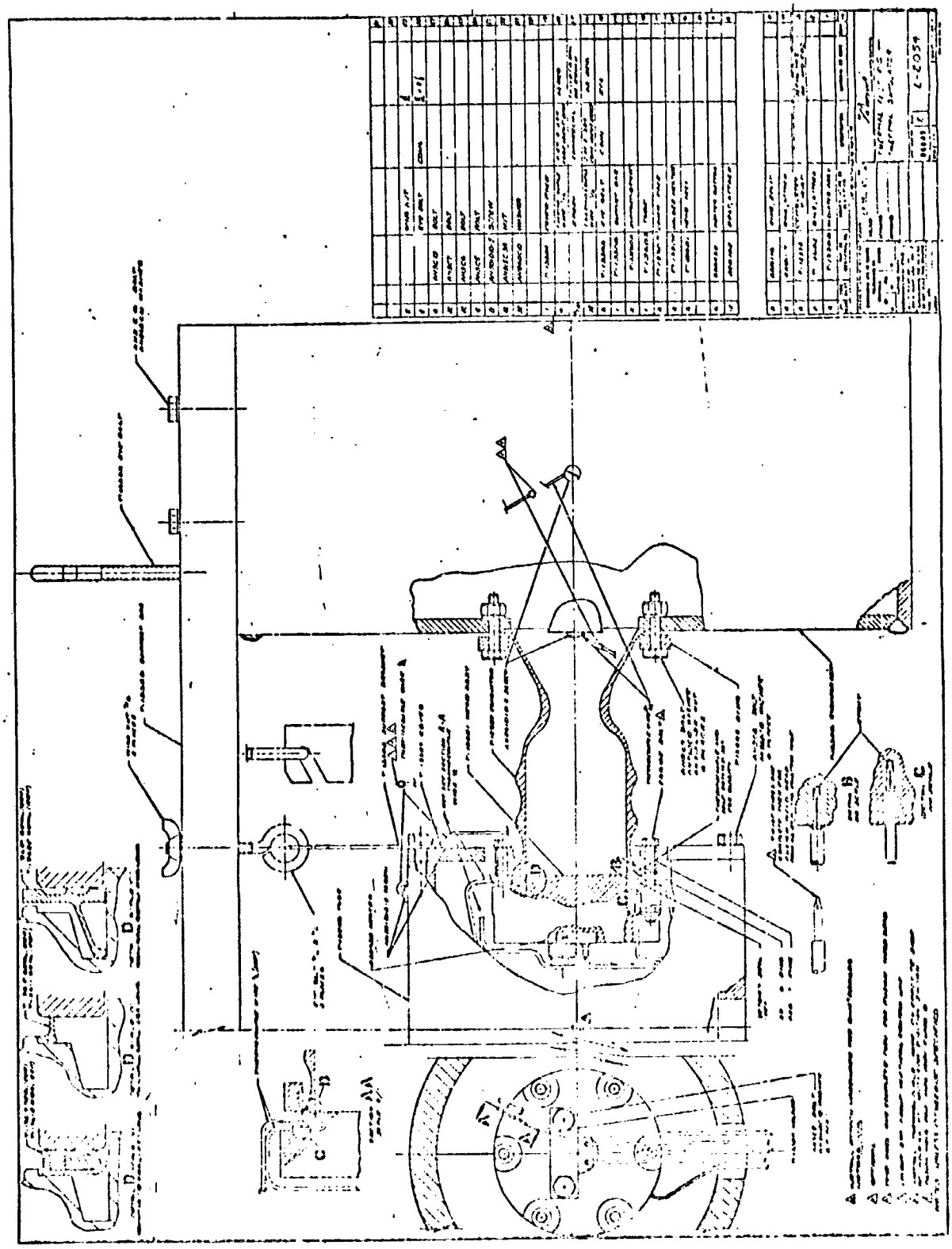

Figure 19

REPRODUCIBILITY OF THE ORIGINAL PAGE IS POOR.

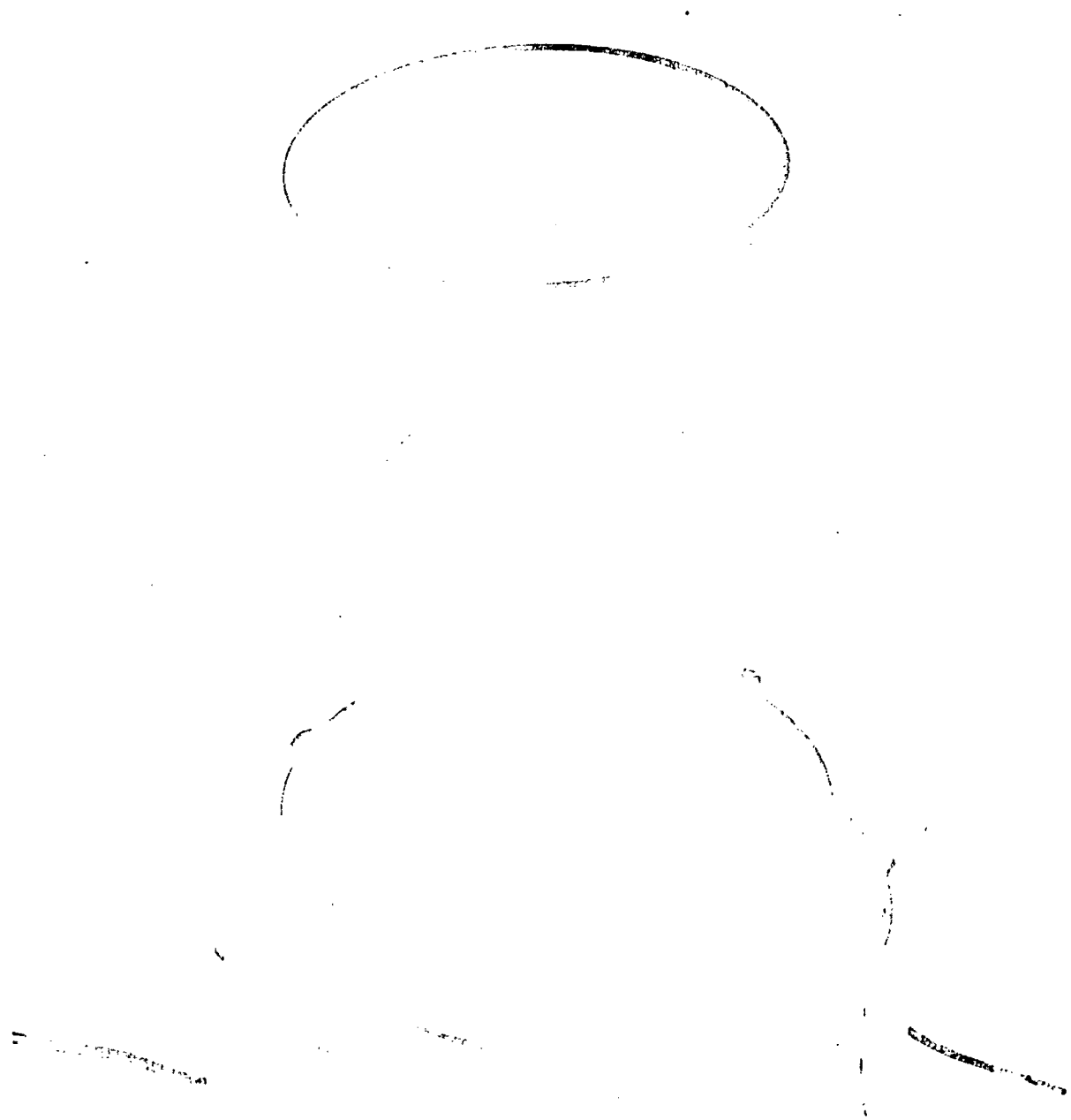

NEG. 7003-2

Combustor-Injector Heat Transfer Test Hardware

Figure 20

SEAL THERMAL RESISTANCE TEST RESULTS

Seal Configuration	P/N	Material	Thermal Resistance			
			Predicted (Neglects Contact Resistance)		Demonstrated	
			Minimum	Maximum	Seal	Joint*
			$\frac{Hr\text{-}^{o}F}{BTU}$	$\frac{Hr\text{-}^{o}F}{BTU}$	$\frac{Hr\text{-}^{o}F}{BTU}$	$\frac{Hr\text{-}^{o}F}{BTU}$
Conical Thinwall	T-13622	Titanium	5.3	6.2	6.6	5.7
	T-13621	Rene' 41	3.7	4.3	5.2	4.6
Straight Thinwall	T-13611	Titanium	1.8	2.2	2.1	2.0
	[illegible]612	Rene' 41	1.2	1.5	1.3	1.2
Composite	T-13618	Titanium	4.7	5.3	3.0	2.8
	T-13619	Rene' 41	3.8	4.3	2.8	2.6
Zirconia Cylinder	T-13617	Zirconia	8.1	8.3	3.5	3.2

* Overall thermal resistance of head/seal chamber

Figure 21

Firing Tests

The candidate seals were fired in two engines which were modified to accept a composite seal and conical titanium seal. The predicted results were very close to the actual.

The firing tests did demonstrate a potential problem which should be considered for any engine design using a high resistance seal and film cooling. The highest resistance seal $\sim 7 \frac{Hr-^{o}F}{Btu}$ was pulsed at a rate of 50 ms on and 50 ms off to build up pulsing operation time on the engine.

After 980 cycles the run was stopped because the molybdenum flange temperature had reached 1100°F. This is above the steady state operation temperature of 300-400°F and way above the maximum soakback temperature of 650-700°F. This condition did not occur with the lower thermal resistance composite seal, nor has it occurred with the very low thermal resistance L-605 standard Apollo seal.

The apparent cause was the flange temperature increase in temperature during the soakback because heat was unable to dissipate into the head due to the higher seal thermal resistance. As the flange increased in temperature it became impossible for nucleate boiling to occur at the flange and the cooling effect of the fuel cooling flow was considerably reduced.

It has not been demonstrated that this phenomena is in any way detrimental to the operation of the engine but it would result in vastly different performance and thermal behavior if operated in this manner. A very significant input is the large number of cycles which were required for the condition to manifest itself. This type of duty cycle is highly unlikely for any anticipated mission.

D. Lunar Orbiter (Reference 10)

The Lunar Orbiter engine was a modified Apollo engine which provided the Δvelocity for the photographic lunar satellite. The modifications were the addition of a heater, qualification of the engine to a higher vibration spectrum, and extended burn time of up to 700 seconds.

The heater selected was a modification of a Minco button heater. It was incorporated into an assembly which protected the leads and provided a heat path into the injector. The assembly was screwed into an existing 10/32 screw hole in the head.

Design criteria which was used for sizing of the heater was obtained from thermal tests made on the PTC verification testing. Figure 11 shows the engine heat loss vs. chamber throat temperature for two conditions of firing. The worst case was obtained using a chamber operated over 3,000 seconds at 2700+°F and was used to size the heater. The Lunar Orbiter engine was oriented away from the sun at all times and a thermostat was not used. The heater was turned on at launch and operated continuously throughout the mission.

The engine performed very well on its mission in space. The engine temperature was maintained at ~75°F throughout most of the missions and no problems were encountered.

REFERENCES

1. Stechman, R. C., "Thermal Analyzer Computer Program," MIR #213, The Marquardt Corporation, Van Nuys, Calif., March 1968.

2. Bartz, D. R., "A Simple Equation for the Rapid Estimation of Rocket Nozzle Convective Heat Transfer Coefficients," Jet Propulsion 27, pp 49-51, 1957.

3. Dittus, F. W. and Boelter, L.M.K., Univ. of Calif., Pulse Engineering 2, 443 (1930).

4. Industrial and Engineering Chemistry, Vol. 38, p. 1429, December 1936.

5. Kappl, J. J., "Applied Research Report on High Heat Transfer Burning - TMC Report S-421, 7 June 1964.

6. Stechman, R. C. , "THermal Analysis of the R-4D Rocket Engine Using a Columbium Alloy (C-103) Combustion Chamber," TMC Report S-609, 10 July 1967.

7. Belsley, A., Stechman, R. C., "Preliminary Design Report Phase I, Apollo S/M RCS Engine Modification for Moog Valve," TMC Report A1062, 23 September 1966.

8. Hardgrove, J. A., "Thermal Management Final Report," TMC Report S-444, 12 September 1964.

9. Puntar, J., "Apollo Service Module Reaction Control System Engine Injector/Chamber Seal Program," Marquardt Report PR 3008-F, June 1966.

10. Paladin, J. C., Hill, C. S., Pfeifer, G. R., "Final Report on Supplemental Qualification Program for the Lunar Orbiter Velocity Control Engine," Vol. I, Report 6100, 17 January 1966.

CHAPTER 3

SPACE IGNITION CHARACTERISTICS

BY

W. JURAN

TABLE OF CONTENTS

SECTION NO.		PAGE NO.
I.	INTRODUCTION	3-1
II.	SPACE IGNITION ASPECTS OF THE DEVELOPMENT PROGRAM	3-1
III.	IGNITION INSTRUMENTATION	3-9
	A. Dynamic Pressure Measurements	3-10
	B. Dynamic Strain Measurement	3-14
	C. High Speed Movies	3-14
	D. Other Measurements	3-17
IV.	IGNITION TESTING TECHNIQUES	3-17
V.	TYPES OF IGNITION OVERPRESSURE	3-24
	A. Heterogeneous Detonations	3-24
	B. Condensed Phase Explosions	3-32
VI.	INJECTOR MANIFOLD EXPLOSIONS	3-41
VII.	CONCLUSIONS	3-45
	BIBLIOGRAPHY	3-47

LIST OF FIGURES

FIGURE NO.		PAGE NO.
1	Thrust and Chamber Pressure vs. Time	3-3
2	Typical Pressure History at A Point on the Wall	3-11
3	Quartz Pressure Transducer	3-12
4	Peak Meter	3-13
5	Ignition Transient Instrumentation	3-15
6	Strain Gaged Engine in Test Cell	3-16
7	Engine with Transparent Combustor	3-18
8	Space Simulation Facility	3-20
9	Pulser Model 14	3-21
10	Facility Control Room Instrumentation	3-22
11	Facility Control Room Instrumentation	3-23
12	LM Proof Test Computer Program Output	3-25
13	LM Ingition Proof Test Program	3-26
14	Ignition Data Flow	3-27
15	Wave Propogation after Ignition	3-28
16	Valve Opening Mismatch vs. Chamber Pressure	3-30
17	Ignition Limits	3-31
18	Pulse Operation Model Computer Printout	3-34
19	Typical Chamber Pressure Trace	3-36
20	Injector Emptying Times	3-36
21	Liquid Remaining on Wall after Shutdown	3-37
22	Potential Ingition Pressure vs. Pulse Number	3-39
23-26	LM Ignition Proof Test Data	3-40
27	Propellant System	3-43
28	Comparison of Manifold Pressure Traces	3-44
29	Zot Plot	3-46

I. INTRODUCTION

One of the more interesting parts of the program to develop attitude control engines for the Apollo Service Module and Lunar Module was the identification and solution of problems associated with altitude ignition. During some of the ignition tests conducted early in the development program, the engine combustion chambers were failed by what appeared to be large ignition overpressures. As a result of these early failures, changes were made to the design of the engine to provide more satisfactory ignition characteristics. Extensive tests were conducted to document the conditions under which ignition overpressures occurred and, finally, to demonstrate satisfactory ignition characteristics over the range of operating conditions expected during the Apollo missions.

The effort associated with eliminating the ignition problems extended from early 1963 through 1967. As a result of this effort two different types of ignition overpressures were identified. One type of ignition overpressure proved to be associated with the detonation of materials introduced into the combustion chamber during the preignition period. A second type of ignition overpressure was found to be associated with the accumulation and explosion of energy rich materials from previous firings of the rocket engine.

The engine design was modified to include a preignition chamber designed to reduce the frequency and severity of the first type of ignition overpressure. Destructive overpressures of the second kind were eliminated by increasing the power used to heat the engine so that it operated at temperatures where accumulations of energy rich materials were limited. The fuel for the Service Module Reaction Control Engine was changed from Aerozine-50 to the more volatile fuel MMH and the Lunar Module reaction control engine temperature controls were set at a higher temperature to meet the requirements of the Aerozine-50 fuel. As a result of these changes and the knowledge generated during study of the altitude ignition process, confidence was generated that the reaction control engines will perform their intended mission reliably. This report describes the process through which damaging ignition overpressures, once apparently random and poorly understood, were eliminated over the operating range of the Apollo Reaction Control Engines.

II. SPACE IGNITION ASPECTS OF THE DEVELOPMENT PROGRAM

The multiple doublet injector designs evaluated in early 1963 provided performance approaching the design goal of 300 seconds. However, engines using these injectors were subject to excessive heating of the injector and valves during prolonged firings. To reduce the injector and valve temperatures produced during steady state firing and soakback, a fuel cooling annulus was added to a prototype injector head so that the flowing fuel would cool the injector.

After some initial testing to evaluate its thermal characteristics, the engine was installed in the newly completed Cell 6 altitude test facility to document pulse performance. Three, five second steady state firings were successfully completed. On the start of the fourth steady state firing, the molybdenum combustion chamber broke into a number of pieces. The engine was removed from the test cell and examined, the only anomalous observation being that the oxidizer valve was leaking excessively. No connection could be established between this leakage and the failure.

The valve was reworked to an acceptable condition and reinstalled. The engine was rebuilt to the same configuration with a new molybdenum combustion chamber and installed in Cell 6 to duplicate, if possible, the conditions leading to the failure. Twenty, three second steady state firings were conducted successfully. Ten pulses of 10 milliseconds on and 200 milliseconds off were then programmed. During the third pulse of this program the combustion chamber broke again. A post run examination of the injector head and solenoid valves showed that the injector and valves were in good condition.

An investigation was initiated to determine the causes of the explosions. One of the first theories to be explored was that the large fuel dribble volume associated with the fuel cooling loop might empty substantial quantities of fuel into the combustion chamber and into the facility after firing. It was felt that the fuel would vaporize at the low test cell pressures being used and it was known that hydrazine in the vapor state can act as a monopropellant. It was theorized that when the engine was fired, hot combustion products might ignite hydrazine vapors resulting in a detonation in the combustion chamber or test cell. To investigate this possibility, the engine was again rebuilt to the same fuel cooled head configuration except that a stainless steel combustion chamber with a flush mounted chamber pressure transducer was substituted for the molybdenum combustion chamber. Seventy six steady state and pulse firings were made with this engine. The frequency response of the chamber pressure transducer did not allow the accurate determination of the peak value of the ignition pressure transient. However, the data definitely showed significant ignition overpressures at start up. Figure 1 shows a sample of thrust and chamber pressure traces for one of the pulses. Although the pressure appears to peak at about 300 psia, subsequent investigations showed that the actual pressures were significantly higher.

Because of the high ignition overpressures observed, it was decided to stop all development work on the fuel cooled injector and to begin investigation of a twelve on twelve doublet injector that had previously shown some promise for reducing maximum injector temperatures. A number of tests were conducted with variations of this design during July and August of 1963.

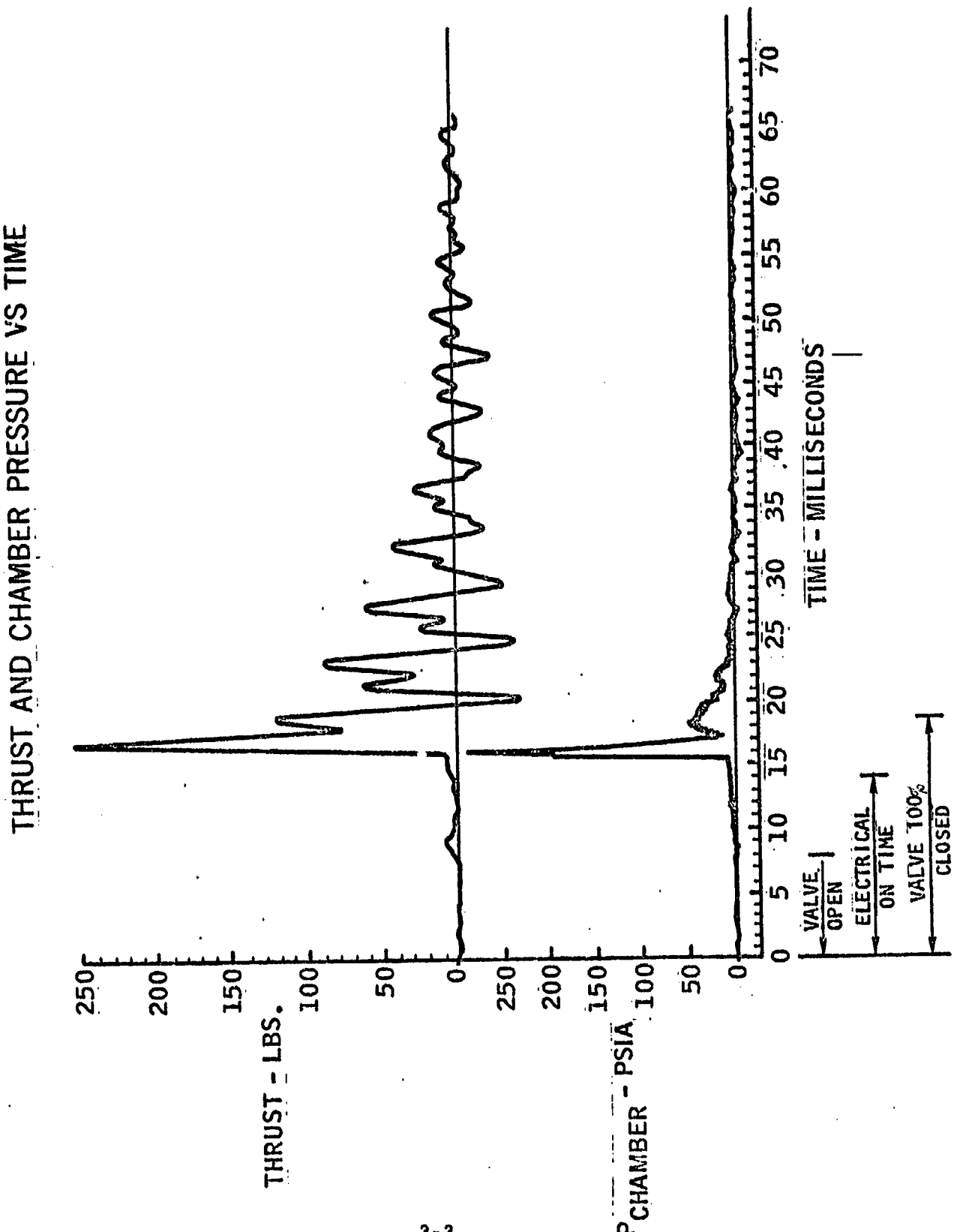
THRUST AND CHAMBER PRESSURE VS TIME
THRUST - LBS.
250
200
150
100
50
0
$P_{CHAMBER}$ - PSIA
250
200
150
100
50
0
0
5
10
15
20
25
30
35
40
45
50
55
60
65
70
TIME - MILLISECONDS
VALVE OPEN
ELECTRICAL ON TIME
VALVE 100% CLOSED

Figure 1

During one of these tests in the ATL facility, three firings of 11, 10 and 5 seconds duration were made. The combustion chamber failed at the start of a planned 5 second run and subsequent examination of the engine showed that about two-thirds of the combustion chamber was missing.

A series of tests was begun in an attempt to determine the conditions causing the molybdenum chambers to shatter. The tests used a segmented combustion chamber with removable molybdenum and plastic combustion chamber sleeves. The transparent plastic chamber sleeves were used with high speed motion pictures to view ignition and combustion phenomena and high response pressure transducers were used to measure ignition pressures.

During the tests, the injector volumes, propellant valve timing and propellant temperatures were varied. An injector design with a 13th doublet located at the geometric center of the injector face was also tested. (This 13th doublet was introduced in an effort to reduce the time between opening the solenoid valves on the engines and subsequent ignition.) A number of plastic and molybdenum chamber sleeves were purposely shattered during these studies of the conditions that contributed to ignition overpressures. (Concurrent dynamic burst tests of the molybdenum sea level chambers being used with the twelve doublet injector showed that two out of three chambers failed between 1500 and 2000 psi. A third chamber successfully withstood a 2000 psi dynamic burst test and then failed at 2700 psi during a static burst test. The large pressures required to burst the chambers supported the observation that large ignition overpressures were occurring during the engine tests.)

By October of 1963, the available test data suggested that two conditions seemed to contribute the most towards causing large ignition overpressures. These conditions were: 1. An oxidizer lead into the combustion chamber caused by timing of the electrical signals to the propellant valves and by differences between the oxidizer and fuel injector dribble volumes and 2. Propellant temperatures being either ambient or colder. (This effect was later shown to be mostly a function of injector and combustion chamber temperatures rather than propellant temperatures.)

During October of 1963 the ability to accurately measure peak ignition pressures was significantly improved by supplementing the previously used Photocon pressure transducers (with a frequency response of 10 KHz) with newly obtained Kistler pressure transducers whose natural frequency was about 140 KHz. (The Kistler transducer had previously been evaluated by Princeton University under a NASA contract for improving rocket thrust chamber pressure measurements.) Data from the Kistler transducers showed significantly higher peak pressures than data taken simultaneously with the Photocon transducer. A water cooled Kistler unit showed approximately double the peak pressure shown by the Photocon transducer and a flush mounted Kistler transducer showed pressures as much as four times higher.

An investigation of the pressure measurement system characteristics was begun to explain the differences in indicated pressure. This investigation subsequently resulted in improved techniques for measuring ignition severity that were very helpful later in the program.

Analysis of high speed movies made using the transparent combustion chamber sleeves suggested that large ignition overpressures were caused by the explosion of propellants accumulated in the combustion chamber during the ignition delay period. It was therefore felt that the best way to reduce the magnitude of ignition overpressures was to reduce the accumulation of propellant by shortening the ignition delay time. Several methods for initiating early combustion were investigated including a "preigniter" for piloting early combustion near the injector face. The preigniter was a small combustion chamber attached to the injector face and exhausting into the main combustion chamber. It was felt that a properly designed injector hydraulic circuit could supply the preigniter with fuel and oxidizer directly from the propellant valve outlets, allowing ignition without the long delay times required to fill the passages in the rest of the injector. The burning preigniter would then pressurize the main combustion chamber with hot exhaust products so the mixture in the main combustion chamber would ignite at the earliest possible time. In December of 1963, design of engine hardware incorporating a preigniter chamber was begun.

While the preigniter engine was being designed, testing was continued to determine the ignition characteristics of various engine designs. Tests were made using strain gages to determine the dynamic response of the combustion chamber to ignition pressure transients. Tests were also made using five Kistler pressure transducers at different locations in the combustion chamber wall to determine the temporal and spatial characteristics of the ignition pressure transient. The results of these tests showed that the peak ignition pressure was sensitive to the injector configuration being tested and to the relative timing between the opening of the oxidizer and fuel valves. (The largest ignition overpressures occurred when the oxidizer valve was opened a few milliseconds before the fuel valve.)

Tests using the strain gaged molybdenum sleeves showed that the peak strain was relatively insensitive to the chamber wall thickness. This meant that adequate design margin could not be provided simply by thickening the chamber wall. The test results did suggest that the dynamic bending stresses could be reduced to the same magnitude as the dynamic hoop stresses by providing circumferential "ribs" on the combustion chamber wall. Two ribs were eventually incorporated in the production engine combustor.

During June of 1964 the first preigniter engine was tested. It had an extra set of propellant valves so that the flow to the preigniter could be controlled independently from the main combustion chamber flow. The tests were aimed at demonstrating the ability of the preigniter to reduce ignition overpressures and at providing design criteria for a flight-type preigniter engine using a single set of valves. A flight-type engine design was fabricated and tested starting the week of 22 June 1964. It used a throatless preigniter with the exit cut at 45°. Preigniter cooling was provided by fuel film cooling holes aimed at the base of the preigniter. Tests of this configuration and of a number of other preigniter engine configurations were conducted through the end of 1964. This testing resulted in selection of the preigniter engine design later to be used for qualification testing.

Testing done in 1965 included a three engine Preliminary Flight Rating Test to qualify the preigniter engine design for use on the first Apollo flights. The test results showed that the preigniter had significantly reduced ignition delay times and overpressures. The test results also showed some evidence of ignition overpressures during pulse trains with short (0.3 to 5 second) intervals between pulses. The overpressures did not occur on the first pulse of a train and their full significance was not immediately grasped. (It was later determined that this type of ignition overpressure was caused by collection and subsequent explosion of residual materials from previous firings and could be prevented by heating the engine above a critical temperature that depends on the propellant used and the duty cycle being fired.)

The test results also showed sharp transient rises in the output of the transducers used to measure the pressure of the propellants supplied to the engine. The pressure rises occurred immediately after the propellant valves were opened and were later shown to be caused by explosion of minute quantities of fuel that entered the oxidizer passages of the engine between firings. A similar type of process was observed on the fuel side of the engine. These "injector manifold explosions" were later studied extensively and were shown to occur only when the test cell pressure was above a critical value that depends on the engine temperature.

The ignition characteristics of the three Pre Flight Rating Test engines were felt to be adequate for meeting program requirements and in August of 1965, Marquardt and North American (the prime contractor for the Apollo Service Module) agreed to proceed with a five engine qualification test program. The qualification tests were to be run with gas-free propellants because previous testing had shown that the presence of dissolved or entrained pressurant gas caused erratic ignition behavior.

(Ignition tests of engines with helium saturated propellants had shown ignition pressures as high as 1550 psia with normal fuel leads. It was felt that the overpressures were caused by gas bubbles in the propellant. Data taken under comparable conditions with gas-free propellant showed no overpressures.)

Since the Apollo mission required that the engine operate with propellants saturated with helium pressurant, it was agreed that Marquardt would also conduct some tests to develop techniques for measuring the amount of gas dissolved in propellants and its effect on ignition characteristics.

The first of five engines began qualification testing on August 16, 1965. On 17 September 1965 qualification engine D experienced a chamber failure during a cold mission simulation firing sequence. Marquardt stopped all qualification tests and production test firings and established a Failure Malfunction Committee. Formal investigation of the failure began immediately. The general sequence of events regarding the failure was established as follows:

> "Excess fuel was deposited in the oxidizer passages of the injector during the cold mission duty cycle. This fuel then reacted with oxidizer when the valve was opened causing an explosion which damaged the oxidizer valve seat. The damaged valve seat created a large oxidizer leak after pulse 6 which permitted an abnormally oxidizer rich mixture in the combustion chamber. Continued pulsing caused an ignition overpressure that failed the chamber on or about the twentieth pulse. The run was terminated after 25 pulses, the cell opened and it was then observed that the combustion chamber had failed."

This failure during qualification testing showed that injector manifold explosions had to be prevented if the engine was to meet its requirements. Five analytical solutions and recovering plans were put forth.

1. The injector explosion was a facility induced phenomenon which would not occur in the space environment.

2. Design an explosion proof valve that would contain injector head explosions.

3. Design an injector baffle to absorb or reflect injector head explosions.

4. Devise local heating or thermal control for the injector standoff to raise local temperatures above the condensation temperature of the fuel vapors.

5. Consider an alternate fuel such as UDMH or MMH of different phase characteristics such that injector head explosions could not occur.

All five plans were aggressively placed in work with a progress report and milestone evaluation presentation of 18 October 1965 to NAA/S&ID and a follow up presentation to NASA, Houston on 21 October 1965 which resulted in a mutual agreement that the failure was a facility induced phenomenon and would not occur in the space environment. Marquardt's Cell No. 9 with its lower pressure capability had proven entirely satisfactory as a ground facility and its use was planned for any further cold mission simulation tests. It was further agreed that qualification testing would be resumed and that Marquardt would continue to produce and ship production engines on the approved schedule. The formal failure malfunction report was published on 5 November 1965. During December of 1965, replacement engine B successfully completed the cold mission simulation test that had resulted in the failure of engine B.

Testing and analysis conducted during 1966 resulted in considerable progress toward understanding both injector manifold explosions and the ignition overpressures observed when engines were restarted after previous firings. A comprehensive program of analysis and engine tests established that injector manifold explosions could not occur if the test cell pressure was low enough to allow free evaporation of residual propellants from the engine. It followed that injector manifold explosions would not occur in space and this was supported by successful engine test programs conducted at lower cell pressures than those used before 1966.

Ignition test data had begun to suggest that the temperature of the engine hardware was important in determining ignition pressure magnitude during multiple pulse firings. Testing during the helium effects program suggested that there was a safe operating region because the combustion chamber flange temperature at the time of an oxidizer lead pulse was observed to correlate with the magnitude of the resulting ignition overpressure. The overpressure magnitude decreased at higher flange temperatures. At the time, the cause of ignition overpressures was thought to be explosion of frozen residual fuel within the engine.

The identification of engine temperature as an important determinant of ignition pressure magnitude resulted in extensive engine test programs being conducted at Marquardt and at the NASA Manned Spacecraft Center to establish the temperature limits for space operation. The Marquardt Pad G facility had been modified to permit engine firing at very low ($\leq 50\ \mu$) pressures, in any attitude with respect to the gravitational field and with a thermal environment representative of space operation.

Ignition testing at Marquardt consisted of Low Temperature Mapping tests and Ignition Proof tests. During the Low Temperature Mapping tests, engines with instrumented aluminum and steel combustion chambers were used to establish the low temperature limits for satisfactory ignition. Verification of the temperature limits established was to be demonstrated by a series of proof tests with production molybdenum combustors.

Formal proof test firings began in August of 1966, firing up with Aerozine-50 fuel at a 50°F chamber exit nut temperature. Testing was stopped when the molybdenum chamber fractured on the 57th run of 88 runs scheduled for this first temperature condition. A second engine failed on the 63rd run of the same sequence. As a result of the two failures, testing with Aerozine-50 fuel was stopped and proof testing with MMH fuel was begun. The MMH tests showed that the engine could be safely operated at lower temperatures with MMH fuel than with Aerozine-50 fuel. The combustion chamber had to be cooled below a nut temperature of 30°F before the molybdenum combustor would fail in any attitude.

The good results obtained during the proof tests with MMH suggested that the Aerozine-50 fuel planned for the Apollo Service Module should be changed to MMH and an MMH Design Substantiation Test Program was conducted by Marquardt to demonstrate that no performance or structural problems would result from this change of fuels. A supplemental qualification program was then run using MMH fuel and then the fuel change for Apollo Service Module was made.

The prime contractor for the Lunar Module Reaction Control Engines, Grumman Aircraft Engineering Corp., did not feel that a switch to MMH was practical for their vehicle. This decision was based on their plans to supply the reaction control engines with residual Aerozine-50 fuel from the ascent engine tanks during parts of some missions. Additional proof testing was performed for Grumman to establish safe temperature limits with Aerozine-50 fuel. As a result of these tests, the Lunar Module heaters were provided with additional capacity to maintain the engine combustion chamber flanges above 120°F, a temperature proven satisfactory by the engine tests.

The combination of preignition chamber, fuel lead valves, and control of engine temperature resulted in elimination of damaging ignition overpressures over the range of operating conditions typical for the Apollo mission. Injector manifold explosions were eliminated by test cell modifications that provided a low pressure judged more representative of space operating conditions. The elimination of ignition overpressures and injector explosions as a source of conern was one of the major mileposts of the Apollo Reaction Control Engine program.

III. IGNITION INSTRUMENTATION

During the program to improve the ignition characteristics of the Apollo Reaction Control Engine, information was needed about the magnitude of ignition severity and about the nature of the processes occurring within the combustion chamber during pulsing operation of the engine. High response dynamic pressure, acceleration and strain measurement systems were developed to meet the need for quantitative data about ignition severity. High speed motion pictures provided the major source of information on the detailed processes that occur within the engine during pulsing operation.

A. DYNAMIC PRESSURE MEASUREMENTS

The earliest measurements of ignition pressure made during the program used Photocon transducers with a frequency response of approximately 10 KHz. Data obtained from the Photocon transducers showed excessive ringing at the transducer natural frequency and were therefore not suitable for determining the peak magnitude of the ignition pressure transient. An effort was made to obtain improved measurements by using a Kistler transducer of improved frequency response characteristics. At the time the only Kistler transducer that was available at Marquardt included a water cooling adapter which acted as an acoustic resonator with a natural frequency of about 10 KHz. In an effort to obtain some useful information about the ignition transient, the output of this pressure transducer was recorded on magnetic tape and processed through a dynamic compensator (Transductron). The compensator was adjusted to the inverse transfer function of a second order system at the natural frequency of the water cooling adapter cavity resonance and oscilloscope photographs were made of the transducer output after processing by the Transductron. These oscilloscope photographs provided the first information about the fine structure of the ignition pressure transient. They showed that the transient consisted of a number of sharp pressure peaks with extremely short rise and fall times. One of these early oscilloscope photographs is shown in Figure 2. The fine structure suggested multiple reflections of a denotation wave from the walls of the combustion chamber.

This hypothesis was later borne out by measurements made with flush mounted Kistler Type 601 pressure transducers similar to Figure 3. These transducers with their associated electronics provided pressure information with a bandwidth of about 140 KHz. The ability of the Kistler instrumentation system to respond rapidly to pressure transients resulted in its use as a primary measurement technique for the study of ignition transients.

Tektronix Type 502 oscilloscopes and Polaroid oscilloscope cameras were used to provide an output device with frequency response capabilities suitable for use with the high response Kistler instrumentation. This combination provided both a record of the peak ignition pressure and information on the variation of transient ignition pressure with time. During the later parts of the ignition study program when the emphasis shifted from applied research to documentation, the oscilloscopes were replaced by newly developed Kistler peak reading voltmeters which provided an indication of the peak pressure since the instrument was last reset. Figure 4 shows a photograph of the Kistler peak reading voltmeter. This instrument proved very useful in measuring the maximum ignition pressure both on single pulses and on trains of pulses.

TYPICAL PRESSURE HISTORY AT A POINT ON THE CHAMBER WALL

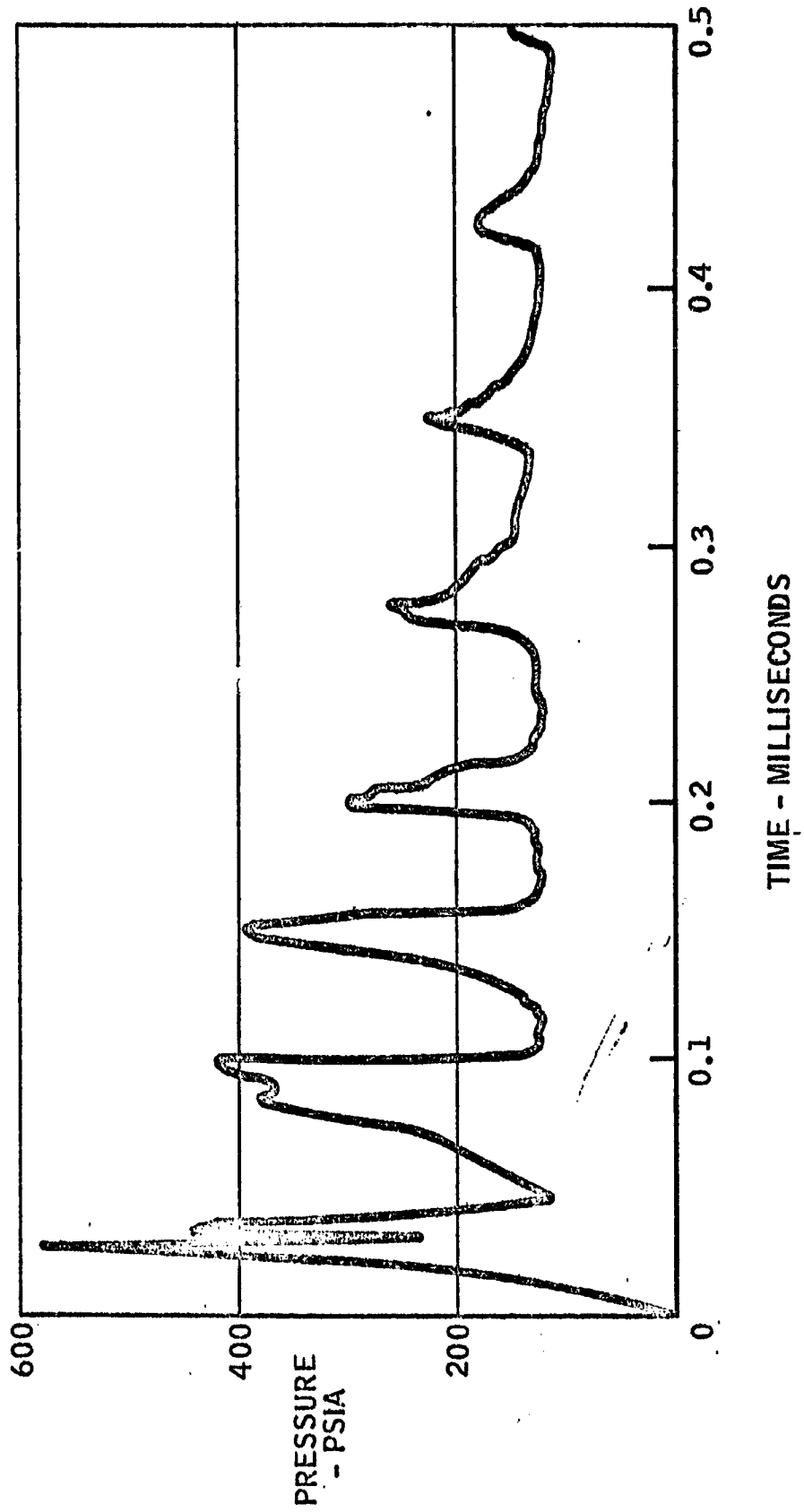

model 601H

quartz pressure transducer

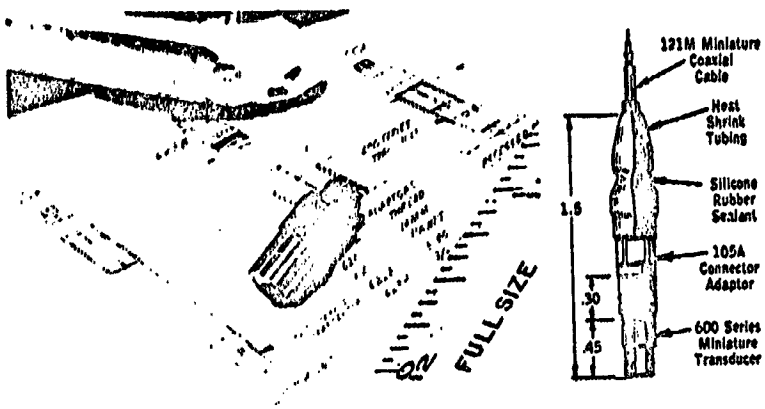

FAST RESPONSE TRANSDUCER MEASURES HIGH LEVEL DYNAMIC PRESSURES

Model 601H heavy diaphragm, fast response, miniature quartz transducer measures dynamic pressure up to 15,000 psi, with limited application to 20,000 psi, in blast, explosion, combustion, hydraulic and pneumatic applications. Mounting adaptors facilitate installation and protect transducer against extreme environments. Electrostatic systems, utilizing quartz transducers, charge amplifiers and low-noise cable, feature short-term static response and static calibration.

SPECIFICATIONS	MODEL 601H
Pressure range	1,000 to 15,000 psi
Resolution	0.5 psi
Maximum pressure	20,000 psi
Sensitivity (nominal)	1 picocoulomb/psi
Resonant frequency (mounted) (nominal)	130,000 cps
Rise time	3 microseconds
Linearity	1 percent
Capacitance (nominal)	5 picofarads
Insulation resistance (minimum)	10^{14} ohms
Acceleration sensitivity	0.01 psi/g
Temperature sensitivity	0.01 percent/°F
Temperature range	−450 to +500°F
Intermittent gas temperature on diaphragm	>3000°F
Shock and vibration	15,000 g's
Cable connector	Kistler 4mm*
Mounting thread with connector adaptor	7 x 0.75mm
Sensing element	crystalline quartz
Case material: body; diaphragm	430F SS; 316 SS
Size	0.25 x 0.6 inch
Weight (approximate)	0.08 oz., 2.25 gm.

*Converts to 2A-32 coaxial with 105A and 105L connector adaptors

KISTLER INSTRUMENT CORP : 0959 SHERIDAN DR : CLARENCE, N. Y. 14031

KISTLER
advanced dynamic instrumentation

Figure 3

REPRODUCIBILITY OF THE ORIGINAL PAGE IS POOR

model 538A

peak meter

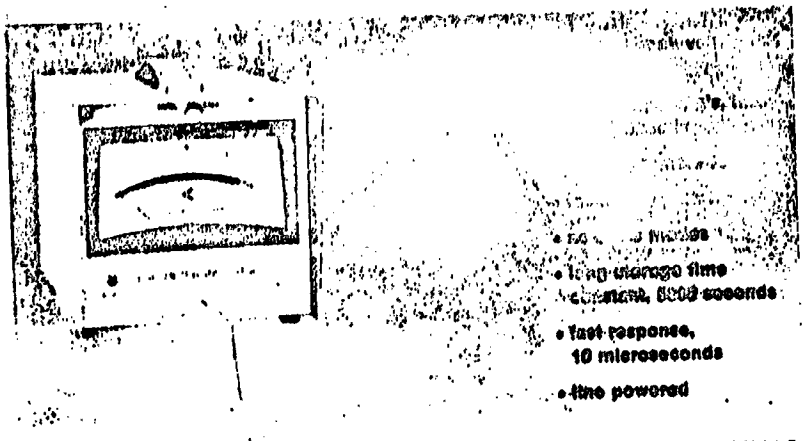

MEASURES AND DISPLAYS PEAK AMPLITUDE OF TRANSIENT SIGNALS

All-solid-state Model 538A Peak Meter detects maximum amplitude of a single pulse or highest pulse of a series, displays the maximum signal on a precision meter, and provides a DC auxiliary output signal corresponding to peak indication for digital display or other data acquisition. With quartz transducers and electrostatic charge amplifiers, it measures peak shock, force, impact, and pressure levels. It detects and indicates either slow or very fast rise time signals—even signals of very short duration.

SPECIFICATIONS	MODEL 538A
Full scale input	± 10 volts
Full scale output	+ 10 volts
Panel meter scales	0-1, 0-2, 0-5
Input impedance, DC mode	44 K ohms
Storage time constant	5000 seconds
Frequency response, DC mode	DC to 100 kHz
Linearity deviation, panel meter	1% F.S.
Linearity deviation, auxiliary output	0.5% F.S.
Auxiliary output current (max.)	4 ma
Auxiliary output load resistance (min.)	2500 ohms
Rise time, peak detection circuit	10 microseconds
Accuracy	±2% F.S.
Temperature environment, operating	+ 30 to + 130 F
Input power	115V, 60Hz, 5VA
Size, with case, inches	5¼ x 5¼ x 8¼
Weight	3.2 lbs

ISTLER advanced dynamic instrumentation

Figure 4

Ignition severity measurements were sometimes required on production engines that were not equipped with taps for chamber pressure measurement. In these cases, piezoelectric accelerometers were mounted on the outside of the engine injector and their output signals, processed by the same electronic system used for pressure measurements, were used to indicate ignition severity. Figure 5 shows a diagram of the signal conditioning circuitry used with piezoelectric transducers to measure ignition severity. The Kistler peak reading voltmeter proved most valuable for gathering large amounts of data on ignition severity. Its output, showing the highest peak value of acceleration or pressure for a selected set of firings, could be read directly from its meter face or could be recorded on a chart recorder or oscilloscope for later data reduction.

B. DYNAMIC STRAIN MEASUREMENT

During the engine development program, information was needed on the stress distribution in the combustion chamber and expansion bell. This information was to serve as a guide for design efforts to improve the resistance of the chamber and bell to loads caused by transient ignition overpressures. The measurement method adopted used a simple single active arm bridge circuit, an oscilloscope and a camera. Tests were conducted with as many as 48 strain gages cemented to selected locations on the engine combustion chamber and expansion bell. Figure 6 shows an instrumented combustion chamber installed in the test cell. Calibration was accomplished with a 60 Hz chopper which intermittently keyed a calibration resistor across the measuring strain gage to produce on the face of the oscilloscope a square wave representing a known gage resistance change.

Strain recordings were made by arming the sweep circuits of the oscilloscopes, opening the camera shutters, firing the engine and then closing the oscilloscope camera shutters. A common trigger signal was used to initiate the sweep on all the oscilloscopes simultaneously.

C. HIGH SPEED MOVIES

Color motion pictures made at speeds from 2,000 to 16,000 frames per second were used to study ignition and related processes in engines equipped with transparent plastic combustion chambers. The high speed movies were first used to compare ignition transients with and without ignition overpressures. When an ignition overpressure occurred, the mixture in the combustion chamber would transform from a nonluminous dark brown preignition appearance to an intense blue-white luminous mixture.

IGNITION TRANSIENT INSTRUMENTATION

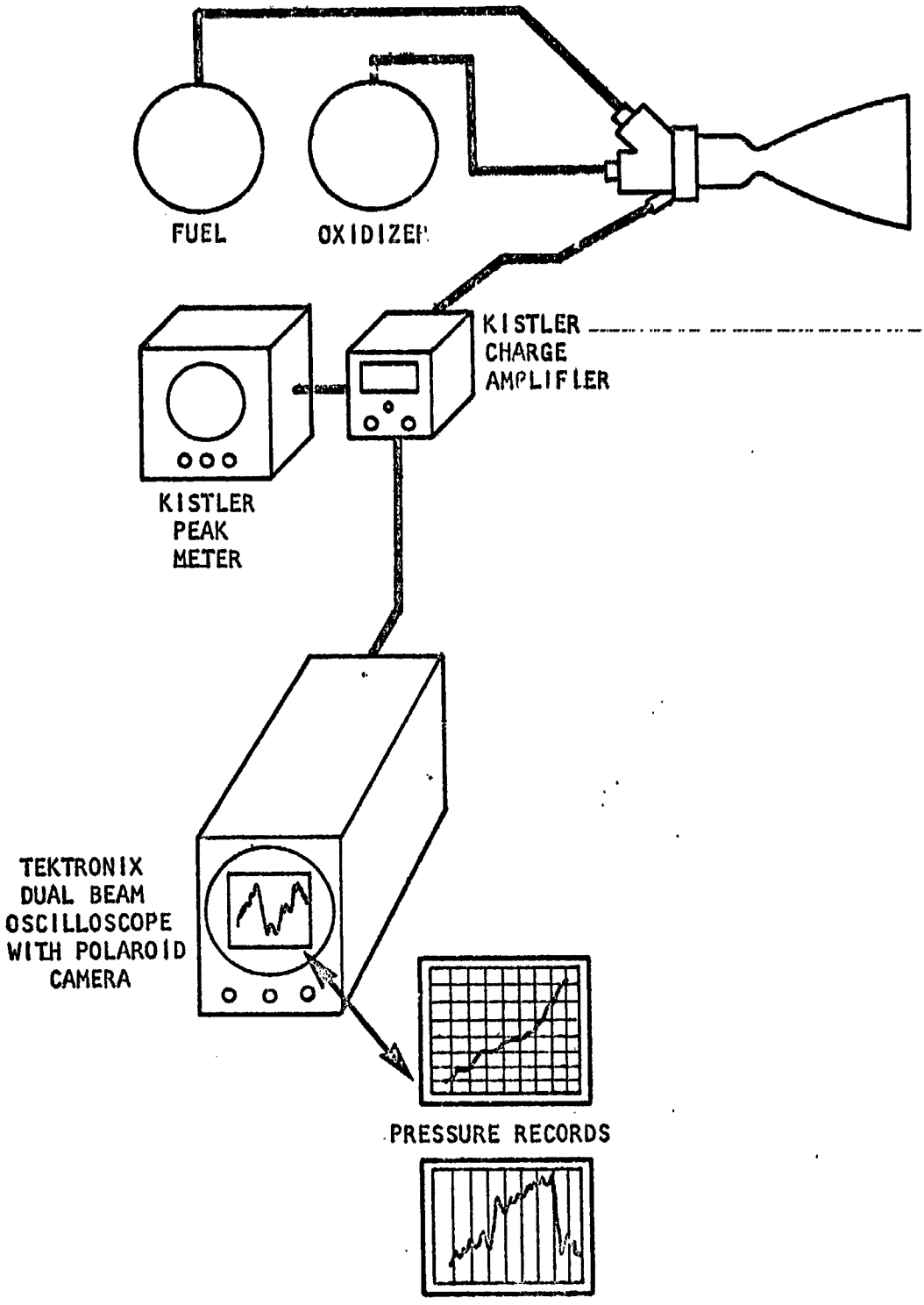

Figure 5

REPRODUCIBILITY OF THE ORIGINAL PAGE IS POOR.

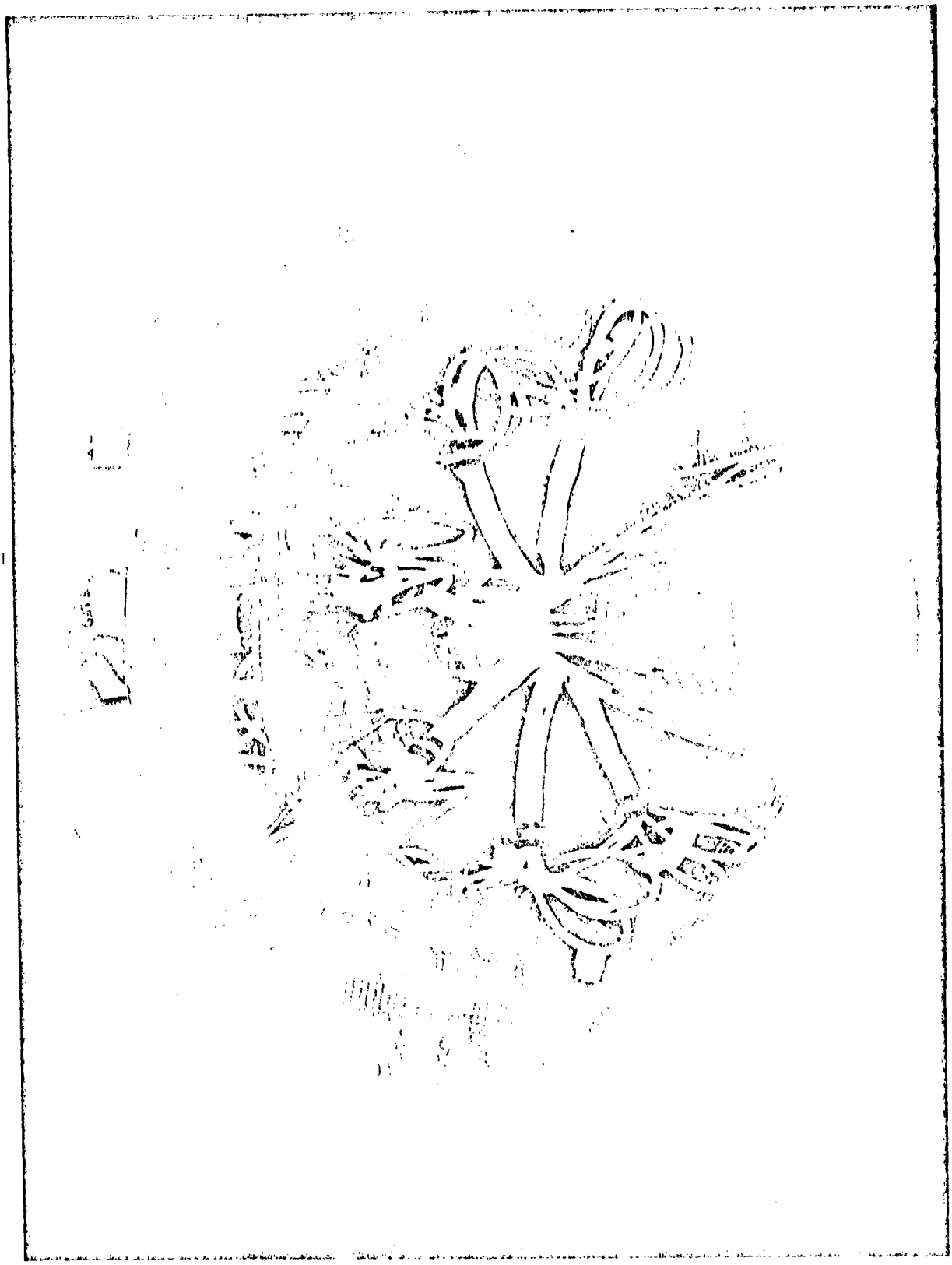

NEG. T3201-23

Strain Gaged Engine in Test Cell

Figure 6

The transformation occurred during the short interval between frames. This was the first concrete evidence that a detonation wave had propagated through the material in the chamber. The presence of detonation waves during ignition overpressures was also detected by high response pressure measurements. High speed movies were used later in the program to study the timing of the events in the combustion chamber during pulsing operation and to study injector emptying as a function of attitude and temperature. Figure 7 shows an engine with a transparent combustion chamber installed in the test cell for a movie run.

D. OTHER MEASUREMENTS

Information from the high speed movies was compared with data from both high and low range Kistler transducers. The high range transducer was used to measure pressures after ignition and the low range Kistler transducer was used to measure the pressure in the combustion chamber before ignition occurred. A combination of a low range transducer and a solenoid valve was used to study the chamber pressure after combustion ceased. The solenoid valve was held shut during the preignition and combustion periods to protect the transducer (which was more sensitive then the Kistler transducers) and then opened after the propellant valves were closed. This provided a measurement of the chamber pressure decay after firing ceased. This information was used, in conjunction with the movies, to help understand the processes that occurred after engine firing.

Later in the program, when extensive tests were being conducted to document the ignition characteristics of production engines without chamber pressure taps, a technique was developed for determining relative ignition severity by monitoring the output signal from the piezoelectric accelerometer mounted on the rocket injector. The signal from the accelerometer was processed through the same Kistler instrumentation used with the Kistler pressure transducers. Large bodies of accelerometer data were gathered over a range of engine firing conditions and the data were reduced using a statistical analysis of variance technique to determine which test parameters significantly affected ignition behavior. These tests showed that the combustion chamber temperature had a strong effect on ignition severity. This discovery provided the basis for use of hardware temperature control to alleviate the problems associated with accumulation of residues from previous pulses.

IV. IGNITION TESTING TECHNIQUES

The development of effective ignition testing procedures and facilities was one of the key elements in the effort to understand the factors affecting altitude ignition and in the documentation of the Apollo reaction control engine ignition characteristics.

REPRODUCIBILITY OF THE ORIGINAL PAGE IS POOR.

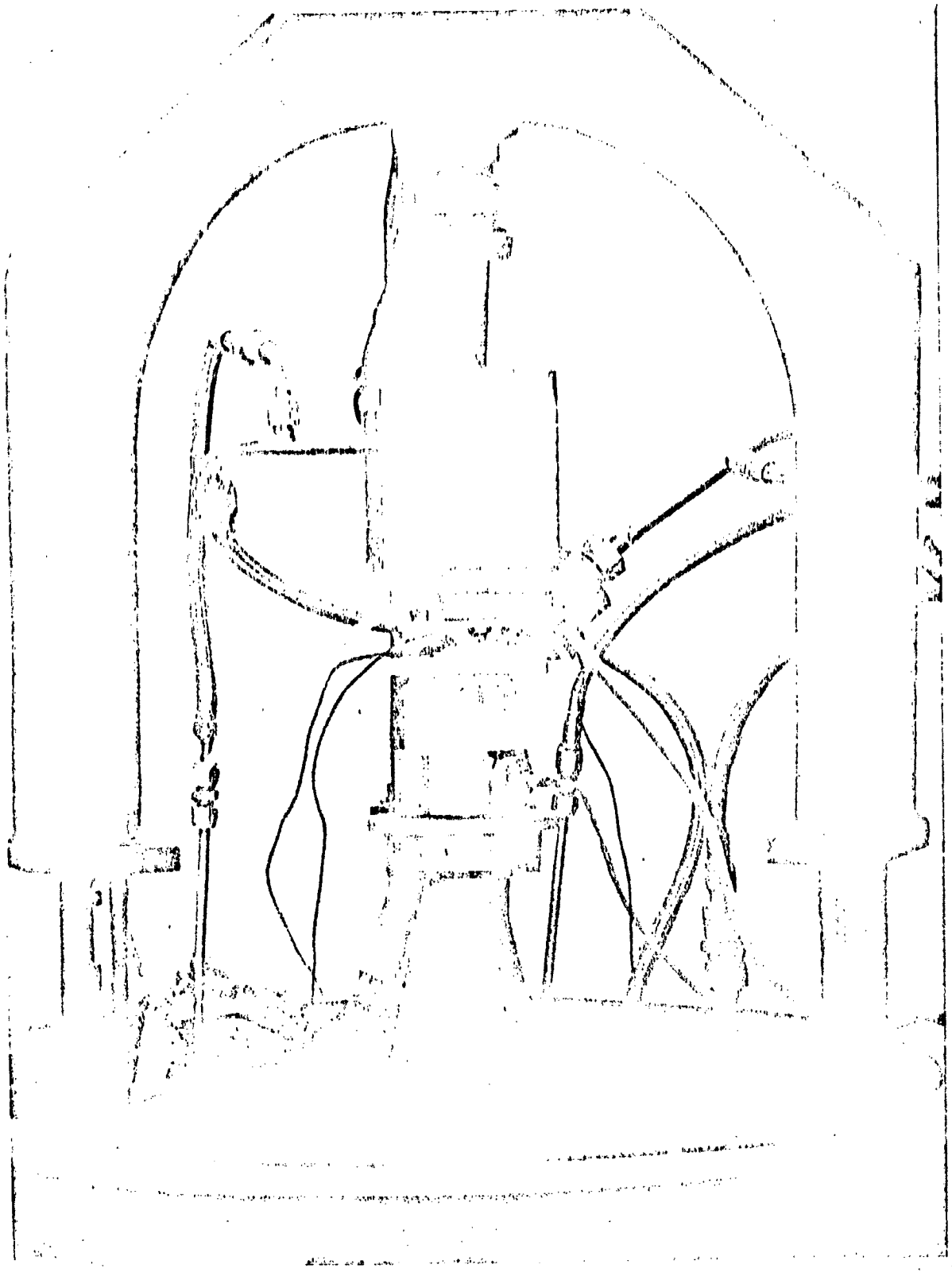

NEG. C6334-2

Engine with Transparent Combustor

Figure 7

Experience gained during the Apollo program showed that ignition pressure data included a large random component and that both the mean and variance of the data were significantly affected by a number of variables including engine orientation in the gravitational field, the duty cycle being fired, the temperature of the engine and propellants, the type of fuel being used, the number of pulses per run and the pressure within the test cell. During the program, techniques were developed for identifying the significant variables affecting ignition pressure, for controlling them during engine ignition tests and for data reduction and presentation in meaningful and useful forms. Control of the variables affecting ignition pressure was made possible by construction of a multi-attitude space simulation facility. This facility provided the capability for firing the rocket engine in any desired attitude with respect to the gravitational field. The facility pressure prior to ignition was held at less than 25 microns of mercury by the combination of a cold trap and a 9,000 cfm roots blower backed by a three stage steam injector. During ignition tests the engine was exposed to a simulated black space thermal environment in the form of a liquid nitrogen cooled shroud which surrounded but did not touch the combustion chamber and expansion bell. Engine temperature control was accomplished in a manner similar to that used on actual space vehicles by electrically heating the rocket engine's injector head while allowing the engine to radiate heat to its cold surroundings. Operation of the engine propellant valves was controlled by a Marquardt designed "pulser" with provisions for independent control of the firing pulse width, time between pulses, number of pulses and relative timing of the oxidizer and fuel valves. Figure 8 shows the multi-attitude space simulation facility and Figure 9 is a photograph showing the control panel of the pulser.

Special instrumentation required for ignition tests included high response piezoelectric transducers to measure chamber pressure (or injector acceleration when the engine had no tap) and the high response electronics for conditioning the resulting signals and for electronically identifying and recording the peak value measured during a run. Oscilloscopes and Polaroid oscilloscope cameras were used to study the fine structure of transients. The special ignition instrumentation and equipment required to control the facility were located in the facility control room shown in Figures 10 and 11.

During the course of the program these facilities were used to accumulate data on over 610,000 altitude ignitions of the final version of the Apollo reaction control engine so that a thorough statistical study of the engine ignition characteristics could be made over the range of conditions typical of the Lunar mission. The large amount of ignition data required to adequately define space ignition characteristics and the complex relation between the test data and the engine test conditions required the development of a technique for handling and interpreting large masses of data. The technique that was finally developed consisted of punching IBM cards with information on the test conditions and the peak ignition pressure or acceleration observed during each run.

REPRODUCIBILITY OF THE ORIGINAL PAGE IS POOR.

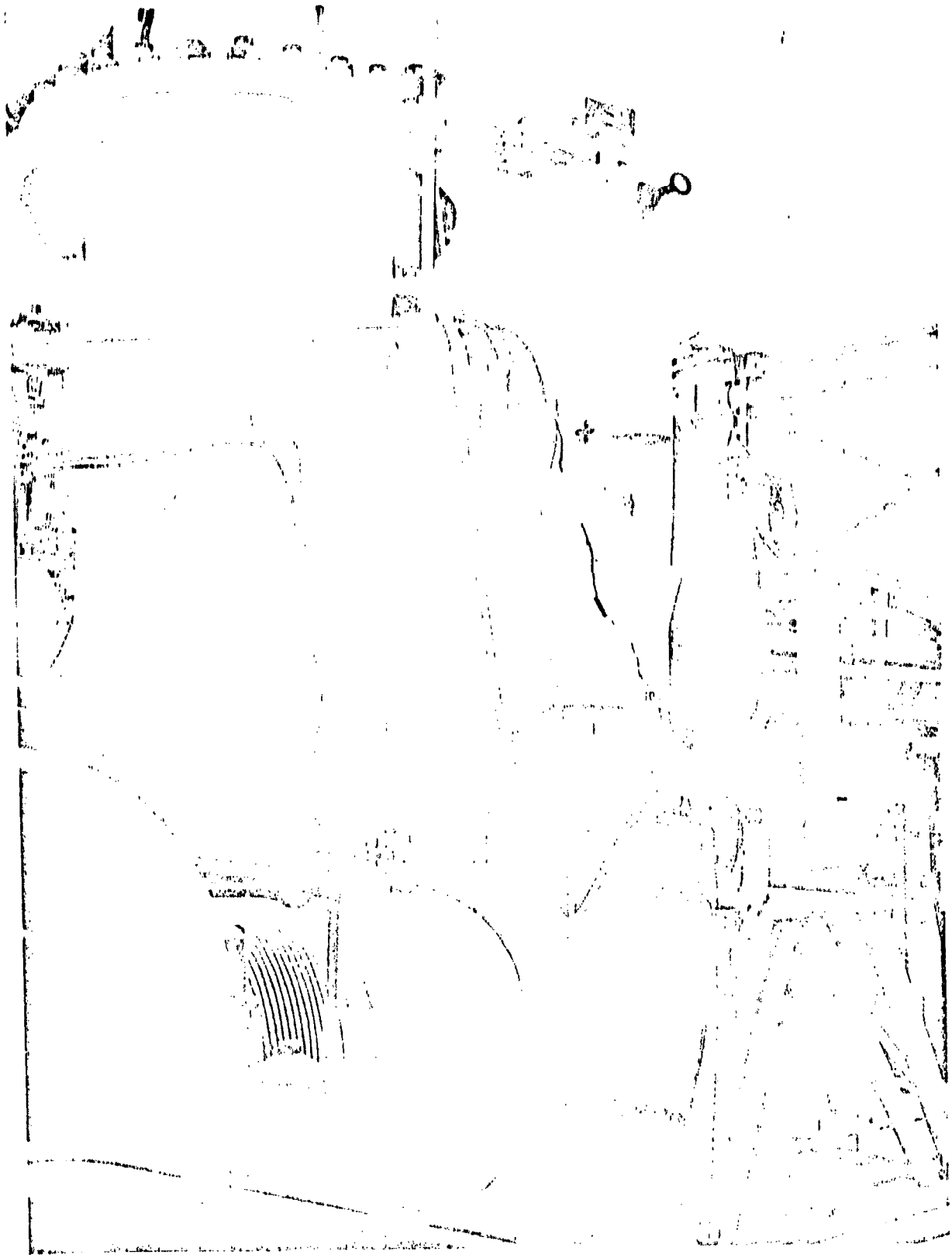

NEG. 8357-1

Space Simulation Facility

Figure 8

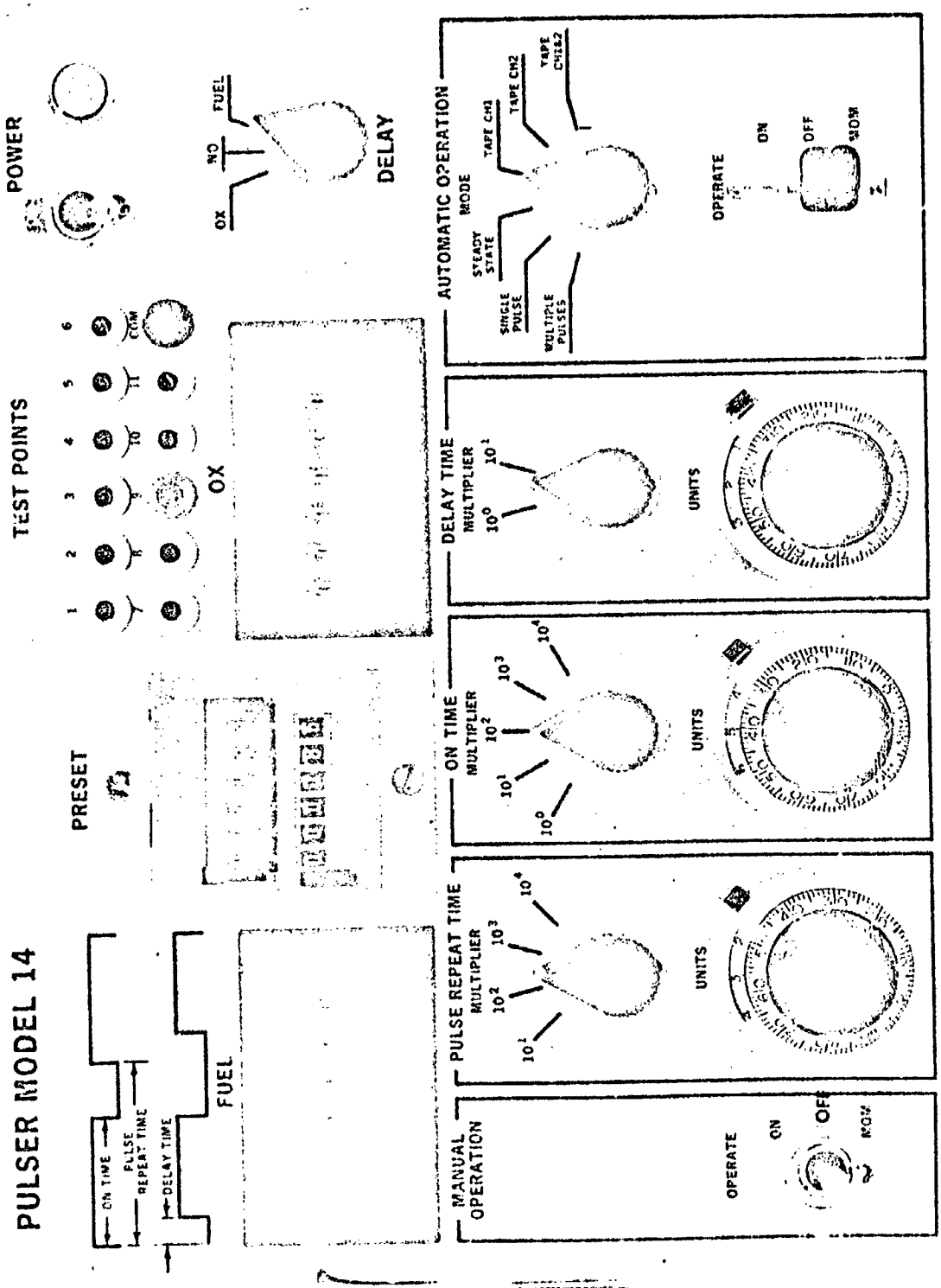

NEG. 6849-1

PULSER MODEL 14

Figure 9

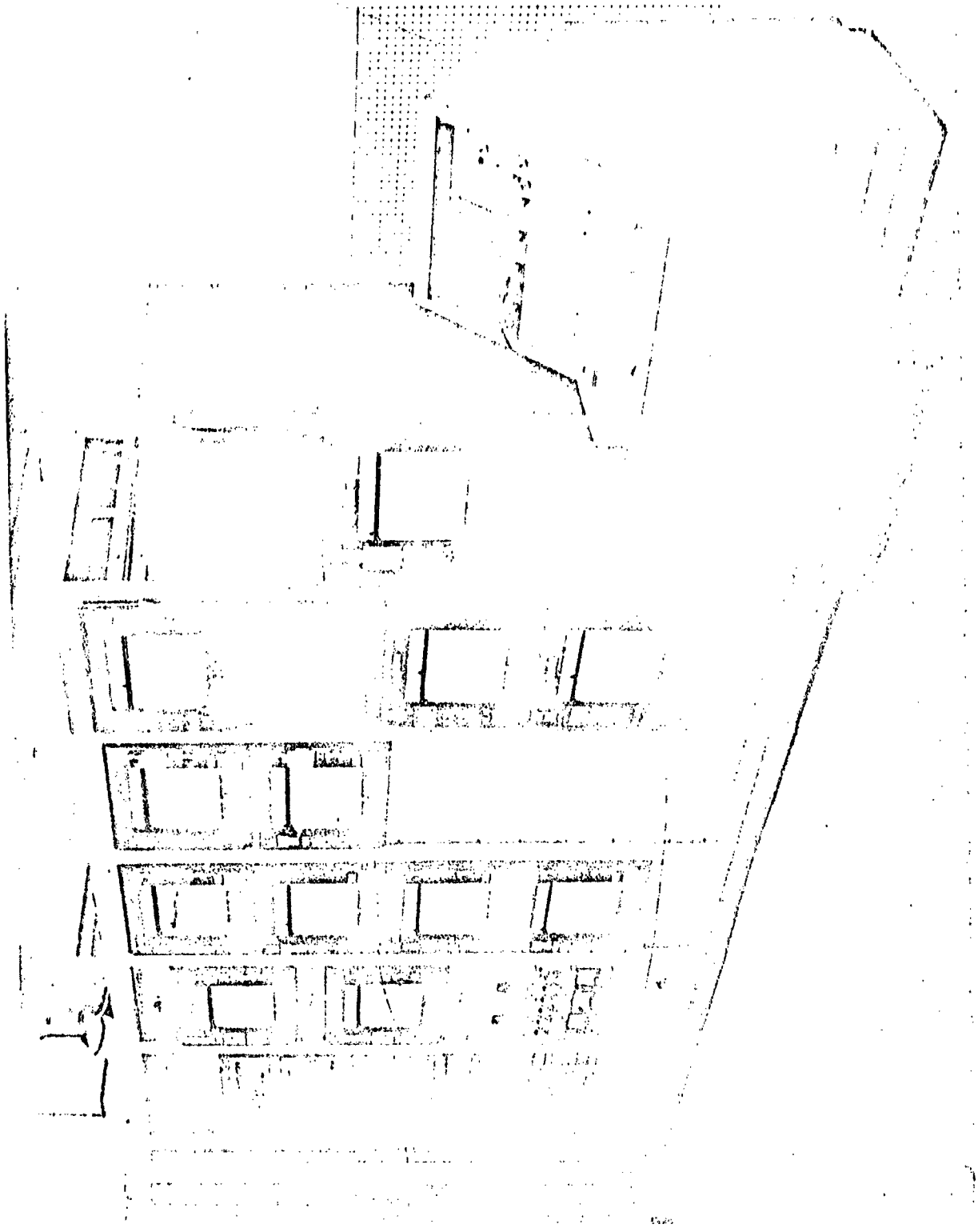

NEG. T3390-6

Facility Control Room Instrumentation

Figure 10

REPRODUCIBILITY OF THE ORIGINAL PAGE IS POOR.

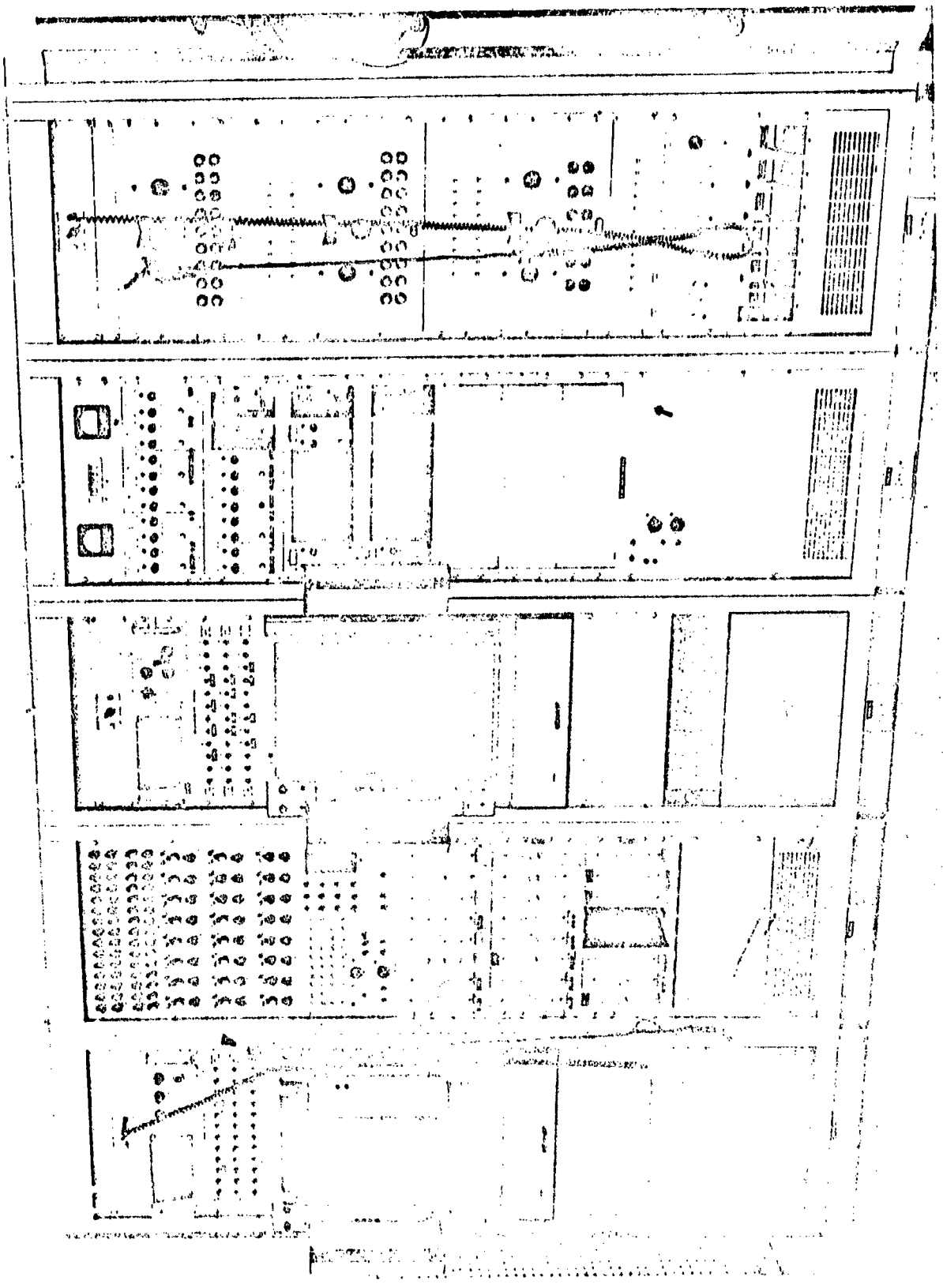

NEG. T3390-7

Facility Control Room Instrumentation

Figure 11

The ignition test data cards were used as input to an analysis of variance computer program which determined those variables and combinations of variables that significantly affected ignition severity during each test. (For example, if the temperature of the combustion chamber had a statistically significant influence on ignition severity and if the engine off times between firings did not, but certain combinations of off time and chamber temperature produced ignition severities significantly different from what would be predicted from the chamber temperature effect alone, the computer program would identify chamber temperature and the combination of chamber temperature and off time as significant variables).

A typical computer program printout of a sample of ignition test data is shown in Figure 12. It shows that during this test, chamber temperature, number of pulses and off time were the variables that significantly affected ignition severity. After firing the engine through a set of runs selected by statistical experiment design techniques and identification of the significant variables using the analysis of variance computer program, a computer plotting routine was used to prepare plots of the ignition pressure against the significant variables. Figure 13 is a typical plot of ignition data showing the effect of combustion chamber temperature on ignition severity. Figure 14 schematically shows the system used for handling the large amounts of ignition test data.

V. TYPES OF INGITION OVERPRESSURES

Two types of ignition overpressure were identified during the development of the Apollo Reaction Control Engines. The first type(later named "heterogeneous detonation")was a detonation wave that propagated through the material that collected in the combustion chamber during the preignition period. (Later in the program, a second type of ignition overpressure was identified, a detonation involving residual materials left on the combustion chamber internal surfaces from prior engine firings.) The preigniter was added to the engine to reduce heterogeneous detonation pressures by shortening the time between entry of propellants into the combustion pressure and their subsequent ignition.

A. Heterogeneous Detonations

Movies made to help explain early engine failures provided the first evidence that a detonation wave could form in the combustion chamber. These high speed movies showed a rapid transition from a slowly moving flame front to a rapidly travelling wave that swept through the material in the combustion chamber in less time than the fraction of a millisecond between movie frames. These rapidly moving waves during ignition overpressures were also detected by comparison of transient pressure measurements made simultaneously at a number of locations within the combustion chamber using five high response Kistler pressure transducers. A set of simultaneous pressure records is shown in Figure 15. The progress of the detonation wave past each of the transducer stations can be seen.

REPRODUCIBILITY OF THE ORIGINAL PAGE IS POOR.

LM PROOF TEST
COMPUTER PROGRAM OUTPUT

ANALYSIS OF VARIANCE.....A5U-H1

LEM PROOF TEST - ACCELEROMETER Ax1
ENGINE ATTITUDE - VERTICAL UP
AEROZINE-50, "GREEN" N2O4 PROPELLANTS
RUNS 1-371
ENGINE P/N 228686-501, S/N's 0002, 0234
RRL "G", 9-9 thru 9-13-66

ACCELEROMETER LOCATED ON HEAD FLANGE IN LINE WITH THE ENGINE AXIS

LEVELS OF FACTORS

L	3 - Oxidizer lead = 0, .006, .015 seconds
C	5 - Off time = .100, .350, .600, 1.000, 1.500 seconds
N	4 - Tmat = 100, 92, 76, 59 °F
P	3 - # of pulses = 4, 7, 9
R	2 - Repetition = 2

GRAND MEAN 254.72610

ERROR MEAN SQUARE = 61,645.92414422
180 DEGREES OF FREEDOM
STANDARD DEVIATION OF ERROR = 248.28597

SOURCE OF VARIATION	SUMS OF SQUARES	DEGREES OF FREEDOM	MEAN SQUARES	F RATIO	
L	273393.69531	2	136696.84766	2.2175	
C	578624.17969	4	144656.04492	2.3466	
LC	355831.91406	8	44478.99926	0.7215	
N	1547927.45313	3	515975.81641	8.3700	***
LN	551017.02813	6	91836.30469	1.4897	
CN	3917930.37500	12	326494.19531	5.2963	***
LCN	1458335.32813	24	60763.97168	0.9857	
P	2105345.34375	2	1052672.67188	17.5629	***
LP	282496.87109	4	70624.21777	1.1456	
CP	907202.47656	8	113400.30957	1.8395	
LCP	383073.88281	16	55242.11768	0.8961	
NP	261178.80273	6	43529.80029	0.7061	
LNP	1428972.67188	12	119081.05566	1.9317	*
CNP	2282729.87500	24	95113.74414	1.5429	
LCNP	2350659.46875	48	48972.07227	0.7944	
R	19562.92603	1	19562.92603		
LR	111544.55766	2	55772.29883		
CR	334083.50781	4	83520.87695		
LCR	226755.79102	8	28344.47388		
NR	41614.16064	3	13838.05347		

* SIGNIFICANT AT 5% LEVEL
** SIGNIFICANT AT 1% LEVEL
*** SIGNIFICANT AT 0.1% LEVEL

Figure 12

LM IGNITION PROOF TEST PROGRAM
A-50 FUEL, VERTICAL UP ORIENTATION

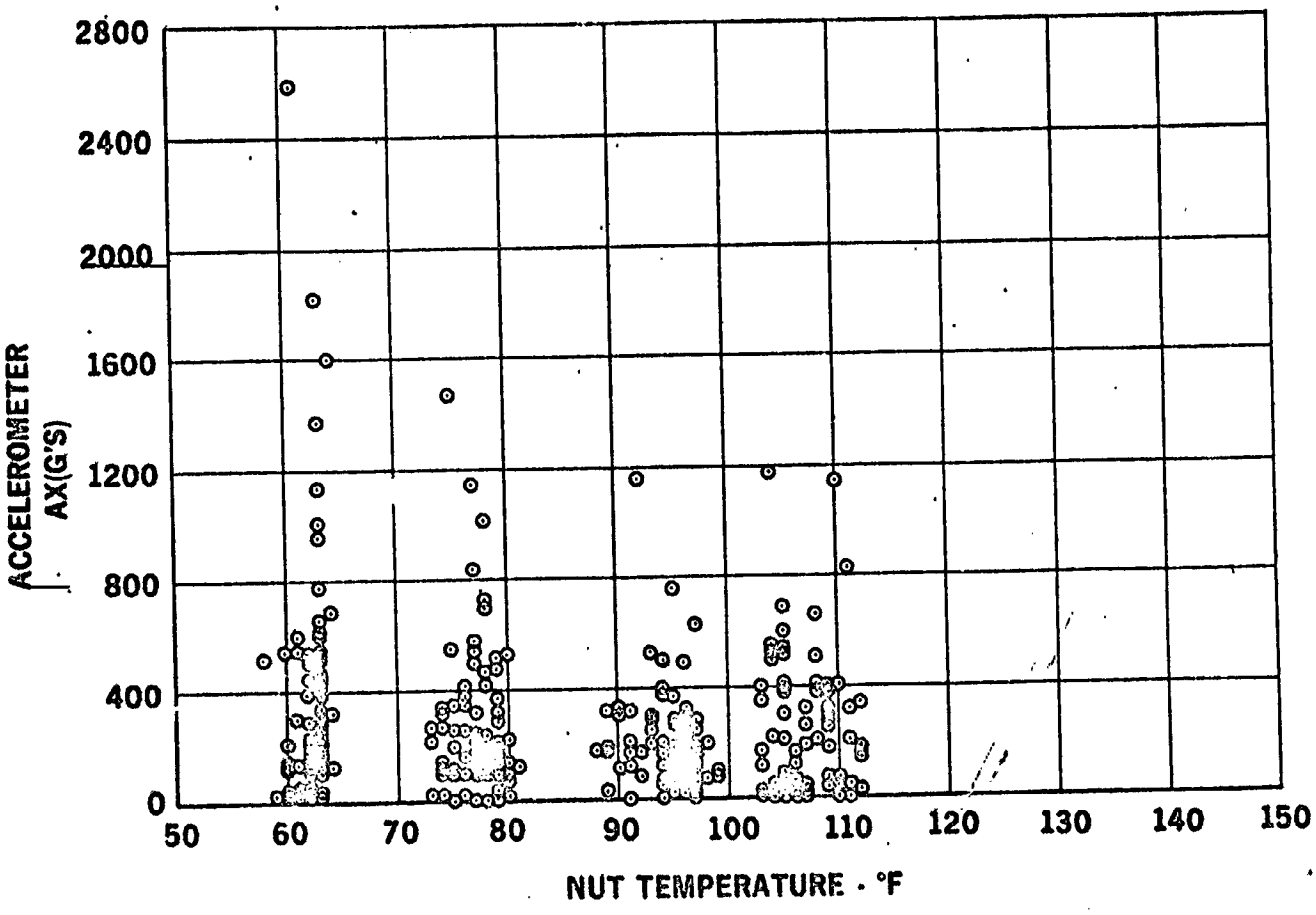

Figure 13

IGNITION DATA FLOW

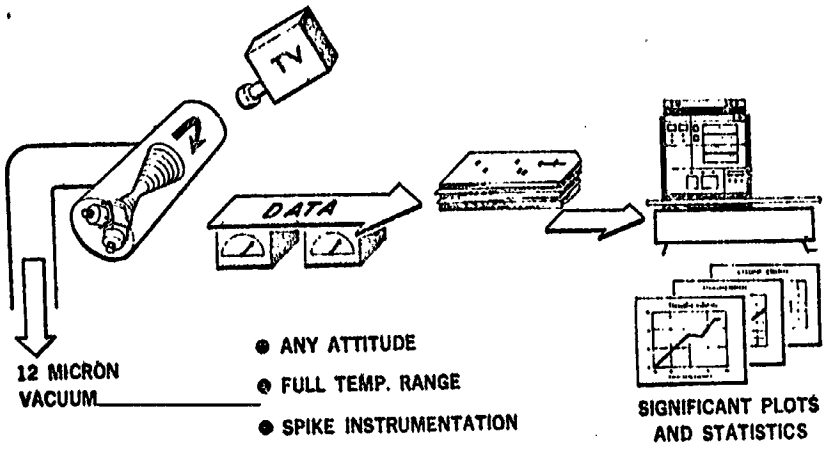

Figure 14

WAVE PROPAGATION AFTER IGNITION

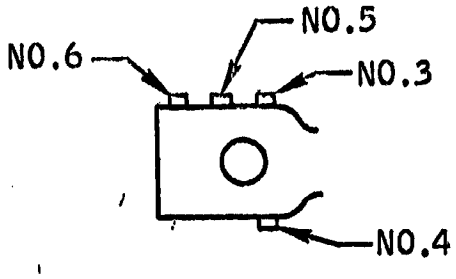

TRANSDUCER LOCATIONS

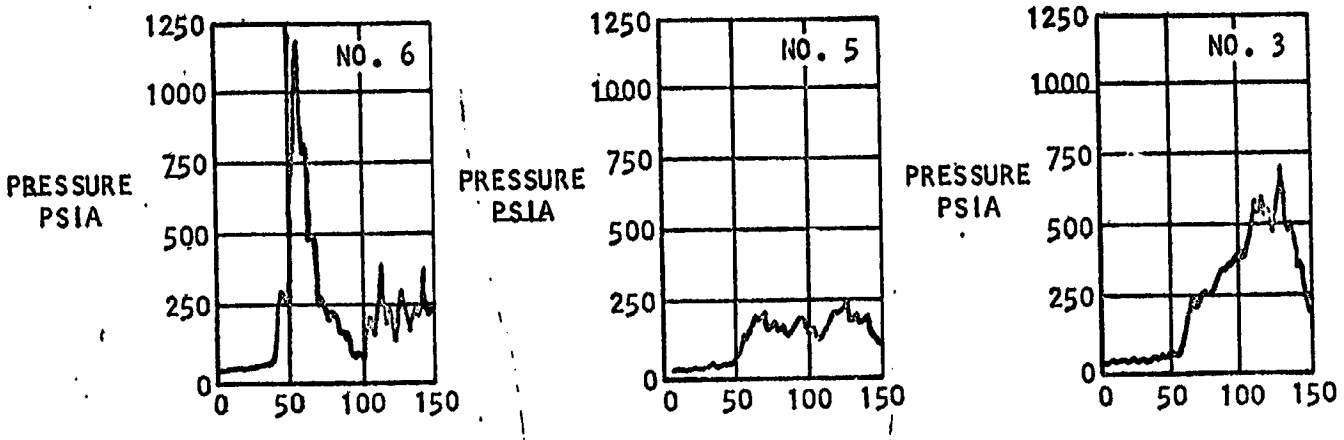

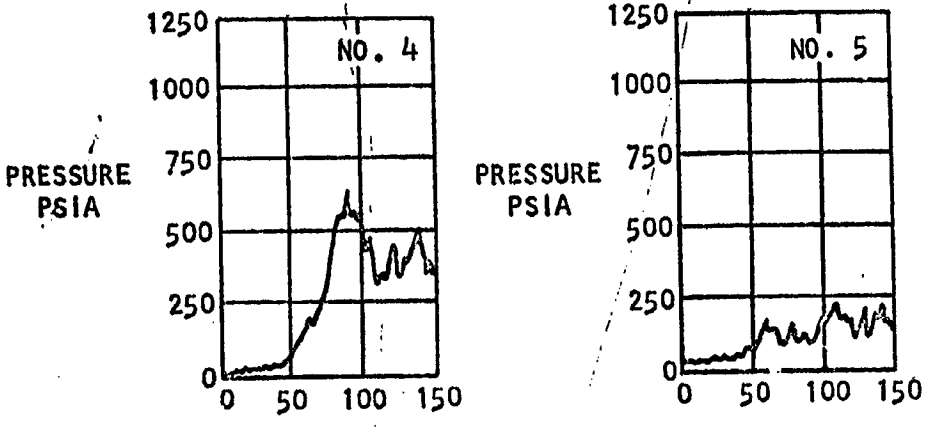

Figure 15

Pressure measurements made with low-range Kistler transducers during the preignition period showed that a preignition reaction raised the temperature and pressure of the mixture within the combustion chamber until the initiation of the travelling detonation wave occurred. Analytical estimates based on detonation theory and the amount of material injected before ignition predicted that ignition pressure around 2,000 psi might be produced during a heterogeneous detonation. Extensive engine test programs were conducted to determine the engine test conditions that produced ignition overpressures and the effect of the overpressures on the molybdenum combustion chamber and bell. These early test results showed that the timing of the propellant valve opening influenced the peak ignition pressure. The highest pressures occurred when the oxidizer valve was opened before the fuel valve. Figure 16 shows a sample of peak ignition pressure data plotted as a function of valve timing. (Another factor that seemed to affect ignition pressure magnitude was propellant temperature. The largest ignition pressures were obtained during tests run with cold propellants. It was only later in the program that condensed phase explosions associated with cold engine hardware were found to be responsible for this apparent propellant temperature effect.)

The observed relation between ignition overpressures and engine operating variables did not explain all the data characteristics because of the influence of uncontrolled but significant variables such as hardware temperature and time between pulses. However, it was felt that satisfactory ignition characteristics could be obtained by eliminating the heterogeneous detonations and early tests of the preigniter engine design seemed to indicate that the preigniter could eliminate large ignition overpressures.

Tests were conducted to determine the configuration of a preigniter injector that would provide satisfactory ignition characteristics over a wide range of propellant valve timing. It was found, Figure 17., that the ignition limits for preigniter operation were a function of O/F ratio, preigniter characteristic length, and the propellant weight flow divided by preigniter throat area. These data were used to design the preigniter injector eventually incorporated in the production engine. This injector incorporated a combination of hydraulic restrictions and volumes arranged to provide propellants to the preigniter before allowing propellant flow into the combustion chamber. A computer program was used in conjunction with engine tests to design the hydraulic circuitry for positive preigniter operation.

The preigniter engine design seemed to substantially reduce the magnitude of ignition pressures. However, a growing body of data suggested that ignition overpressures might still occur when the engine hardware was cold or when the engine had been previously operated a short time before attempting to reignite it. This clouded picture was brought into focus by the failure of a preigniter engine during qualification testing.

VALVE OPENING MISMATCH VS CHAMBER PRESSURE - (PCK NO. 1)

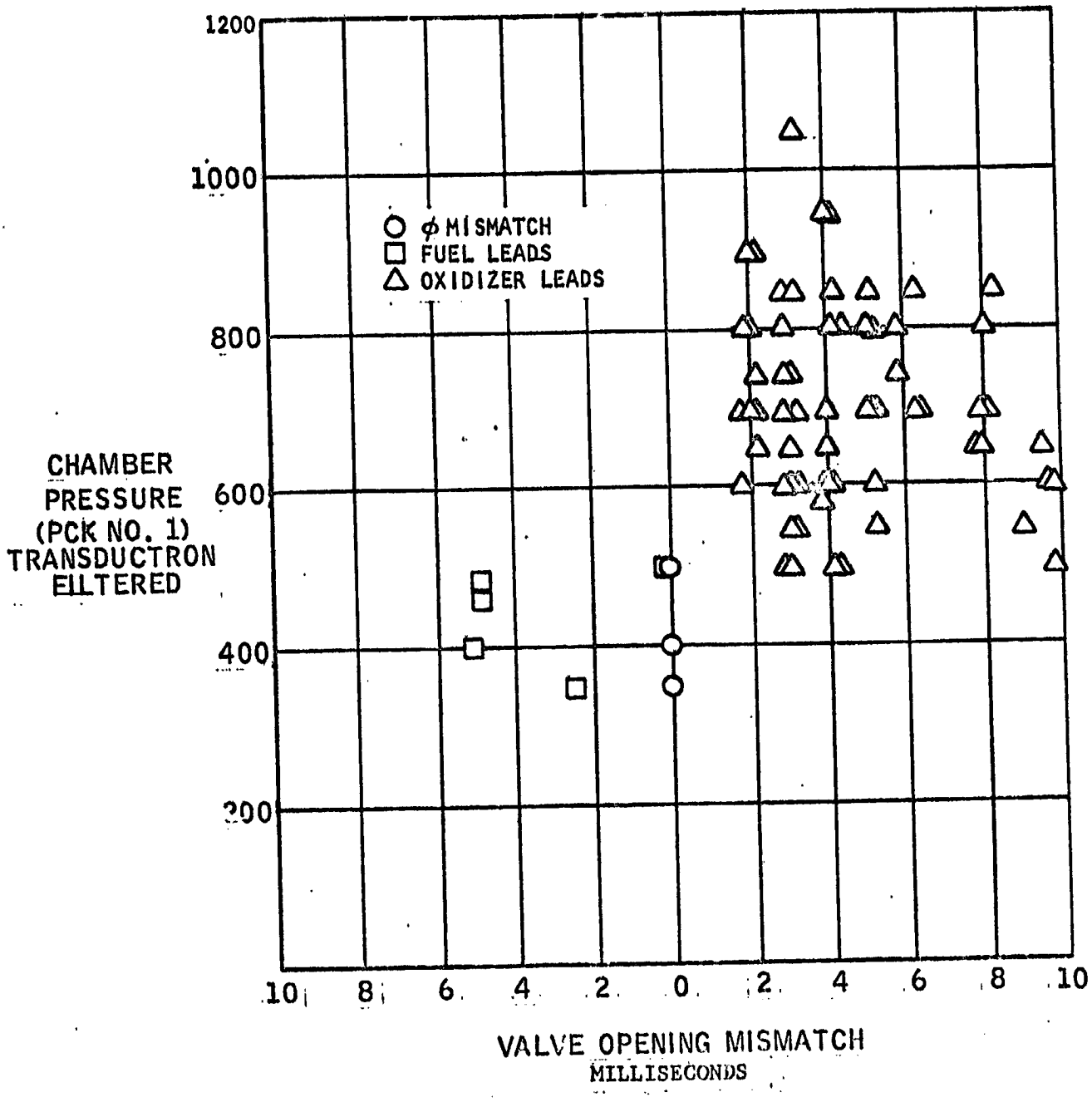

Figure 16

IGNITION LIMITS

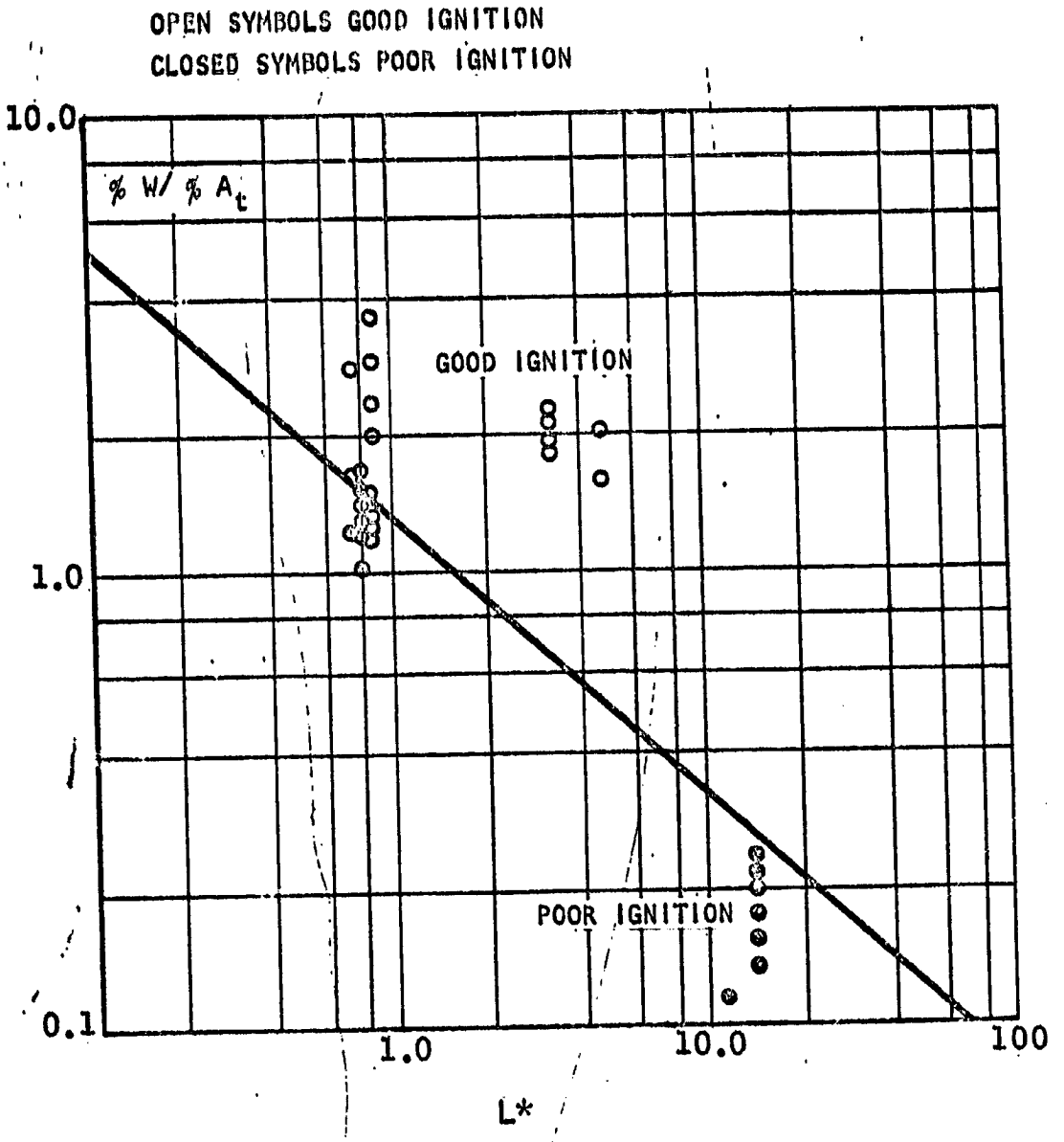

Figure 17

The cause of the failure was identified as a large oxidizer leak caused by an injector manifold explosion. While the causes and cures of injector manifold explosions were being determined, engine testing at the NASA Manned Spacecraft Center resulted in the failure of a heavy boilerplate steel chamber. The energy required to produce the observed deformation of the steel chamber was estimated to be greater than the energy that could be extracted from propellants entering the chamber prior to ignition. This observation pointed the way to the discovery of detonations of condensed residual materials as a second cause of ignition overpressures. This second type of ignition overpressure was later controlled by establishing operating temperature limits for the engine.

B. Condensed Phase Explosions

The heterogeneous detonation theory had explained some but not all of the ignition overpressures observed during engine testing. The temperature and duty cycle dependence of ignition pressure and the large energy yields required to produce some of the observed engine hardware damage strongly suggested the presence of a second type of ignition overpressure associated with the detonation of residual materials from prior pulses. Later support of this hypothesis came from visual observation of liquid deposits in rocket engines being tested at Marquardt and at NASA's Manned Spacecraft Center. In May of 1966, Marquardt, North American Aviation and the NASA Manned Spacecraft Center began a cooperative program to investigate condensed phase explosions.

The program consisted of engine tests to determine the conditions causing condensed phase explosions and analytical and experimental studies aimed at providing a model for the physical processes that transfer materials into and out of rocket combustion chambers. It was felt that such a model would help interpret engine test data and would help identify techniques for ensuring low ignition pressures.

The model developed provided analytical estimates of the amount of residual fuel remaining in the rocket combustion chamber as a function of time, temperature and firing duty cycle. The estimates considered heat transfer, evaporation and gravity flow of residual fuel. The model predicted the same functional dependence of ignition pressure on operating parameters that was observed during engine tests.

Residues collected from rocket combustion chambers after firing were chemically analyzed and found to contain water, nitrates derived from the fuel (particularly hydrazine nitrate) and unreacted fuel. Work is still continuing at a number of institutions to provide a more complete understanding of the formation of residual materials and their role in producing condensed phase explosions. However, the success of the residual fuel model in predicting ignition pressures as a function of fuel being used, engine temperature and pulsing duty cycle does suggest that the residual fuel is important either as an energy source, or indirectly as a contributor to residue formation.

The mathematical model developed for condensed phase explosions was a computer program that periodically calculated the amount of residual fuel in the combustion chamber. This amount was based on the amount of residual fuel calculated one computing interval previously and adjusted for additions and losses associated with injector emptying, evaporation and gravity drainage. At the time corresponding to ignition for a pulse firing, the program computed the ignition pressure associated with instantaneous stoichiometric combustion of the residual fuel present at the moment of ignition. Figure 18 is a sample of the information generated by the computer program.

When the engine is fired in pulsing duty cycles, a number of processes sequentially take place. The relative timing of these processes was determined by analysis of high speed movies and high response chamber pressure measurements. The engine solenoid valves open shortly after being electrically energized and the propellants begin to fill the injector passages. Because the injector is evacuated by the space environment between engine firings, some of the incoming propellant vaporizes. This vaporization allows formation of a two-phase mixture in the injector. Flow from the injector into the combustion chamber begin as a tenuous mist whose liquid content increases as the injector begins to fill with liquid. Preignition reactions begin to take place in the combustion chamber, raising both the temperature and pressure of the two propellant mixture. Approximately five milliseconds after the propellant valves open, the preignition reaction rate becomes fast enough for ignition to take place.

Ignition may take the form of a deflagration that spreads through the chamber at subsonic speeds or a supersonic detonation wave may sweep through the chamber and rapidly raise the chamber pressure. (This latter was named "heterogeneous detonation." The heterogeneous detonation seemed to occur more frequently when the engine valves were timed so that the oxidizer valve opens first. If residual energy rich material is present on the combustion chamber it may explode and contribute mass and energy in the form of a "condensed phase explosion." Test data suggested that the condensed phase explosions were more likely on pulses with oxidizer leads than on pulses with fuel leads. This suggested that the conditions produced by a "heterogeneous detonation" may induce explosion of energy rich materials in the combustion chamber walls. A coupling of this type has been observed in detonation tube experiments by Dabora and his co-workers at the University of Michigan.

After the ignition transient dissipates, the propellant flow rates and chamber pressure tend toward their steady state values. When the propellant valves are closed, a new set of transient processes begins. The flow rates into the injector stop and the flow rates from the injector into the combustion chamber begin to diminish. The fuel flow from the injector decreases more rapidly because the vapor pressure of the fuel is lower than the vapor pressure of the oxidizer. During the period while the propellant flow rates are decreasing, a sporadic combustion takes place in the chamber with a periodic characteristic caused by coupling between the combustion chamber pressure and the flow rate from the injector.

PULSE OPERATION MODEL
COMPUTER PRINTOUT

MARQUARDT PULSE OPERATION MODEL

TRY NUMBER 1
0.013 SEC ON 0.087 SEC OFF 20 PULSES INITIAL WALL TEMPERATURE= 40.00

PULSE NO	EVENT	TIME AFTER ELECT ON (MILLISEC)	FUEL IN MANIFOLD (LBS)	UDMH ON WALL (LBS)	N2H4 ON WALL (LBS)	WALL TEMP (F)	IGN PRESS (PSIA)
1	IGNITION	7	0.15100E-03	0.0	0.0	40.002	0.0
1	MAN FULL	16	0.14300E-02	0.0	0.0	40.004	0.0
1	BURN STOP	24	0.10784E-02	0.37624530E-04	0.57169033E-04	52.693	21.827
2	IGNITION	7	0.78660E-03	0.15119986E-05	0.12042641E-03	50.655	226.272
2	MAN FULL	12	0.14300E-02	0.15119986E-05	0.12355836E-03	50.570	232.035
2	BURN STOP	24	0.10784E-02	0.56524426E-04	0.22937010E-03	69.176	597.266
3	IGNITION	7	0.78660E-03	0.15119986E-05	0.26747724E-03	66.608	496.845
3	MAN FULL	12	0.14300E-02	0.15119986E-05	0.26941905E-03	66.503	500.418
3	BURN STOP	24	0.10784E-02	0.15271886E-04	0.37085125E-03	84.529	729.709
4	IGNITION	7	0.78660E-03	0.15119986E-05	0.37291110E-03	81.687	690.843
4	MAN FULL	12	0.14300E-02	0.15119986E-05	0.37331413E-03	81.559	691.585
4	BURN STOP	24	0.10784E-02	0.15119986E-05	0.47317171E-03	99.250	875.323
5	IGNITION	7	0.78660E-03	0.15119986E-05	0.51142368E-03	97.028	945.707
5	MAN FULL	12	0.14300E-02	0.15119986E-05	0.51314803E-03	96.919	948.879
5	BURN STOP	24	0.10784E-02	0.15119986E-05	0.61389036E-03	114.401	1134.245
6	IGNITION	7	0.78660E-03	0.15119986E-05	0.60498295E-03	111.452	1117.855
6	MAN FULL	12	0.14300E-02	0.15119986E-05	0.60492055E-03	111.316	1117.741
6	BURN STOP	24	0.10784E-02	0.15119986E-05	0.69589284E-03	128.444	1285.130
7	IGNITION	7	0.78660E-03	0.15119986E-05	0.61332574E-03	124.374	1133.206
7	MAN FULL	12	0.14300E-02	0.15119986E-05	0.61007077E-03	124.188	1127.217
7	BURN STOP	24	0.10784E-02	0.15119986E-05	0.68809208E-03	140.937	1270.776
8	IGNITION	7	0.78660E-03	0.15119986E-05	0.51466306E-03	135.489	951.667
8	MAN FULL	12	0.14300E-02	0.15119986E-05	0.50760340E-03	135.246	938.677
8	BURN STOP	24	0.10784E-02	0.15119986E-05	0.57053473E-03	151.610	1054.471
9	IGNITION	7	0.78660E-03	0.15119986E-05	0.29625953E-03	144.636	549.804
9	MAN FULL	12	0.14300E-02	0.15119986E-05	0.28513651E-03	144.331	529.338
9	BURN STOP	24	0.10784E-02	0.15119986E-05	0.33225957E-03	160.329	616.044
10	IGNITION	7	0.78660E-03	0.15119986E-05	0.15119986E-05	152.497	7.469
10	MAN FULL	12	0.14300E-02	0.15119986E-05	0.15119986E-05	152.359	7.469
10	BURN STOP	24	0.10784E-02	0.15119986E-05	0.35359277E-04	168.042	69.748

Figure 18

This sporadic combustion ceases when the oxidizer is exhausted (typically about 100 milliseconds after the valves are closed). The fuel still remaining in the injector then empties for approximately 200 milliseconds more.

Fuel is deposited on the combustion chamber walls by the film cooling flow used to lower steady state operating temperatures and by the emptying of the injector after the valves are closed. If the combustion chamber walls are relatively cool, this fuel can accumulate from pulse to pulse. The accumulated fuel represents a reservoir of energy as do combustion intermediate compounds such as nitrates formed by reaction of this fuel with oxidizer during the preignition and post combustion transient processes. Identification of the sequence of transient processes during pulsing of the rocket engine is the first step toward understanding the ignition process. Figure 19 shows a typical chamber pressure record with some of the transient processes identified.

Data for modelling the injector emptying transient were based on analysis and laboratory experiments. During the laboratory experiments, glass vials of propellant were opened in an evacuated bell jar while high speed movies were used to determine the effect of propellant temperature and gravitational orientation on the emptying process. The movies showed that emptying took place by two-phase liquid-vapor flow except when the vials were filled with chilled propellant and oriented to empty by flow upward against gravity. In this latter case, emptying took much longer and took place by solid-vapor flow with periodic stoppages caused by frozen plugs in the vial neck. Injector emptying curves similar to those in Figure 20 were calculated for two-phase flow and used as part of the computerized Pulse Operation Model.

Fuel added to the combustion chamber walls is affected by gravity and by vaporization. The vaporization rate is heavily influenced by heat transfer considerations and is, therefore, quite dependent on the thickness of the layer of fuel. During ground testing, gravity flow has an important effect on the thickness of fuel films as shown by Figure 21, constructed by equating gravity forces and viscous forces in a layer of liquid on a vertical wall. This curve shows that 50% of a 0.01 inch thick layer of monomethylhydrazine will drain from a 2 inch vertical wall in 0.43 seconds. 95% drainage requires 43 seconds.

Because of the low pressure outside the engine, deposits within the combustion chamber tend to be vaporized by boiling or by evaporation (or sublimation) from the free surface of the deposit. For conditions under which evaporation from the free surface occurs, the time to evaporate an 0.001 inch thick layer of monomethylhydrazine covering a portion of combustion chamber surface with four times the area of the combustion chamber throat is 0.05 seconds for a chamber temperature of 70°F.

TYPICAL CHAMBER PRESSURE TRACE

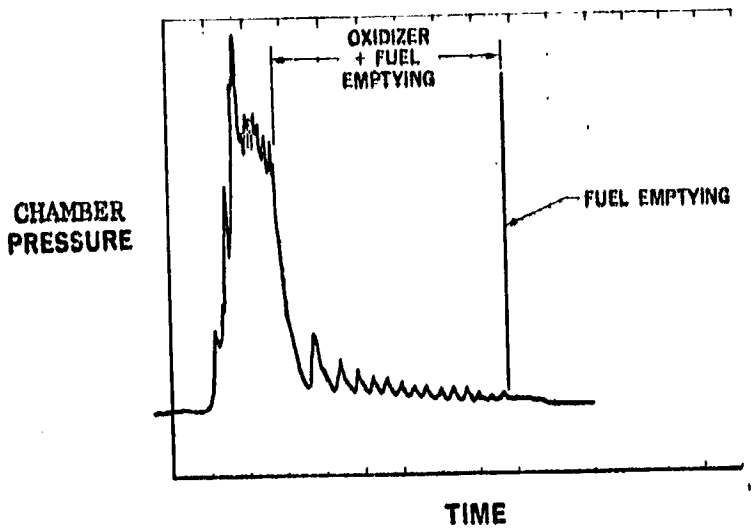

FIGURE 19

INJECTOR EMPTYING TIMES

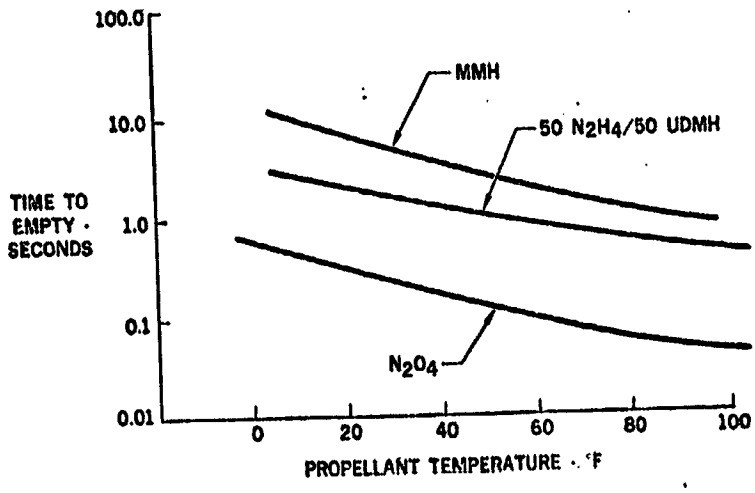

FIGURE 20

LIQUID REMAINING ON WALL AFTER SHUTDOWN

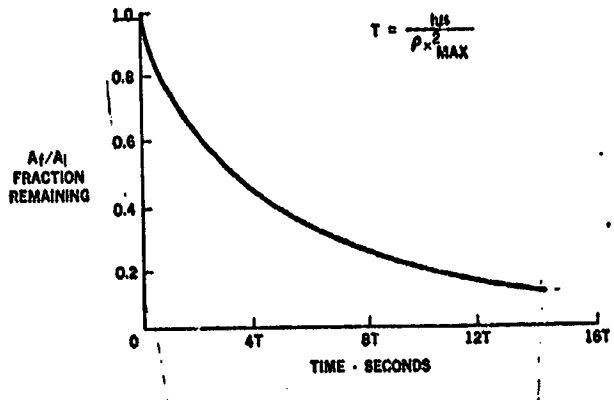

Figure 21

Computer runs made with the Pulse Operation Model using the analytical expressions for injector emptying time, wall drainage time and fuel evaporation times (and including the effect of evaporation and combustion heat fluxes on the combustion chamber temperature) showed two different types of behavior. Large accumulations of fuel were predicted for cases where the heat added by combustion was less than the heat required to evaporate the fuel deposited on the combustion chamber walls during a firing. A high initial wall temperature delayed this accumulation until the heat deficit from a number of pulses reduced the combustion chamber temperature so that the residual fuel could not evaporate between firings.

Firing the engine for longer periods provided enough heat to remove all the material deposited on the wall by a firing. This produced a rise in chamber temperature and no fuel accumulation when the initial temperature was warm enough to evaporate all the residual fuel between firings. Starting a pulse train at lower temperatures produced accumulations only until the excess heat warmed the chamber to a temperature high enough for complete vaporization. Figure 22 shows the behavior of chamber temperature and potential ignition pressures (based on instant combustion of the residual fuel) for the two situations discussed.

After recognition of condensed phase explosions as a source of ignition overpressures, the significant variables affecting condensed phase explosions were identified by studying Pulse Operation Model results. Engine tests were conducted to explore the effects of engine temperature, attitude, duty cycle, and propellant selection on the ignition pressure magnitude. The tests established engine temperatures required for avoiding condensation phase explosions and showed the following trends in the data.

1. Ignition severity decreased as engine temperature increased, suggesting that evaporation is an important factor in emptying residues from the combustion chamber.

2. Ignition severity was lowest for very short and very long times between firing.

3. Ignition severity generally increased as the engine firing direction was rotated from downward to horizontal to upward showing the influence of gravity in spreading and draining residual material deposits.

4. Ignition overpressures were more frequent with oxidizer leads.

5. Monomethylhydrazine fuel produced lower ignition pressures than Aerozine-50 fuel under the same conditions.

Typical data plots from the ignition tests are shown in Figures 23 through 26. The scattered nature of the data shows the value of using statistical methods to identify trends and patterns in ignition test data.

POTENTIAL IGNITION PRESSURE VS PULSE NUMBER

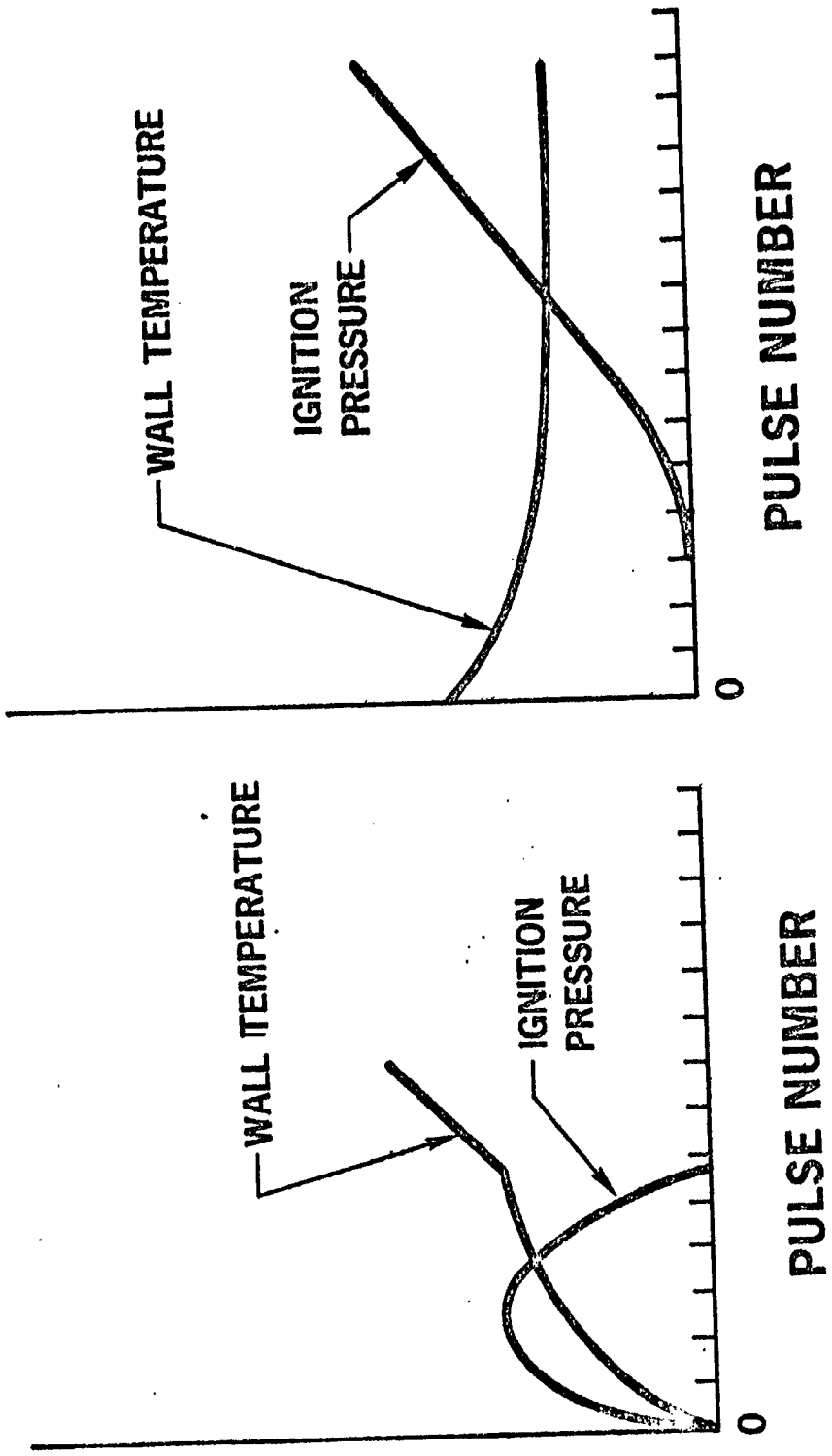

Figure 22

REPRODUCIBILITY OF THE ORIGINAL PAGE IS POOR.

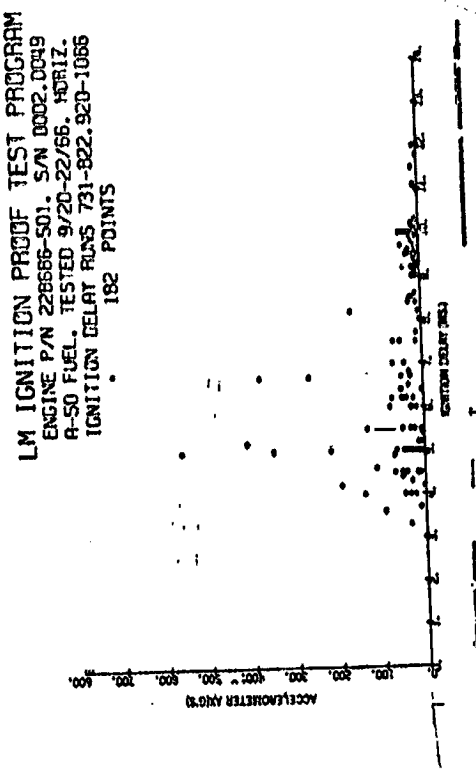

FIGURE 24

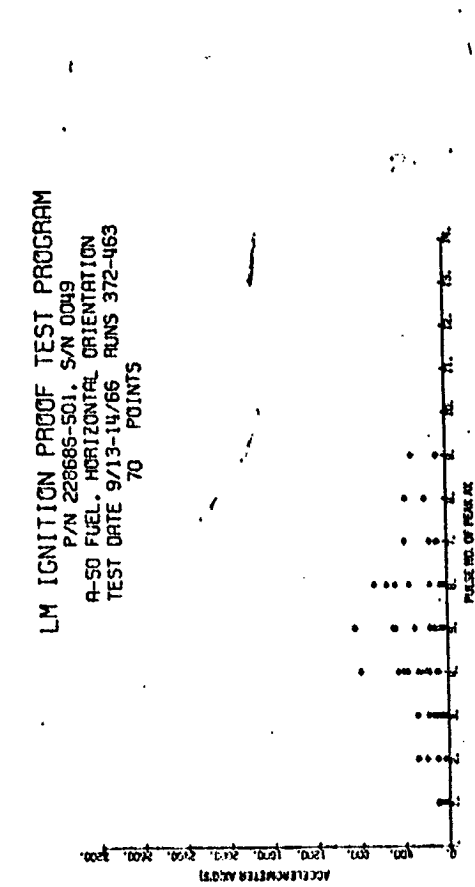

FIGURE 23

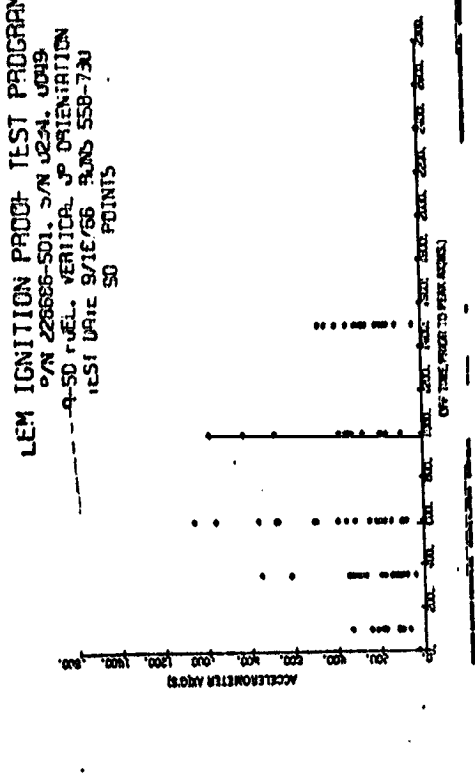

FIGURE 26

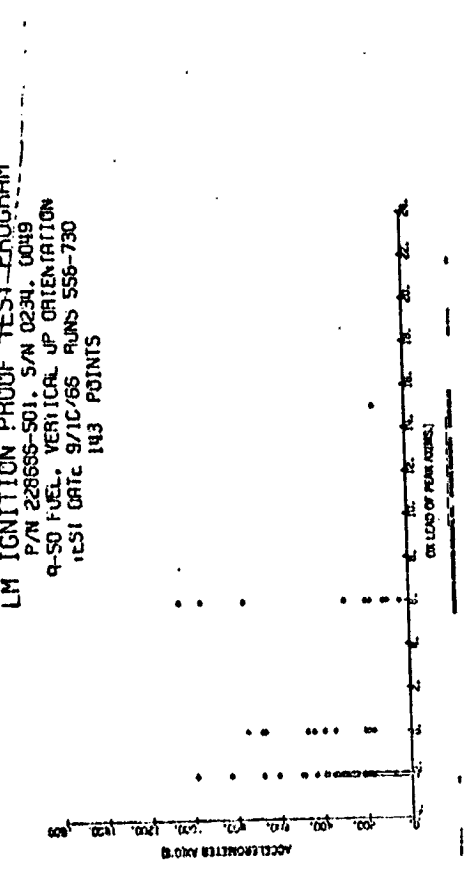

FIGURE 25

Recognition of condensed phase explosions as an important type of ignition overpressure and the subsequent establishment of low temperature limits (and the Service Module change from Aerozine-50 to MMH fuel) resulted in elimination of this phenomenon as a cause of mysterious damaging overpressures and provided confidence in satisfactory ignition performance during the Apollo missions.

VI. INJECTOR MANIFOLD EXPLOSIONS

During much of the program to develop the Apollo reaction control engines, engine test firings were made at test cell pressures which were high compared to those used during the later parts of the program. One of the factors leading to the use of lower test cell pressures (below 100 microns) was the occurrence of injector manifold explosions when engines were fired repeatedly at much higher cell pressures. These injector manifold explosions caused a characteristic pressure rise in the output of pressure transducers located upstream of the engine valves in the propellant feed lines. In some cases the injector manifold explosions caused damage to the test engine injector or to a propellant valve. The first clearly recognized case of engine damage due to an injector manifold explosion was Qualification Engine B whose valve seat was damaged by an injector manifold explosion so that it subsequently was unable to properly seal. (The resulting leak cooled the combustion chamber of the engine and resulted in an ignition overpressure which damaged the combustion chamber). Subsequent study of the injector manifold explosion phenomenon showed that the injector manifold explosions were caused by accumulations of one propellant in the injector passages intended for the other propellant. These accumulations occurred when the test cell pressure was high enough to prevent normal boiling and evaporation of propellants during the shut-down transients at the end of an engine firing. When the engine was subsequently reignited with an accumulation of one propellant in the passages for the other propellant, the confined reaction produced undesirably high pressures.

When the first injector manifold explosions were observed, a task force was set up to determine the causes of injector manifold explosions, their frequency of occurrence, the nature of the associated physical and chemical processes and, finally, whether they would be expected to occur during missions in space. The investigation consisted of laboratory experiments, engine tests and supporting analysis and showed that injector manifold explosions could not occur at the low ambient pressures typical of space operation.

The first portion of the investigation of injector manifold explosions was a review of available test data to determine if injector manifold explosions could be detected in cases where no damage to the engine hardware occurred. A review of engine test data showed that the pressure transducers located in the propellant supply lines did indeed sometimes show a peculiar pressure transient that might be attributed to explosions within the rocket engine injector.

The pressure transducers normally used at the time for measuring propellant supply pressures were Taber transducers located in the propellant by-pass lines used for recirculation of propellant during temperature conditioning. This arrangement is shown in Figure 27. In an effort to improve the frequency response of the transient pressure measurement and to gain more information about the nature of the injector manifold explosions, a propellant supply system was instrumented with high response Kistler piezoelectric pressure transducers (Model 601H) located within a few inches of the engine inlet. A test program was conducted to determine if injector manifold explosion would occur and what their characteristics were. The test program consisted of a number of engine firings at engine injector temperatures ranging from 25°F to 110°F with test cell pressures ranging from 0.03 to 10 psia. Figure 28 provides a comparison between the normal pressure transients in the propellant supply lines and the pressure transients associated with explosions within the injector passages.

A study of the data from these engine tests suggested to members of the task force that explosions were occurring in the injector passages. An analysis was performed to determine the magnitude of internal injector pressures required to produce the observed propellant feed system transients. The analysis was based on the assumption that the pressure transients propagated through the injector and valve within these internal passages. Application of water hammer analysis showed that the observed 200 to 300 psia feed system pressure rises must be associated with pressure transients of the order of 10,000 psi at the propellant valve seat and perhaps even higher values if the source of the pressure transient were further downstream in the injector. Such high pressures could only be caused by explosions confined within the injector passages and the task force effort was therefore focused on explaining how such explosions occurred.

Since most of the injector manifold explosions occurred in the oxidizer side of the engine and since the oxidizer (N_2O_4) is not known to decompose explosively, it seemed apparent that somehow fuel was being transported into the oxidizer passages between firings of the engine. In order to verify the hypothesis that the observed phenomena could be caused by the transport of one propellant into the passages of the other propellant, fuel was purposely placed within the oxidizer passages of an injector prior to opening the oxidizer valve. The fuel samples (hydrazine, Aerozine-50 and UDMH) were placed at various locations within the injector using a hypodermic needle. The test personnel then retreated behind a barricade and electrically actuated the oxidizer valve while recording the output of a Kistler pressure transducer located just upstream of the valve. The pressure transients measured by the transducer were identical to those previously observed during engine testing and suggested that the "injector manifold explosions" were indeed caused by transport of one propellant into the passages normally used by the other. An intensive analytical study was then undertaken to determine the conditions under which such transport might occur.

REPRODUCIBILITY OF THE ORIGINAL PAGE IS POOR.

Propellant System

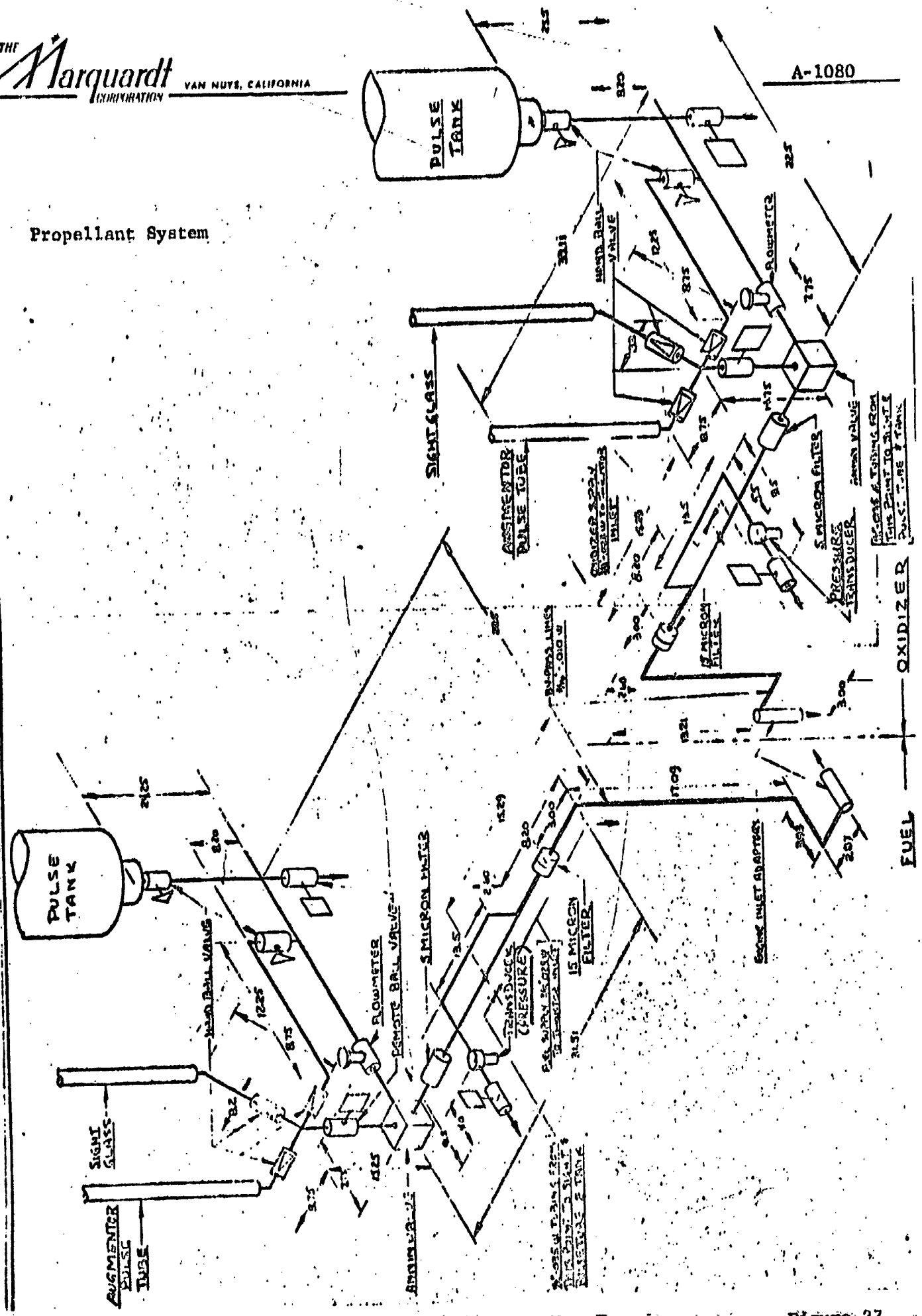

COMPARISON OF MANIFOLD PRESSURE TRACES

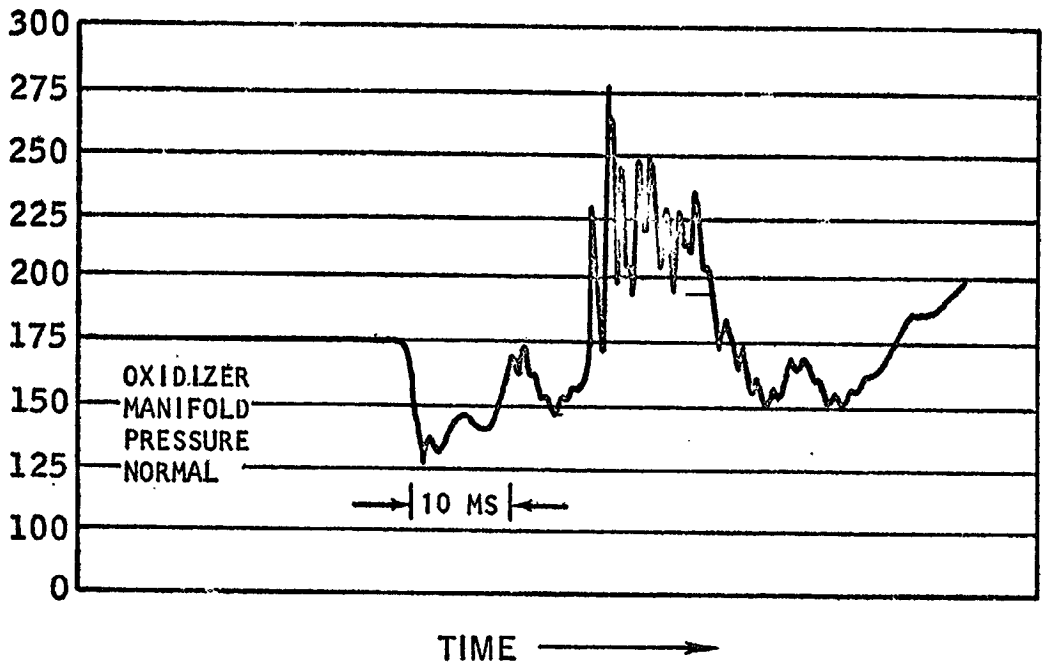

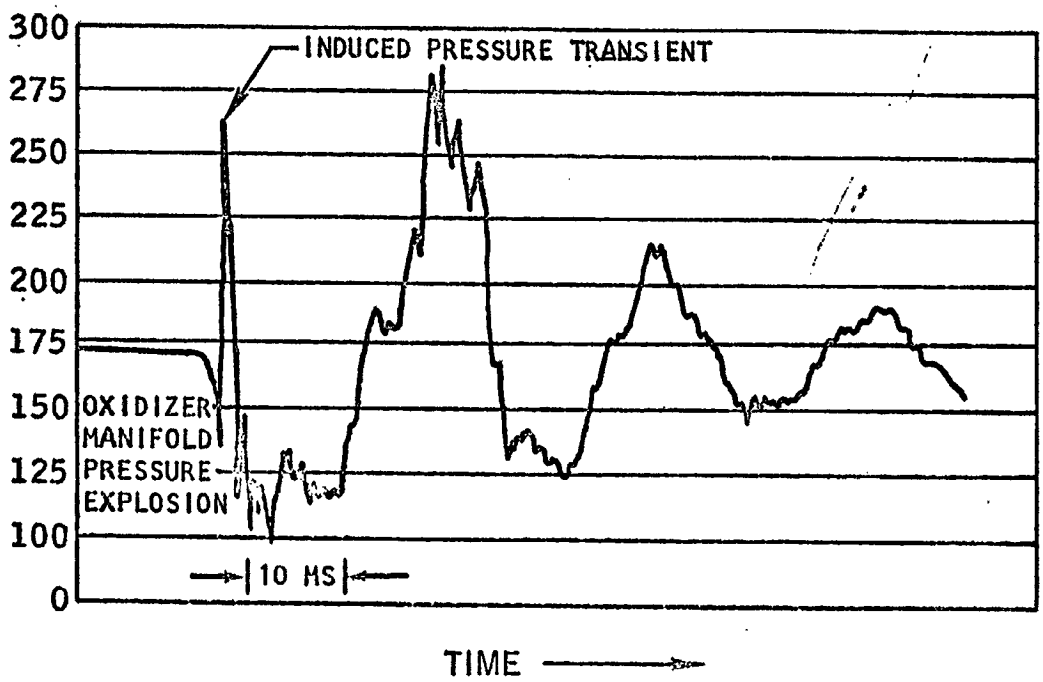

Figure 28

The analyses studied the dynamics of the injector emptying process after a pulse firing, the possible phase transformations with the propellant system being used, the processes of condensation and evaporation of propellants with the engine, and the possibility of propellant valve leakage causing deposits of propellants at various locations within the engine. The analyses showed that although propellants might take several hundred milliseconds to empty from the engine injector they can never accumulate in the wrong side of the injector unless the pressure within the engine test cell is high enough to inhibit this free evaporation at normal rates for space operation. The analytical studies also showed that the internal engine pressures associated with propellant valve leaks (less than 1,000 cc's of propellant per hour) were such that propellants would not be deposited in the wrong parts of the injector.

Based on the analytical studies a plot was prepared giving, as a function of injector temperature, the cell pressure level required to allow accumulation of one propellant in the other propellant's passages. This plot, shown in Figure 29, was based on the propellant's vapor pressure properties. Analysis of available engine test data showed that all the injector manifold explosions that had been observed occurred at test cell pressures above the lowest line on Figure 29 and that injector manifold explosions had not been observed with test cell pressures below the lowest line in Figure 29.

The agreement between the analytical predictions and the observed pressure regions where injector manifold explosions occurred was encouraging because it showed that this phenomenon would not be encountered during operation of the engine in space.

VII. CONCLUSION

One of the important features of the Apollo Reaction Control Engines is their ability to provide reliable ignition over a wide range of pulsing duty cycles. This capability was developed as the result of extensive testing and analysis to document engine behavior and to understand the factors affecting space ignition. In addition to the engine configuration and temperature control techniques that provide control of ignition pressure magnitude, the engine development program provided techniques for measuring ignition transients, for simulating space operation during engine ground tests and for handling and interpreting large amounts of ignition test data. Progress was made toward understanding the basic processes involved in space ignition and the injector manifold explosions that can occur during ground testing at elevated cell pressures. The knowledge gained during the Apollo Reaction Control Engine development program should provide a valuable contribution to rocket technology and to the development of future reaction control engines.

ZOT PLOT

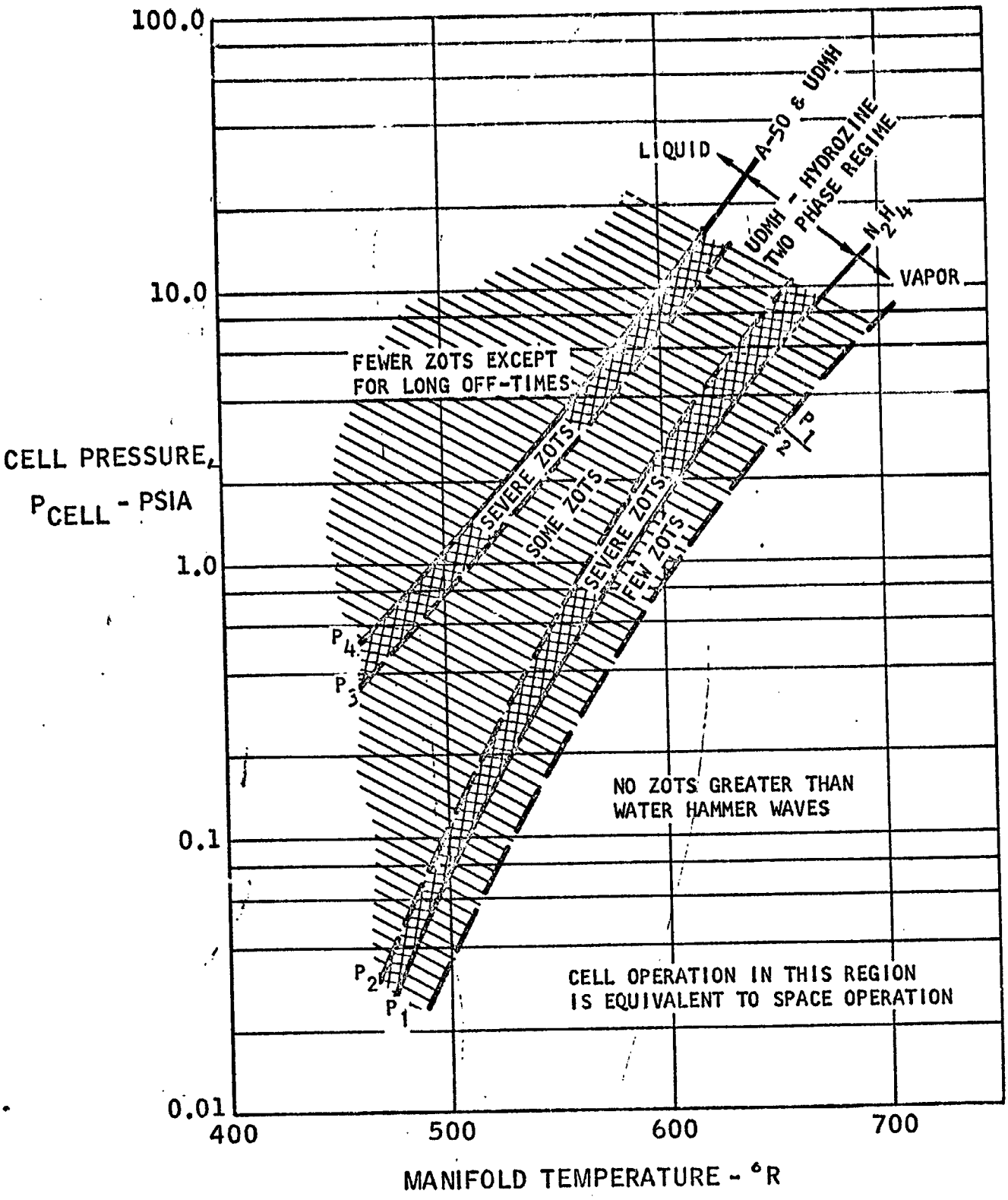

Figure 29

BIBLIOGRAPHY

(1) Knox, R. M., Minton, S. J. and Zwick, E., "Space Ignition."

(2) Kappl, J. J. and Knox, R. M., "Altitude Ignition of Hypergolic Bipropellant Rockets."

(3) Juran, W. and Stechman, R. C., "Ignition Transients in Small Hypergolic Rockets."

(4) Perlee, H. E. and Christos, T., "Summary of Literature Survey of Hypergolic Ignition Spike Phenomena, Phase I," Bureau of Mines.

(5) Seamans, T. F. and Dawson, B. E., AFRPL-TR-67-129

CHAPTER 4

GAS PRESSURIZATION EFFECTS

BY

J. F. FOOTE
and
W. JURAN

TABLE OF CONTENTS

SECTION		PAGE NO.
I.	INTRODUCTION	4-1
II.	HISTORICAL REVIEW	4-2
III.	THRUST OSCILLATIONS	4-12
	A. Nitrogen	4-12
	B. Helium	4-24
IV.	THRUST OSCILLATION MODELS	4-43
	A. Stability Analysis	4-43
	B. Gas Flow Limit Model	4-62
	C. Cavitation in the Valve	4-62
IV.	CONCLUSIONS	4-67

LIST OF ILLUSTRATIONS

FIGURE NO.		PAGE NO.
1	Float Working	4-3
2	Float Sunk	4-4
3	Thrust Oscillation due to Nitrogen Gas Accidentally Introduced into the Engine	4-6
4	Thrust Oscillation due to Nitrogen Gas Purposely Introduced into the Engine	4-14
5	Bubbling Saturation Procedure	4-23
6	Short Duration Oscillation	4-29
7	Thrust Oscillation Summary	4-31
8	Thrust Oscillation Summary	4-32
9	Unsaturated	4-34
10	Saturated	4-35
11	Typical Helium Gas Entrainment Trace	4-41
12	Typical Helium Gas Entrainment Trace	4-42
13	Rocket Engine Model	4-44
14	Rocket Engine Model Block Diagram	4-48
15 & 16	Reduced Rocket Engine Model Block Diagrams	4-49
17	Frequency Response of the Open Loop Transfer Function	4-52
18	Frequency Response Contribution of the Combustor	4-53
19	Attentuating Effect of Combustor	4-54
20	Attentuating Effect of Combustor	4-56
21	Stability Dependence	4-57
22	Stability Dependence	4-59
23	Helium - NTO Saturation Weight Ratio	4-64
24	Oxidizer Valve Seat Geometry & Flow Pattern	4-65

LIST OF TABLES

TABLE NO.		PAGE NO.
I.	Nitrogen Tests - PFRT	4-7
II	Helium Tests	4-10
III	Warm Propellant Test Results	4-15
IV	Effect of Time, Propellant Temperature and Tank Level on Oscillations	4-19
V	Engine 228439 - Cell 1	4-25
VI	Pre-Qualification Test with Helium	4-26
VII	Helium Test Run Summary	4-28
VIII	Stability Test Runs with GHe Saturated Propellants	4-37
IX	Gas Flow Limit	4-63

I. INTRODUCTION

The R-4D engine is a pressure fed bipropellant rocket engine used for attitude control or ΔV applications. Most space missions require that the engine operate after many months in space. For example, on Lunar Orbiter II the propellants had been pressured for 338 days before the last engine firing that transferred the vehicle to a moon crashing orbit to end the flight. During ground tests with bladderless tanks, the effects of dissolved or entrained gas on engine operation were discovered. First the oxidizer flow did not repeat from test to test after the oxidizer had been pressurized for several hours. Second, thrust oscillations occurred if the propellants contained entrained or dissolved gas. Both of these problems do not occur in flight because the bladders protect the propellants. The chapter discusses Marquardt's test experience with propellants containing the pressurant gas.

II. HISTORICAL REVIEW

At the start of the development program the test facilities did not have the capability of running with either hot or cold propellants. Around August of 1963 Cell 6 was modified so that the propellant temperatures could be controlled between 30° and 120°F. With hot propellants the oxidizer flow rate would vary from run to run even though the test conditions remained the same. In general, the flow would decrease from run to run and it seemed to be connected with how long the propellants had been in the run tanks. Also, when the propellant tanks were refilled the flow rate would return to the expected value.

The problem was solved by installing a float in the cylindrical run tanks (6 in. dia. × 18 in. long). Apparently nitrogen gas dissolved in the propellants would come out of solution either in the flow meter to give an error in flow measurment or in the injector head. The float eliminated this because it decreased the surface area between the propellant and the pressurant gas and consequently the gas could not dissolve in the propellants as easily. The float was a flat cylinder whose diameter was a little smaller than the diameter of the tank. It was made from stainless steel with a honeycomb center so it would be light enough to float.

Sometimes a float would sink after it had been in the oxidizer tank for a while. When this happened, the oxidizer flow would vary from run to run in unpredictable manner. Figures 1 and 2 show the injector pressure drop vs. flow correlation for a test where the float was working and where the float had sunk. There is very good agreement between pressure drop and flow with the float and poor correlation without the float. In fact, the poor flow repeatability was used as an indication that the float had sunk. Whenever it was noticed that the oxidizer flow rate was not repeatable a check would be made on the float. In almost all cases the float would be sunk.

Dissolved or entrained gas in the propellant also caused thrust oscillation to occur. This first occurred on the PFRT (October 1964) program with nitrogen. During acceptance testing of the first two engines, nitrogen gas was introduced into the propellant by a new and improper operational procedure. The thrust load cell is calibrated in the test facility by applying a calibrated force of 100 lb. on the thrust cell with the nominal propellant pressures at the engine. Previously the propellant tanks are pressurized to the nominal value to duplicate the pressure at the engine. For the first acceptance tests of engines 1 and 2, however, the lines were pressurized by applying the run pressure in the purge lines. A bubble of nitrogen gas was trapped in the purge line (30" of 1/4" line) which then could enter the engine along with the propellant. The procedure was changed so that the propellant tanks were pressurized during the thrust calibration. This eliminated the oscillation until they returned when tests were made with warmer propellant later in the program.

FLOAT WORKING

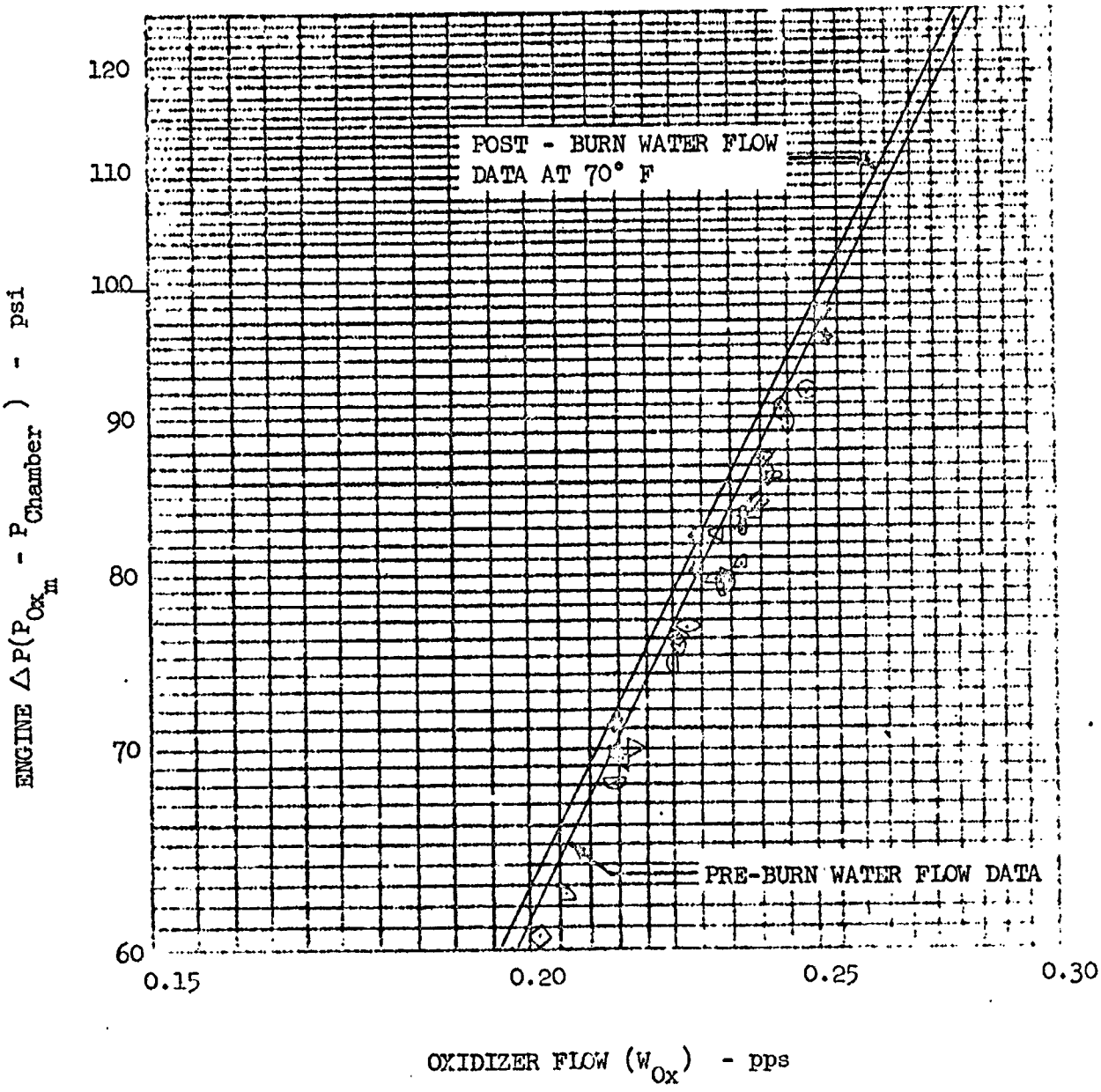

Figure 1

FLOAT SUNK

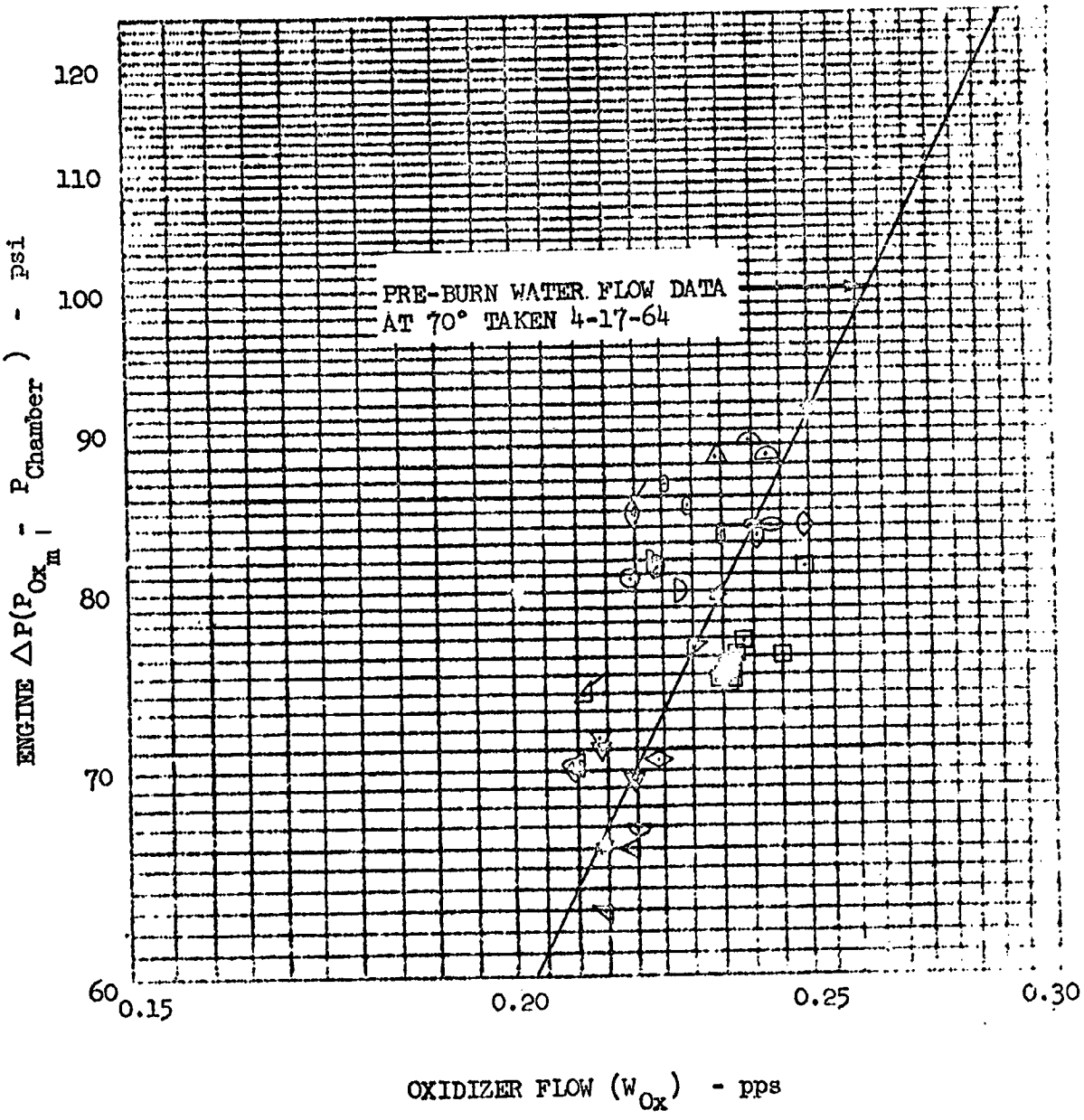

Figure 2

The engine (PRFT #1) again oscillated when the propellant temperatures were above 90°F. Because the one cause was gas in the propellant, the test facility was checked for nitrogen gas leaks. No leaks were found. However, we also knew from past experience that nitrogen gas could dissolve in the propellants. One way to eliminate the dissolved gas is to heat the propellant while venting the tanks. At the higher temperature (100°) the gas is driven out of solution. The propellants were degassed this way and the thrust oscillations were eliminated. The rest of the PFRT test with warm propellant were conducted with degassed propellants.

Figure 3 is a typical example of the thrust oscillations. The magnitude is 40% of full thrust at a frequency of 350 cps. The chamber pressure instrumentation is designed for steady state operation and can not follow the oscillations. The engine has never been damaged by the oscillations. Performance sometimes decreases but with the thrust oscillating it is difficult to measure performance. The engine does not run hotter.

After the PRFT experience, additional tests were run with purposely saturated propellant in an effort to understand the problem. Also, oscillations occurred with ambient propellants where the float had sunk and where the float was working but the tanks were pressurized for a long period of time. Table I tabulates the engines and general conditions where oscillations occurred with nitrogen gas as the pressurant gas.

The thrust oscillations were not considered a serious problem because the engine was not damaged by the oscillations, the flight tanks would have bladders that would protect propellant from the pressurant gas, and the pressurant for the flight would be helium which is not as soluble as nitrogen.

However, about two months before the start of the qualification program Marquardt was directed to use helium as the pressurant gas and to run with helium saturated propellants during the Qualification Program. Because the engines characteristics with helium saturated propellants were unknown, a small program was conducted to investigate engine operation with helium saturated propellants, to develop saturation techniques, and ways of determining the saturation level. The first 3 engines in Table II are the three engines tested with helium saturated propellants during this program prior to qualification.

Partly because of the results of this program, oscillations did not occur at nominal O/F or thrust, but primarily because the overall program schedule was not long enough to permit the development of saturation techniques and complete the qualification program on schedule, the qualification program was conducted with unsaturated propellants. Helium was used as the pressurant gas but a limit was put on how long the propellant could be pressurized and on the tank level since it had been learned that both had an effect on the occurrence of thrust oscillations.

The engine successfully completed the qualification program without any oscillations.

THRUST OSCILLATION DUE TO NITROGEN GAS ACCIDENTLY INTRODUCED INTO THE ENGINE

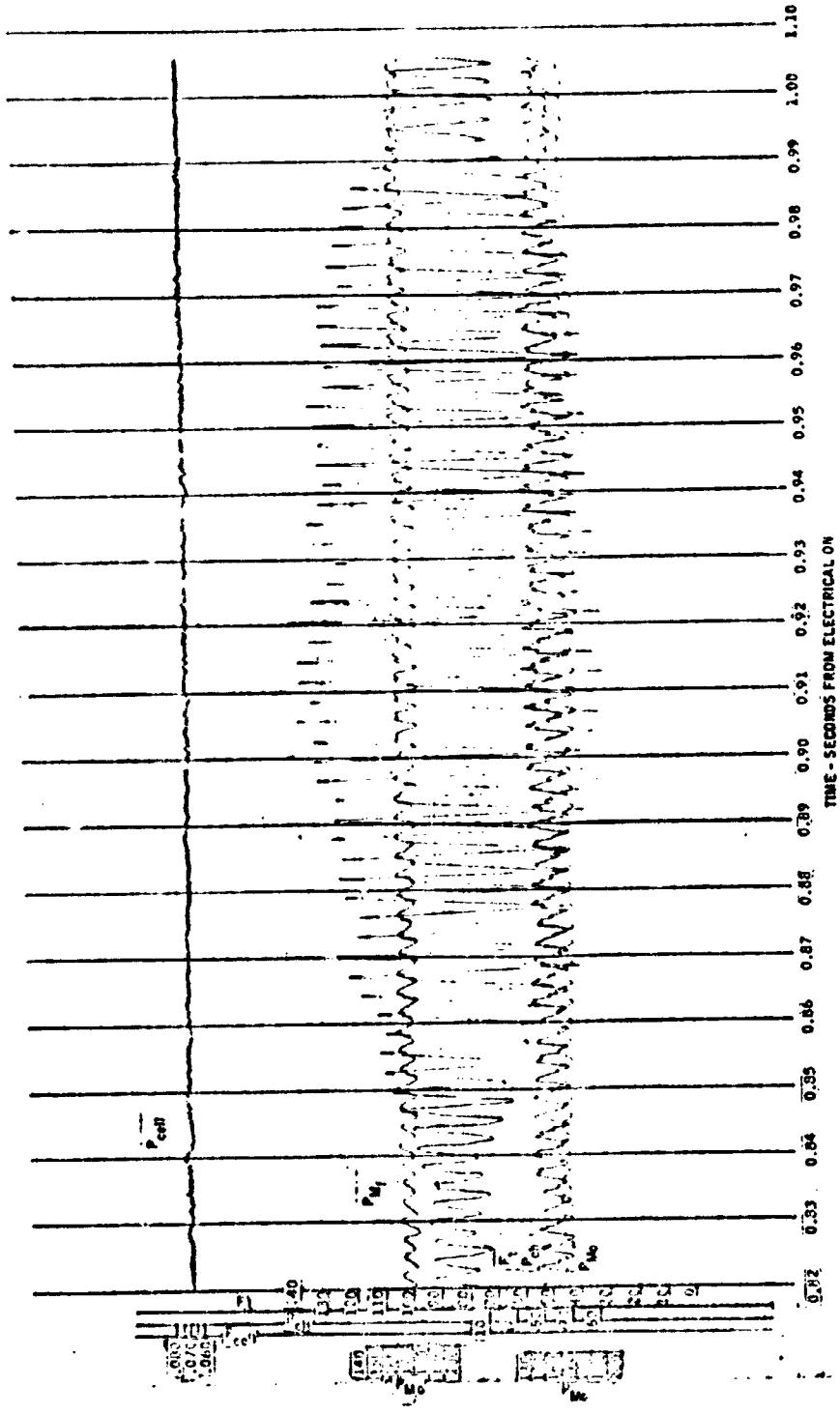

Figure 3

TABLE I

NITROGEN TESTS - PFRT

ENGINE AND TEST	DATE	CELL	RUNS	PROPELLANTS	REMARKS
X21424, S/N 0002 PFRT Acceptance Test	10/26/64	1	8710-11	N_2O_4-A 50	Due to N_2 in bypass line.
X21424, S/N 0001 PFRT Acceptance Test	10/31/64	1	8712-8722	N_2O_4-A 50	Due to N_2 in bypass line.
X21424, S/N 0001 Instability Invest. Test	11-1 to 11/2/64	1	8723-8743	N_2O_4-A 50	Due to N_2 in bypass line. Induced by introducing GN_2 into propellants.
X21424, S/N 0001 Appendix * - Calib. Tests	11/21 to 11/23/64	1	8822-8870	N_2O_4-A 50	Oscillated with propellants 90° or above Degassed for first time.
X21424, S/N 0001 Appendix B - Pulse Operation Survey	11/23 to 11/25/64	1	8871-8958	N_2O_4-A 50	Oscillated on one pulse run (8881)
X21424, S/N 0001 Appendix A - Calib. Test	12/2/64	1	9004-9015	N_2O_4-A 50	T_p = 95°. Degassed 2.0 to 2.5 hours before oscillating runs.
X21424, S/N 0003 Appendix A - Calib. Test	4/20/65	1	11159-11191	N_2O_4-A 50	(11188) Float sunk
X21424, S/N 0003 Appendix B - Pulse Operation Survey	4/21 to 4/22/65	1	11192-11275	N_2O_4-A 50	Float sunk
X21424, S/N 0003 Appendix N - Direct coil	4/22 to 4/24/65	1	11276-11289	N_2O_4-A 50	Float sunk
X21424, S/N 0003 Appendix W - Mission Duty Cycle	4/24/65	1	11290-11291	N_2O_4-A 50	Float sunk
X21424, S/N 0003 Appendix A - Calib. Test	4/25 to 4/27/65	1	11292-11322	N_2O_4-A 50	Float sunk

TABLE I (continued)

NITROGEN TESTS - PFRT

ENGINE AND TEST	DATE	CELL	RUNS	PROPELLANTS	REMARKS
X21424, X/N 0003 Appendix W - Mission Duty Cycle	4/27 to 4/28/65	1	11323-11325	N_2O_4-A 50	Float sunk
X21424, S/N 0003 Appendix A - Calib. Test	5/5 to 5/7/65	1	11938-11975	N_2O_4-A 50	Hot Propellants. Degassed and did not oscillate.
			NITROGEN TESTS - ACCEPTANCE		
227486, S/N 0007 Acceptance Test	2/26/65	1	10308-10317	N_2O_4-A 50	No degassing
227486, S/N 0012 Acceptance Test	2/26/65	6	7378-7386	N_2O_4-A 50	N_2 leak
227486, S/N 0020 Acceptance Test	3/25/65	1	10459-10467	N_2O_4-A 50	Degassed two hours, 35 min. before run.
227486, S/N 0024	4/10/65	6	7494-7505	N_2O_4-A 50	Degassed two hours before run.
227486, S/N 0022	4/12/65	6	7506-7515	N_2O_4-A 50	Degassed three hours before run.
228687-517, S/N 0560	10/25 and 10/27/67	6		N_2O_4-A 50	Float sunk
228687-517, S/N 0560	11/10/67	6		N_2O_4-A 50	Float sunk
228687-517, S/N 0551	11/15 to 11/16/67	6		N_2O_4-A 50	Float sunk
705762 FMR 5022-002	11/20 to 11/27/67	6		N_2O_4-A 50	Test to study time under pressure required to make an engine oscillate.

TABLE I (cont.)

NITROGEN TESTS - PFRT

ENGINE AND TEST	DATE	CELL	RUNS	PROPELLANTS	REMARKS
T-11042, S/N 0001-4	12/18/64	6	6555-6586	N_2O_4-A-50	Bubble N_2 through propellants.
T-11043, S/N 0001-1	12/31/64	6	6649-6663	N_2O_4-A-50	Bubbled N_2 through propellants. No oscillations.
T-11400, S/N 0001-11	1/7/65	1.	9943-9963	N_2O_4-A-50	100° not degassed.
T-116065, S/N 0001-5 DST Test	5/26 to 6/2/65	1	-	N_2O_4-A-50	.
228390-501, S/N 0001 Lunar Orbiter Qualification Test	3/29 to 11/8/65	Pad D	-	N_2O_4-A-50	Propellant purposely saturated at two levels by bubbling.

TABLE II

HELIUM TESTS

ENGINE AND TEST	DATE	CELL	RUNS	PROPELLANTS	REMARKS
X228439	7/8/65	1		N_2O_4-A-50	First test with He saturated propellants. No oscillations
T-12285, S/N 0001-1 Pre Qual.	7/12 to 7/30/65	1	L-301	N_2O_4-A-50	
T-12340, S/N 0001-1 Helium Effects		1		N_2O_4-A-50	
T-12321, S/N 0001-5 Contoured Valve Seat.	5/15/66	6	10484-10487	N_2O_4-A-50	Bubbled, no oscillation
T-11606, S/N 0001-15	7/13/66	1	3453-3471	N_2O_4-A-50	Bubbled He at 400 psia. No oscillation. Engine orificed for an O/F = 1.6.
T-14200, S/N 0001-7 MMH - DST Test	8/24 to 8/26/66	1	3608-3700	N_2O_4-MMH	
			APOLLO SUPPLEMENTAL QUAL		
228686-501, S/N 0049 Hot Calibration	10/10/66	1	3967-3987	N_2O_4-MMH	Unsaturated propellants.
228686-501, S/N 0234 Hot Calibration	10/15/66	1	4073-4092	N_2O_4-MMH	Unsaturated propellants.
228686-501, S/N 0049 Ambient calibration.	10/12/66	1	4015-4032	N_2O_4-MMH	Saturated by bubbling.
228686-501, S/N 0234 Ambient calibration	10/16/66	1	4094-4110	N_2O_4-MMH	Saturated by bubbling.
228686-501, S/N 0234 Orbit retrograde	10/20/66	1	4316	N_2O_4-MMH	Propellant stored at 180 psig helium pressure for 84 hrs. Did not oscillate
228686-501, S/N 0234 Mission ambient.	10/18/66	1	4111-4203	N_2O_4-MMH	Bubbled - did not oscillate
228686-501, S/N 0234 Mission hot.	10/19 to 10/20/66	1	4204-4299	N_2O_4-MMH	Bubbled - did not oscillate

TABLE II
(Continued)

HELIUM TESTS

ENGINE AND TEST	DATE	CELL	RUNS	PROPELLANTS	REMARKS	
			LM SUPPLEMENTAL QUAL			
228686-501, S/N 0331 Cold calibration	12/29/66	1	4773-4793	N_2O_4/A-50	Saturated by stirring. oscillation.	No
228686-501, S/N 0261 Cold calibration	1/17/67	1	4949-4969	N_2O_4/A-50	Saturated by stirring. oscillation.	No
228686-501, S/N 0261 Mission abort	1/14/67	1	4926-4928	N_2O_4/A-50	Saturated by stirring. oscillations.	No
228686-501, S/N 0331 Ambient calibration	11/29/66	1	4597-4613	N_2O_4-A-50	Saturated by stirring. oscillations.	No
228686-501, S/N 0261 Ambient Calibration	12/1/66	1	4641-4658	N_2O_4-A-50	Saturated by stirring. oscillations.	No
228686-501, S/N 0261 Ambient calibration	1/3/67	1	4817-4827	N_2O_4-A-50	Saturated by stirring. oscillations.	No
228686-501, S/N 0331 Ambient calibration	12/30/66	1	4794-4810	N_2O_4-A-50	Saturated by stirring. oscillations.	No
228686-501, S/N 0261 Ambient calibration	1/18/67	1	4910-4986	N_2O_4-A-50	Saturated by stirring. oscillations.	No
228686-501, S/N 0331 Hot calibration	12/26/66	1	4755-4771	N_2O_4-A-50	Saturated by stirring. oscillations.	No
228686-501, S/N 0261 Hot calibration.	1/16/67	1	4930-4946	N_2O_4-A-50	Saturated by stirring. oscillations.	No

After the Qualification program a saturation technique was developed. To saturate the propellants the tanks are pressurized to the desired pressure and slowly stirred for a given amount of time. The amount of gas dissolved in the propellant is determined by freezing a sample of propellant, exposing the frozen sample to an evacuated volume, recording the pressure increase in the volume and identifying the gas constituents. JPL conducts the analysis in their laboratory. By running a few controlled tests, it is possible to determine the stirring time required at a given pressure to reach the desired saturation level.

Another method used to saturate the propellant was to bubble the gas through the tank from the bottom. The disadvantage of this technique is that it may supersaturate by leaving entrained bubbles in the propellants. This technique was used during the test just prior to the Qualification tests and during the Lunar Orbiter program. It was also used after the Qualification program before the stirring technique was developed.

Two formal programs were run after Qualification with saturated propellants. The Service Module MMH Supplemented Qualification test with bubbled propellants and the Lunar Module A-50 Supplemented Qualification tests with stirred propellants. In the Service Module test oscillations occurred. But it is felt that the oscillations were due to entrained bubbles in the propellant rather than just saturated propellants. No oscillations occurred during the Lunar Module tests.

Today all Apollo testing is done with helium pressurization except for the acceptance tests which still use nitrogen; since the engine performance is the same with both and the tests have always been run with unsaturated propellants.

The only steady state testing done with a known level of helium saturated propellants has been on another program. The results of these tests have lead to a conclusion that the engine will oscillate if the amount of gas that comes out of solution exceeds a certain value.

III. THRUST OSCILLATIONS

Dissolved or entrained gas in the propellants may cause thrust oscillations. This was first discovered during the PFRT program when a test facility operational error introduced nitrogen into the propellants. Since that time many tests have been run to understand under what conditions, with either nitrogen or helium as the pressurants, oscillations occur.

A. Nitrogen

Tabulated in Table 1 are those engines that have oscillated with nitrogen as the pressurant. The results from these tests are reviewed below in some detail.

PFRT Tests

During the acceptance test of PFRT engines 1 and 2, thrust oscillations occurred (Run 8711 for engine 1 and 8713 for engine 2). The cause of the oscillations was that nitrogen gas was mistakenly being introduced into the propellants (FMR's 279-056 and 054). The oscillations were duplicated on Runs 8723-8743 by purposely injecting nitrogen into the propellants. A copy of the oscillograph for the two cases is shown in Figures 3 and 4.

During calibration tests with warm propellants (90° or greater) the engine oscillated again. Tabulated in Table III are the runs from 8826 to 8867 showing the test conditions. Several conclusions were reached from this test. One, if the propellants were hotter than 90° the engine would oscillate, but if the propellants were degassed by venting the tanks when the propellants were hot, the engine would not oscillate. Also, the oscillations were somewhat random in that the engine did not always oscillate with hot propellants.

During this time period the main propellant storage tanks were kept at a pressure of around 100 psig so that the propellants were already saturated to this pressure when they were loaded into the run tank. Furthermore these specific tests were run during the winter when the propellants were cold (40°-60°) and they could absorb more gas. Consequently it was postulated that it was necessary to degas hot oxidizer to drive out the gas absorbed during storage and also any gas that was absorbed while the propellants were in the run tanks.

Engine No. 3 oscillated with hot propellants (Runs 9007 and 9008) even though these propellants had been degassed. However, the time between degassing and the runs was 2.5 hours. It was felt that 2.5 hours under pressure was enough time for the propellants to become saturated enough to cause thrust oscillations.

Engine 3 oscillated during the period from April 21 to April 28, 1965. After the testing on the 28th, the float was found to be sunk and it is thought that the oscillations that occurred on these runs were because the propellant became saturated very quickly without the float to act as a barrier between the propellant and the pressurant.

Engine No. 3 oscillated with hot degassed propellants during the calibration tests; Runs 11955, 11956, 11959 and 11960. This test showed that with hot propellants (100°F) and the float installed, the propellants became saturated enough in about an hour to cause oscillations. Two sets of runs were made after degassing. They are tabulated below.

THRUST OSCILLATION DUE TO NITROGEN GAS PURPOSELY INTRODUCED INTO THE ENGINE

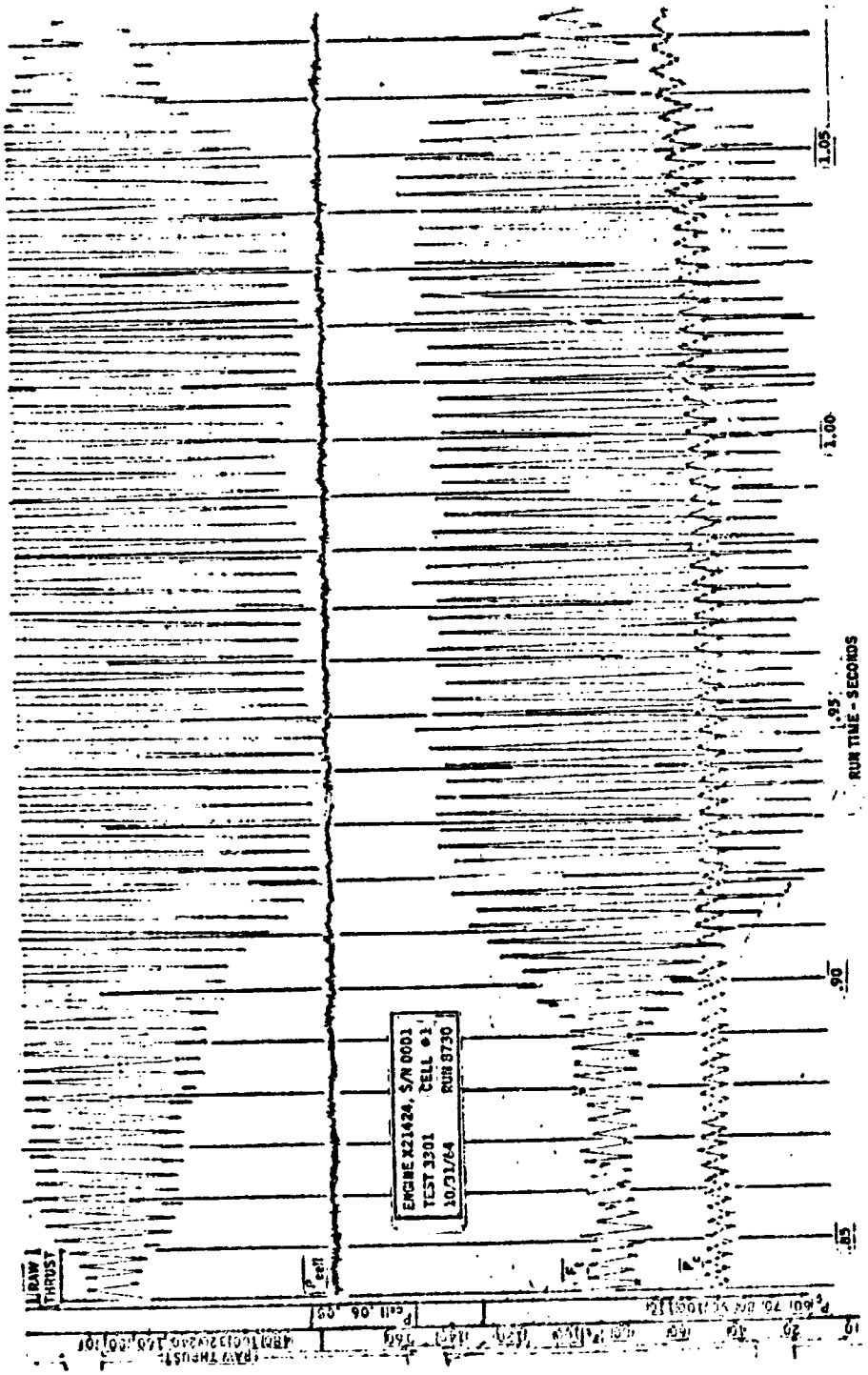

Figure 4

TABLE III

WARM PROPELLANT TEST RESULTS

UNDEGASSED						DEGASSED (oxidizer)					
Stable	Unstable	T<90	T>90	Bypassed	Refill Tanks	Stable	Unstable	T<90	T>90	Bypassed	Refill Tanks
	8826		×	No		8857			×	No	
	8827		×	No		8858			×		
8828		×		No		8859			×		
8829		×		No		8860			×		
8830			×	No							
	8831		×	No							
	8832		×	No							
	8833		×	No							
	8834		×	No							
	8835		×	No							
8836		×		No							
8837		× Fuel	× Ox	No							
	8838	× Fuel	× Ox	No							
8839		× Ox	× Fuel	No							
8840		× Ox	× Fuel	No							
	8841		×	No							
	8842		×	No							
	8843		×	No							
	8844		×	Yes							
	8845		×	Yes							
8846		×		No							
8847		×		No							
8848		×		No							
8849		×		Yes							
8850		×		Yes							
	8851	×		No							
8852		×		No							
8853		×		No							
8854		×		No							
	8855	×		No							
	8856		×	No							
*8861			×	No							
*8862			×	No							
*8863			×	No							
	8864		×	No							
	8865		×	No							
	8866		×	No							
	8867		×	No							

DEGASSED - Tank heated to 100°F with no tank pressurization and let set. Pressurize and cool off to run.

*Probably degassed propellants as tanks were reloaded after only three 5 second runs. It's normally done after 7 or 8.

un Sequence 1
egas complete at 18:25

Run		Time	Comments
11952	(5 sec.)	18:32	Normal Thrust
11953	(5 sec.)	18:42	Normal Thrust
11954	(5 sec.)	18:55	Normal Thrust
11955	(5 sec.)	19:05	Slightly unstable
11956	(5 sec.)	19:24	Highly unstable

Run Sequence 2
Degas complete at 20:17

Run	Time	Comments
11957	20:28	Normal Thrust
11958	21:17	Normal Thrust
11959	21:32	Slightly unstable
11960	21:40	Highly unstable

Development Tests

Special tests were made during the development program with purposely saturated propellants. Also some engines oscillated because the propellants became saturated during the normal testing.

T-11042, S/N 0001-4 12/18/64 Cell I - Runs 6555-6586

The primary objective of this test was to determine the thermal characteristics of the PFRT engine with a pyrolytic graphite chamber seal. At a part of this test three 80 second runs were made with propellant that had nitrogen gas bubbled through it for 10 minutes. For one run the oxidizer was bubbled, for another run the fuel was bubbled; the third both propellants were bubbled. The results are tabulated below.

Run	Propellants Bubbled	Comments
6584	Fuel	Normal
6585	Oxidizer	Oscillated
6586	Both	Oscillated

During the bubbling the tank pressure was maintained above the run pressure. Before the engine was fired, the propellants were held at the run set pressure for 5 minutes.

When the oxidizer was saturated or both propellants were saturated, the engine oscillated at 350 cps with a peak to peak amplitude of 25 lbs. When the fuel was saturated the engine did not oscillate.

T-11043, S/N 0001-1 12/31/64 Cell 6 - Runs 6649-6663

The primary objective of this test was to determine at what saturation pressures the engine did and did not oscillate. The propellants were saturating by bubbling nitrogen through them at pressures of 100, 140, 170 and 200 psia for 10 minutes. Each propellant was saturated separately and then both together for a total of 12 runs. The runs were made at the normal tank pressures (190 psia).

The engine did not oscillate on any of these runs.

Run	Bubbling Pressure	Propellant	Results
6652	140	Oxidizer	Normal
6653	170	Oxidizer	Normal
6654	200	Oxidizer	Normal
6655	100	Oxidizer	Normal
6656	140	Fuel	Normal
6657	170	Fuel	Normal
6658	200	Fuel	Normal
6659	100	Fuel	Normal
6660	140	Both	Normal
6661	170	Both	Normal
6662	200	Both	Normal
6663	200	Both	Normal

This engine was a little different than the normal PFRT engine. Instead of 8 coolant holes for the preigniter and main chamber it had four fuel coolant holes for the preigniter and four for the chamber. Also the pressure drop across the final fuel orifices had been increased by 10 psi by decreasing the fuel doublet diameter.

In the previous test with engine T-11042-001-4 there was a five (5) minute wait after bubbling before the run was made. In this test the run was made within a few minutes of the end of bubbling.

T-11400, S/N 0001-11 1/7/65 - Cell 1 Runs 9943-9663

The objective of this test was to determine engine performance. Three runs oscillated with hot undegassed propellant. The oscillating runs occurred between 1-2 hours after the tanks had been pressurized which was similar to previous experience during PFRT.

T-11606, S/N 0001-5 - DST Test 5/26/65 to 6/3/65 Cell 1
Runs 12,016 to 12,097

As part of the DST test, prior to qual, a series of runs were made to investigate the effect of time from degassing to run, propellant temperature and tank level on the occurrence of thrust oscillations.

Tabulated on Table IV are the special tests made to investigate the time level, and temperature effect.

With propellant temperatures of 100° the engine oscillated if the run was made more than 3/4 hour after degassing. The propellants were pressurized to the normal tank pressure right after degassing. Note from the table that usually four or five runs were made from one degassed load of propellants and that the engine usually oscillated on the fourth or fifth run which was 3/4 to 2 hours or more after degassing. The tank level at this time was also generally about 1/4 full.

There is a general belief that tank level also has an effect; that the engine will oscillate with saturated propellant if the tank level is low. This is indicated by the fact that most of the time when the engine oscillated, the tanks were only about 1/4 full. However, several runs indicate that this is not always true. Runs 12031, 12071 and 12074 oscillated with the tank more than 1/2 full.

Most of the runs during this test were with 100° propellant. A series of four runs were made with 80° propellant. The last run of the series made 1.5 hours after degassing, did not oscillate. This seems to indicate that 80° propellant does not become saturated as quickly as 100° propellant or does not become saturated enough to cause oscillations as rapidly as the 100° propellant.

Acceptance Tests

All engine acceptance testing is done with nitrogen as the pressurant. Several engines have oscillated during acceptance test. These engines are tabulated in Table I. Each engine passed a later acceptance test after the propellants were degassed.

Serial number 7 oscillated when the propellants were pressurized 4.75 hours before the run and the propellants had not been degassed.

Serial number 12 oscillated because there was a nitrogen gas leak into fuel during the engine run.

Serial numbers 20, 22, and 24 oscillated after the propellant tanks had been pressurized for 2-3 hours before the run.

Serial numbers 560 and 551 oscillated because the float had sunk. A failure investigation (FMR 5022-002) that used engine 705762 showed that if the tanks were pressurized for 1 hour without the float, the engine would oscillate.

TABLE IV

EFFECT OF TIME, PROPELLANT TEMPERATURE AND TANK LEVEL ON OSCILLATIONS T-11606, S/N 0001-5

Run	Length	Operation	Tp	Time From Degas	Level cm
12018	5	Unstable	100	3.5	28.5
12019	5	Stable	100	Did not degas	48.6
12020	5	Stable	100	Did not degas	56.8
12021	5	Stable	100	25 min.	32.1
12022	5	Stable	100	1.25	30.6
12023	5	Unstable	100	1.6	27.6
12024	5	Unstable	100	1.8	25.6
12025	5	Unstable	100	2.1	23.6
12026	5	Unstable	100	2.5	21.3
12027	5	Stable	100	.75	47.5
12028	5	Stable	100	1.0	44.4
12029	5	Unstable	100	2.1	41.7
12031	5	Unstable	100	1.0	43.5
12032	5	Unstable	100	1.5	28.0
12033	5	Stable	100	10 min.	47.3
12034	5	Stable	100	1.0	34.1
12035	5	Stable	100	1.3	28.2
12036	5	Unstable	100	1.6	21.9
12037	5	Stable	100	.5	45.2
12038	5	Stable	100	.75	32.0
12039	5	Stable	100	1.0	26.4
12040	5	Unstable	100	1.4	20.5
12041	5	Stable	100	.6	45.5
12042	5	Stable	100	1.0	33.5
12043	5	Stable	100	1.5	27.6
12044	5	Unstable	100	2.0	21.9
12045	5	Stable	100	.5	39.4
12046	5	Stable	100	.75	26.3
12047	5	Unstable	100	1.1	20.8
12048	5	Stable	100	.6	40.8
12049	5	Stable	100	1.2	28.3
12050	5	Unstable	100	1.9	22.0

TABLE IV (continued)

EFFECT OF TIME, PROPELLANT TEMPERATURE
AND TANK LEVEL ON OSCILLATIONS T-11606, S/N 0001-5

Run	Length	Operation	Tp	Time From Degas	Level cm
12051	5	Stable	100	.3	42.7
12052	5	Stable	100	.9	30.2
12053	5	Unstable	100	1.0	24.3
12054	5	Stable	100	.25	42.8
12055	5	Stable	100	.5	30.4
12056	5	Stable	100	.75	24.2
12057	5	Unstable	100	.8	18.0
12058	5	Stable	100	.2	43.8
12059	5	Stable	100	.5	30.8
12060	5	Stable	100	.75	24.6
12061	5	Unstable	100	1.0	18.3
12062	5	Stable	80	1.75	- From Pulse Tubes, Tanks vented.
12063	5	Stable	80	2.0	- From Pulse Tubes
12064	5	Stable	85	?	- Pulse Tube Run
12065	5	Stable	85	?	-
12066	5	Stable	85	?	-
12067	5	Stable	85	?	-
12068	5	Stable	85	?	-
12069	43	Stable	85	0	40.5
12070	46	Stable	100	0	41.7
12071	50	Unstable	100	1	38.7
12072	50	Stable	100	1.2	45.7
12073	50	Stable	100	1.0	46.6
12074	60	Unstable	100	.75	40.1
12075	5	Stable	70	.5	47.1
12076	5	Stable	70	1.0	38.1
12077	5	Stable	70	1.1	-
12078	5	Stable	70	1.5	30.8

TABLE IV (continued)

EFFECT OF TIME, PROPELLANT TEMPERATURE
AND TANK LEVEL ON OSCILLATIONS T-11606, S/N 0001-5

Run	Length	Operation	Tp	Time From Degas	Level cm
12079	10/490	Stable	100	5.75	-
12080	10/490	Stable	100	7.5	-
12081	10/490	Stable	100	9.3	-
12082	13/487	Stable	100	10.3	-
12083	15/485	Stable	100	10.8	-
12084	15/485	Stable	100	11.25	-
12085	20/20	Stable	100	11.8	-
12086	20/480	Stable	100	12.25	-
12087	40/10	Unstable	100	12.50	-
12088	40/10	Stable	100	-	-
12089	30/470	Stable	100	.5	-
12090	40/410	Stable	100	.75	-
12091	60/100	Stable	100	1.0	-
12092	100/100	Stable	100	1.25	-
12093	200/300	Unstable	100	1.8	17.0
12094	500/100	Unstable	100	2.5	16.0

Lunar Orbiter

The R-4D engine used on the Lunar Orbiter Vehicle is pressurized by nitrogen gas. As part of its Qualification Program, it was operated with propellants saturated with nitrogen gas by a bubbling process. The engine oscillated with what was called 90% saturation and did not oscillate with a 60% saturation level.

Nitrogen was bubbled through the propellants by a perforated circular tube located at the bottom of the tank. For the 90% level the ullage pressure was raised from 176 to 186 psia and then vented back to 176 psia. Each cycle took 15 minutes and it was performed 8 times in about two hours. Following the bubble cycles, the ullage pressure was maintained at the saturation pressure for at least 30 minutes prior to the pressure required for the run. The saturation procedure for 90% level is shown graphically in Figure 5. For the 60% saturation level, the ullage pressure was raised from 134 to 144 psia in 15 minutes and then vented back to 134 psia. The float was installed for these tests.

The Lunar Orbiter has flown four (4) flights without thrust oscillations occurring. Thrust and I_{sp} of the engine have agreed within 1% of the ground test data.

Conclusion - Nitrogen

Summarizing what we know about the effect of nitrogen as a pressurant on thrust oscillations:

1. Nitrogen entrained (bubbles) or nitrogen saturated (to an unknown level) propellant will cause thrust oscillations.

2. With hot propellants and the float installed oscillations will occur if the propellants are not degassed. If they are degassed, oscillations may occur if the propellants are pressurized for 3/4 of an hour before the run.

3. If the float sinks oscillations will occur with ambient propellants after 1 hour at pressure.

4. With the float working, oscillations will occur with ambient propellants after 2-3 hours at pressure.

5. Based on the Lunar Orbiter tests, the propellants must be saturated to a pressure greater than 134-144 psia before oscillations will occur.

PROCEDURE FOR NITROGEN SATURATION OF PROPELLANTS TO 90% SATURATION LEVEL

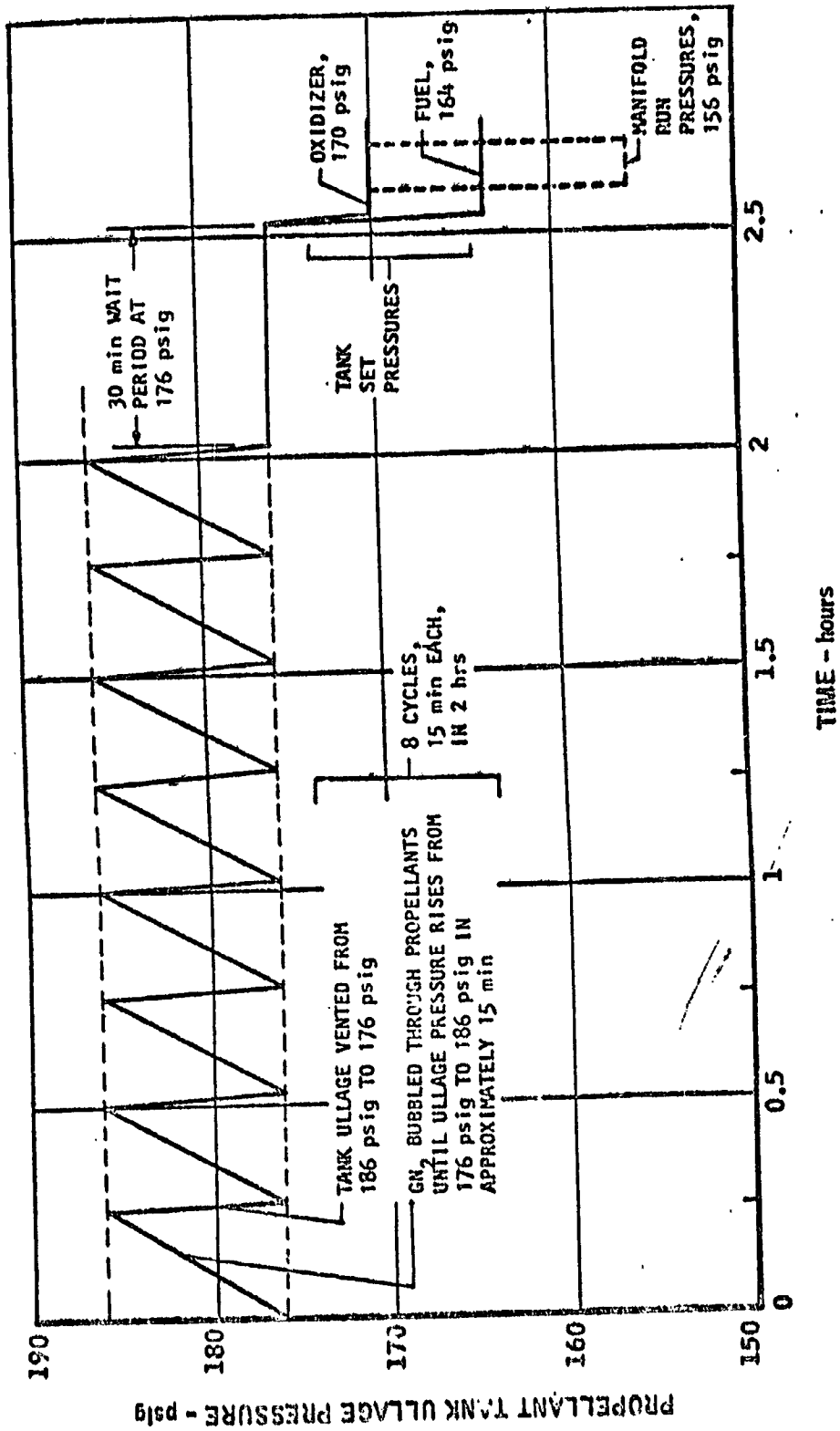

Figure 5

B. Helium

Tabulated in Table II are those engines that have oscillated or been tested with helium saturated propellants. The results from these tests are reviewed below.

X-228439, S/N 0001-2 — 7/8 to 7/9/65 Cell 1, Runs 12327 - 12340

This test was the first made with helium as the pressurant. Ten runs were made with helium dissolved in the propellants. Thrust oscillations did not occur. Under similar test conditions the engine oscillated with nitrogen dissolved in the propellants. With both gases the propellants were saturated by bubbling for 20 minutes prior to a run. Table V shows the test conditions.

T-12285, S/N 0001-1 - Pre-Qualification Test — 7/12 to 7/30/65 Cell 1, Runs 1 - 301

This test was the Pre-qualification test, run to confirm that the engine and test facility (including procedures) were ready for the Qualification test. Helium was the pressurant gas. The engine oscillated four times during the test. Table VI shows the conditions for these runs and three other runs that did not oscillate.

The first time on Run 169 the propellant was purposely saturated by bubbling helium through the propellant for four hours at 250 psia with the propellants at 100°F. Just before the run, the tanks pressure was reduced to 170 psia and the propellant cooled to 40°F. It was thought that the propellant would hold more helium hot than cold, so saturating hot and running cold would be the most severe test. The engine oscillated for the last 10 seconds of the 20 second run.

The rest of the runs were made with propellant that had been pressurized for different lengths of time. Oscillations occurred when the tanks had been pressurized for 4, 7 and 8 hours and they did not occur when pressurized for 2.2, 2.0 and 3.0 hours. The tank level of those runs that oscillated was also less than 1/2 full. Consequently, for the Qualification tests, the propellant tanks were reloaded when they became less than 1/2 full and if they had been pressurized for 4 hours. The engine did not oscillate during the Qualification test.

T-12340, S/N 0001-1 - Helium Effects Test — 8/1 to 8/5/65 Cell 1, Run 302 - 411

The objective of this test was to document engine performance, both steady state and pulsing, at design and off design mixture ratios and thrust levels using propellants containing helium gas.

ENGINE 228439 - CELL 1 DATE: JULY 8 and 9, 1965

TABLE V

Run	Length	Dissolved Gas	Bubbling Pressure Ox/Fuel (psia)	Tank Set Pressure Ox/Fuel (psia)	Bubbling Temperature Ox/Fuel °F	Run Temperature Ox/Fuel °F	Normal Engine Operation	Remarks
12327	5.0 sec.	Nothing	-	181.6/176.1	-	68/67	Yes	Trim run with N_2 gas.
12328	5.0 sec.	Nothing	-	182.5/177.3	-	69/68	Yes	Trim run with N_2 gas.
12329	55.0 sec.	He	182.4/176.9	182.3/176.8	40/40	38/40	Yes	
12330	50.0 sec.	He	182.9/177.4	182.8/177.3	90/90	85/88	Yes	
12331	28.0 sec.	He	181.3/176.3	180.3/176.3	100/100	48/50	Yes	Facility problem shutdown run - no performance data.
12332	40.0 sec.	He	181.8/177.3	181.8/177.3	40/40	79/108	Yes	
12333	35.0 sec.	He	181.3/176.3	181.3/176.3	100/100	36/38	Yes	
12334	55.0 sec.	He	250/250	181.3/176.3	36/36	40/41	Yes	
12335	55.0 sec.	He	250/250	181.3/176.3	100/100	96/99	Yes	
12336	72.0 sec.	He	250/250	182.3/177.3	40/40	101/108	Yes	
12337	47.0 sec.	He	250/250	181.8/177.3	100/100	43/47	No*	Engine not primed.
12338	54.0 sec.	He	250/250	181.8/177.3	100/100	40/44	Yes	Repeat of Run 12337.
12339	63.0 sec.	N_2	182.3/177.3	182.3/177.3	104/110	96/108	No**	N_2 test.
12340	74.0 sec.	Nothing	-	182.3/177.3	-	104/99	Yes	N_2 gas as pressurant.

*Ran out of oxidizer on previous run. Did not prime engine. Thrust oscillations noted during first 2 seconds of run, due to gas in line.

**Thrust oscillations of ± 15 pounds experienced throughout run.

A-1080

TABLE VI

PRE-QUALIFICATION TEST WITH HELIUM

T-12285, S/N 0001-1

Run	Length (secs.)	Operation	Tp	Time Under Pressure	Tank Level	Remarks
169	20	Unstable	40°	-	-	Bubble for 4 hours at 100° and 250 psia
255	10	Unstable	100°	8 hrs.	20 cm	
262	5	Unstable	70°	7 hrs.	-	Pulse Tube Run
268	17	Unstable	100°	4.2	3/8 Full	
299	5	Stable	100°	2.2	50 cm	
300	5	Stable	100°	2.0	44 cm	
301	5	Stable	100°	3.0	-	

The propellants had been stored in the main storage tanks under helium gas at a total pressure of 180 psia. The main storage tanks were at this pressure from one day before the test to the end of the test. In addition, each run tank load of propellants was treated in the following manner to attempt to saturate them with helium.

1. Helium was bubbled through the propellants from a ring in the bottom of the pulse tank for 5 minutes at 180 psia and the run temperature.

2. The tank was held at 180 psia and the run temperature for 15 minutes with no helium bubbling.

3. Steps 1 and 2 were repeated three more times.

At no time during the test was the pressure reduced below 180 psia except during off-design runs (O/F = 2.2, F = 90 pounds, etc.). The helium was always bubbled through the propellant at a pressure of 180 psia even when the run pressures were lower or higher than 180 psia. When the propellants were transferred from the storage tanks to the pulse tanks, the pressure was held above 180 psia to avoid outgassing of the propellants.

Run Conditions Where Thrust Oscillations Occurred

The engine was tested at nominal O/F's of 1.8, 2.0, and 2.2 at 100 pounds thrust, and thrusts of 90 and 120 pounds at an O/F of 2.0. Nominal propellant temperatures were 40°, 75°, and 100°F. Both pulse and steady state runs were made at each condition. The steady state runs were made in duty cycle groups of three to determine the effect of hot injector head on both performance and the occurrence of thrust oscillations. Injector head temperature at the start of the third run of a sequence was greater than 200°F due to soakback from the first two runs.

Table VII lists the runs made at each condition and indicates whether oscillations did or did not occur. As shown, oscillations occurred 12 times. These oscillations can be divided into two types; those caused by dissolved helium in the propellants, and those probably caused by bubbles of helium entrained in the propellants.

A bubble in the propellant usually resulted in short duration oscillations, while the dissolved gas resulted in long duration oscillations. An example of short duration oscillations is shown in Figure 6. Seven of the thrust oscillations were apparently due to dissolved helium and five to entrained bubbles. Three thrust oscillation periods occurred at nominal conditions of 100 pounds thrust and O/F of 2.0, but in each case the oscillations appeared to be due to entrained gas and not dissolved gas. Two of these (Runs 309-3 and 325-1) lasted for only 200 milliseconds and were probably the result of entrained helium bubbles. The third (Run 382) was the result of poor priming prior to the test that left helium gas in the propellant lines upstream of the engine.

TABLE VII

HELIUM TEST RUN SUMMARY

Helium Test Run Summary Engine T12340-001-1 Cell 1 August 1-5 1965. Propellants Stored under 180 PSIA Helium Pressure and Conditioned by Bubbling Helium thru Propellants at 180 PSIA for 5 Minutes, Waiting 15 Minutes and Repeating 3 More Times.

Nominal O/F	Thrust (lbs.)	Nominal Propellant Temperature					
		40°		75°		100°	
		Normal	Oscillations	Normal	Oscillations	Normal	Oscillations
1.8	100	367-1 367-2 367-3	None	350 357-1 351 357-2 352 357-3	None	362-2 362-3	362-1**
2.0	100	325-2 326-2 325-3 326-3 326-1	325-1*	302 309-1 303 309-2 308 383	309-3* 382**	315 316 317	None
2.2	100	347-1 347-2	347-3	328 336-2 329 336-3 330 335 391 336-1	327* 336-4	341-1 341-2 341-3	None
2.0	90	None	411-1 411-2 411-3 411-4	391 401-1 392 401-2 393 401-3	None	406-1 406-2	40[illegible]-3
2.0	120	390-1 390-2 390-3	None	368 376-1 369 376-2 370 376-3 371	None	381-1 381-2 381-3	None

* Oscillation caused by entrained bubbles

**Oscillation cuased by poor priming that left bubbles in the propellant lines.

SHORT DURATION OSCILLATION

T12340, S/N 0001 RUN 309-3

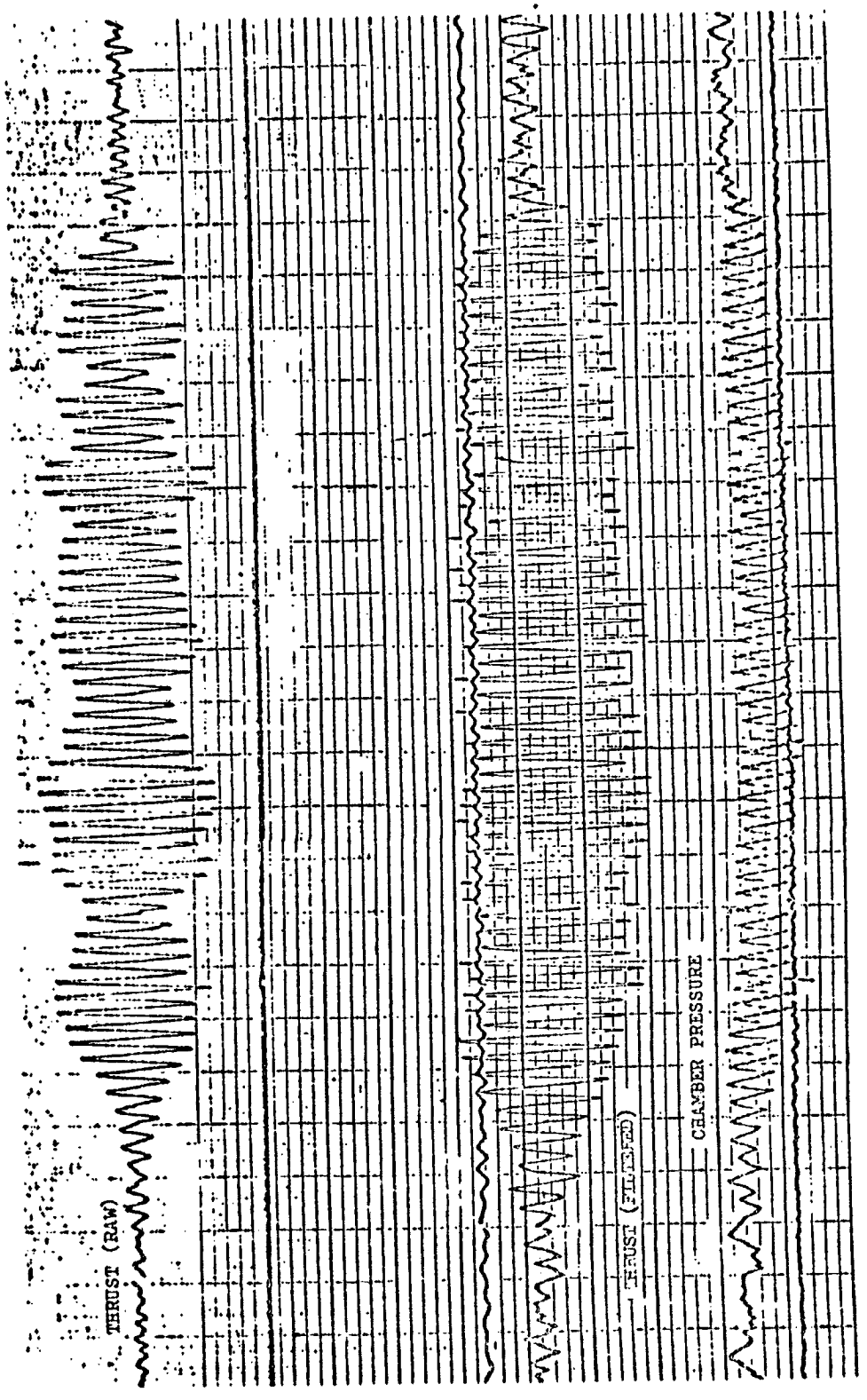

Figure 6

The steady state run data are plotted on Figures 7 and 8 as a function of thrust level and O/F ratio. The shaded symbols in Figure 7 are runs where oscillations occurred, and the open symbols denote normal operation. Only those runs where oscillations occurred are plotted on Figure 8, but the oscillations are separated into two types; those of long duration (probably due to dissolved gas), and those due to gas bubbles in the propellants which were indicated by the short duration of the oscillations. No oscillations due to dissolved gas occurred at the design point O/F of 2.0 and thrust of 100 pounds.

One purpose of running the steady state runs in a group of three was to evaluate the effect of high injector head temperatures on the occurrence of thrust oscillations. Tabulated below are the seven runs where oscillations occurred due to dissolved gas, along with the correponding head temperature.

Run	Head Temperature
336-4	209°
347-3	275°
406-3	264°
411-1	113°
411-2	154°
411-3	246°
411-4	220°

These data indicate that thrust oscillations occur more frequently with elevated head temperatures (200° or greater) since the first three runs tabulated were the third run of sequences of three where the first two runs of the group were at lower temperatures and oscillations did not occur. This implies that oscillations are more likely to occur with a hot injector head, but that a hot head is not the only requirement for oscillations to occur as indicated for Runs 411-1 and -2 where head temperatures were significantly lower.

T-12321, S/N 0001-5 - Contoured Valve Seat — 5/15/66 Cell 6, Runs 10484-10487

One model to explain why the engine oscillates with saturated propellants is that the static pressure in the oxidizer valve seat is low enough (85 psia) to cause gas cavitation. If this model is correct, a fix would be to redesign the oxidizer valve seat to eliminate the cavitation. The oxidizer valve for this test was contoured to eliminate this effect. Two runs were made with saturated helium at conditions where thrust oscillations had occurred with other engines. The contoured valve seat engine did not oscillate.

Testing was conducted with N_2O_4/A-50 propellants saturated with helium. The saturation procedure consisted of bubbling helium gas from the bottom to the top of the propellant pulse tank at an initial tank pressure of 178 psig and allowing

THRUST OSCILLATION SUMMARY

ENGINE T-12340-001-1, CELL 1, 8-1 to 8-5-65

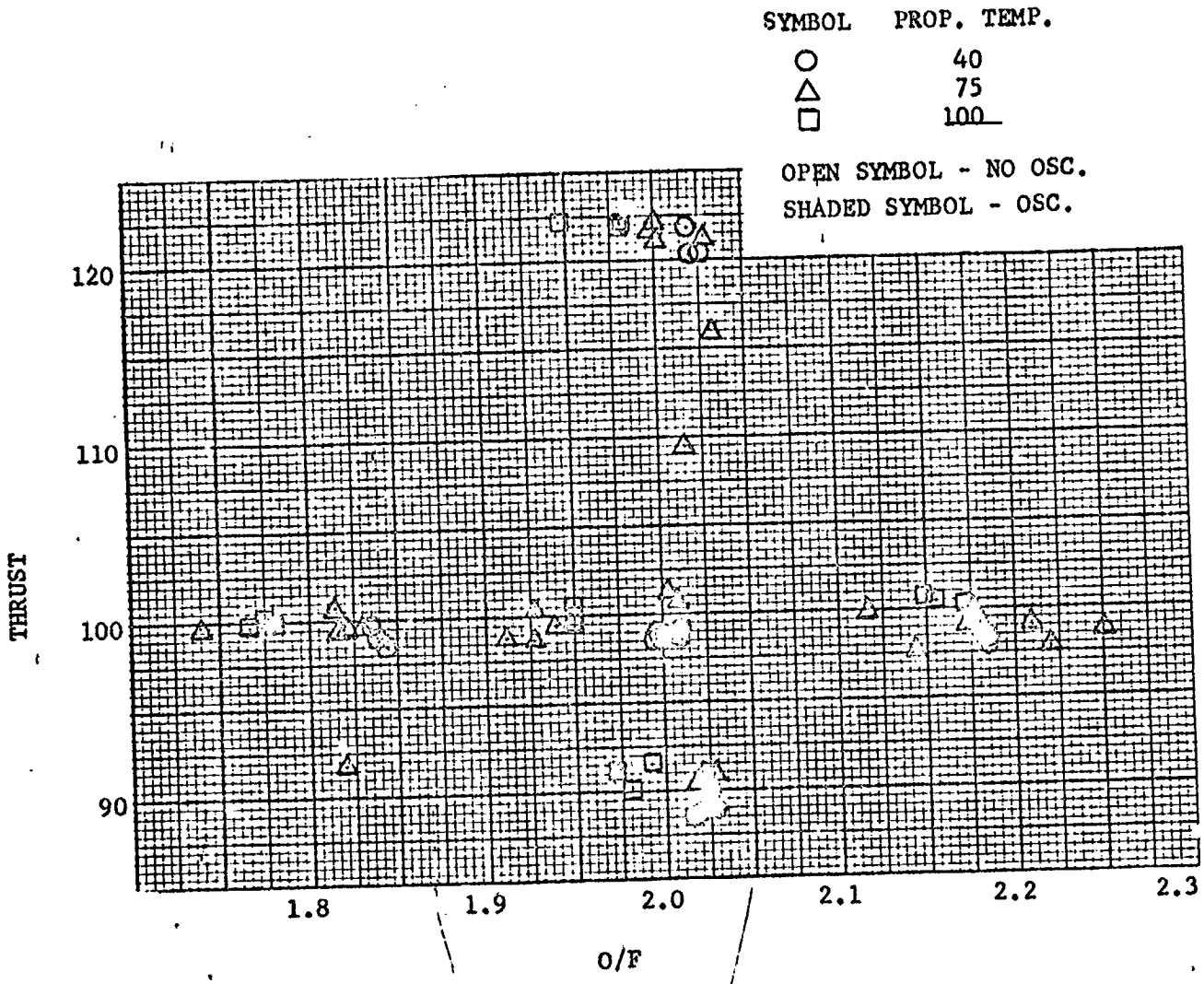

Figure 7

THRUST OSCILLATION SUMMARY

ENGINE T-10340-001-1, CELL 1, 8-1 to 8-5-65

OPEN SYMBOLS - SHORT DURATION OSCILLATIONS
SHADED SYMBOLS - LONG DURATION OSCILLATIONS

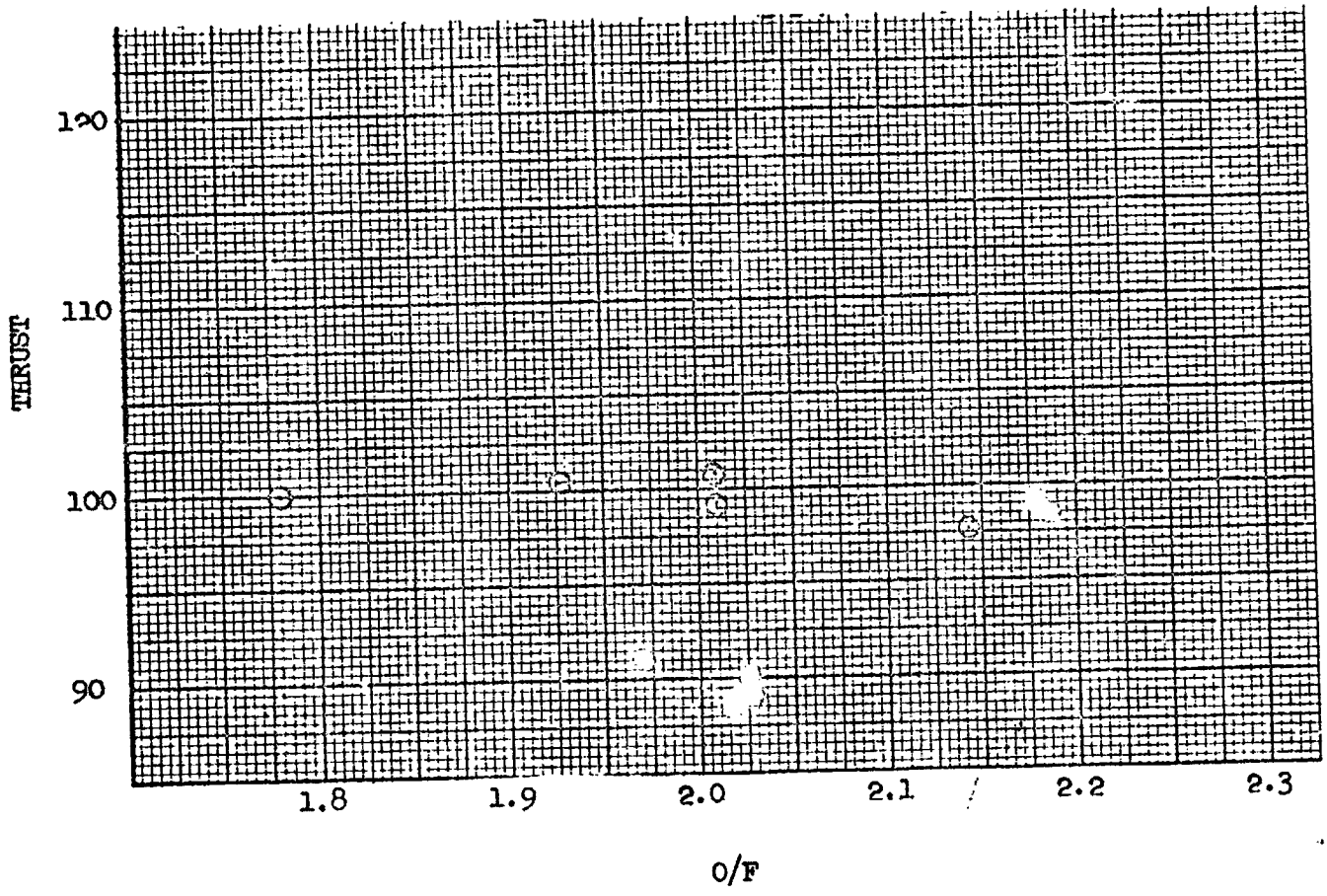

Figure 8

the pressure to increase to 190 psig over a 15 minute period. At the end of this period, the tank was vented and pressure reduced to 178 psig. This cycle was repeated 3 times. Pressure was then held at 178 psig for 30 minutes, reset to run pressures and firing within one minute. All test firings were conducted with propellants at ambient temperature. The quantitative degree of gas saturation using this procedure with helium has not yet been specifically determined. However, previous tests have resulted in thrust oscillations under less stringent saturating conditions.

The runs which were conducted are as follows:

Run No.	Duration (sec.)	O/F	F_N LBF	I_{sp} (sec.)	Remarks
10484	5	2.19	100	267	Unsaturated
10485	50	2.17	100	267	Unsaturated
10486	50	2.18	100	267	Saturated
10487	50	2.17	100	267	Saturated

The O/F and thrust level conditions for the runs were selected on the basis of conditions at which previous engines had demonstrated thrust oscillations with the standard valve configuration.

A copy of a section of the oscillograph record for Runs 10485 and 10487 is shown in Figures 9 and 10, respectively. The dynamic characteristics of the thrust and pressure traces are identical, thus indicating stability for the gas saturated condition.

T-11606, S/N 001-15 — 7/13/66 Cell 1, Runs 3453-3471

The objective of this test was to determine engine performance at an O/F = 1.6 with helium saturated propellant at tank pressures from 150 to 400 psia. The engine was orificed for an O/F of 1.6 and 100 lb. thrust at a tank pressure of 182 psia. To provide a comparison, runs were also made with unsaturated propellant and nitrogen saturated propellants at tank pressures from 150 to 400 psia.

The propellants were saturated by bubbling gas from the bottom to the top of the propellant pulse tank at an initial tank pressure of 430 psia over a 15 minute period. At the end of this period, the tank was vented and the pressure reduced to 410 psia. This cycle was repeated seven times (total 8 times), in two hours. Twelve second runs were then made at tank pressures of 150, 185, 300 and 400 psia.

UNSATURATED
ENGINE No. T-12321, S/N 0001-15
RUN No. 10485, 30 SECOND TIME POINT
CELL #6 TEST DATE: 5-15-66

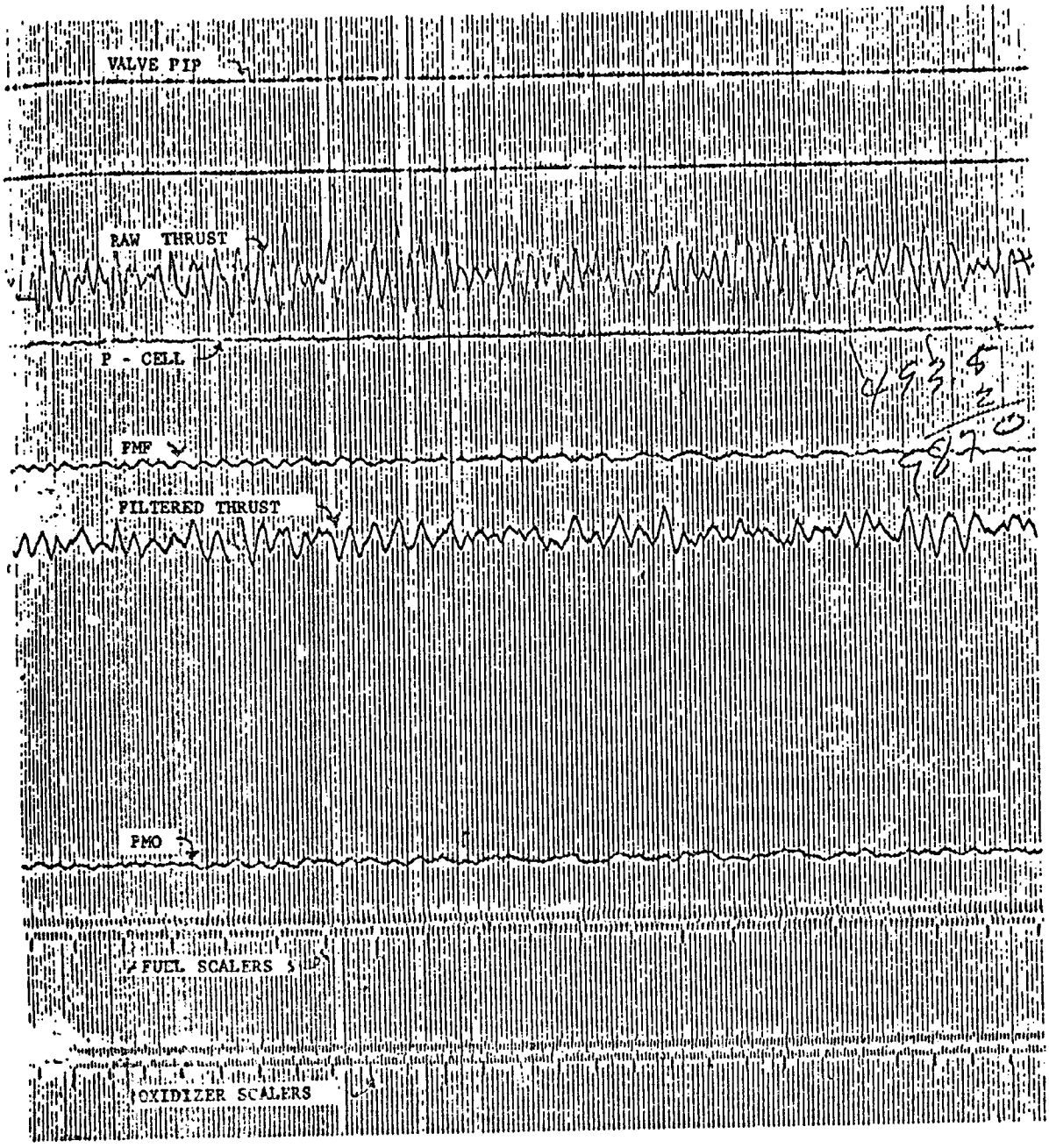

Figure 9

SATURATED
ENGINE No. T-12321, S/N 0001-15
RUN No. 10487 30 SECOND TIME POINT
CELL #6 TEST DATE: 5-15-66

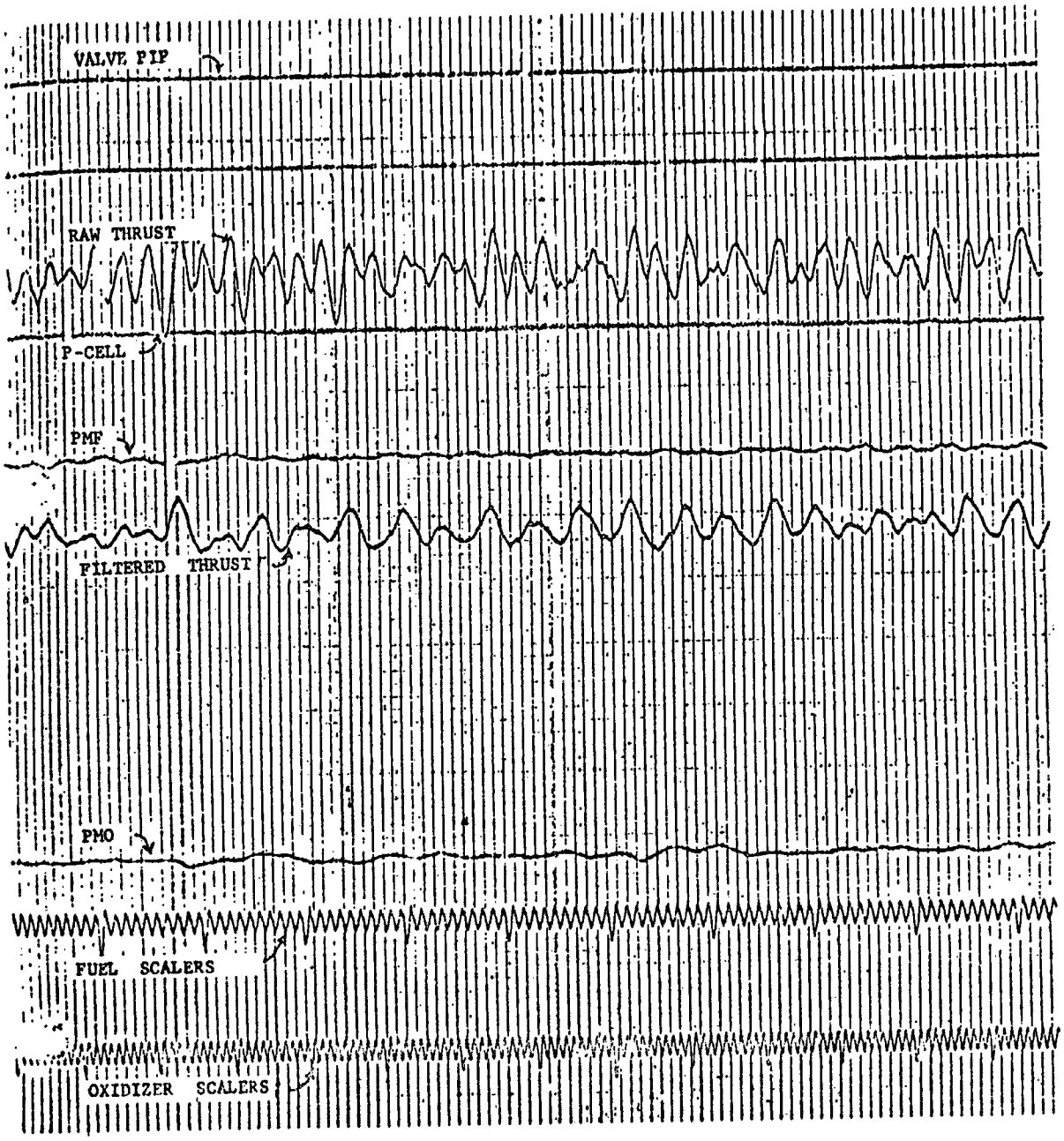

Figure 10

Engine operation was normal with helium saturated and unsaturated propellant. The engine oscillated with nitrogen saturated propellant. The test results are summarized below.

Run	Saturated	P_{tank}	T_p	Results
3455	No	185	80	Stable
3456	No	400	80	Stable
3457	No	400	75	Stable
3458	No	300	75	Stable
3459	No	150	80	Stable
3460	He	400	80	Stable
3461	He	300	80	Stable
3462	He	180	80	Stable
3463	He	150	80	Stable
3464	N2	400	80	Stable
3465	N2	300	80	Unstable
3466	N2	180	80	Unstable
3467	N2	150	80	Unstable

T-14200, S/N 0001-7 MMH DST Test — 8/24 to 8/26/66 Cell 1 Runs 3608-3700

The objective of this test was to demonstrate MMH steady state and pulse performance, to eveluate long duration firing with MMH, and to determine the effects of helium saturated propellants on engine performance prior to the formal supplemental Qualification test with MMH.

Testing with helium saturated A-50 and NTO on engine T-12340, S/N 0001-1 showed a tendency for thrust oscillations to occur at high O/F ratios and low thrust levels. This pehnomenon was investigated with propellants saturated by bubbling helium through the propellant tanks from bottom to top. During this bubbling, the tank pressures were cycled from 196 psia to 206 psia, eight equal times over a two hour period. Five second and 60 second runs were made at ambient conditions. Hot hardware tests with ambient propellants were also made by conducting firing sequences similar to the Apollo Mission Maneuver No. 1 (10 seconds ON - 30 seconds OFF - 3 seconds ON - 360 seconds OFF - 20 seconds ON) where the heat soakback from the engine firing heats the engine. Table VIII lists the thrust level, O/F ratio combinations tested and the results for the runs conducted. In general, the engine oscillated less with MMH than Aerozine-50.

A long run (500 seconds) was also made with dissolved helium in the propellants and the engine did not oscillate. The main propellant storage tanks were pressurized to 180 psia with helium for about 40 hours prior to the run.

TABLE VIII

STABILITY TEST RUNS WITH CH_3 SATURATED PROPELLANTS

MMH FUEL AND GREEN N_2O_4
ENGINE T-14200, S/N 0001-7

Cell 1 TEST DATA: TEST #3343
MMH DST TEST PROGRAM

Run No.	Run Length Seconds	Nominal O/F	Normal Thrust Level Pounds	Thrust Level During Oscillations Pounds	Normal Pch Level psia	Pch Level During Oscillations psia	Time of Run Oscillations Occur Seconds	Duration Seconds	Amplitude Thrust Oscillations Pounds	Amplitude Pch Oscillations psi	COMMENTS
3667	5.0	2.047	100.0	-	96.0	-	None	-	-	-	Trim Run
3668	5.0	2.050	123.0	-	117.0	-	None	-	-	-	Trim Run
3669	5.0	2.002	123.0	-	115.0	-	None	-	-	-	Trim Run
3670	5.0	1.818	101.0	-	97.0	-	None	-	-	-	Trim Run
3671	5.0	2.253	99.0	-	95.0	-	None	-			Trim Run
3672	5.0	2.209	99.0	-	95.0	-	None	-			Trim Run
3673	5.0	2.010	92.0	-	88.0				16.7	9.5	Trim Run - Mild Oscillations throughout run
3674	5.0	2.219	89.0	87.0 87.0	87.0	79.0 82.0	0.080 3.120	0.200 1.600	53.8 57.6	21.2 13.3	Trim Run
3675	5.0	2.019	100.0	-	96.0	-	None	-	-	-	Trim Run
3676	60.0	2.037	100.0		97.0	-	None	-	-	-	
3677	60.0	1.816	102.0	-	98.0	-	None	-	-	-	
3678-1	10.0	1.820	99.0	-	98.0	-	None	-	-	-	
3678-2	3.0	1.814	99.0	-	98.0	-	None	-	-	-	
3678-3	20.0	1.813	99.0	-	97.0	-	None	-			Ran out of Propellant at 18.5 seconds
3679	5.0	2.014	88.0	-	88.0	-	None	-			Trim Run
3680	60.0	2.004	88.0	-	88.0	-	None	-			

TABLE VIII (continued)

STABILITY TEST RUNS WITH GH_e SATURATED PROPELLANTS

MMH FUEL AND GREEN N_2O_4

ENGINE T-14200, S/N 0001-7

Cell 1 TEST DATA: TEST #3343

MMH DST TEST PROGRAM

Run No.	Run Length Seconds	Nominal O/F	Normal Thrust Level Pounds	Thrust Level During Oscillations Pounds	Normal Pch Level psia	Pch Level During Oscillations psia	Time of Run Oscillations Occur Seconds	Duration Seconds	Amplitude Thrust Oscillations Pounds	Amplitude Pch Oscillations psi	COMMENTS
3681	60.0	2.174	96.0	-	96.0	-	None	-	-	-	
3682	60.0	2.004	118.0	-	115.0	-	None	-	-	-	
3683	60.0	2.246	88.0	-	86.0	-	None	-	-	-	
3684-1	10.0	2.015	119	-	113	-	None	-	-	-	
3684-2	3.0	2.015	117	-	115	-	None	-	-	-	
3684-3	20.0	2.011	117	-	114	-	None	-	-	-	
3685-1	10.0	2.018	90	-	89	-	None	-	20.3	9.0	Mild Oscillations throughout run
3685-2	3.0	2.009	90	-	89	-	None	-	-	-	
3685-3	20.0	1.994	90	-	88	-	None	-	-	-	
3686-1	10.0	2.031	97	-	95	-	None	-	-	-	
3686-2	3.0	2.038	97	-	95	-	None	-	-	-	
3686-3	20.0	2.030	97	-	95	-	None	-	-	-	
3687-1	10.0	2.220	88	-	87	-	None	-	-	-	
3687-2	3.0	2.167	89	-	87	-	None	-	-	-	
3687-3	20.0	2.199	89	-	88	-	None	-	-	-	

TABLE VIII (continued).

STABILITY TEST RUNS WITH CH_4 SATURATED PROPELLANTS

MMH FUEL AND GREEN N_2O_4
ENGINE T-14200, S/N 0001-7

Cell 1 TEST DATA: TEST #3343
MMH DST TEST PROGRAM

Run No.	Run Length Seconds	Nominal O/F	Normal Thrust Level Pounds	Thrust Level During Oscillations Pounds	Normal Pch Level psia	Pch Level During Oscillations psia	Time of Run Oscillations Occur Seconds	Duration Seconds	Amplitude Thrust Oscillations Pounds	Amplitude Pch Oscillations psi	COMMENTS
3688-1	10.0	2.191	97	-	96	-	None	-	-	-	
3688-2	3.0	2.198	96	-	95	-	None	-	-	-	
3688-3	20.0	2.191	95	-	93	-	None	-	-	-	
3689-1	10.0	2.068	92	-	91	-	None	-	-	-	
3689-2	3.0	2.076	92	-	90	-	None	-	-	-	
3689-3	20.0	2.058	92	-	90	-	None	-	-	-	

NOTE: P_{ch} and thrust from oscillograph.

Apollo Supplemental Qualification

The objectives of the R-4D Supplemental Qualification Test for the Apollo Service Module Reaction Control System Engine were: (1) to demonstrate that the SM RCS engine will operate safely utilizing helium saturated monomethylhydrazine as the fuel and helium saturated nitrogen tetroxide, which has nitric oxide content of between 0.4 and 0.8% by weight, as the oxidizer; (2) to demonstrate that the SM RCS engine will operate safely when arc suppression circuitry is incorporated into the electrical engine valve command system; (3) to acquire and document engine performance data with both unsaturated and helium saturated propellants.

The engine oscillated during the hot calibration test with unsaturated propellants and during the ambient calibration test with propellants saturated by bubbling. A study of the test data indicates that most likely cause of the oscillations was the presence of entrained gas in the propellants. The presence of the entrained gas can sometimes be identified by its effect upon the response of the propellant manifold pressures on start-up and shut-down. Two oscillograph records showing indications of helium entrainment in the oxidizer are shown in Figures 11 and 12, from the ambient and hot calibration test. The oxidizer manifold pressure (Pmo) exhibited sluggish response which can be attributed to the damping effect of the helium entrained in the propellant. Further indications of gas entrainment was evident in the chamber pressure trace of both runs. At approximately 80% pressure rise, a marked change in the chamber pressure and thrust transient occur as a result of gas ejection. These transient irregulations were followed almost immediately by the onset of thrust oscillations.

The engine did not oscillate during three other tests made with purposely saturated propellant. The propellants for the orbit retrograde test were saturated by storing the propellants with helium at 180 psia for 84 hours before the test. The engine did not oscillate. The propellant for the hot and ambient mission simulation tests were saturated by bubbling helium through the propellant tanks from bottom to top. During this bubbling the tank pressures were cycled from 196 psia to 206 psia, eight equal times over a period of two hours. Following the bubbling, the propellants were maintained under 186 psia pressure for at least 30 minutes prior to reduction to run pressures. The engine did not oscillate for these two tests.

LM Supplemental Qualification

The primary objective of the LM RCS Supplemental Qualification Test was to demonstrate that the LM RCS engine will operate safely utilizing helium saturated Aerozine-50 as the fuel and helium saturated nitrogen tetroxide, which has a nitric oxide content between 0.4 and 0.8% by weight, as the oxidizer.

The propellants were saturated for all tests by stirring the propellants for four hours while the tanks were pressurized to 180 psig with helium. The engines did not oscillate for any of the tests.

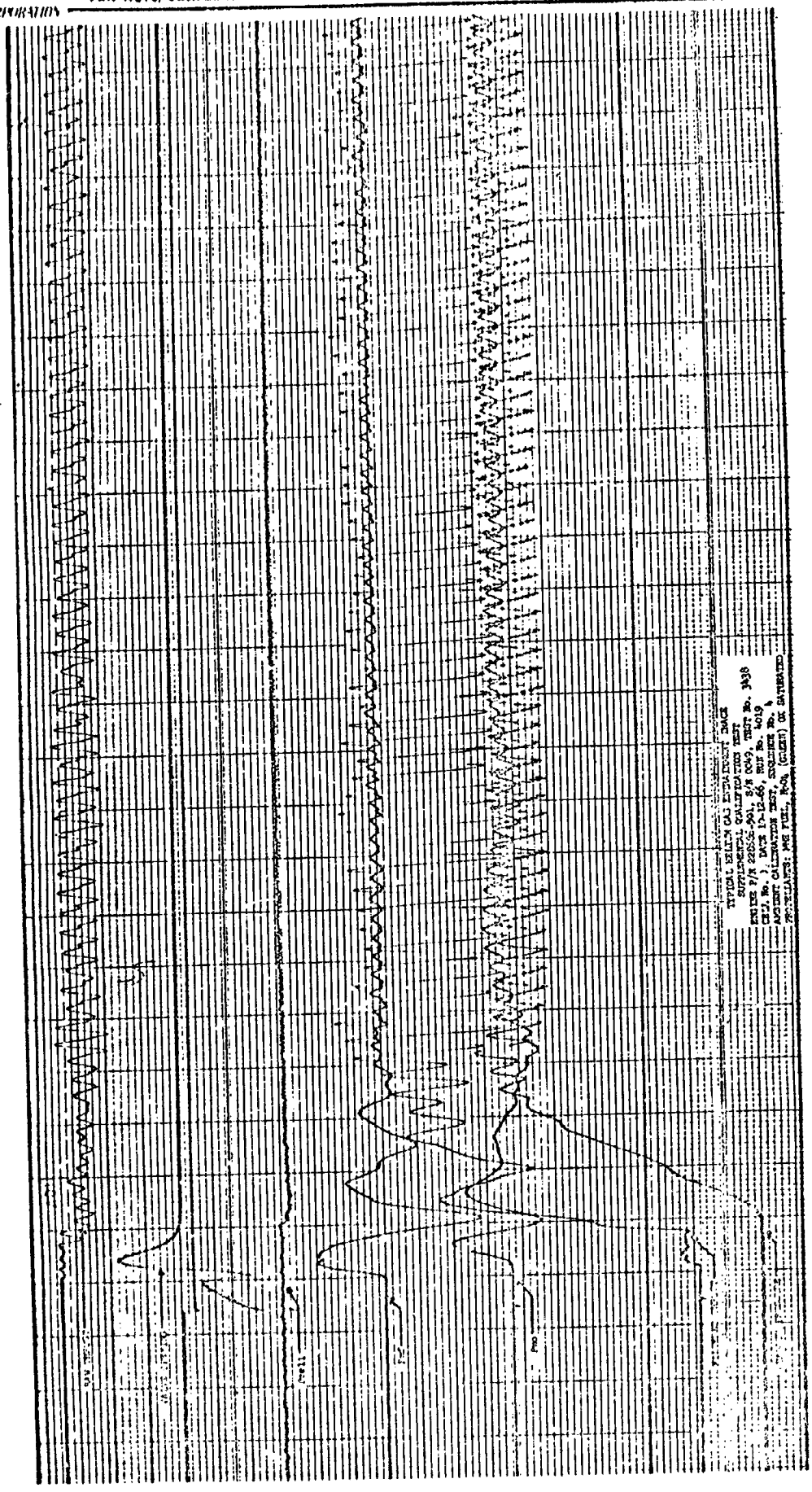
TYPICAL HELIUM GAS ENTRAINMENT TRACE
SUPPLEMENTAL QUALIFICATION TEST
ENGINE P/N 22556-901, S/N 0049, TEST No. 3438
CELL No. 1, DATE 10-12-66, RUN No. 4019
AMBIENT CALIBRATION TEST, SEQUENCE No. 4
PROPELLANTS: MMH FUEL, N2O4 (GREEN) OX SATURATED

FIGURE 11

REPRODUCIBILITY OF THE ORIGINAL PAGE IS POOR.

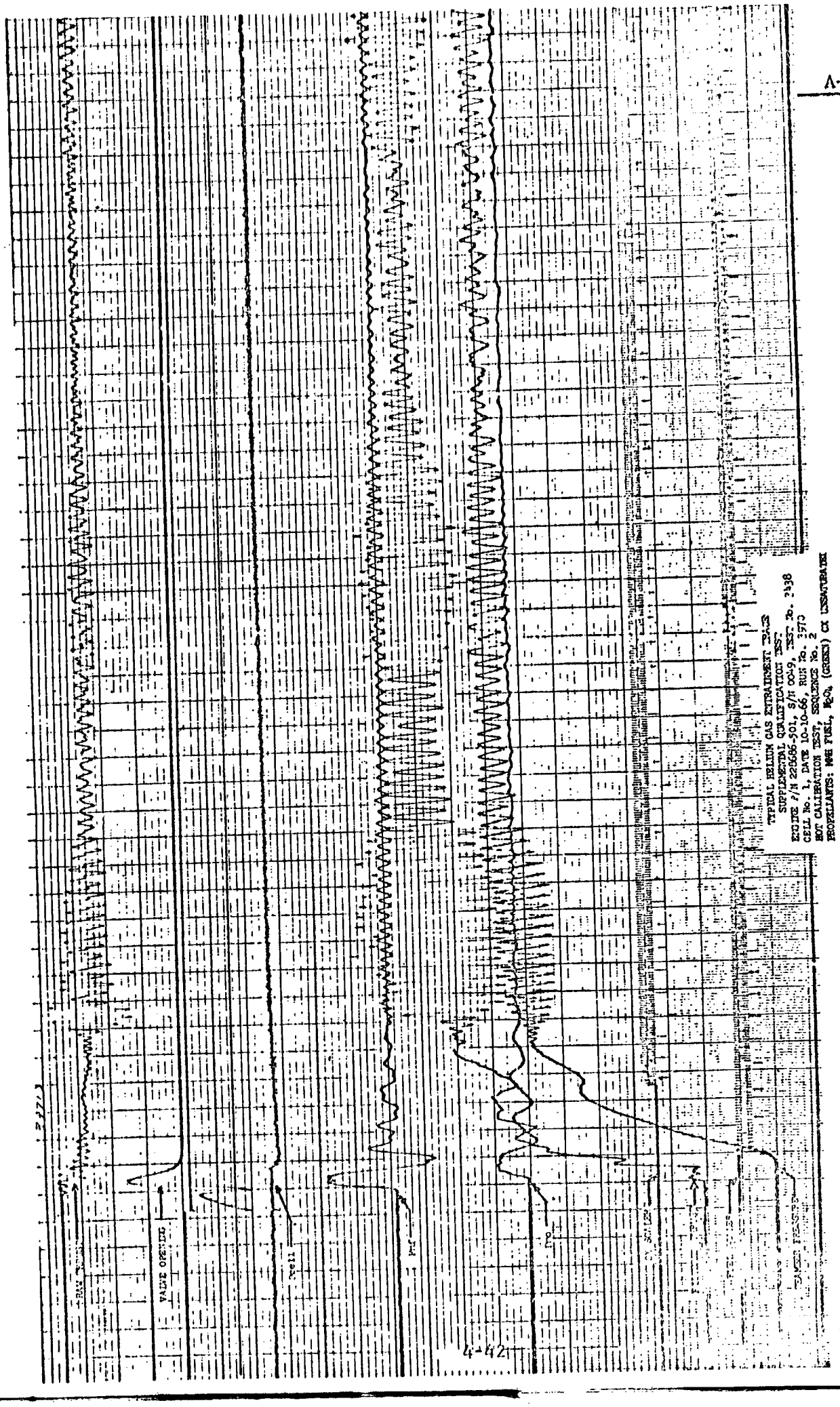

FIGURE 12

IV. THRUST OSCILLATION MODELS

To better understand why the engine oscillates with gas in the propellants, various analytical models were developed.

A stability analysis of the bipropellant rocket with free gas (bubble) in the injector was made. The analysis showed that free gas in the injector might cause thrust oscillations. Based on recent testing with the R-4D engine on a different program, a gas flow limit was determined above which oscillation seemed to occur. An analysis was also made of the injector pressure drop to see where the dissolved gas might come out of solution. It was determined that at the valve seat the static pressure might be as low as 85 psia. A special engine test with a contoured valve seat to eliminate the large pressure drop, resulted in the engine operating without oscillations under conditions where oscillations had occurred with the normal valve seat.

A. Stability Analysis of a Rocket Engine with Free Gas in the Injector Passages

A general stability analysis of a bipropellant rocket with free gas in the injector passages was made. The analysis shows how much gas must collect in the injector before thrust oscillations would be expected. The analysis uses linear control system theory and does not include any effect of gas on the shape and mixing of the streams leaving the injector. (This least effect may be another mechanism for producing oscillations)

An analytical model was developed relating the amount of free gas required for oscillations and the amount of gas dissolved in the oxidizer to cause low frequency instability of a rocket engine.

Figure 13 shows the simplified rocket engine model that was analyzed. The propellant supply pressures are P_A and P_B. P_1 and P_2 are the pressures in the injector dribble volumes. P_c is the combustion chamber pressure. W_α and W_B are the weights of propellant displaced by the free gas bubbles. W_1 and W_2 are the flow rates of the two propellants into the combustion chamber. W_A and W_B are the flow rates of the two propellants into their respective injector volumes.

The model in Figure 13 is described by the following set of equations. These dquations include pressures and flow rates in the model as variables, some constants of proportionately (denoted by k with an appropriate subscript), constants representing the supply pressures and propellant weight displaced by free gas and a constant (γ) for the ratio of specific heats of the gas. A dynamic transfer function G, appears in one of the equations. G is the transfer function that converts a change in propellant flow rate into the chamber to a change in chamber pressure.

$$\left(G = \frac{e^{-\tau_d S}}{(1 + \tau_1 S)}\right)$$

ROCKET ENGINE MODEL

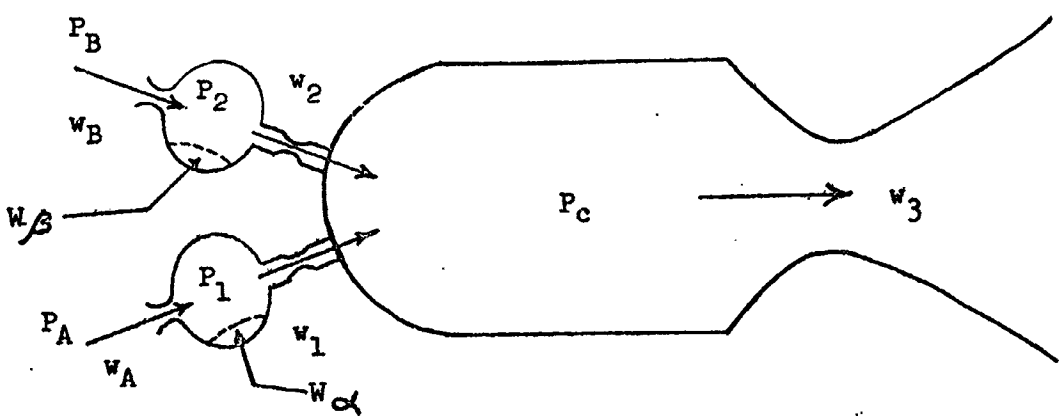

Figure 13

Total Propellant Flow

$$w_3 = w_1 + w_2$$

Oxidizer Flow Into Combustor

$$w_1 = k_1(P_1 - P_c)^{1/2}$$

Oxidizer Flow Into Injector

$$w_A = k_A(P_A - P_1)^{1/2}$$

Fuel Flow Into Combustor

$$w_2 = k_2 (P_2 - P_c)^{1/2}$$

Fuel Flow Into Injector

$$w_B = k_B (P_B - P_2)^{1/2}$$

Chamber Pres ure Generation

$$P_c = k_3 w_3 G$$

Oxidizer Pressure In Injector

$$P_1 = \frac{P_{1_0}(W_\alpha)^\gamma}{(W_\alpha + W_1 - W_A)^\gamma} \qquad W_1 = \int_0^t w_1 dt \qquad \text{etc.}$$

Fuel Pressure in Injector

$$P_2 = \frac{P_{2_0} (W_\beta)^\gamma}{(W_\beta + W_2 - W_B)^\gamma}$$

By taking the logarithm of each of these equations and then differentiating, the equations can be transformed into dimensionless linear equations. This proces is illustrated below for the equation giving the oxidizer flow into the combustion chamber.

$$\ln w_1 = \ln k_1 + 1/2 \ln (P_1 - P_c)$$

$$\frac{d\,w_1}{w_1} = \frac{d\,k_1}{k_1} + 1/2 \frac{d(P_1 - P_c)}{(P_1 - P_c)}$$

$$\frac{d\,w_1}{w_1} = \frac{d\,k_1}{k_1} + \frac{\frac{1}{2} P_1}{(P_1 - P_c)} \frac{d\,P_1}{P_1} - \frac{\frac{1}{2} P_c}{P_1 - P_c} \frac{d\,P_c}{P_c}$$

Recognizing k_1 as a constant and using letter symbols for the coefficients in the equation above gives

$$\frac{d\,w_1}{w_1} = \frac{AdP_1}{P_1} - \frac{BdP_c}{P_c}$$

For small perturbations, the variables $\frac{dX}{X}$ give the change in X as a fraction of its nominal value. Adopting the change in notation that $X \cong \frac{dX}{X}$, the equation for fuel flow into the combustion chamber becomes

$$W_1 = AP_1 - BP_c$$

Applying the above linearization process to the set of equations describing the model gives the following set of dimensionless linear equations.

Chamber

$$w_3 = Y w_1 + Z w_2$$

$$P_c = G\, w_3$$

Oxidizer

$$w_1 = A P_1 - B P_c$$

$$w_A = - C P_1$$

$$P_1 = (D w_A - E w_1)\, 1/S$$

Fuel

$$w_2 = a P_2 - b P_c$$

$$w_B = - c P_2$$

$$P_2 = (d\, w_B - e\, w_2)\, 1/S$$

Where:

$$Y = \left[\frac{O/F}{1+O/F} + \frac{dk_3}{dW_1}\right] \quad Z = \left[\frac{1}{1+O/F} + \frac{dk_3}{dW_2}\right] \quad *$$

$$A = \frac{P_1}{2(P_1 - P_c)} \qquad B = \frac{P_c}{2(P_1 - P_c)} \qquad C = \frac{P_1}{2(P_A - P_1)}$$

$$D = \gamma \frac{w_A}{W_\alpha} \qquad E = \gamma \frac{w_1}{W_\alpha}$$

$$a = \frac{P_2}{2(P_2 - P_c)} \qquad b = \frac{P_c}{2(P_2 - P_c)} \qquad c = \frac{P_2}{2(P_B - P_2)}$$

$$d = \gamma \frac{w_B}{W_\beta} \qquad e = \gamma \frac{w_2}{W_\beta}$$

The preceding set of equations can now be represented in block diagram form and the techniques of block diagram reduction used to combine them into a single transfer function for the dynamic interaction between the pressures and flow rates in the system. Figures 14, 15 and 16 show the reduction of the system to a combustion chamber transfer function and two injector transfer functions for the fuel and oxidizer.

By substituting for A, B, C, D and E, their definitions, recognizing that the initial flow rates in and out of the oxidizer side of the injector are equal (ie. $w_1 = w_A$) and by making the following new definitions

$$\frac{P_1 - P_c}{P_c} = n \qquad \frac{P_A - P_1}{P_c} = m \qquad \frac{w_1}{W_\alpha} = \omega_b \qquad \zeta = \frac{\gamma(1+n)}{2m}$$

---

* The coefficients Y and Z have been modified to include the effect of O/F ratio on Isp.

ROCKET ENGINE MODEL BLOCK DIAGRAM

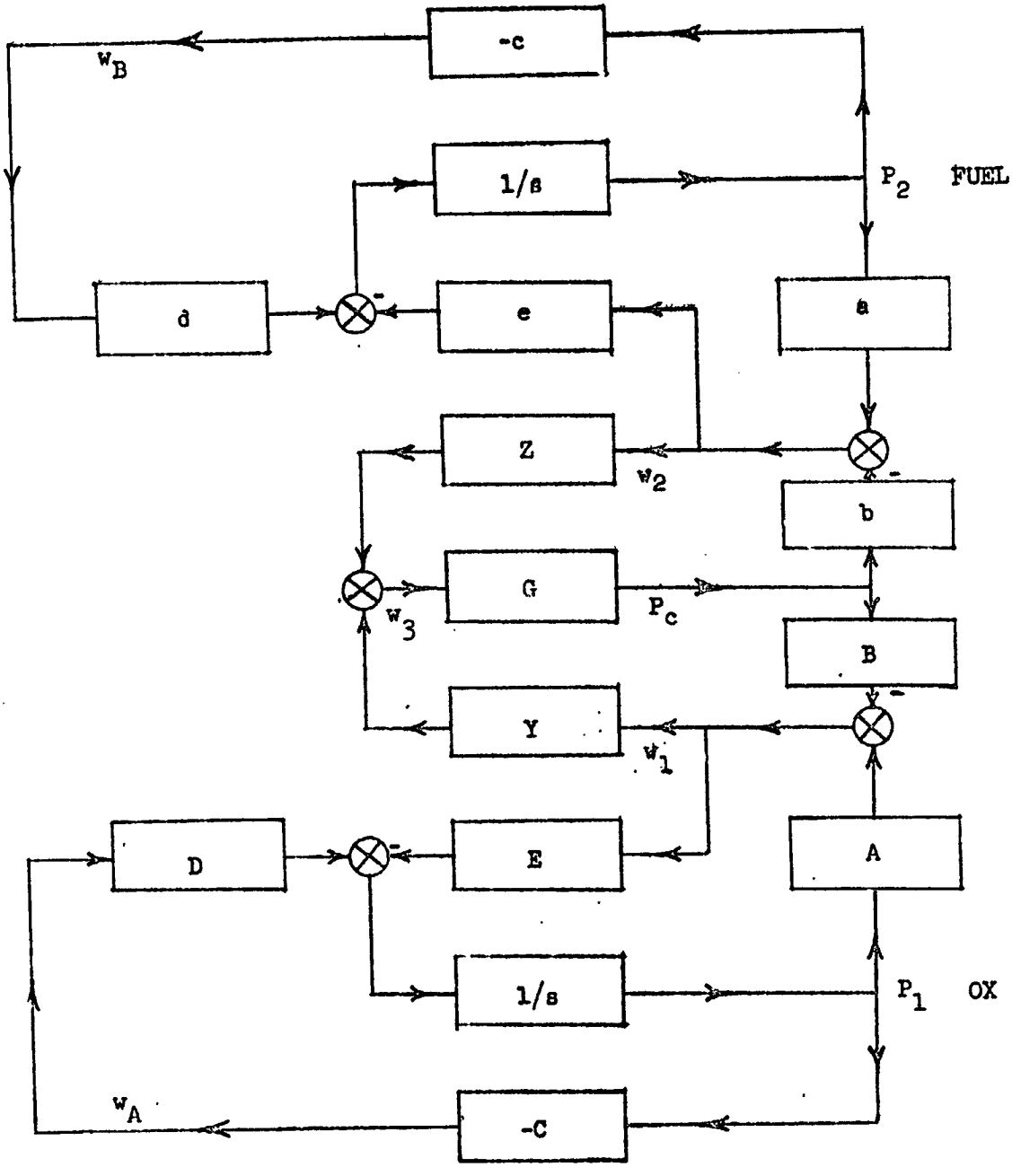

Figure 14

REDUCED ROCKET ENGINE MODEL BLOCK DIAGRAMS

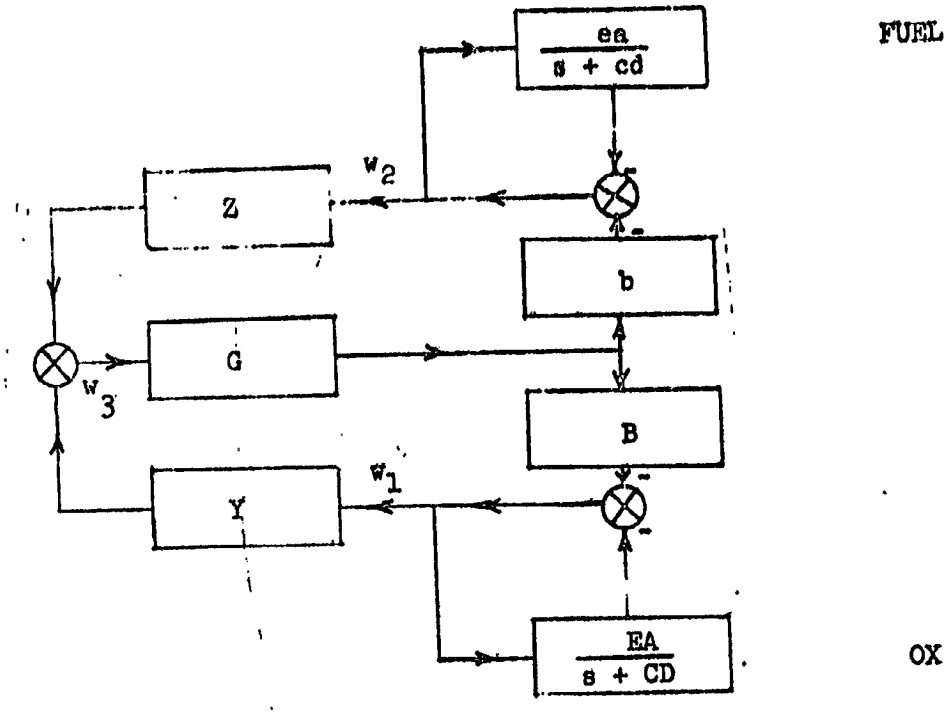

Figure 15

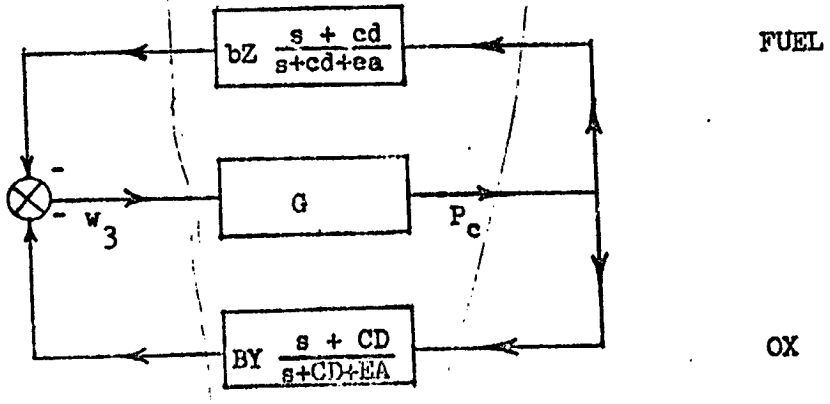

Figure 16

The expression BY $\frac{S + CD}{S + CD + EA}$ can be written in the form:

$$\frac{Y}{2n} \frac{S + \zeta \omega_b}{S + (1 + \frac{m}{n}) \zeta W_b}$$

Similarly, the expression on the fuel side can be written in the form:

$$\frac{Z}{2n'} \frac{S + \zeta' \omega_b'}{S + (1 + \frac{m'}{n'}) \zeta' W_b'}$$

The open loop transfer function around the interaction loop can now be written by forming the product of G and the sum of the two injector terms. This transfer function takes the form

$$G \left[\frac{Y}{2n} \frac{S + \zeta \omega_b}{S + (1 + \frac{m}{n}) \zeta \omega_b} + \frac{Z}{2n'} \frac{S + \zeta' \omega_b'}{S + (1 + \frac{m'}{n'}) \zeta' \omega_b'} \right]$$

The stability of this expression can be easily determined if the simplifying assumption of no free gas on the fuel side of the engine is made. The fuel term then reduces to

$$\frac{Z}{2 (n' + m')}$$

If it is further assumed that the fuel and oxidizer supply pressures are equal ($m' + n' = m + n$), the transfer function can be written

$$G \left[\frac{Y}{2n} \frac{S + \zeta \omega_b}{S + (1 + \frac{m}{n}) \zeta \omega_b} + \frac{Z}{2 (m + n)} \right]$$

Combining terms, this becomes

$$G \left[\frac{\frac{Y}{2n} (S + \zeta \omega_b) + \frac{Z}{2(m+n)} \left[S + (1 + \frac{m}{n}) \zeta \omega_b \right]}{S + (1 + \frac{m}{n}) \zeta \omega_b} \right]$$

Algebraic manipulation yields

$$G\left[\frac{Y(m+n)+mZ}{2n(m+n)}\right]\left[\frac{S+\frac{(m+n)(Y+Z)}{Y(m+n)+nZ}\zeta\omega_b}{S+(1+\frac{m}{n})\zeta\omega_b}\right]$$

Substituting for G, ζ and ω_b gives

$$\frac{e^{-\tau_d S}}{1+\tau_1 S}\;\frac{Y(m+n)+nZ}{2n(m+n)}\;\frac{S+\left\{\frac{(Y+Z)}{[Y(m+n)+nZ]}\right\}\left\{\frac{\gamma(1+n)(m+n)}{2m}\frac{W_1}{W_\alpha}\right\}}{S+\frac{1}{n}\left\{\frac{\gamma(1+n)(m+n)}{2m}\frac{W_1}{W_\alpha}\right\}}$$

Figure 17 shows the frequency response of the open loop transfer function without the combustor contribution

$$\frac{e^{-\tau_d S}}{1+\tau_1 S}$$

Figure 18 shows the contribution of the combustor transfer function

$$\frac{e^{-\tau_d S}}{1+\tau_1 S}$$

A sufficient criterion for stability is that the pressure drop across the oxidizer injector holes be large enough so that the open loop gain never exceeds unity. This sufficient criterion for stability is

$$\frac{Y}{2n}+\frac{Z}{2(m+n)}<1$$

If $\frac{Y}{2n}+\frac{Z}{2(m+n)}>1$, stability is still achieved provided that the attenuating effect of the $(1+\tau S)$ lag term in the combustor transfer function prevents the system gain from exceeding unity. This stabilizing effect is shown in Figure 19.

The effect of the combustor lag will prevent the loop gain from exceeding unity provided the ratio of the combustor lag frequency to the lead frequency associated with the gas bubble is less than the reciprocal of the injector gain term evaluated at zero frequency. This criterion is written as follows:

FREQUENCY RESPONSE OF THE OPEN LOOP TRANSFER FUNCTION
WITHOUT THE COMBUSTOR CONTRIBUTION

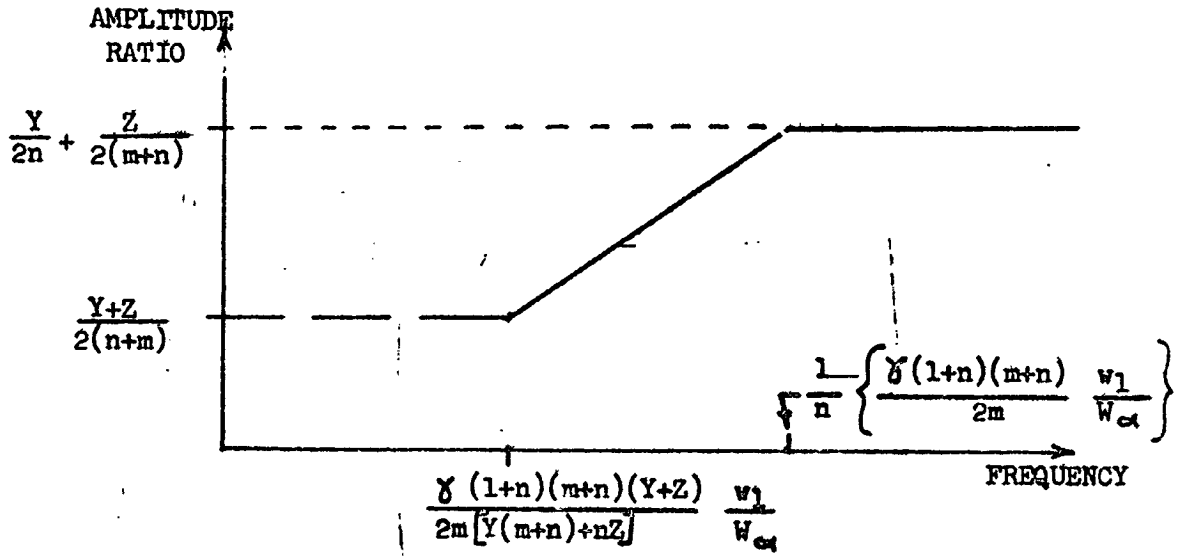

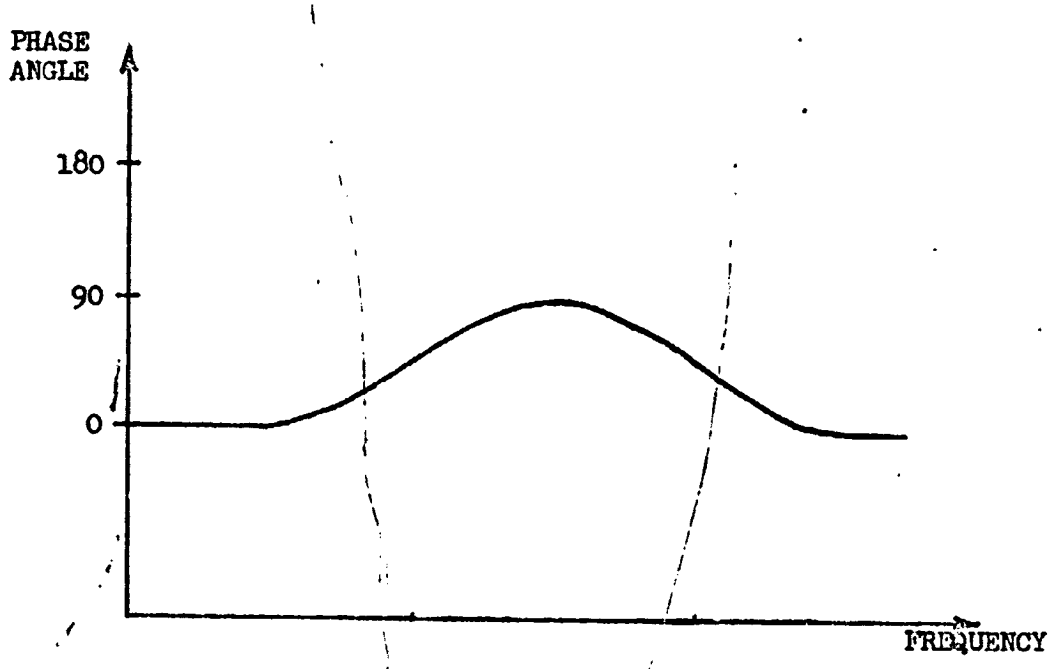

Figure 17

FREQUENCY RESPONSE CONTRIBUTION OF THE COMBUSTOR

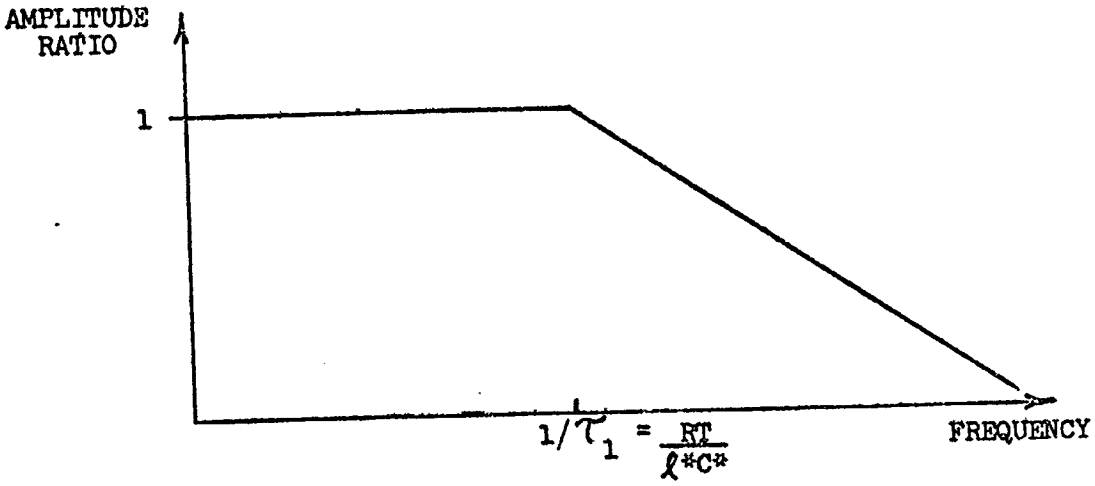

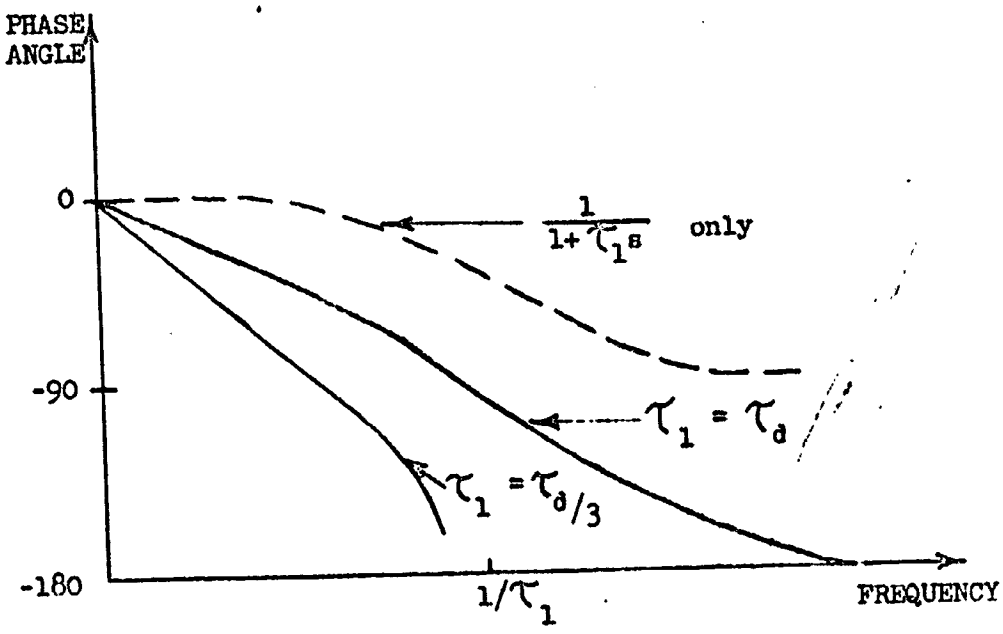

Figure 18

ATTENUATING EFFECT OF COMBUSTOR CONTRIBUTION UNDER CERTAIN CONDITIONS

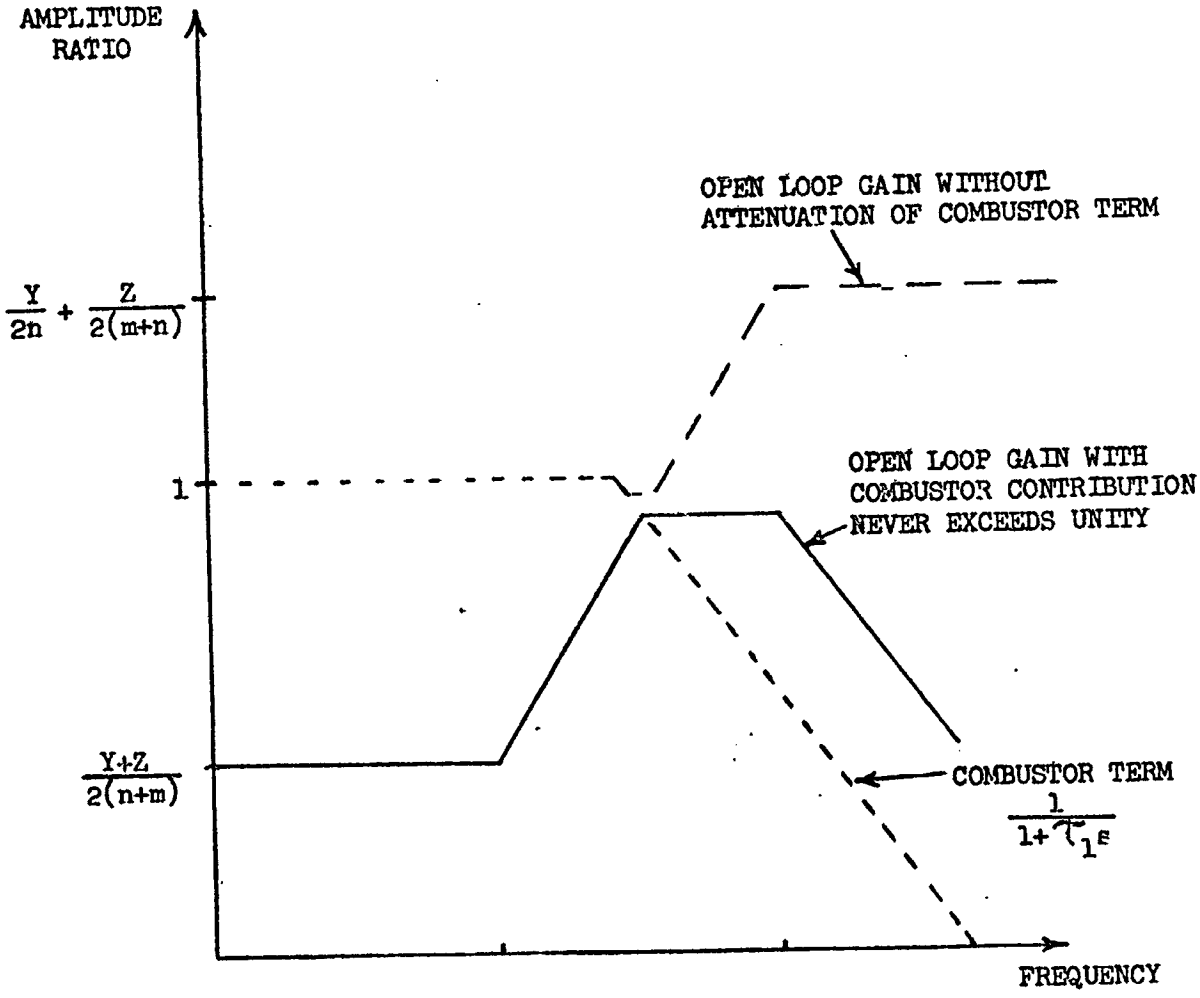

Figure 19

$$\frac{1}{\tau_1} \frac{2\,m\,[Y\,(m+n)+n\,Z]}{\gamma\,(1+n)(m+n)(Y+Z)} \frac{W_\alpha}{W_1} < \frac{2\,(n+m)}{Y+Z}$$

Which may be written

$$\frac{1}{\tau_1} \frac{1}{\gamma} \frac{W_\alpha}{W_1} \frac{m\,[Y\,(m+n)+nZ]}{(1+n)\,(m+n)^2} < 1$$

Another condition that insures that the gain never exceeds unity corresponds to the case when the combustor lag begins attenuating at a frequency below the frequency of the injector lead term. This case is shown in Figure 20.

This condition, sufficient for stability may be written

$$1/\tau_1 < \frac{\gamma\,(1+n)(m+n)(Y+Z)}{2m\,[Y(m+n)+n\,Z]} \frac{W_1}{W_\alpha}$$

Another sufficient criterion for stability is that the phase angle of the open loop transfer function be less than 180° when the loop gain is above unity. For the case sketched in Figure 21 this sufficient stability criterion is obtained when

$$\frac{[Y\,(m+n)+n\,Z]}{2\,n\,(m+n)} \frac{\tau_d}{\tau_1} + \tan^{-1} \frac{[Y(m+n)+n\,Z]}{2\,n\,(m+n)} < \pi$$

ATTENUATING EFFECT OF COMBUSTOR CONTRIBUTION UNDER CERTAIN CONDITIONS

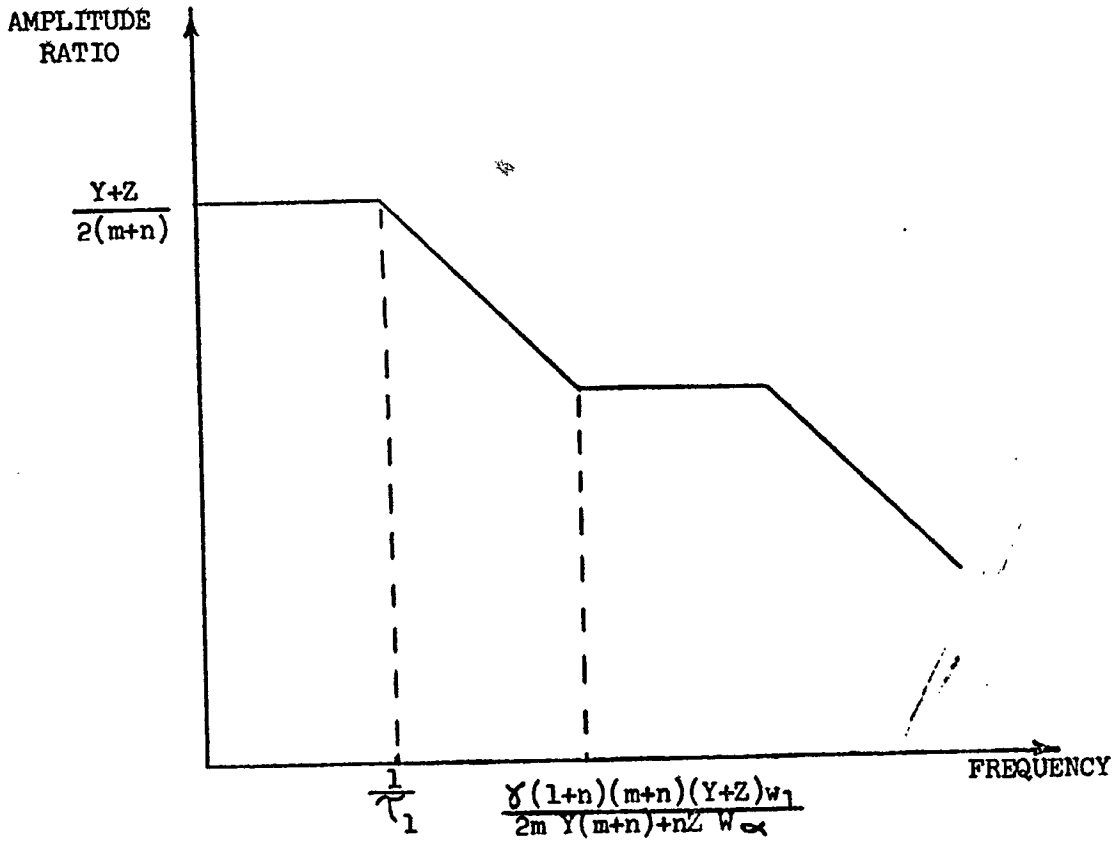

Figure 20

STABILITY DEPENDENCE ON OPEN LOOP TRANSFER FUNCTION

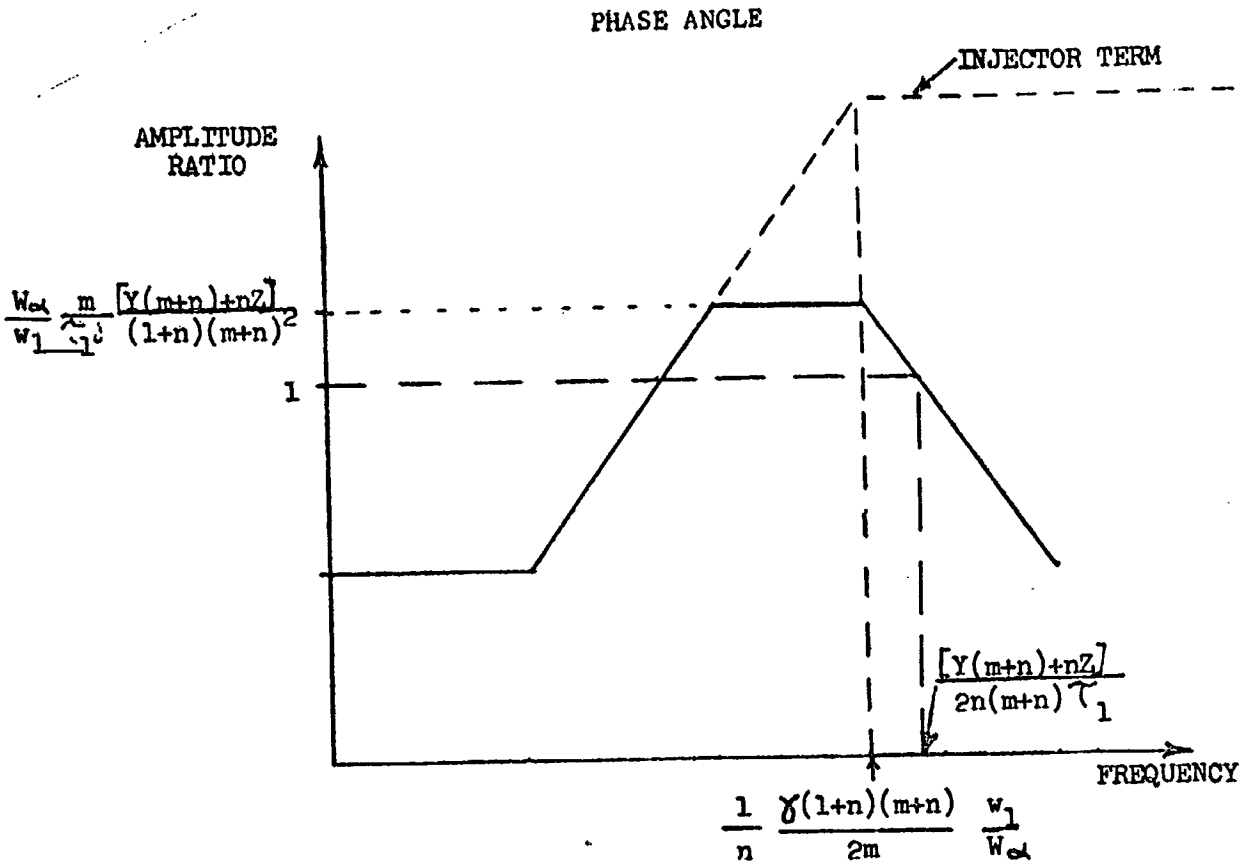

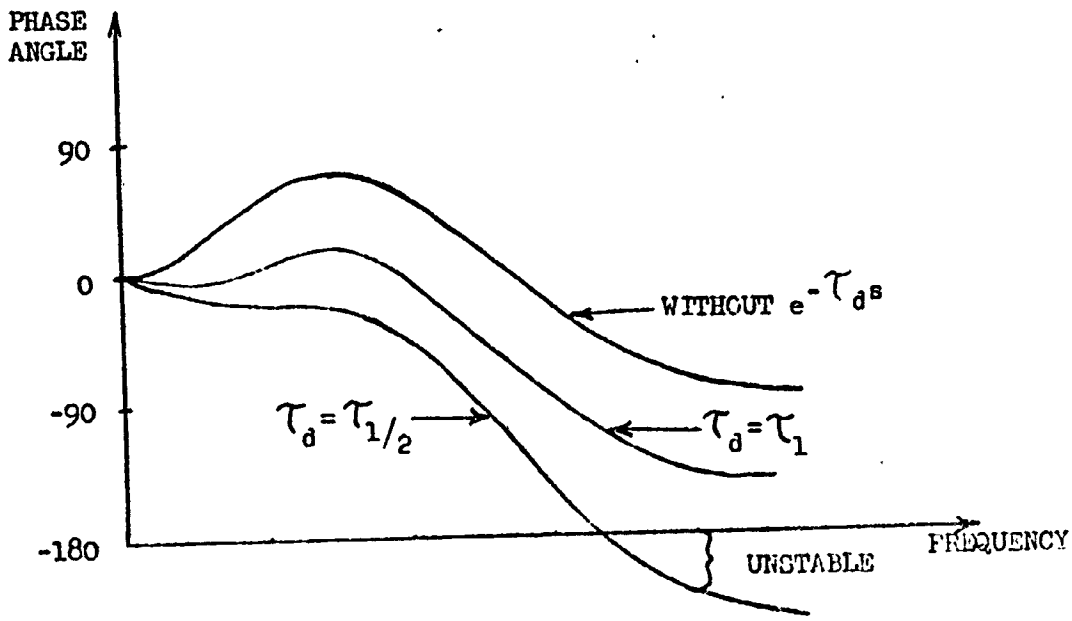

Figure 21

Which takes into account the phase contributions of the lagging terms and conservatively leaves out the contribution of the leading term.

For the case sketched in Figure 22, the phase criterion becomes

$$\frac{Y(m+n)+nZ}{2n(m+n)}\frac{\tau_d}{\tau_1}+\tan^{-1}\frac{Y(m+n)+nZ}{2n(m+n)} < \pi$$

Which is the same as derived for the case where the combustor lag occurred at a frequency between the injector load frequency and the injector lag frequency.

The phase criterion for stability is to be applied when

$$\frac{1}{\tau_1} > \frac{\gamma(1+n)(m+n)(Y+Z)}{2m\left[Y(m+n)+nZ\right]}\frac{w_1}{W_\alpha}$$

The stability criteria derived, any one of which provides stability are listed below:

$$\frac{Y(m+n)+nZ}{2n(m+n)} < 1$$

$$\frac{\gamma(1+n)(m+n)(Y+Z)}{2m\left[Y(m+n)+nZ\right]}\frac{w_1}{W_\alpha} > \frac{1}{\tau_1}$$

$$\frac{m\left[Y(m+n)+nZ\right]}{(1+n)(m+n)^2\gamma}\frac{W_\alpha}{\tau_1 w_1} < 1$$

$$\frac{\left[Y(m+n)+nZ\right]}{2n(m+n)}\frac{\tau_d}{\tau_1}+\tan^{-1}\frac{\left[Y(m+n)+nZ\right]}{2n(m+n)} < \pi$$

The values for Y and Z can now be substituted into the term $\left[Y(m+n)+nZ\right]$ that appears in the stability criteria. If this is done and

$$\frac{dk_3}{dw_1} = \frac{dk_3}{dw_2}$$

Then

$$Y(m+n)+nZ = \frac{O/F(m+n)+n+m(1+O/F)\frac{dk_3}{dw_1}}{(1+O/F)}$$

STABILITY DEPENDENCE ON OPEN LOOP TRANSFER FUNCTION

PHASE ANGLE

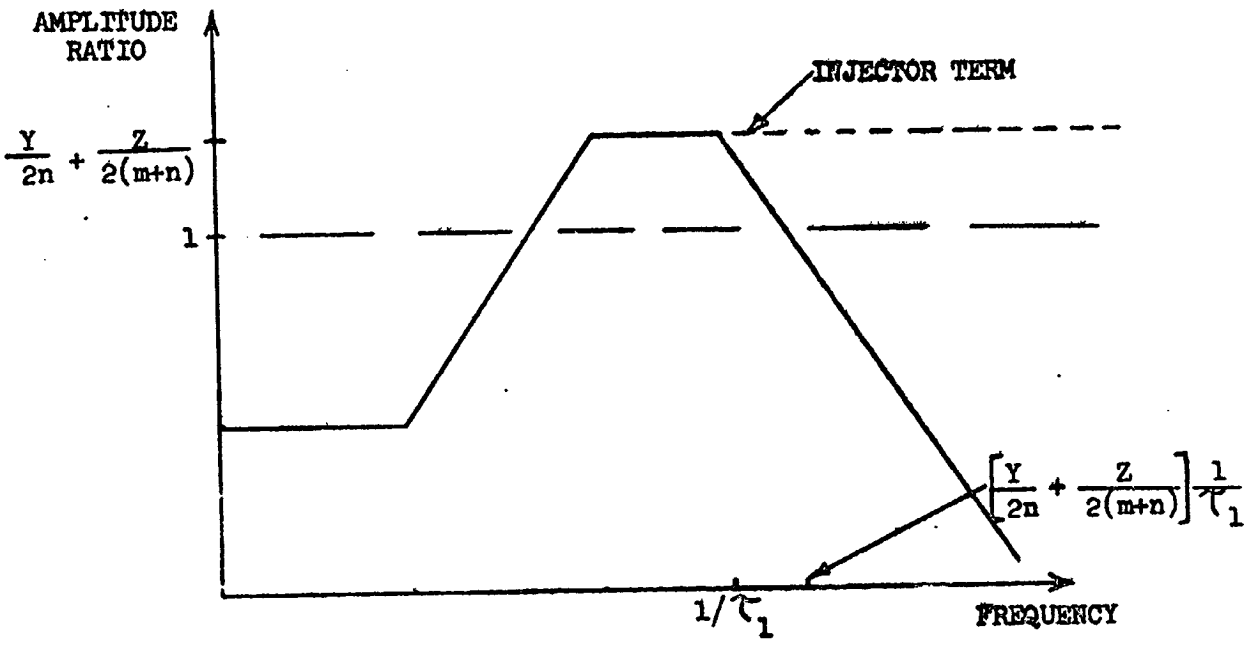

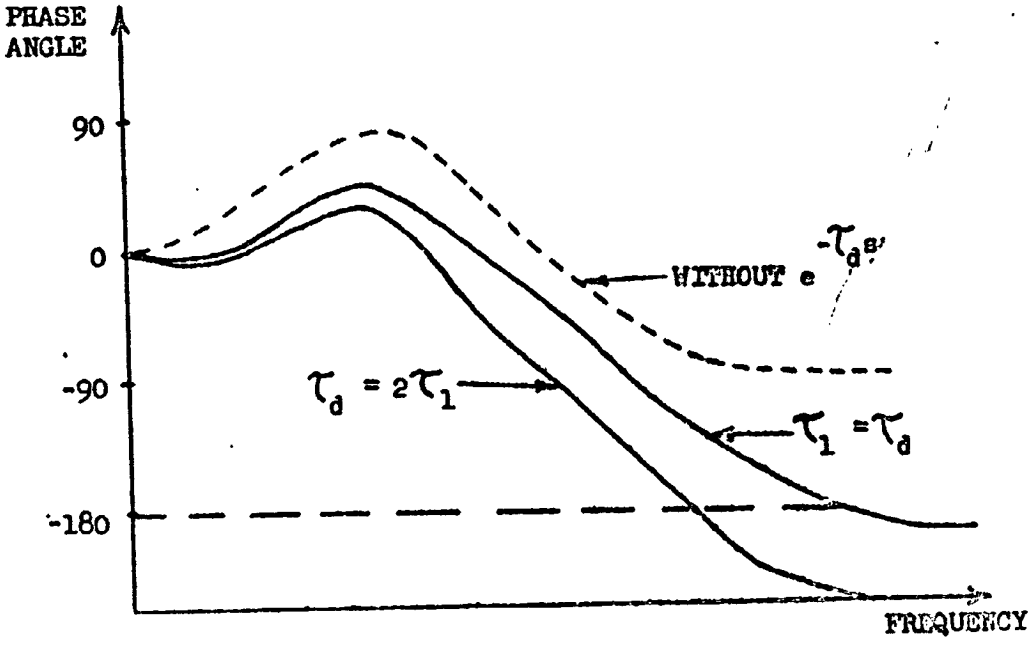

Figure 22

The stability criteria then take the form

$$\frac{O/F\,(m+n) + n + m\,(1+O/F)\,\frac{d\,k_3}{d\,w_1}}{(1+O/F)\,2\,n\,(m+n)} < 1$$

$$\frac{2\,m\left[O/F\,(m+n) + n + m\,(1+O/F)\,\frac{d\,k_3}{d\,w_1}\right]}{\gamma\,(1+n)\,(m+n)(1+O/F)}\;\frac{W_\alpha}{w_1\,\tau_1} < 1$$

$$\frac{m\left[O/F\,(m+n) + n + m\,(1+O/F)\,\frac{d\,k_3}{d\,w_1}\right]}{\gamma\,(1+n)\,(m+n)^2\,(1+O/F)}\;\frac{W_\alpha}{w_1\,\tau_1} < 1$$

$$\frac{O/F\,(m+n) + n + m(1+O/F)\,\frac{d\,k_3}{d\,w_1}}{(1+O/F)\,(2\,n)\,(m+n)}\;\frac{\tau_d}{\tau_1} + \tan^{-1}\frac{O/F\,(m+n) + n + m(1+O/F)\frac{dk_3}{d\,w_1}}{(1+O/F)\,(2n)\,(m+n)} < \pi$$

For most systems, $m + n > 0.5$ and the third criterion will be satisified if the second one is. It is therefore not necessary to further consider the second criterion.

The three remaining criteria are then

$$Q < 1$$

$$RQ\;\frac{W_\alpha}{w_1\tau_1} < 1$$

$$Q\,\frac{\tau_d}{\tau_1} + \tan^{-1}Q < \pi$$

Where

$$Q = \frac{O/F\,(m+n) + n + m\,(1+O/F)\frac{d\,k_3}{d\,w_1}}{2n\,(m+n)\,(1+O/F)}$$

$$R = \frac{2\,n\,m}{\gamma(1+n)(m+n)}$$

The following example shows the results of applying these three criteria to the Apollo R-4D engine.

$$O/F = 2.0 \quad n = 0.205 \quad m = 0.515 \quad \frac{d\,k_3}{d\,w_1} = -0.290 \quad \gamma = 1.67 \text{ (Helium)}$$

$$\tau_1 = 0.42 \times 10^{-3} \text{sec.} \qquad \tau_d = 1.5 \times 10^{-3} \text{sec.}$$

$$Q = \frac{2.0\,(0.72) + 0.205 + 0.515\,(3.0)(-0.290}{2(0.205)(0.72)\,(3.0)}$$

$$Q = 1.35$$

$$R = \frac{2 \times 0.205 \times 0.515}{1.67\,(1.205)(0.72)} = 0.146$$

The first criterion is not met. The second criterion is met when

$$\frac{0.146 \times 1.35}{0.42 \times 10^{-3}} \quad \frac{W_d}{w_1} < 1$$

or when

$$\frac{W_d}{w_1} < 2.15 \times 10^{-3} \text{ seconds}$$

The third criterion is

$$1.35 \times \frac{1.5}{0.42} + \tan^{-1} 1.35 < \pi$$

It is not met but would be if

$$\tau_d < 0.69 \times 10^{-3} \text{ seconds}$$

If the ignition delay time is greater than 0.69 milliseconds and there is a bubble in the head that displaces 2.15 ms of steady state flow (about 20% of the D.V.) then the engine will oscillate.

Gas Flow Limit Model

Based on recent test data from another program, an upper gas flow limit has been determined above which oscillations will probably take place.

The propellants for the tests were saturated to a known amount by the stirring method. This is the only test with the R-4D engine where the propellants were saturated to a known level.

Tabulated in Table IX are test conditions and results of the runs made with helium saturated propellant. In the last two columns are the gas volume flow and weight ratio ($W_{He}/W_{N_2O_4}$), that would come out of solution in the injector dribble volume upstream of the final injector pressure drop and the oxidizer doublet orifice.

The amount of gas was determined by assumming that in dropping from the tank pressure or saturated pressure to the doublet pressure, the helium in the propellant reached equilibrium condition. The difference in weight ratio between the two pressures was calculated from Figure 23, the saturation curve for helium in N_2O_4. Knowing the weight ratio and consequently the weight of gas, the volume flow rate was calculated from the perfect gas law.

It can be seen from this table that the engine starts to oscillate when the weight ratio exceeds 0.300×10^{-4} lb. He/lb. oxidizer or gas flow rate exceeds 2.50 cc/sec.

Cavitation in the Valve

A possible source of bubble formation in the engine is cavitation in the oxidizer seat area.

The geometry of the oxidizer valve seat and flow pattern is shown in Figure 24. The sudden enlargement in flow area at the end of the tapered portion of the valve seat will lead to flow separation. The separated flow will continue to converge to a minimum area at the vena contracta, and will then re-expand toward the walls of the flow passage.

The geometry of the flow passage at the end of the valve seat is

$$D = 0.125''$$
$$H = 0.014''$$
$$A = 0.0055 \text{ in}^2$$

At a flow rate and density given by

$$W = 0.24 \text{ \#/sec}$$
$$\rho = 90 \text{ \#/ft}^3$$

TABLE IX

GAS FLOW LIMIT

ENGINE 229202-503, S/N 0001

Run	Oscillated	Psat	Tsat	Set/Run	Set/Run	O/F	°F	PDo	cc/sec.	$W_{He}/W_{N_2O_4} \times 10^{-4}$
5449	Yes	204	70°	194/182	167/159	1.91	91	104.6	2.50	.299
5450	Yes	204	70°	196/184	167/159	1.93	91	104.6	2.50	.299
5464	Yes	224	70°	224/210	191/182	1.90	99.6	117.8	2.50	.308
5467	Yes	224	70°	229/214	192/182	1.94	100.1	117.8	2.50	.308
5468	Yes	224	70°	229/214	192/182	1.94	100.0	117.8	2.50	.303
5489-5493	No	213	80°	213/200	213/202	1.63	102	115.7	2.29	.290
5494-5498	No	213	80°	194/184	194/186	1.62	95	108.8	2.55	.320
5516-5520	No	213	90°	194/183	194/185	1.60	94	108.8	2.67	.300
5521-5525	No	213	100°	194/183	194/185	1.60	94	108.8	2.82	.342
5526-5531	Yes	213	110°	194/183	194/185	1.60	92	108.8	3.24	.385
5532-5536	Yes	213	110°	213/200	213/204	1.59	99	115.7	2.84	.340
5572-5580	Yes	253	70°	258/239	203/191	2.07	105	127.4	2.98	.360
5617-5621	Yes	213	107°	195/182	195/185	1.60	94	108.8	2.88	.345
5622-5626	Yes	213	107°	213/200	213/203	1.63	102	115.7	2.7	.325

HELIUM - NTO SATURATION WEIGHT RATIO vs SATURATION PRESSURE

PRESSURE RANGE: 0 TO 300 PSIA

TEMPERATURE RANGE: 20 TO 120°F

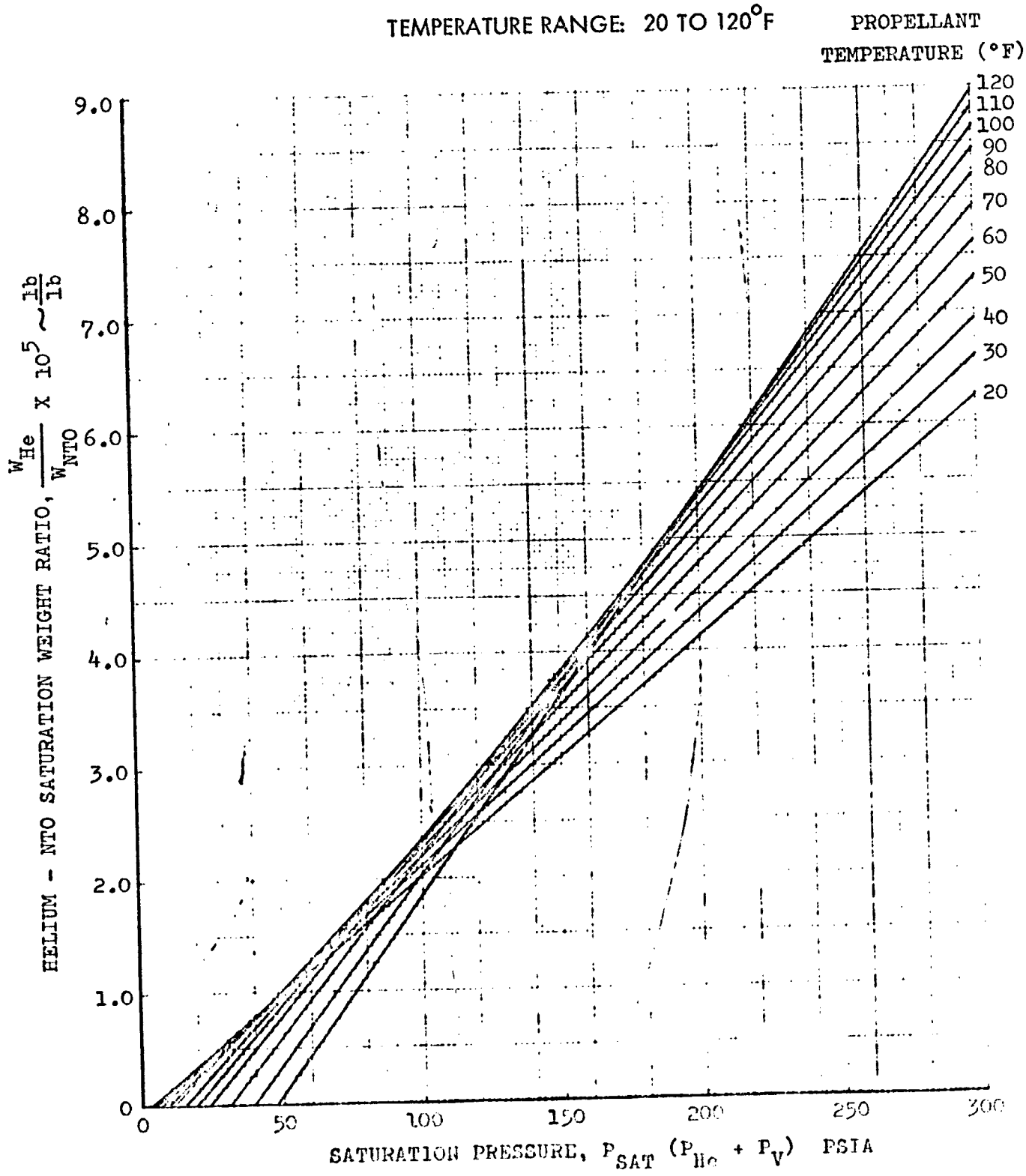

Figure 23

OXIDIZER VALVE SEAT GEOMETRY AND FLOW PATTERN

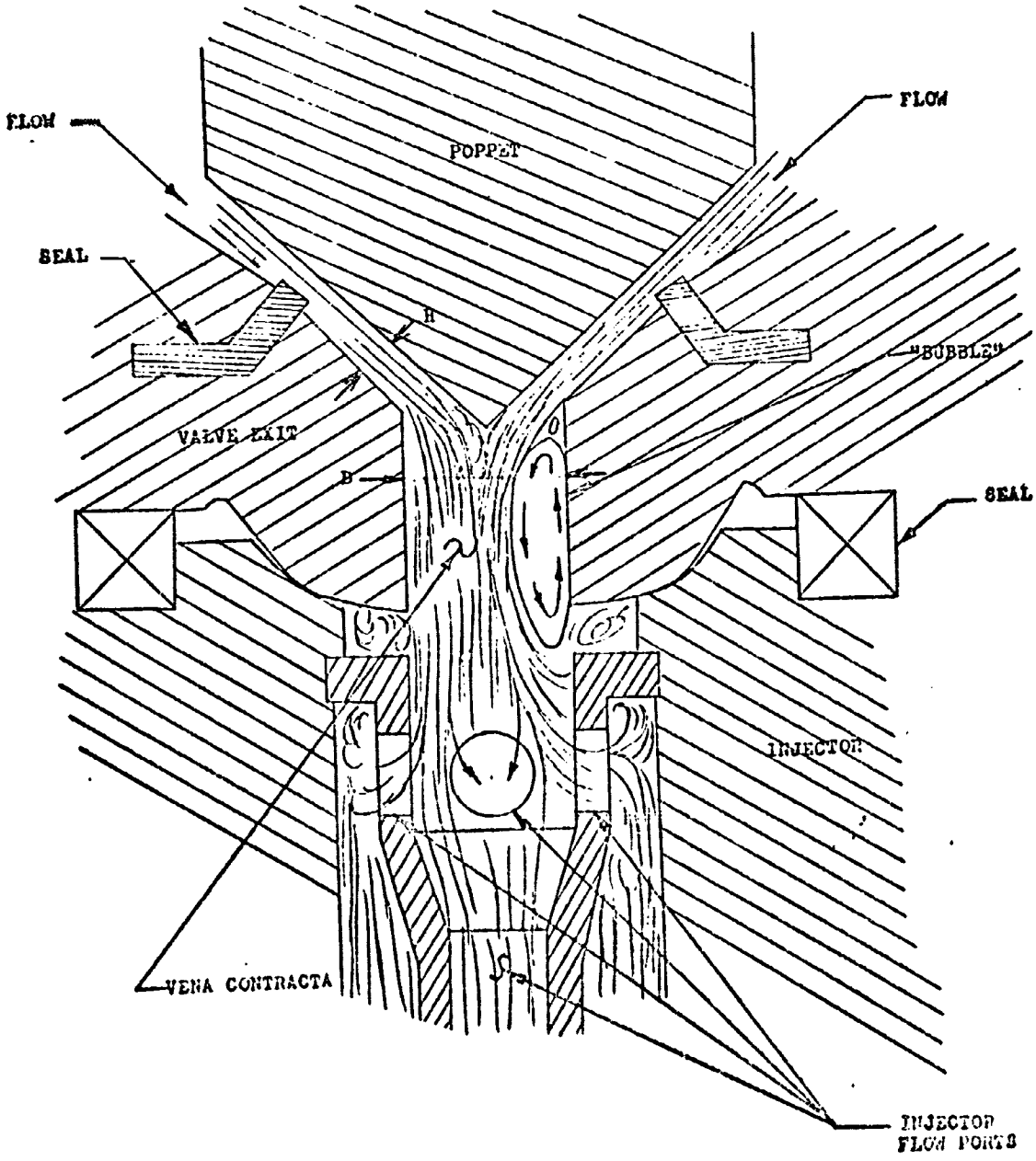

Figure 24

The volume flow rate is

$$Q = 4.62 \text{ in}^3/\text{sec.}$$

which yields a flow velocity at the valve seat exit of

$$V_e = 70 \text{ ft/sec.}$$

The contraction area ratio for a 40° conical nozzle is

$$\frac{Ac}{A} = 0.75$$

Then

$$V_c = 93.4 \text{ ft/sec.}$$

The total to static pressure differential at the vena contracta is

$$\Delta P_c = 1/2 \, PV_c^2$$
$$= 83.5 \text{ psi.}$$

The pressure upstream of the valve in the engine is nominally 170 psia. Allowing for a small drop to the valve seat, the pressure at the vena contracta will be about

$$P_c = 85 \text{ psia.}$$

Consequently if the propellant is saturated with helium at a pressure greater than 85 psia, some of the helium will come out of solution in the valve seat. The bubbles may remain in the valve area or they may be swept into other parts of the injector head or into the chamber to cause thrust oscillations.

V. CONCLUSION

While the bladders in the flight vehicle propellant tanks protect the propellants from the pressurant gas, ground tests are usually made with propellants containing either entrained or dissolved pressurant gas. This gas can cause unrepeatable oxidizer flow from test to test and also engine thrust oscillations. The engine is more susceptable to oscillations with nitrogen gas than helium. Three possible causes of the oscillations are a trapped gas bubble in the injector, a gas flow rate limit, and cavitation in the oxidizer valve. Oscillations during ground tests can be avoided by limiting the time the propellants are exposed to the gas. In space there is no problem because the bladders protect the propellants from the gas as indicated by the Lunar Orbiter flights.

CHAPTER 5

CONTAMINATION CONTROL

BY

Q. R. CALL

TABLE OF CONTENTS

		PAGE
I.	INTRODUCTION	5-1
II.	HISTORICAL DEVELOPMENT SUMMARY	5-2
	A. General	5-2
	B. Propellant Valve Contamination Problems	5-5
	C. Propellant Injector Contamination Problems	5-9
	D. Engine Contamination Problems	5-13
III.	EVOLUTION OF CONTAMINATION CONTROL FACILITIES AND PROCEDURES	5-18
	A. General	5-18
	B. Clean Rooms at The Marquardt Corporation - Van Nuys	5-18
	C. Contamination Control Procedures	5-32
	D. Contamination Control Committee	5-33

LIST OF ILLUSTRATIONS

FIGURE NO.		PAGE NO.
1	Summary of Apollo SM-LM RCS Engine Contamination Problems	5-3
2	Chronology Frequency Summary	5-4
3	Gross Surface Damage to Teflon Valve Seat	5-7
4	Head and Valve Assembly - Model R-4D Rocket Engine	5-10
5	Injector Contamination	5-11
6	600 Micron (.024 in) Glass Particle Imbedded in Valve Teflon Seal	5-14
7	Injector Contamination	5-16
8	Valve Contamintation	5-16
9	White Room Air Shower	5-19
10	White Room Cleaning Area	5-20
11	White Room Subassembly and Valve Test Area	5-21
12	White Room Final Inspection and Packaging Area	5-22
13	Laminar Flow Room	5-24
14	Laminar Flow Room - Engine Assembly	5-25
15	Laminar Flow Room - Cluster Assembly Inspection	5-26
16	Assembly Leaving Controlled Area No. 1 for Test	5-28
17	Acceptance Test Controlled Area No. 2 Laminar Flow Bench	5-29
18	Acceptance Test Controled Area No. 2 Water Flow Bench	5-30
19	Acceptance Test Controlled Area No. 2 Laminar Flow Bench Leak Test	5-31

I. INTRODUCTION

The development of contamination control at Marquardt has been an integral part of the Apollo SM-LM RCS engine development program. It was learned early in the program that proper performance and reliable operation of the engines were affected by contamination. The most sensitive areas affected by contamination were found to be the propellant passages of the injector head and valves and the propellant valve seat.

The propellant passages are affected by both film residues and particulate contamination. Plugged or restricted propellant passages may cause decrease in thrust and specific impulse. Also, abnormal flow distribution, inadequate preignitor chamber cooling, or improper combustor cooling may result in a combustor burn-through.

The sealing capability of the propellant valves may be degraded by trapped particles between the poppet and the seat or by resulting damage to the Teflon seal from temporarily trapped particles. Valve leakage may be a serious failure resulting in loss of propellant and possible engine explosion.

Contamination control for the RCS engine has resulted through the development and implementation of a philosophy of building the components and engine assembly clean and maintaining them clean during subsequent testing and handling. Clean room facilities and special cleaning process were developed to provide the necessary fabrication control. Special handling procedures and protection against contaminated test fluids were implemented to maintain the required cleanliness of the engines.

II. HISTORICAL DEVELOPMENT SUMMARY

A. General

Contamination control by design and training have received primary effort during the Apollo SM-LM RCS engine development program. It is believed that by adequate design of requirement and procedures, and proper training and motivation of the technicians and operators who work with the hardware, contamination control will be achieved with a minimum of problems. However, failure analysis of engine hardware contamination problems and functional failures resulting from contamination have played a significant roll in the development of contamination control techniques. An evaluation of all hardware failure/malfunction investigations on qualification/production type hardware during the period July 1965 to June 1968, showed that contamination was the most frequent problem (being 39% or 99 of the 252 failure/malfunction investigations which occurred).

A summary of the 99 contamination problems mentioned above are summarized in Figure 1. As can be seen, 58 of the 99 problems were either propellant valve leakage or low flow characteristics of the injector head fuel passages which resulted from contamination. Thirty-five of the problems were found as contamination prior to any functional failure. Figure 2 shows a chronological frequency summary of these contamination problems. It is estimated that the production rates and test programs and hence, the opportunities for problems, was fairly constant from 1965 through 1967.

SUMMARY OF APOLLO SM-LM

RCS ENGINE CONTAMINATION PROBLEMS

(JULY 1965 TO JUNE 1968)

PART DESCRIPTION	PROBLEM EXPERIENCED	NUMBER OF OCCURRENCES
RCS Engine	Contamination	25
	Valve leakage	18
	Low flow of oxidizer system	4
	Failure of filter rinse test	1
Injector Head & Valve	Low preignitor cooling flow	28
	Low chamber cooling flow	6
	Low fuel preignitor flow	4
	Contamination	4
	Valve leakage	1
	Failure to pass orifice rinse test	1
Propellant Valves	Contamination	6
	Valve leakage	1
	TOTAL	99

Figure 1

CHRONOLOGICAL FREQUENCY SUMMARY
OF APOLLO SM-LM RCS ENGINE
CONTAMINATION PROBLEMS
(JULY 1965 TO JUNE 1968)

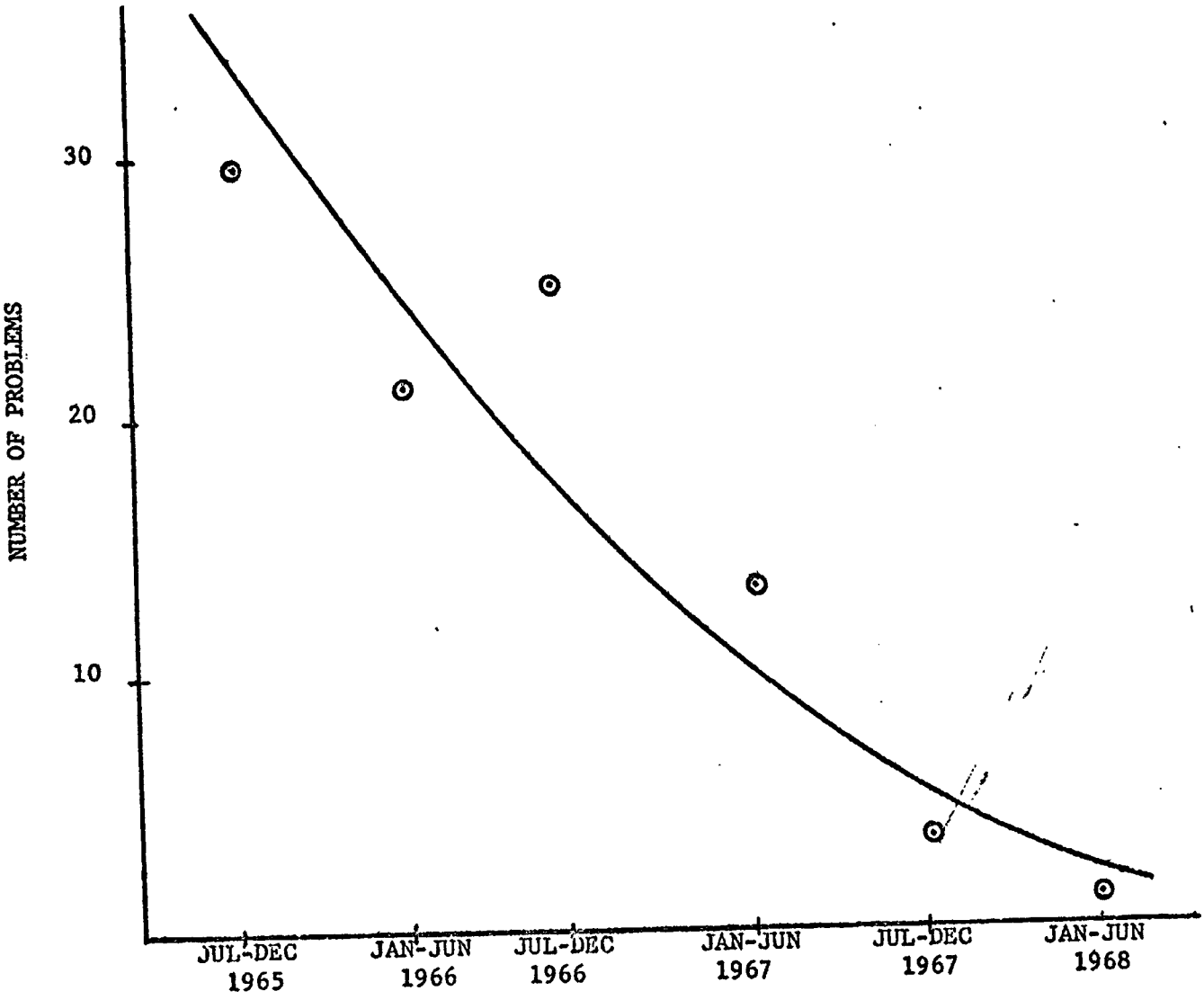

Figure 2

II. HISTORICAL DEVELOPMENT SUMMARY (CONTINUED)

B. Propellant Valve Contamination Problems

Valve leakage is one of the most serious failures resulting from engine contamination. Valve leakage may be a minor or a catastrophic failure mode depending on the magnitude. Excessive propellant leakage may result in depletion of the propellant supply or cause an explosion. Gas leakage as used for acceptance criteria is of minor concern except as an indication of possible propellant leakage. Gas leakage above the allowable specification limit of 15 cc/hr does not necessarily mean propellant leakage. The relationship between GN_2 leakage and liquid leakage has been checked numerous times at TMC, however, with very inconsistent results. This is believed to be due to the many different flow relationships which govern the many different types of leakage paths. The experience does indicate that the GN_2 leakage which indicates zero propellant leakage may be significantly higher than 15 cc/hr.

Particulate contamination can cause valve leakage by two separate actions. Particles entrapped between the armature pintle and the Teflon seal or metal stop of the seat assembly can result in a gap and consequently leakage. Also, particles may cause damage to the Teflon sealing surface with resultant leakage.

The size of contamination which will cause valve leakage has not been established and may be very difficult to establish. However, analysis and experience indicates that filtration to approximately 30 microns is necessary to protect the valve.

Since July 1965, when the qualification valve configuration was established, there have been 29 occurrences of valve leakage. All but three of these problems were excessive GN_2 leakage. During the LM

system testing at Magic Mountain, one oxidizer and one fuel leakage occurred due to contamination, and one oxidizer leakage occurred due to an injector explosion. Of the total 29 occurrences of valve leakage, 19 were concluded to have been caused by some form of contamination.

Nine of the 29 valve leakage problems occurred during acceptance testing. Only 4 of these were due to contamination and these all occurred between July and December 1965. Since then, the contamination control procedures used during assembly and acceptance testing have prevented any additional acceptance test valve leakage problems due to contamination. The control of engine contamination during test programs and customer handling was less effective during this same period.

Only infrequently have the actual particles of contamination which caused the valve leakage been recovered and identified during the investigations. Usually, only the Teflon surface damage in the form of depressions or scratches is evidence of contamination which previously passed through the valve. Almost half of the valve leakage problems resulting from contamination were GN_2 leakages below 60 cc/hr. In all of these cases, only scratches or Teflon surface depressions were found to evidence the effects of contamination. Figure 3 is an example of gross Teflon surface damage due to contamination passing through the valve. This valve was tested without adequate facility filters.

Particles smaller than about 100 microns, trapped between the armature poppet and seal of the valve generally do not cause leakage. The high unit force on the particle from the poppet load either smashes the particle against the seat stop or causes it to be imbedded into the soft Teflon seal. With additional cycles the particle is either smashed, flushed through the valve, or imbedded deep enough to allow the valve to seal. Partially imbedded particles which are subsequently

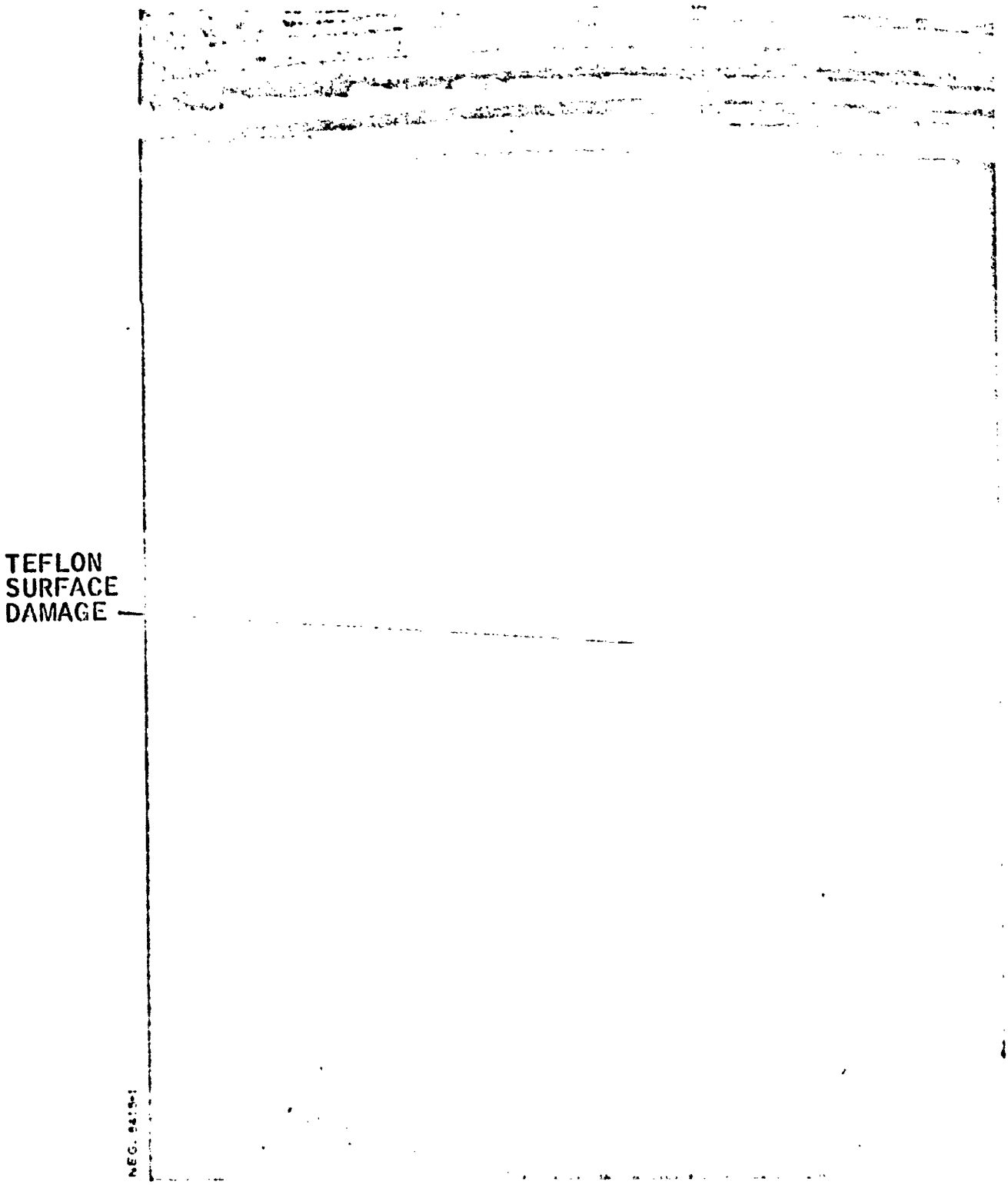

FIGURE 3. GROSS SURFACE DAMAGE TO THE TEFLON VALVE SEAT (APPROX. 120X) REF. FAILURE/MALFUNCTION REPORT 329-80

dislodged result in Teflon seal surface defects discussed in the preceeding paragraph. Experience with large particle contamination is discussed in Section A-3.

Development of contamination control procedures for the propellant valves has been quite effective for fabrication and acceptance test operations as mentioned above. Care has been taken to eliminate any internal or external contamination considered to be injurious to the valve or downstream hardware (injector assembly).

Sources of internal contamination include burrs, Teflon particles from the valve seat, and foreign particles trapped inside the valve. Manufacturing procedures of detail parts include special care to prevent burrs. The possibility of Teflon particles from the valve seat is reduced to a minimum by assembly of the valve and conducting 2,000 break-in actuations with water flow. Subsequent to this break-in procedure, the valve is disassembled, the seat inspected to a visual inspection standard, and recleaned before final assembly.

Protection of the valve from external contamination sources is accomplished by keeping the valve inlet covered at all times, except during testing. During all testing where fluids are introduced into the valve, a 15-30 micron filter is attached at the valve inlet in piggyback style.

II. HISTORICAL DEVELOPMENT SUMMARY (Continued)

C. Propellant Injector Contamination Problems

The propellant injector of the Apollo SM-LM RCS Engine has experienced many rejections during acceptance testing due to contamination problems. However, since the production of the qualification design configuration began in 1965, no engine functional failure has resulted from injector contamination during any of the test programs.

The injector design contains many propellant passages which include fuel cooling for the preignitor and the combustor.

Figure 4 is a layout of the engine which shows most of the propellant passages. Acceptance tests for the engine include monitoring the flow from each port to verify proper levels. Two types of flow problems caused by contamination have been experienced. Individual ports have been found blocked due to large particle contamination and and the total preignitor cooling flow has been found to be too low due to particulate and film type contamination.

Prior to development of adequate cleaning procedures for the injector head assembly and adding a screen at the valve inlets, several engines were rejected due to clogging of the fuel preignitor passage at the 10 degree included angle in the insert assembly. This conical shaped passage acted as a trap for fibers and subsequently other particulate contamination.

Large particle contamination of the injector assembly has been a problem in a few instances. One such problem was experienced when a chamber cooling hole was found partially blocked by a piece of Teflon. Figure 5 shows the blocked hole and the particle. Other large particle contamination problems are discussed in Section D, Engine contamination problems.

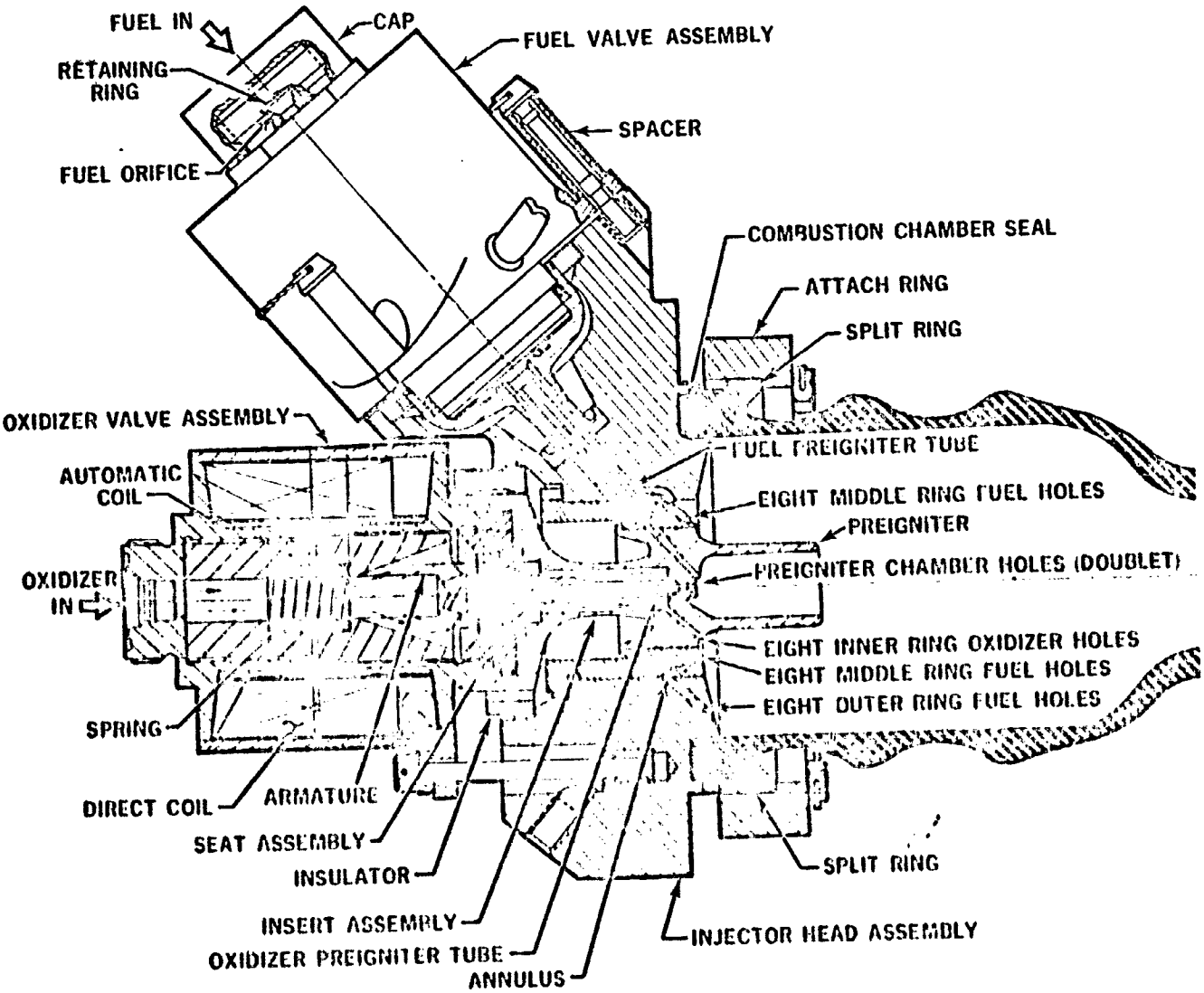

FIGURE 4. HEAD AND VALVE ASSEMBLY - MODEL R-4D ROCKET ENGINE

5-10 Figure 4

NEG. 8432-1

FIGURE 5A. BLOCKED CHAMBER COOLING HOLE AND PARTICLE (14X)

NEG. 8432-2

FIGURE 5B. PARTICLE THAT BLOCKED CHAMBER COOLING HOLE (14X)

FIGURE 5. INJECTOR CONTAMINATION (REF. FAILURE/MALFUNCTION REPORT 8417/M-129)

The most frequently experienced contamination problem with the injector assembly has been low total preignitor cooling flow. This flow impinges on the outside of the preignitor chamber for cooling purposes. There are 7 holes which are .0098/.0102 inches (these are the smallest propellant ports in the engine) and one hole .0199/.0203 inches. Total flow requirements for these 8 holes is 12.5 to 15 percent of the total flow. Failure to meet the required flow was, in nearly every case, due to a general flow restriction rather than a blockage of any individual hole. It is believed that film type contamination and surface held particulate was responsible for the flow restriction.

Although experience of this problem indicated a very close line between contamination and basic material surfaces, it was found that additional cleaning of the injector assemblies brought the flows to within the required limits.

Development of the cleaning procedures for propellant passages eventually resulted in flushing the passages with clean water at a flow rate of 400 to 1,000 ml per minute while the part is submerged in an ultrasonic bath for a 5-minute period. This operation is followed by purging with alcohol and then with Freon under a minimum pressure of 50 psig.

The above flushing operations are done in a direction opposite to the normal flow direction and prior to installation of the preignitor tubes and the propellant valves. When the injector is clean, the preignitor tubes and previously cleaned and acceptance tested propellant valves are installed. The complete assembly is then forward flushed with at least one quart of Freon through each valve with several valve actuations during flow. This procedure has proved quite successful as shown by the low rejection rate since requiring this method of cleaning the injector assembly.

II. HISTORICAL DEVELOPMENT SUMMARY (Continued)

D. Engine Contamination Problems

The following discussion is presented to review engine contamination problems which have occurred during handling and usage outside of TMC acceptance test and controlled test programs. Based on the evidence of the occurrences of gross contamination problems (see examples below), it became evident that careful control of contamination during assembly and acceptance test at Marquardt was not enough to assure reliable engine operation free from contamination failures.

An example of gross contamination occurred at TMC during a test of a monopropellant engine using an Apollo type valve. Failure was experienced when the engine could not be shut off indicating failure of the valve to close due to gross contamination or other possible causes. Investigation revealed a 600 micron (.024 inches) glass particle imbedded in the Teflon seal of the valve (see Figure 6 photograph). This particle was sufficiently large to prevent the poppet from closing properly to shut off the propellant flow.

The first significant engine contamination problem which occurred to an engine delivered to the customer was during check-out of Quad "A" Engines on Apollo S/C 009 at John F. Kennedy Space Center. Investigation of leakage from two of the engines resulted in finding excessive contamination in all four of the engines. The contaminants were varied in identity including sand, metal, human hair, Teflon, wood, rutile, RTV rubber, corrosion products, and other unidentified contaminants. It was concluded that the source of the contaminants was both internal and external to the quad engine system. Recommended action of the NASA investigation team included; 1) provisions for protecting the engines from contamination through the combustor exit bell during test and check-out; 2) checking engines at all levels of manufacture and test to determine and eliminate the sources of contamination; and 3) provide filters immediately upstream of each valve to entrap any internal foreign particles.

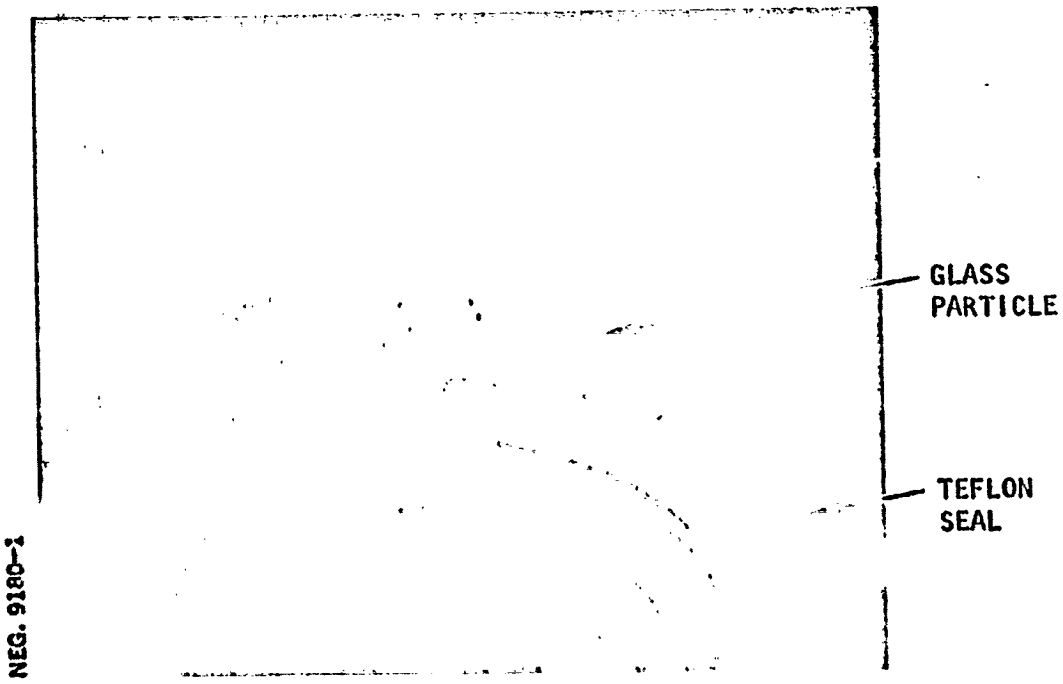

FIGURE 6. 600 MICRON (0.024 IN.) GLASS PARTICLE INBEDDED IN VALVE TEFLON SEAL (18X) (IR&D ENGINE TEST)

Another significant contamination problem to a delivered engine occurred during check-out of Quad "C" engines on Apollo S/C 012 at John F. Kennedy Space Center. An indicated flow restriction in the #4 engine resulted in returning the engine to Marquardt for failure analysis. Investigation disclosed that a piece of nylon plastic (.22 x .23 inches and .0017 inches thick) was lodged at the cross holes of the fuel preignitor tube and was causing a 22.5% decrease in the fuel flow (see Figure 7). The plastic material was probably from a widely used nylon bag.

During check-out of a Quad "B" engine on Apollo S/C 020 also at John F. Kennedy Space Center, the fuel valve of the #2 engine was found to have excessive leakage. Investigation after return to Marquardt disclosed that leakage was caused by pieces of white paint of the type used for striping fittings after proper torquing. Figure 8 shows photos of the paint on the valve Teflon seal and also on the outside of the valve inlet near the area where the paint is normally used.

Based on the above experiences and other similar occurrences, three specific actions were taken to protect the engines from contamination during handling and usage operation. First, protective covers are used on the exit bell of the engine which provide considerable protection for inadvertent external contamination. Second, 25-30 micron filters are provided in the RCS propellant systems upstream of the engines. Third, all engines are being retrofitted with a 160 micron strainer element which is installed into the valve inlet and is an integral part of the engine. It is believed that this strainer will prevent most of the injurious large particle contamination of the type described above from entering the valve or the injector.

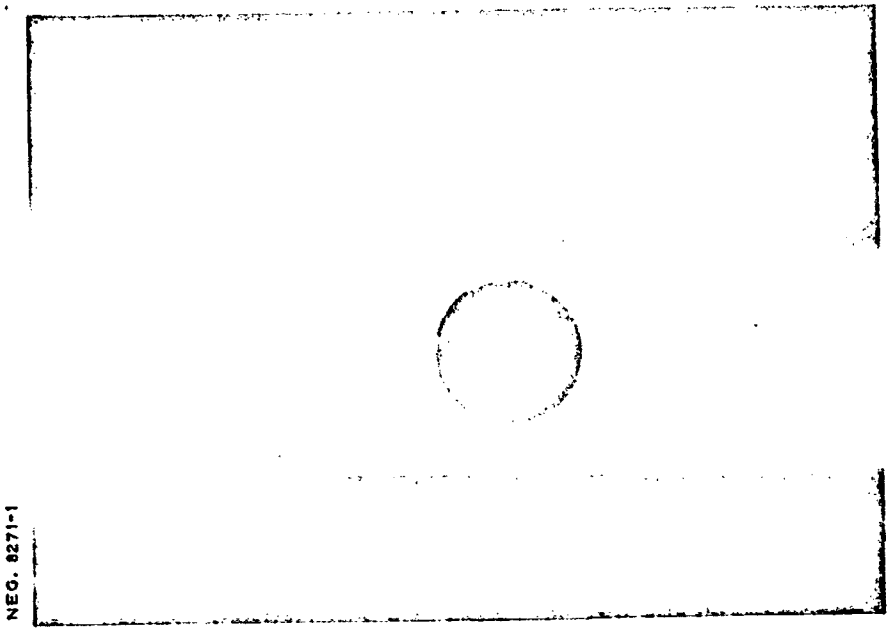

FIGURE 7A. PLASTIC IN PREIGNITOR TUBE (8X)

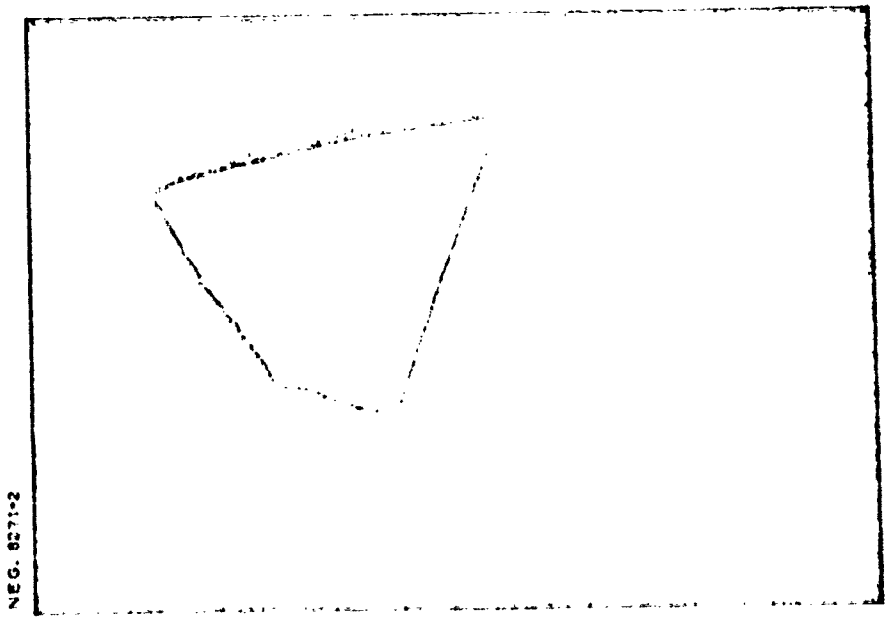

FIGURE 7B. PLASTIC AFTER REMOVAL FROM PREIGNITOR TUBE (8X)

FIGURE 7. INJECTOR CONTAMINATION (REF. FAILURE/MALFUNCTION REPORT CR-056)

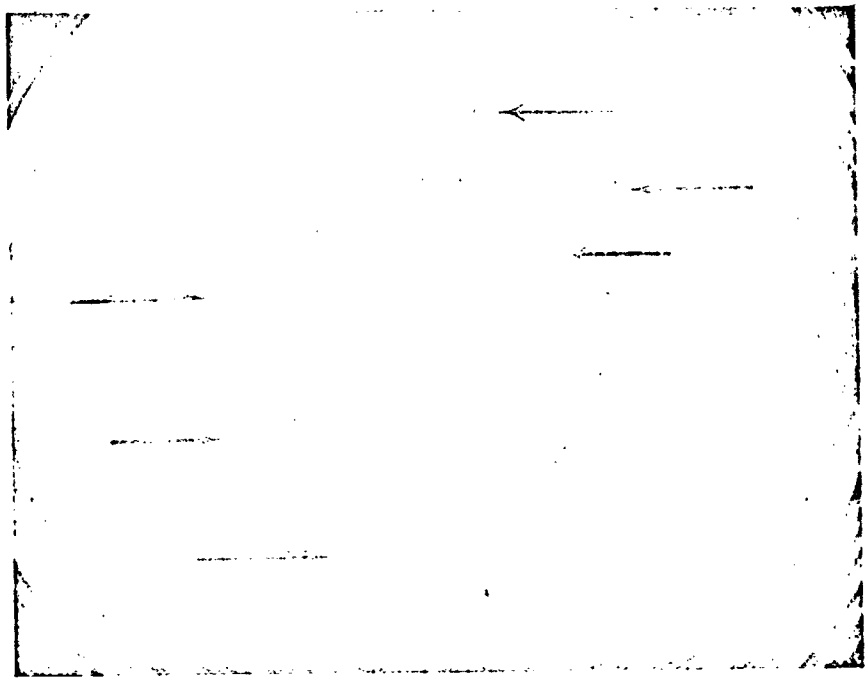

FIGURE 8A. WHITE PAINT ON VALVE TEFLON SEAL FACE (11X)

FIGURE 8B. WHITE PAINT ON THE TOP OF VALVE

FIGURE 8. VALVE CONTAMINATION (REF. FAILURE/MALFUNCTION REPORT CR-075)

III. EVOLUTION OF CONTAMINATION CONTROL FACILITIES AND PROCEDURES

A. General

With the advent of development of reaction control engines for man-rated systems at Marquardt, the need for clean rooms and contamination control procedures became apparent. Three special clean room facilities have been built and put into use to provide the proper facilities for contamination control. Cleaning procedures, test procedures, and handling procedures have been developed to provide the required operational control during fabrication and acceptance test. A contamination control committee was established to monitor contamination control activities and provide technical guidance for the solution of problems as they arise.

B. Clean Rooms at Marquardt-Van Nuys

1. White Room

A 1,500 square foot, Class 100,000 clean room facility, in conformance with Federal Standard 209, is in daily use. This facility consists of three pressurized and controlled rooms. It includes an entry air lock; a clothing change area; cleaning, subassembly, and test areas; and a final inspection and packaging area. Figures 9 thru 12 show one of two air showers, the cleaning area, the subassembly and valve test area, and the final inspection and packaging areas respectively.

The cleaning area provides cleaning processes including chemical cleaning, detergent washes, Freon rinses, and ultrasonic cleaning, and it has provisions for vacuum, nitrogen, and oven drying. Illumination at an intensity of 175 foot-candles at the working level is provided. The air conditioning is controlled to 72°F with a minimum of 12 changes of air per hour at a relative humidity of 45 to 50 percent, and 0.3 micron filters are utilized for maximum control of dust particles.

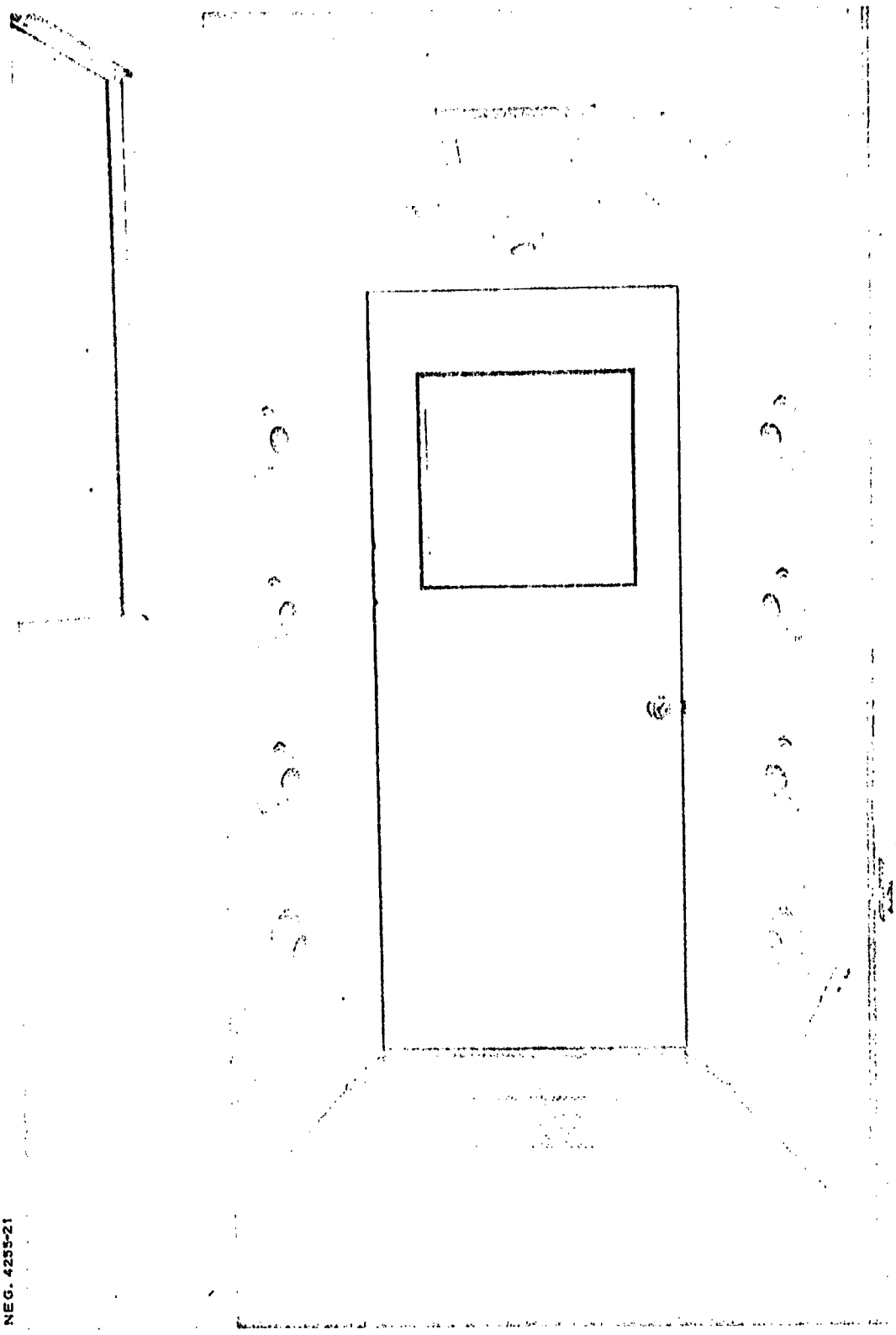

NEG. 4255-21

FIGURE 9. WHITE ROOM AIR SHOWER

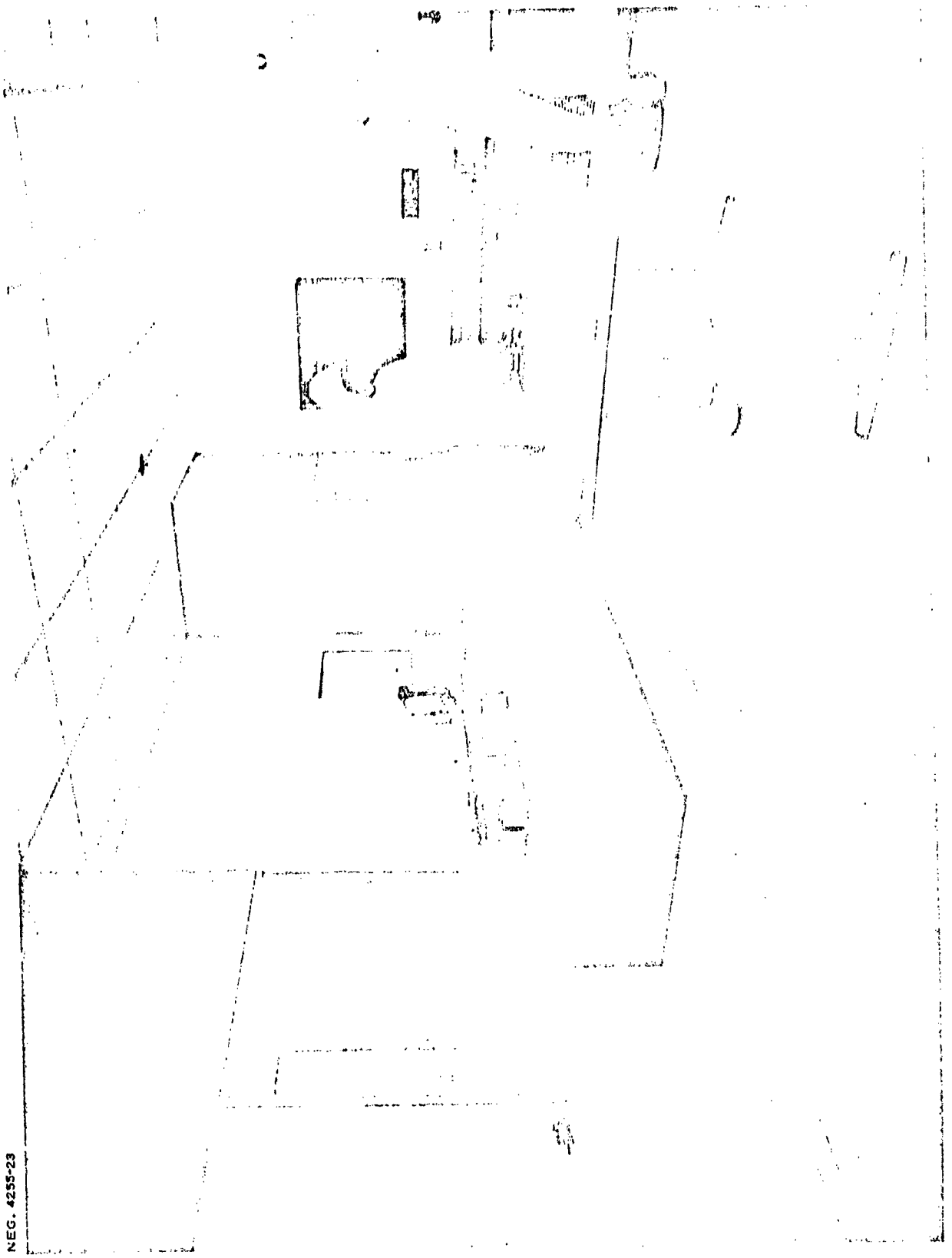

FIGURE 10. WHITE ROOM CLEANING AREA

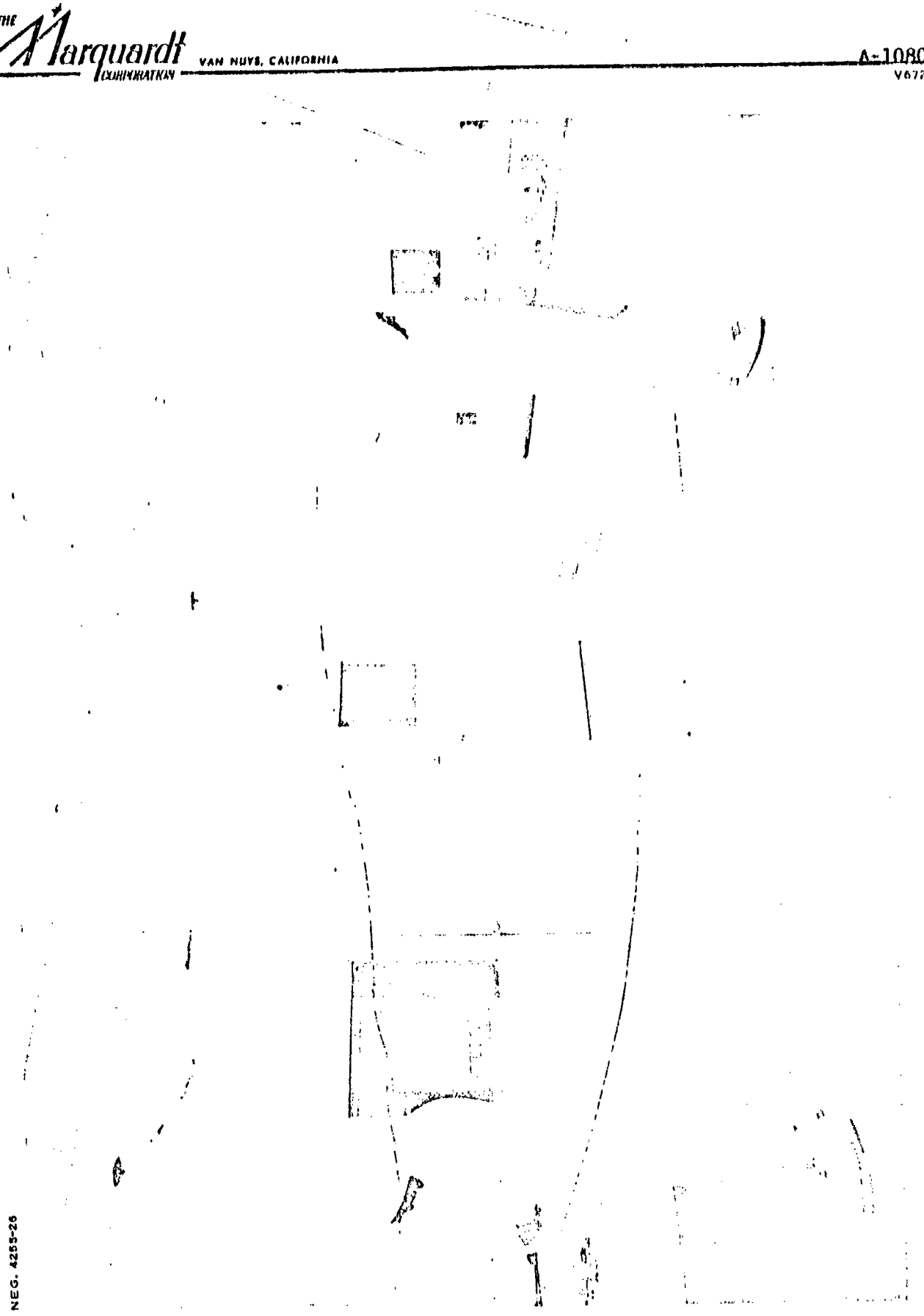

FIGURE 11. WHITE ROOM SUBASSEMBLY AND VALVE TEST AREA

NEG. 4255-26

Figure 11

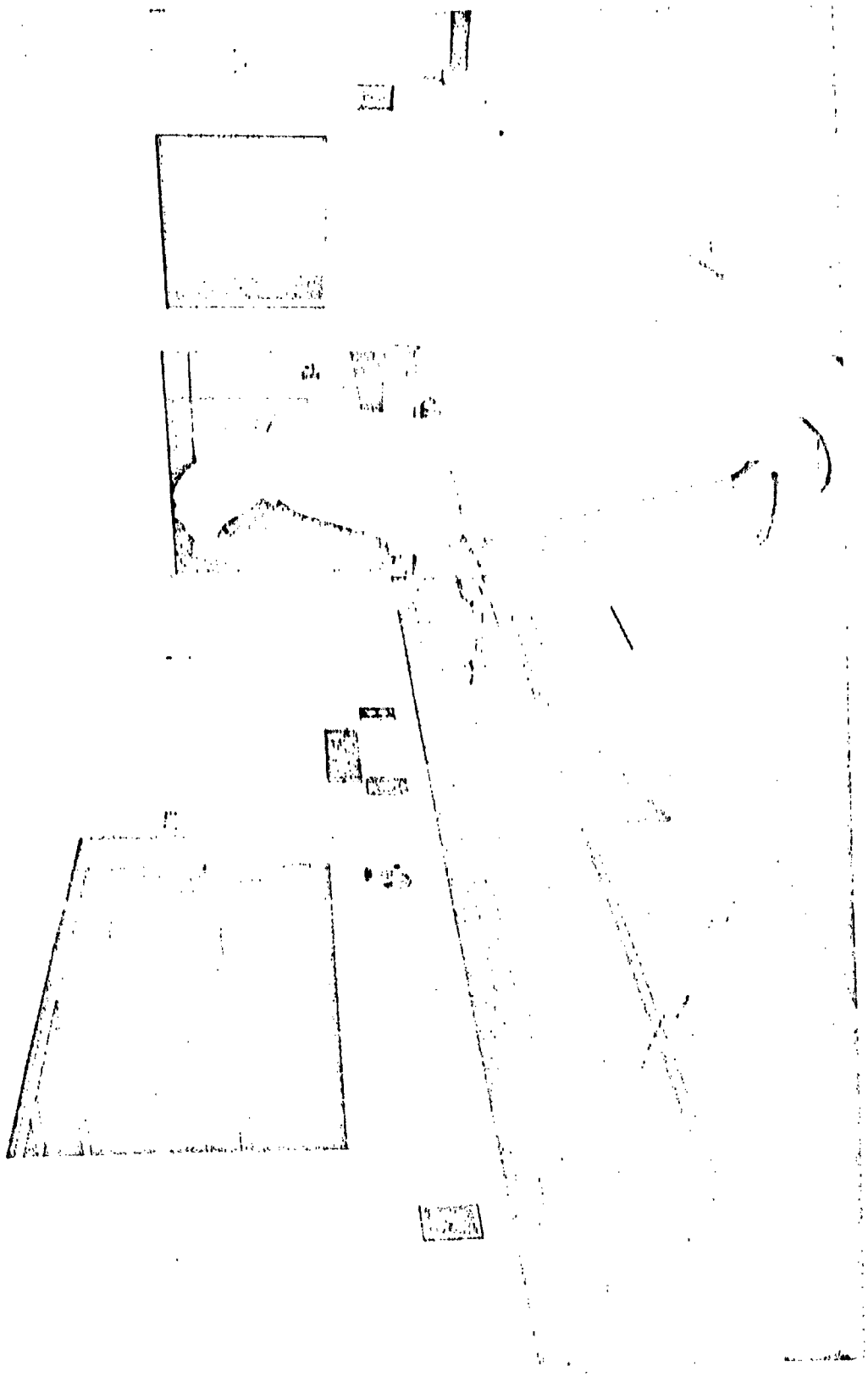

FIGURE 12. WHITE ROOM FINAL INSPECTION AND PACKAGING AREA

NEG. 4255-27

2. Laminar Flow Room

A laminar flow clean room is also available in the assembly area for such activities as press and shrink fit operations, engine final assembly and shake down, and engine disassembly for rework activities. The cleanest part of the room, adjacent to the filtered air flow source, is used to evaluate samples for particulate contamination. An automatic particle counter is presently being implemented for counting facility samples. It is planned that in the future it will probably be used for hardware rinse samples as well (present method is in accordance to SAE-ARP-598).

This facility includes an entry air lock, a clothing change area, and a 900 square foot assembly and test area. The assembly area is equipped with 14 work stations, each with power outlets and a piping bulkhead. The illumination is 175 foot-candles at working level. The air conditioning provides a minimum room air velocity of 90 fpm, temperature control at 72°F, relative humidity at a maximum of 45 percent, and 0.3 micron air filtration throughout for optimum control of dust particles. Figures 13 thru 15 show the Laminar flow room and some work activities.

3. Acceptance Test Controlled Areas

Two controlled areas in the test facility have been developed to provide contamination control during acceptance testing. Controlled Area No. 1 is used for the assembly of engines to the test stand, including attachment of filters to protect the engine, and processing of the engine after the burn test in preparation of postburn acceptance testing. Controlled Area No. 2 is used for preburn and postburn acceptance testing of the reaction control engines and has also been used for valve acceptance testing.

FIGURE 13. LAMINAR FLOW ROOM

NEG. 6912-2

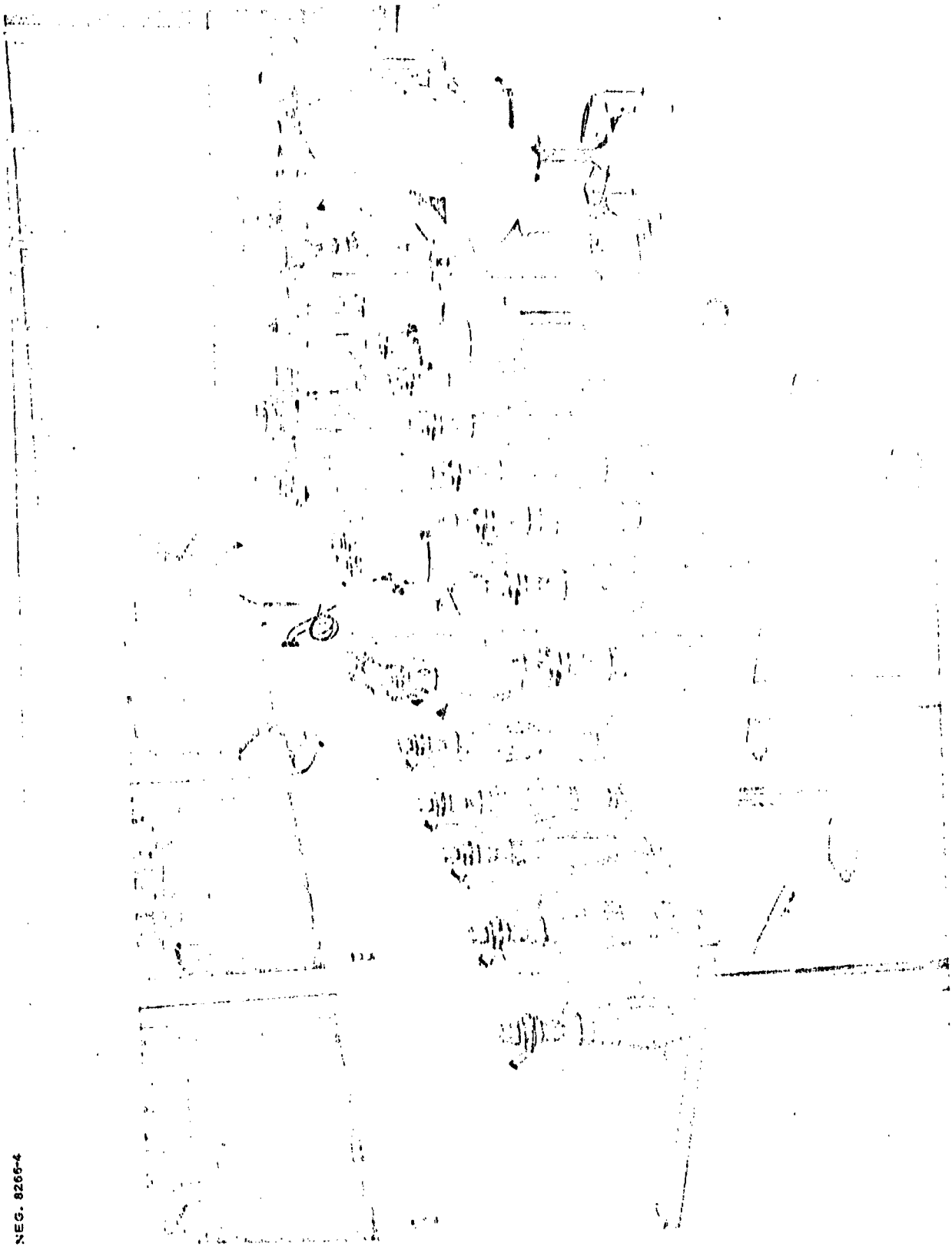

FIGURE 14. LAMINAR FLOW ROOM - ENGINE ASSEMBLY

NEG. 8266-4

Figure 14

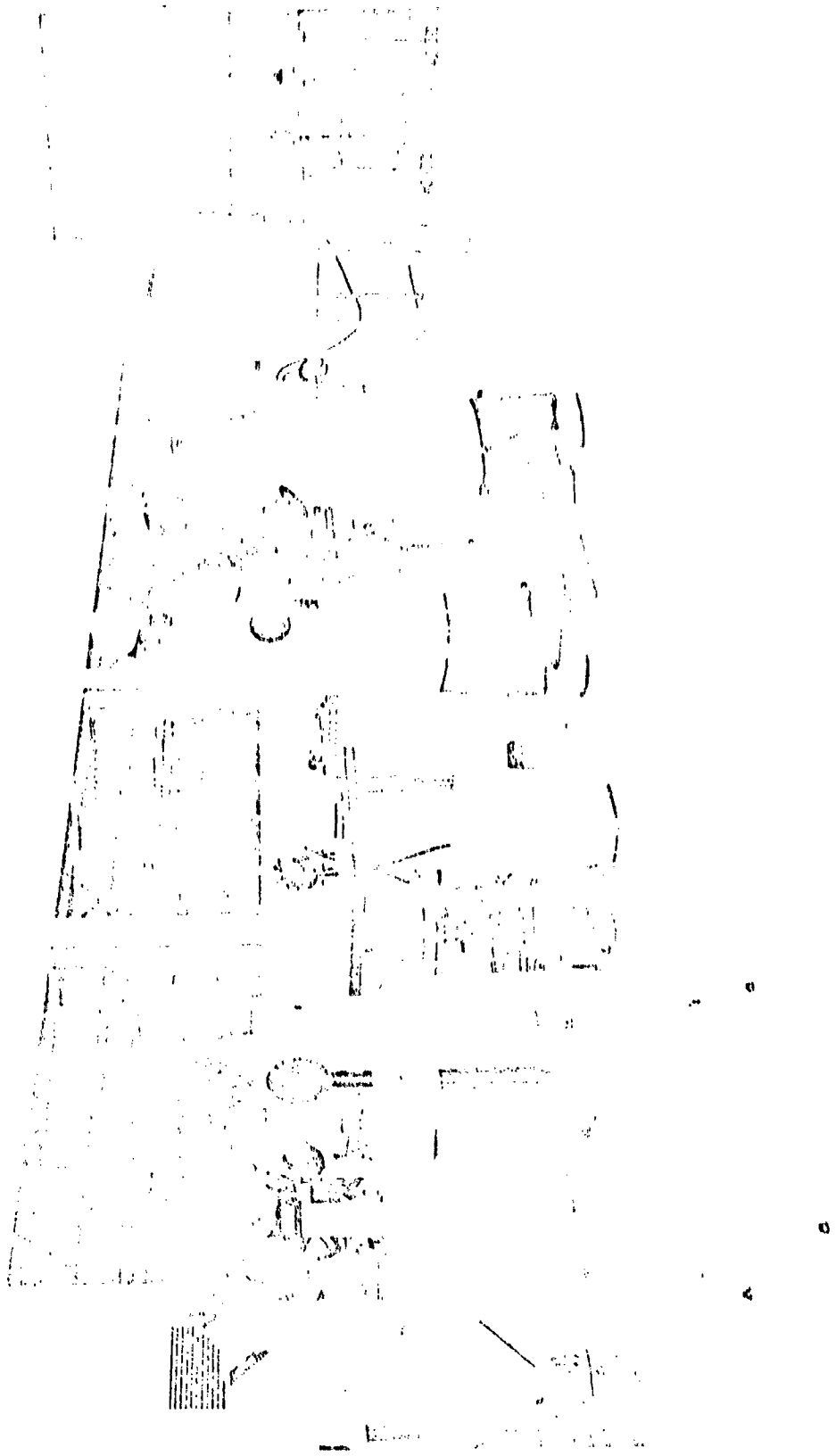

FIGURE 15. LAMINAR FLOW ROOM - CLUSTER ASSEMBLY INSPECTION

NEG. 8379-5

Figure 16 shows an engine assembled on a thrust stand waiting just outside the controlled area No. 1 before going to the test cell for burn acceptance testing. In addition to facility filters, 15-30 micron filters are installed directly to each valve inlet. These "hot fire" filters are removed during the postburn test and replaced. The "hot fire" filters are rinse-tested to verify that adequate protection existed during the burn test.

When engines come back to controlled area #1 after the "hot fire" test in the cells, they have considerable contamination on the external surfaces which at times was carried into the controlled area #2 where postfire tests are conducted. To resolve this problem, a Lady Kenmore dishwasher was modified and put into controlled area #1. When the engines are removed from the thrust stand, they are placed in the washer and the external surfaces cleaned with distilled water. The engines are subsequently dried in a vacuum oven before entering controlled area #2 for postburn testing.

Controlled area #2 is a 1,200 square foot, Class 100,000 clean room facility in conformance with Federal Standard 209. This room consists of an air lock entry which also serves for changing clothes, a large test room, and a room for oven drying and packaging. Figures 17 thru 19 show the test area of the room including the instrumentation, Laminar flow benches, and the flow bench. The air conditioning is controlled 72°F with a minimum of 17 changes of air per hour at a relative humidity of 70 percent maximum, and 0.3 micron filters are utilized for maximum control of dust particles.

Several original improvements to these controlled areas have been implemented as indicated below:

a. During preburn of head and valves in controlled area #2, there was a need for a quick, easy way to remove orifices from the valves without contaminating or damaging the unit. To accomplish

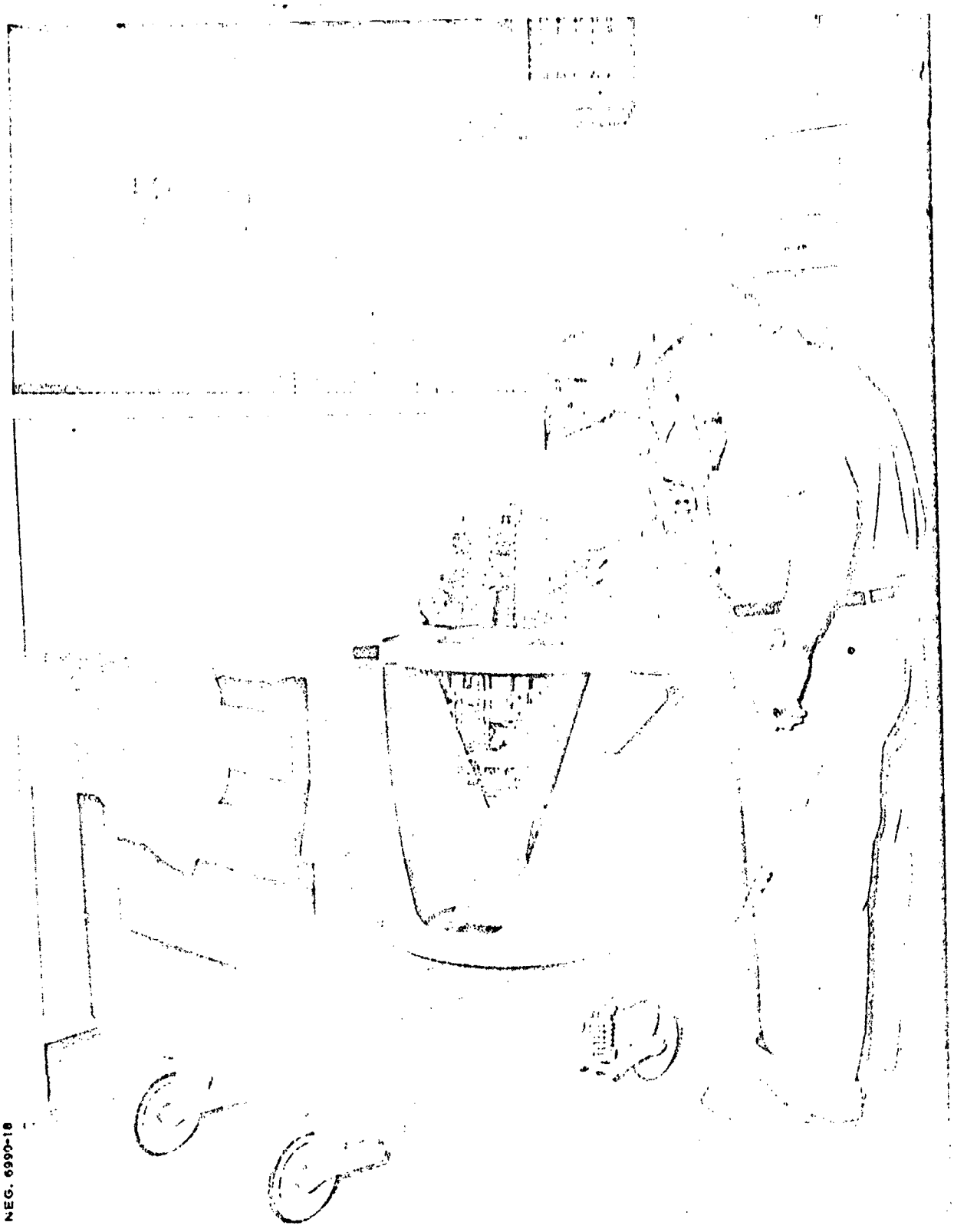

FIGURE 16. ASSEMBLY LEAVING CONTROLLED AREA NO. 1 FOR TEST

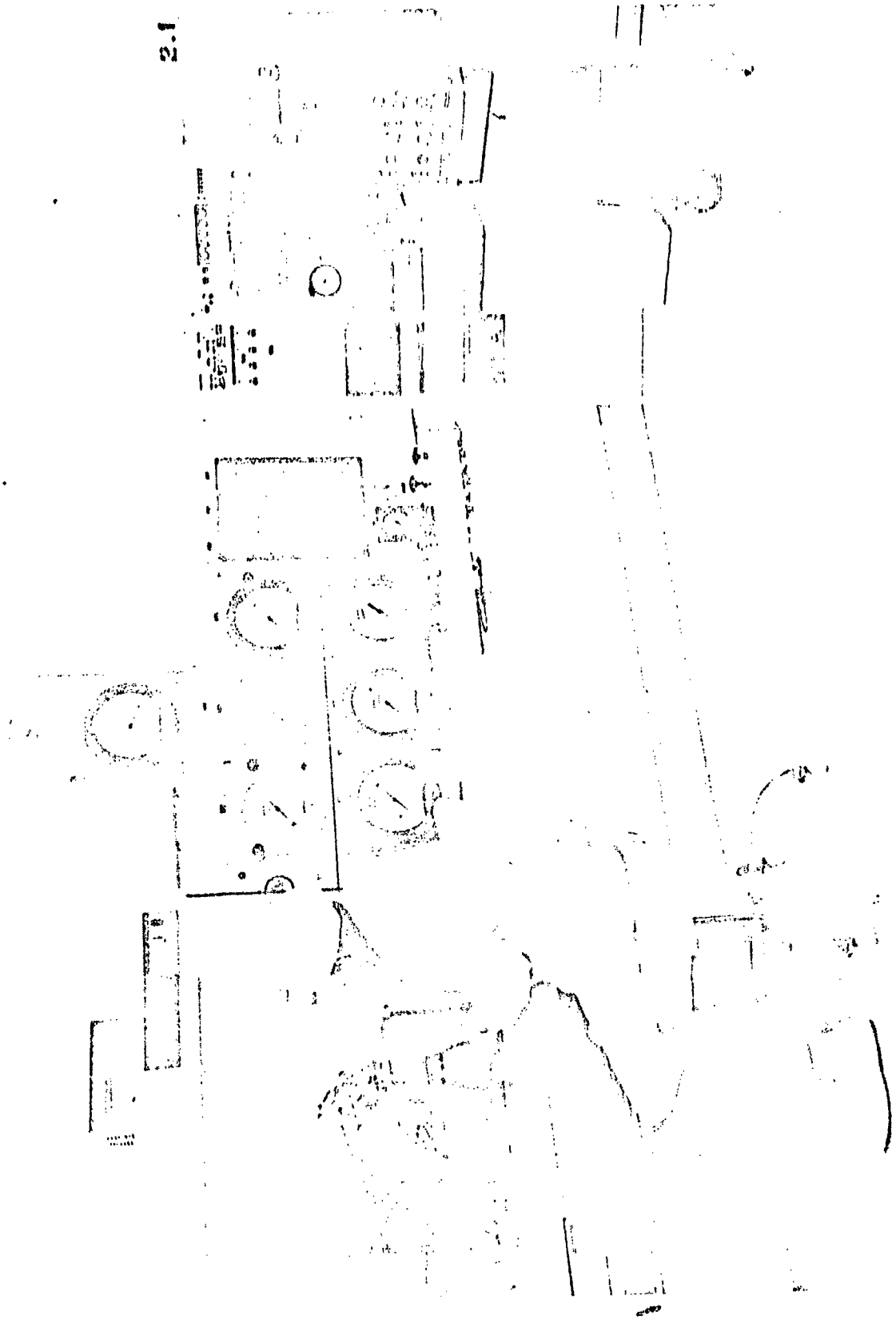

FIGURE 17. ACCEPTANCE TEST CONTROLLED AREA NO. 2 - LAMINAR FLOW BENCH

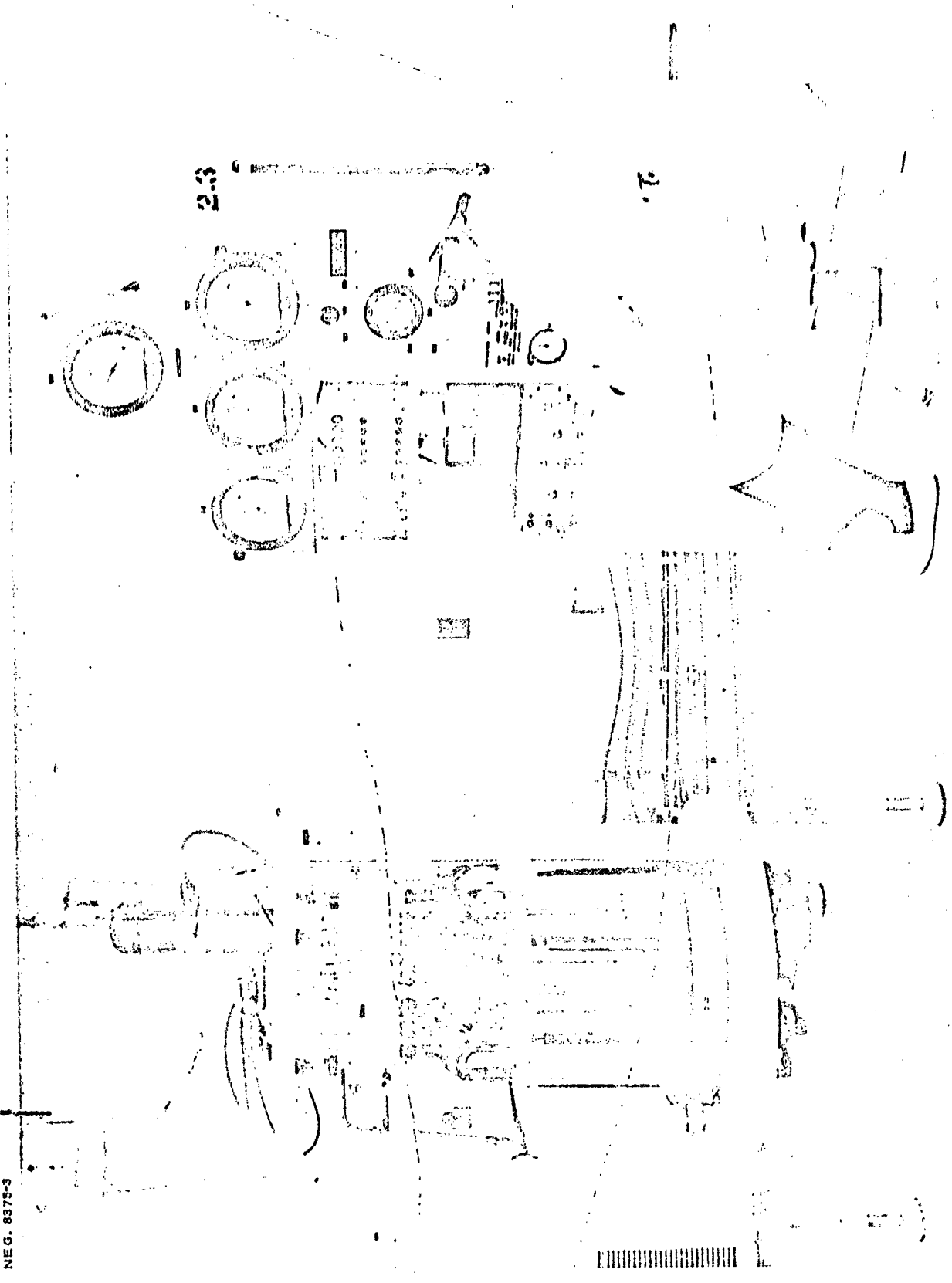

NEG. 8375-3

FIGURE 18. ACCEPTANCE TEST CONTROLLED AREA NO. 2 - WATER FLOW BENCH

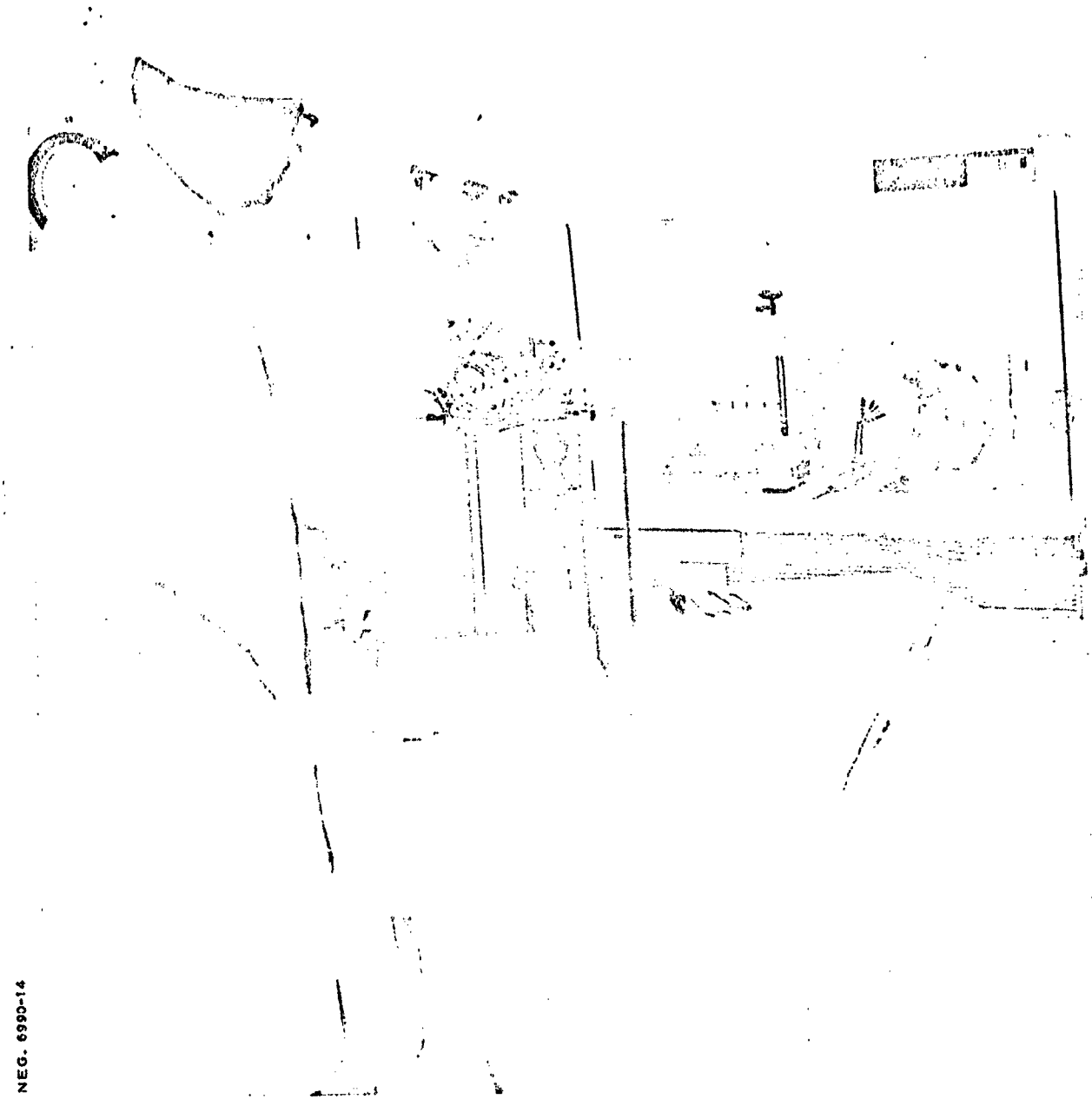

NEG. 6990-14

FIGURE 19. ACCEPTANCE TEST CONTROLLED AREA NO. 2
- LAMINAR FLOW BENCH LEAK TEST

this task, a vacuum line was plumbed to the bench with a small nylon nozzle attached to a stainless flex hose. When the vacuum was turned on, the orifice was very easily plucked from the solenoid valve. This method not only removed the orifice, but removed any possible contamination at the same time.

b. A vacuum hose was installed on each bench to allow the operator to vacuum his person as well as clean any contamination from the work station before installing any hardware on the benches.

c. Wheels were installed on the chairs in the controlled areas to allow the operators more freedom of movement while operating the test benches. Also, this helps to eliminate extra maintenance on the floor that occurred from sliding the chairs on it.

C. Contamination Control Procedures

The primary document which controls the cleanliness of RCS hardware at Marquardt is a Materials & Process Specification (MPS-210), "Cleanliness Requirements for Reaction Control System Engines". This specification defines the requirements for the clean rooms, influent system filtration, particulate contamination limits for influents and hardware, nonvolatile residue (NVR), packaging, and contamination monitoring methods. In addition, this specification contains appendices which define specific requirements for filters, clean room operation and control, and cleaning procedures for RCS hardware.

Other related documents have been prepared which also assist in the control of contamination. Procedures exist for the operation and control of the controlled areas in the test facility. Packaging specifications exist for RCS engines. Also, other detailed procedures exist for some of the cleaning and assembly operation.

D. Contamination Control Committee

A contamination control committee was established as an integral part of the contamination control program at Marquardt. This committee is considered an essential part of the Marquardt aerospace production operation. The committee consists of representatives from Manufacturing, Engineering, Materials & Processes, Test, Quality Assurance, and Reliability with the reliability member acting as chairman.

General responsibilities of this committee include:

1. The committee is to review the program requirements for contamination control facilities with recommendations being submitted to Plant Operations and Program Management.

2. Coordination between all departments, with respect to equipment contamination control, is a responsibility of the committee with the members of the committee being responsible for contamination control in their respective departments.

3. The committee is to secure and exchange information between members to minimize duplication of work and facilities. This information is to be consistent with the state-of-the-art as available through recognized technical society activities, government technical orders and MIL standards.

4. The duties of the committee include the following additional actions to assure the control of contamination:

   Review customer requirements related to contamination.

   Review of product design drawings.

   Review manufacturing processes related to contamination control.

Review manufacturing facilities design as related to contamination control.

Review test facilities design as related to contamination control.

Review test department procedures as related to contamination control.

Review process specifications as related to contamination control.

Provide educational program to maintain and improve workmanship in the contamination control areas.

CHAPTER 6

SYSTEM DYNAMIC EFFECTS

BY

R. Y. YOSHIDA

TABLE OF CONTENTS

SECTION NO.		PAGE NO.
I.	INTRODUCTION	6-1
II.	PART 1 - ENGINE-SYSTEM INTERACTION	6-1
	A. Propellants Feed System Dynamics	6-1
	B. System Natural Frequency	6-4
	C. Duty Cycle Influence of Feed System Dynamics	6-5
	D. Pressurant Saturation of Propellant	6-5
III.	PART 2 - LUNAR MODULE REACTION CONTROL SYSTEM TEST	6-7
	A. Introduction	6-7
	B. System Description and Function	6-7
	C. System Operation	6-10
	D. Engine Data Correlation	6-11
	E. Summary of Tests	6-11
	F. Control Events Tests	6-19
	G. Duty Cycle Tests	6-33
	H. Off-Design Operation	6-38
	I. Failure Mode Operation	6-38
	J. Failure Mode Operation	6-41
	K. Decontamination and Examination	6-41
IV.	CONCLUSIONS	6-42
V.	REFERENCES	6-43

LIST OF ILLUSTRATIONS

FIGURE NO.		PAGE NO.
1	Typical Pressure Transients of Bipropellant Engine	6-3
2	Possible Combinations of Two Engines Firing	6-6
3	LM System Pictorial	6-8
4	Schematic - LM RCS System	6-9
5	LM RCS DVT System	6-12
6	LM RCS DVT "A" System Tankage Module	6-13
7	LM RCS DVT System - Engine Cluster Number I	6-14
8	LM RCS Engine Cluster Assembly	6-16
9	Chamber Pressure Time History	6-20
10	Engine Performance	6-21
11	Propellant System Manifold Pressure Time History	6-22
12	Propellant System Manifold Pressure Time History	6-23
13	Propellant System Manifold Pressure Time History	6-24
14	Propellant System Manifold Pressure Time History	6-25
15	Chamber Pressure Time History	6-28
16	Chamber Pressure Time History	6-29
17	Chamber Pressure Time History	6-30
18	Chamber Pressure Time History	6-31
19	Chamber Pressure Time History	6-32
20	DVT System Impulse, Pulse Width Correlation	6-34
21	Specific Impulse vs. Pulse Width	6-35
22	Propellant Consumption Correlation	6-36
23	Propellant Consumption Correlation	6-37
24	Engine Performance, Manifold Pressure Correlation	6-39
25	Chamber Pressure, Manifold Pressure Correlation	6-40

LIST OF TABLES

TABLE NUMBER		PAGE NO.
I	Typical Maximum Water Hammer Pressure	6-2
II	Correlation of Chamber Pressure with Thrust & Specific Impulse	6-15
III	Lunar Module RCS System Test Summary	6-17
IV	Summary of Apollo Lunar Module Reaction Control System Tests	6-18
V	Comparison of Integrated Chamber Pressure	6-27

SYSTEM DYNAMIC EFFECTS

I. INTRODUCTION

In the design of a spacecraft reaction control system (RCS) utilizing liquid propellant engines, the coupling of the engine to the propellant feed system is of paramount importance. When the engine "on" times are in the order of milliseconds and/or multiple engine firings are required, the feed system pressure may never reach a quiescent value and the system must respond to the engine's demand instantaneously and predictably.

This chapter discusses the system dynamic characteristics that should be considered in the design of the RCS. A review of the salient dynamic characteristics of the feed system - engine interaction is given in Part 1.

Part 2 describes the results of the Apollo Lunar Module (LM) Reaction Control system tests, wherein the system dynamic effects discussed in Part 1 are exemplified by test results.

II. PART 1 - ENGINE - SYSTEM INTERACTION

A. Propellant Feed System Dynamics

When an engine valve is suddenly closed or opened, the flow rate of the propellant in the line is decelerated or accelerated and acoustic waves are created in the propellant line. The magnitude of the compression wave caused by the abrupt closing of a valve, or the rarefaction caused by abrupt opening, is influenced by the properties of the propellant and physical characteristics of the propellant lines. This phenomena is commonly referred to as "water hammer".

The sudden closure of an engine valve increases the pressure just upstream of the valve and this pressure propagates upstream through the line at the local speed of sound. The increase in pressure is proportional to the arrested velocity of flow and to the speed of propagation of the pressure wave. The maximum pressure increase may be expressed as follows:

$$\Delta P = \rho \frac{VC}{g} \qquad (1)$$

Where

ΔP = pressure increase (lb/ft^2)

V = arrested flow velocity (ft/sec)

C = speed of sound in propellant (ft/sec)

ρ = propellant density (lbm/ft^3)

g = gravitational constant ($32.2\ ft/sec^2$)

The increase in pressure expressed in Equation (1) will be attained only in the case where the valve closure time is less than one cycle of the pressure wave, where the cycle time is a function of the plumbing geometry and speed of sound.

The speed of sound in the propellant can be expressed as follows:

$$C = \sqrt{\frac{1}{\frac{\rho}{g}\left(\frac{1}{K} + \frac{DC_1}{bE}\right)}} \qquad (2)$$

Where

- C = speed of sound (ft/sec)
- K = propellant bulk modulus (lb/ft^2)
- D = inside diameter of line (ft)
- E = elasticity of line (lb/ft^2)
- b = wall thickness of line (ft)
- C_1 = dimensionless constant determined by the type of support provided to the line. For lines anchored against longitudinal movement throughout its length $C_1 = 1 - \mu^2$, where μ is the Poisson's ratio of the line material.

Table I presents typical numerical examples of Equations (1) and (2). For the bipropellant example shown, it will be noted that owing to its higher flow rate, the oxidizer will experience higher pressure fluctuations than the fuel.

TABLE I

TYPICAL MAXIMUM WATER HAMMER PRESSURE

Stainless Tubing: OD = .375" b = .020"
Flow, w (at 77°F): W_{ox} = .222 lb/sec, W_f = .111 lb/sec

	Oxidizer N_2O_4	Fuel 50% UDMH-50% N_2H_4
Speed of Sound (ft/sec)	2,460	3,460
Maximum Increase in Pressure (ΔP) psia	196	134

Under comparable conditions the rarefaction wave caused by the sudden opening of a valve are smaller in magnitude than that expressed by Equation (1). Figure 1 represents a typical time history of the feed system pressure of a bipropellant engine during a 50 millisecond pulse. The behavior of the fuel and oxidizer pressures during engine valve opening and closing are clearly indicated in this figure. The damping of the cyclic behavior of the feed

TYPICAL PRESSURE TRANSIENT OF BIPROPELLANT ENGINE

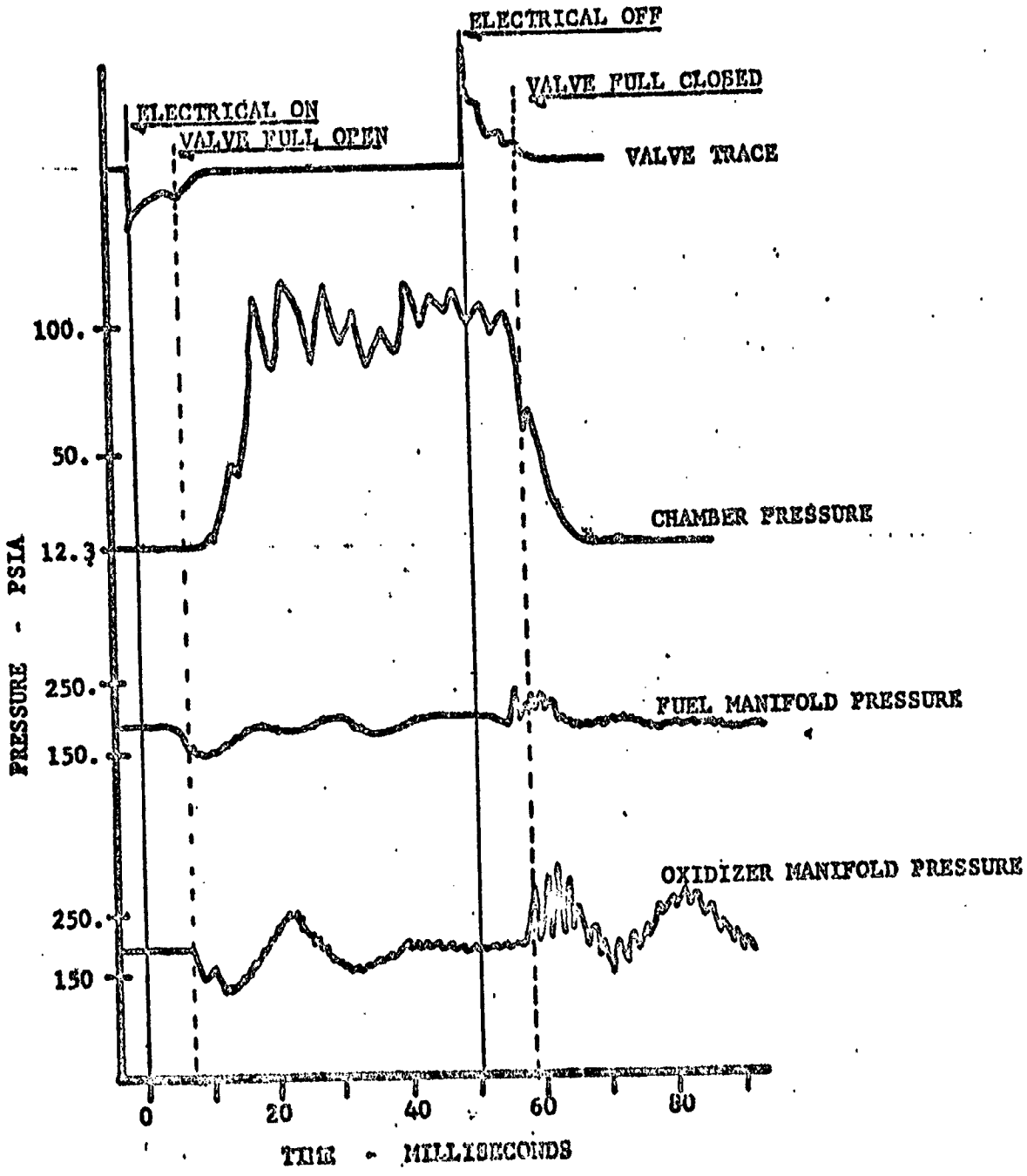

Figure 1

system pressure is caused by friction and fluid damping. In a typical RCS installation the propellant lines feeding the engine take a number of turns (bends) and changes in cross sectional area, these impedance changes all affect the wave propagation of the distributed flow. A detailed treatment of the pressure-time transient associated with both the valve closing and opening are presented in References 1 and 2.

The pressure oscillations of the water hammer phenomena affect the performance of the system in a number of ways. Among them are:

- The time required to reach full flow after engine valves are opened is increased.
- The time required to reach system steady state pressure is delayed when engine valves are closed.
- The performance of other engines utilizing the same propellant feed system is affected.
- Components within the feed system are stressed.
- Creation of gas bubbles and vaporization of propellants are possible.

B. System Natural Frequency

In addition to the water hammer disturbance created by the opening and closing of the engine valve there is an inherent natural frequency of the propellant feed system. This low frequency phenomenon is associated with the elasticity of the propellant line and compressibility of the propellant. Essentially the system reacts to an applied disturbance as a simple spring-mass system. In this analogy the spring constant is an inverse function of the propellant compressibility. The natural frequency can be expressed as follows:

$$f_n = \frac{1}{2\pi}\sqrt{\frac{A}{LM\left(\frac{1}{K} + \frac{DC_1}{bE}\right)}} \qquad (3)$$

Where

f_n = natural frequency (cps)

L = equivalent length of line (ft), for varying cross section

$$L = L_1 + L_2\frac{A_1}{A_2} + L_3 + \frac{A_1}{A_2} + \ldots L_n\frac{A_1}{A_n}$$

A = nominal cross sectional area of line (ft^2)

M = equivalent mass of propellant in line ($lb\ sec^2/ft$)

The mass of a given system remains essentially constant. However, the compressibility may vary with the amount of pressurant (gas) ingested in the propellant or present in the form of bubbles. Data relating to the change in

system natural frequency by pressurant ingestion are discussed in Part 2 of this chapter.

C. Duty Cycle Influence on Feed System Dynamics

A pressurized propellant feed system for typical spacecraft reaction control system application usually provides propellants for a multiple of engines. The pressure oscillations in the feed system created by a single engine firing will affect the performance of other engines which are subsequently fired if they are in close proximity to each other and fired at rapid repetition rates.

As an example of the number of engine firing combinations that might occur in a given mission duty cycle, a simple system with two engines firing from the same propellant source was examined. Assuming that the firing of the individual engines may occur in either a fixed pulse mode (fixed frequency) or steady state (firing time of greater than one second) and with the possibility of either engine being (1) not fired, (2) fired in phase, (3) leading, or (4) lagging, thirty-two (32) different start and shut down transients can be attained as illustrated in Figure 2.

When the number of engines fired from a common feed system increases and the frequency of pulse operation of the individual engines are varied an infinite combination of feed system pressure changes are possible. For bipropellant feed system extreme care must be taken so that the engine mixture ratio is not adversely affected during these pressure fluctuations.

Further, impulse variations and the possibility of attaining no response or zero impulse should be examined when severe duty cycles are imposed on the system. The sensitivity of the engine to lead and lag by either the oxidizer or fuel should also be examined.

Sizing of the propellant lines to minimize these transients is extremely important. The use of cavitating venturis and accumulators have been suggested when system designs have precluded line size changes and precisely controlled impulses are required.

D. Pressurant Saturation of Propellant

The saturation of the propellant by the pressurant plays a dominant role in the stability of a liquid propellant feed system. In feed systems that utilize permeable bladders, the solubility of the pressurant with the propellant must be considered. It has been shown that during long storage periods complete saturation of the propellant is possible. The dominant factors affecting saturation are pressure and temperature (Reference 3). Since the solubility of the pressurant gas increases with pressure, the subsequent drop in pressure that accompanies propellant flow into the engine could release the pressurant from solution forming a two-phase compressible mixture. As a result of this out-gassing the bulk modulus of the feed system is decreased

POSSIBLE COMBINATIONS OF TWO ENGINES
FIRING EITHER STEADY STATE OR PULSING AT FIXED FREQUENCY

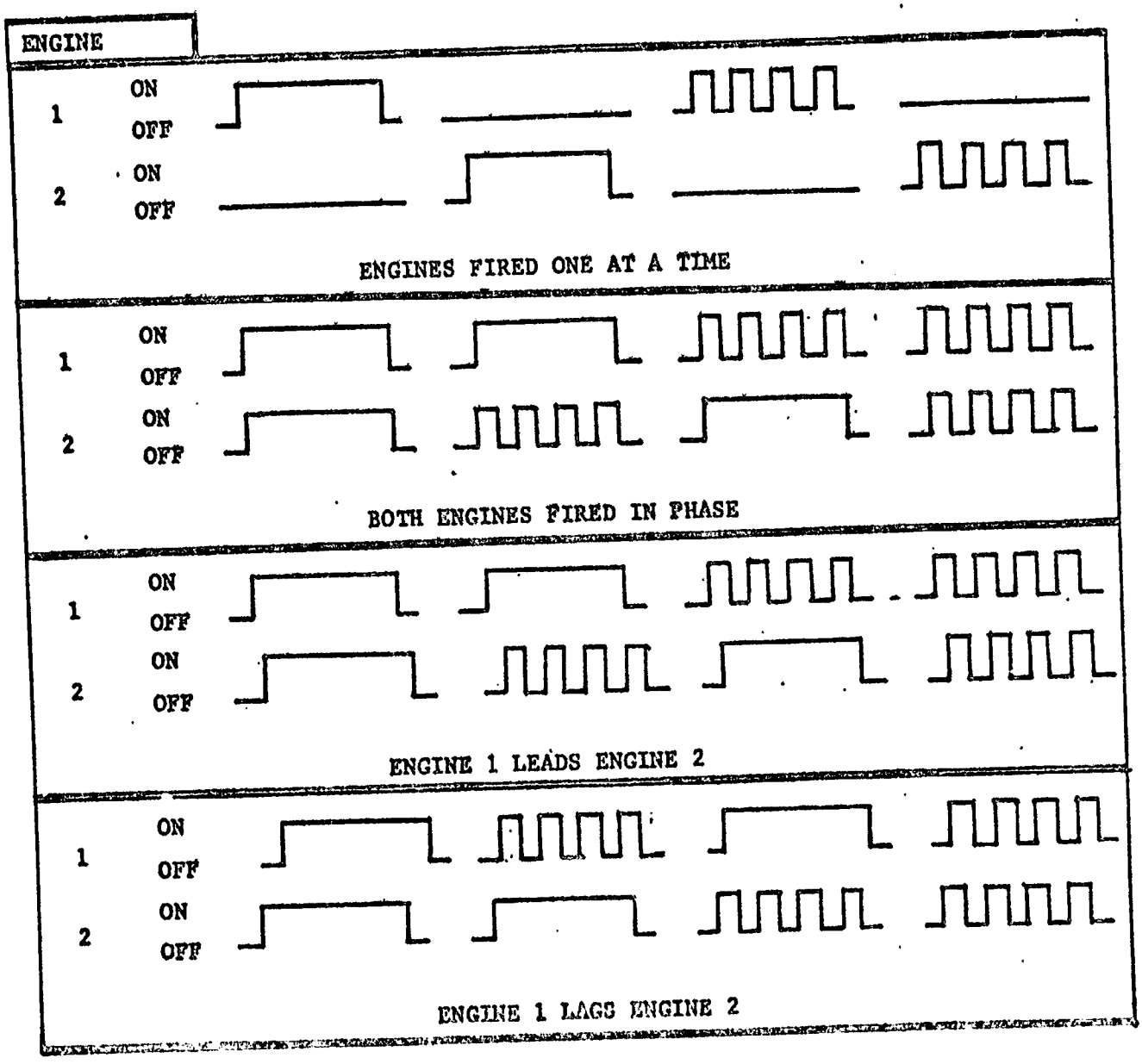

Figure 2

and the natural frequency of the feed system will change from a "hard" system to a "soft" system.

For bipropellant systems utilizing nitrogen tetroxide (N_2O_4) as the oxidizer and a 50-50 blend of unsymmetrical dimethyl hydrazine (UDMH) and hydrazine (N_2H_4) as the fuel, the solubility of the pressurant in the fuel is considerably less than in the oxidizer.

III. PART 2 - LUNAR MODULE REACTION CONTROL SYSTEM TEST

A. Introduction

The Marquardt Corporation under subcontract to the Grumman Aircraft Engineering Corporation of Bethpage, Long Island, New York conducted system tests of the Apollo Lunar Module (LM) Reaction Control System (RCS). These tests were conducted during the period of August 1964 to December 1966. The development and design verification test of the system were conducted in three phases, namely; (1) preproduction, (2) production, and (3) design verification tests. During each progressive stage of development the system was upgraded with design changes and refinements in both hardware and operational procedures. The final design verification tests utilized components that were completely qualified for the lunar mission.

All modes of operation which will be used in the spacecraft mission were simulated repetitively to determine performance criteria and margins. Coupled with the testing of the system was the evaluation and development of support procedures such as propellant filling, priming, purging and decontamination of the system.

The LM system tests were conducted at Marquardt's Magic Mountain test facilities at local barometric pressure. The system test configuration was spatially identical to that of the ultimate flight vehicle (viz. system propellant lines were identical in size and routed in the same manner as on the vehicle).

B. System Description and Function

The Lunar Module reaction control system shown in Figure 3 is composed of two identical independent systems (Systems A and B). Each system contains identical helium pressurization and propellant feed components, together with associated valves and lines necessary to deliver propellants to the bipropellant engine assemblies. The propellants utilized in the system are nitrogen tetroxide (N_2O_4) as the oxidizer and 50% UDMH - 50% N_2H_4 as the fuel with a nominal operating mixture ratio (O/F) of 2.0. A schematic of the system is shown in Figure 4.

Sixteen identical Marquardt 100 lb thrust R-4D engine assemblies are arranged in clusters of four and mounted on four outriggers at the corners of the LM vehicle. Spatially, the clusters are located at the corners of an ap-

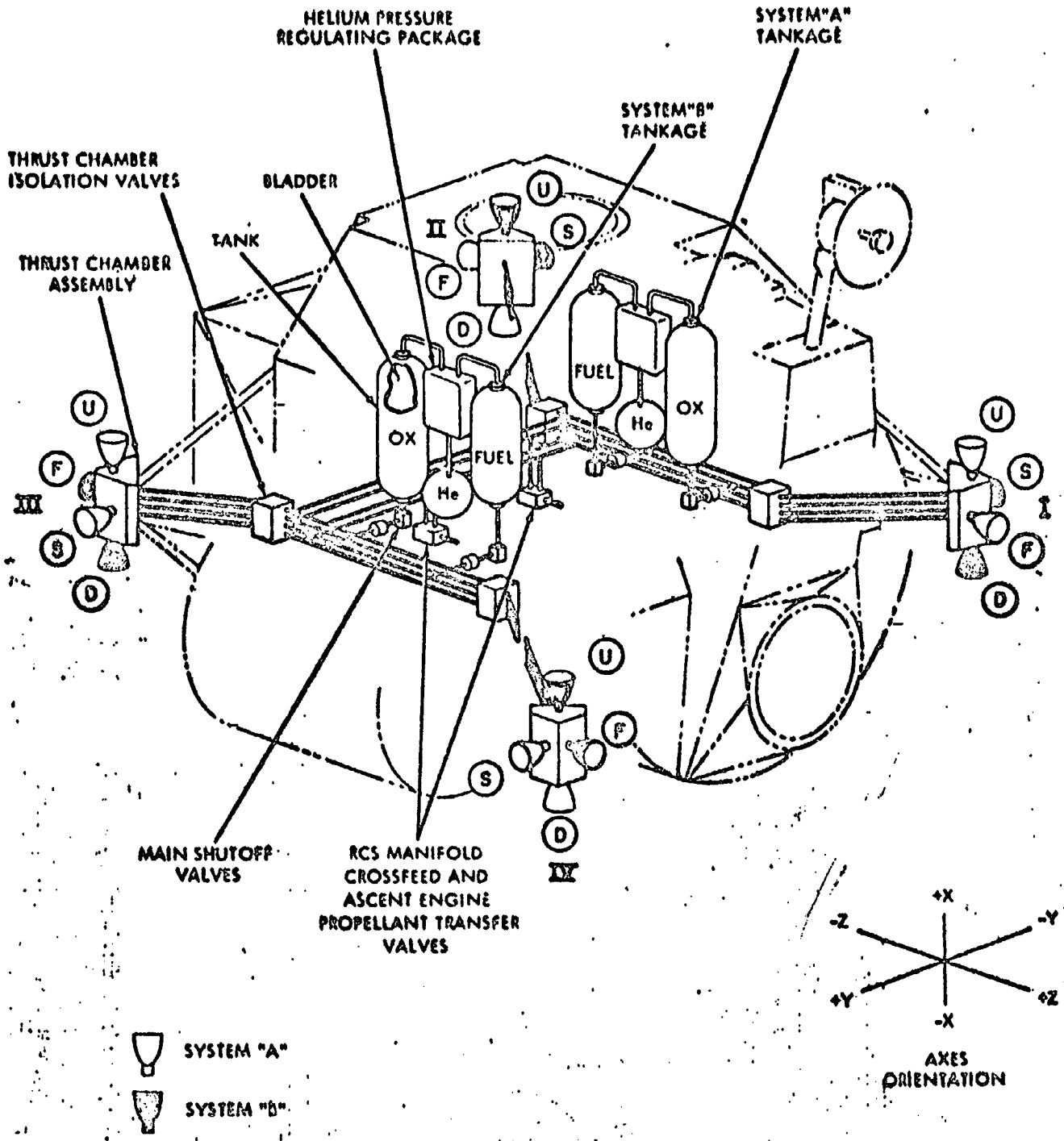

LM System Pictorial

Figure 3

SCHEMATIC - LM RCS SYSTEM

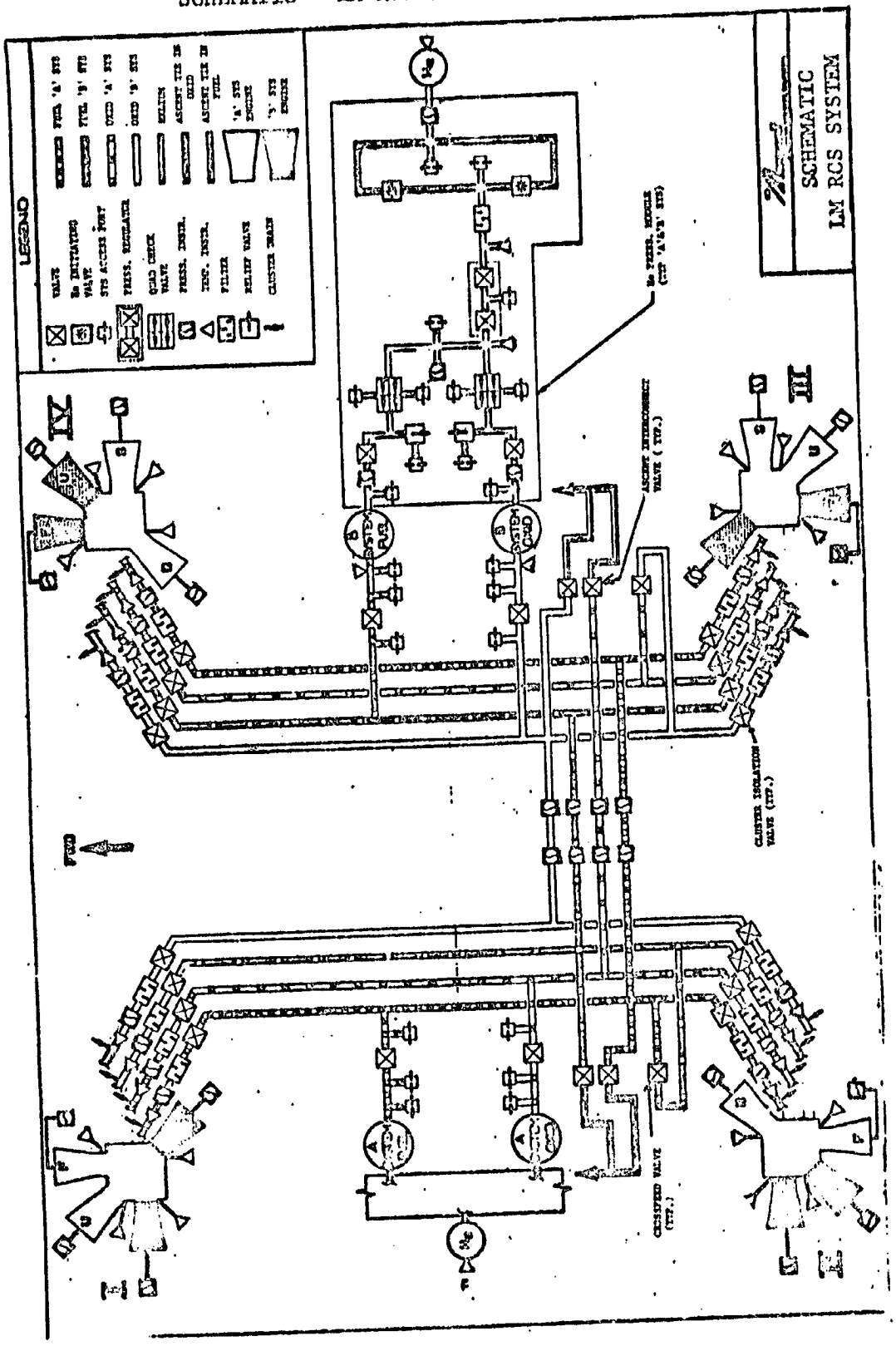

FIGURE 4

proximately 11 foot square around the LM ascent stage. In each cluster two engines are mounted parallel to the vehicle "X" axis, but facing in opposite directions (one engine faces up, the other down). The other two engines are mounted in a plane normal to the "X" axis and spaced 90° apart. The centerline of one engine parallels the vehicle "Y" axis; the centerline of the other parallels the "Z" axis (Figure 3). Two of the engines in the cluster are supplied propellants by System "A"; the other two by System "B". Normally, both systems are operated together, but the arrangement of the engines is such that complete control is all axes is possible despite a failure in either system. The system also has the capability of crossfeeding between System A and B. In the event of upstream failure or propellant depletion in either system, the normally closed crossfeed valves may be opened to connect the propellant manifolds of Systems A and B. Further, an ascent interconnect valve, which connects the RCS propellant manifold to the Ascent Propulsion System (APS) propellant supply is provided to utilize APS propellants for RCS operation.

The RCS performs the following function on the LM vehicle:

1. Provides thrust impulse to stabilize the LM during descent and ascent.
2. Provides thrust impulse to control the vehicle attitude and translation during hover, landing, rendezvous, and docking maneuvers.
3. Provides necessary thrust impulse to accomplish the LM/Service-Command Module separation maneuver.
4. Provides necessary thrust impulse to accomplish acceleration for ullage settling for the descent or ascent propellant storage tanks, when required.

C. System Operation

Gaseous helium is stored at a nominal pressure of 3050 psia at 70°F in two spherical tanks. Each independent system (Systems A and B) contains one helium tank and a set of pressurization components. Upon activation of parallel squib valves the pressurant flows through a filter to the system's series redundant pressure regulator. The regulator maintains a nominal system pressure of 182 psia. The regulated pressure is branched to the gas side of the oxidizer and fuel tanks through quad redundant check valves, which prevent mixing of propellants or propellant fumes in the upstream helium pressurization manifold. A burst disc and relief valve assembly is provided at each tank to prevent system overpressurization. Teflon bladdered propellant tanks feed pressurized fuel and oxidizer through main line latching solenoid valves. The main line valves are normally open, but can be closed in pairs (fuel and oxidizer) to isolate the propellant tanks of one system (A or B) in case of upstream malfunction or when the RCS is operating from the Ascent Propulsion System. All of the aforementioned tanks and components are modularly mounted as an assembly with two modules required per vehicle.

Each tankage module supplies propellants for two engines on each of the four engine clusters. Propellant flow from the main line valves are branched to the four corners of the LM vehicle where the engine clusters are located. Each propellant line (total of four) to the engine cluster assembly has a latching solenoid valve and filter before the flow from these lines are branched to two of the engines. The latching solenoid valve, which is normally open, permits isolation of engine pairs should a malfunction occur downstream of the valve. As shown in Figure 4, pressure and temperature transducers are strategically located throughout the RCS to monitor its performance. Photographs of the Design Verification Test (DVT) setup are shown in Figures 5, 6, and 7.

D. Engine Data Correlation

Prior to installation of the engine in the system, each engine was fired in a thrust stand in both the pulse and steady state mode to obtain necessary correlation between measured thrust and chamber pressure. These correlations were required to determine thrust and/or impulse during the system tests since the system installation would yield no thrust measurements. The single engine thrust stand firing was conducted at both altitude and sea level conditions since the system testings were conducted at local ambient. Table II presents a summary of the equations used to correlate this data.

During steady state firing in the single engine test stand the engine's thrust coefficient and specific impulse were computed from measured thrust, chamber pressure and propellant flow. For pulse operation the integrated values of thrust and chamber pressure together with flow rate data were used to compute a correlation factor (C_{vac}) to determine specific impulse and impulse at specific pulse widths. Once the engines were installed in the system, performance of the engine was monitored by measuring chamber pressure.

A photograph of one of the engine cluster assemblies installed in the system is shown in Figure 8. The expansion bells of the engines were removed since they were not functionally required for sea level tests and to facilitate cluster handling.

E. Summary of Tests

Table III presents a summary of the total system propellant exposure time and engine firing summary for the LM reaction control system tests described herein.

A summary description of the type of tests and their principle objectives are shown in Table IV. Item 3 through 8 of Table IV entailed engine firing either in the steady state and/or pulse mode. The pulse width in the pulse mode varied from 10 to 200 milliseconds with varying off times. The maximum number of engines fired at any one time in a given system (A or B) was six.

REPRODUCIBILITY OF THE ORIGINAL PAGE IS POOR

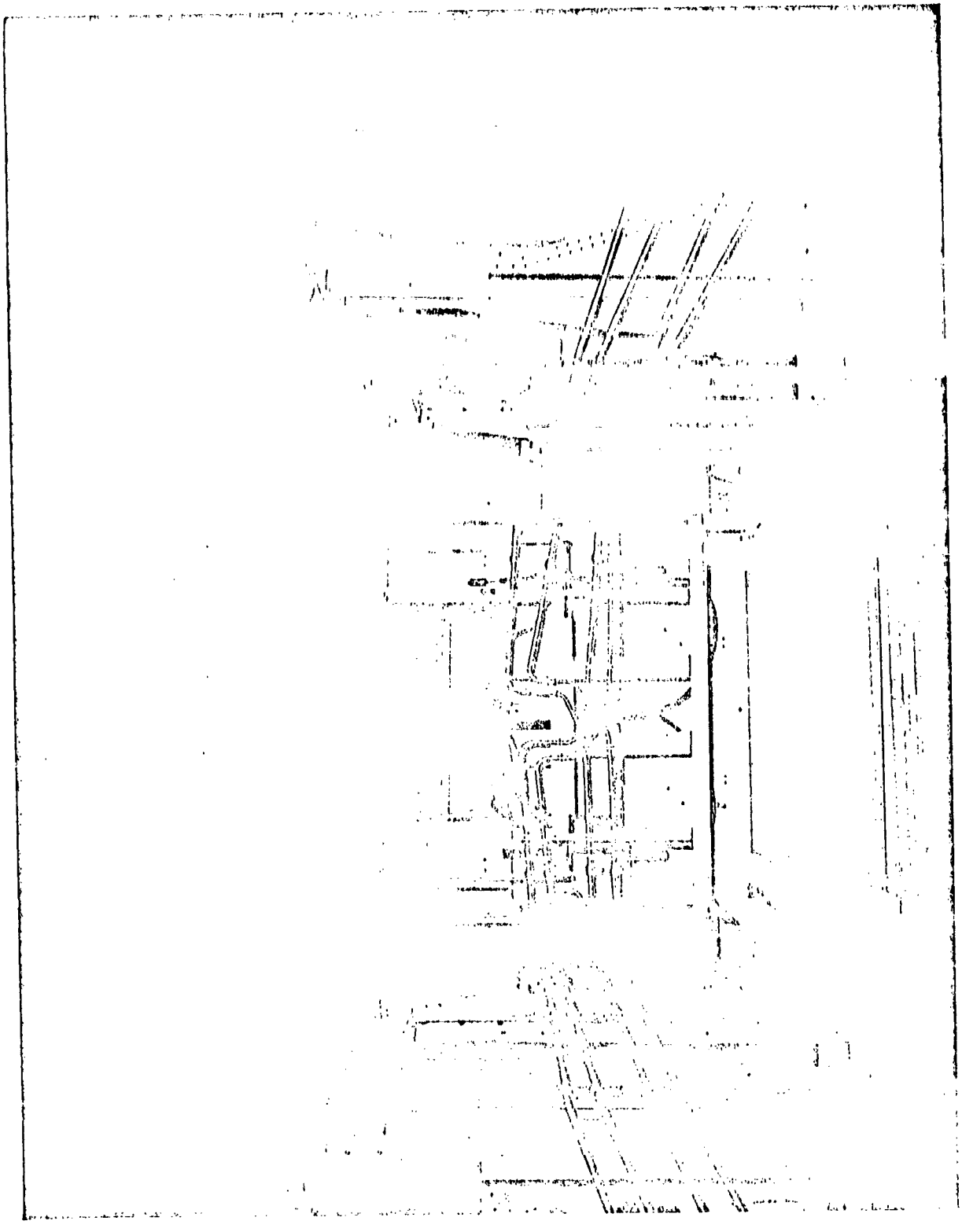

NEG. T6033-4

LM RCS DVT System

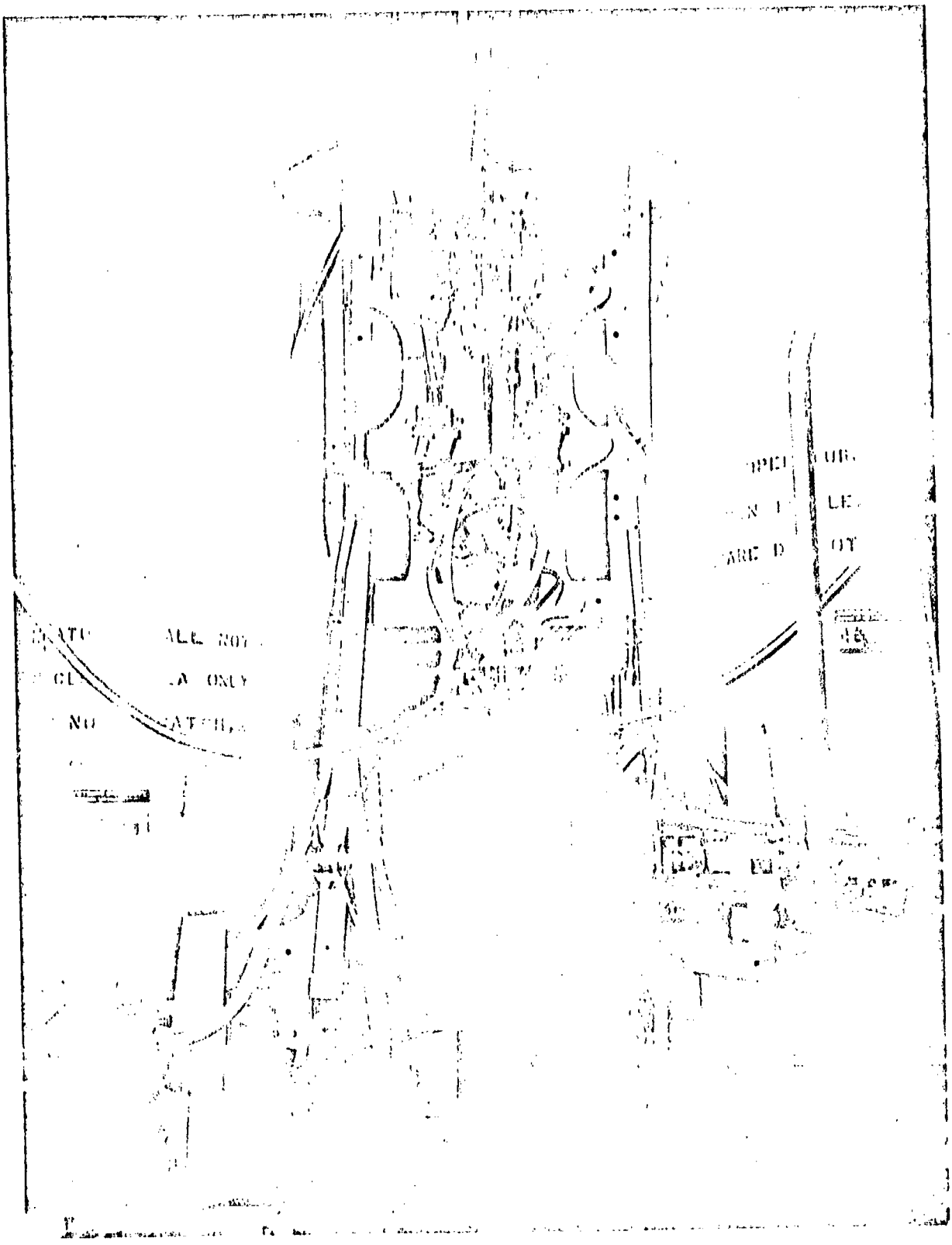

NEG. T6033-1

LM RCS DVT "A" System Tankage Module

Figure 6

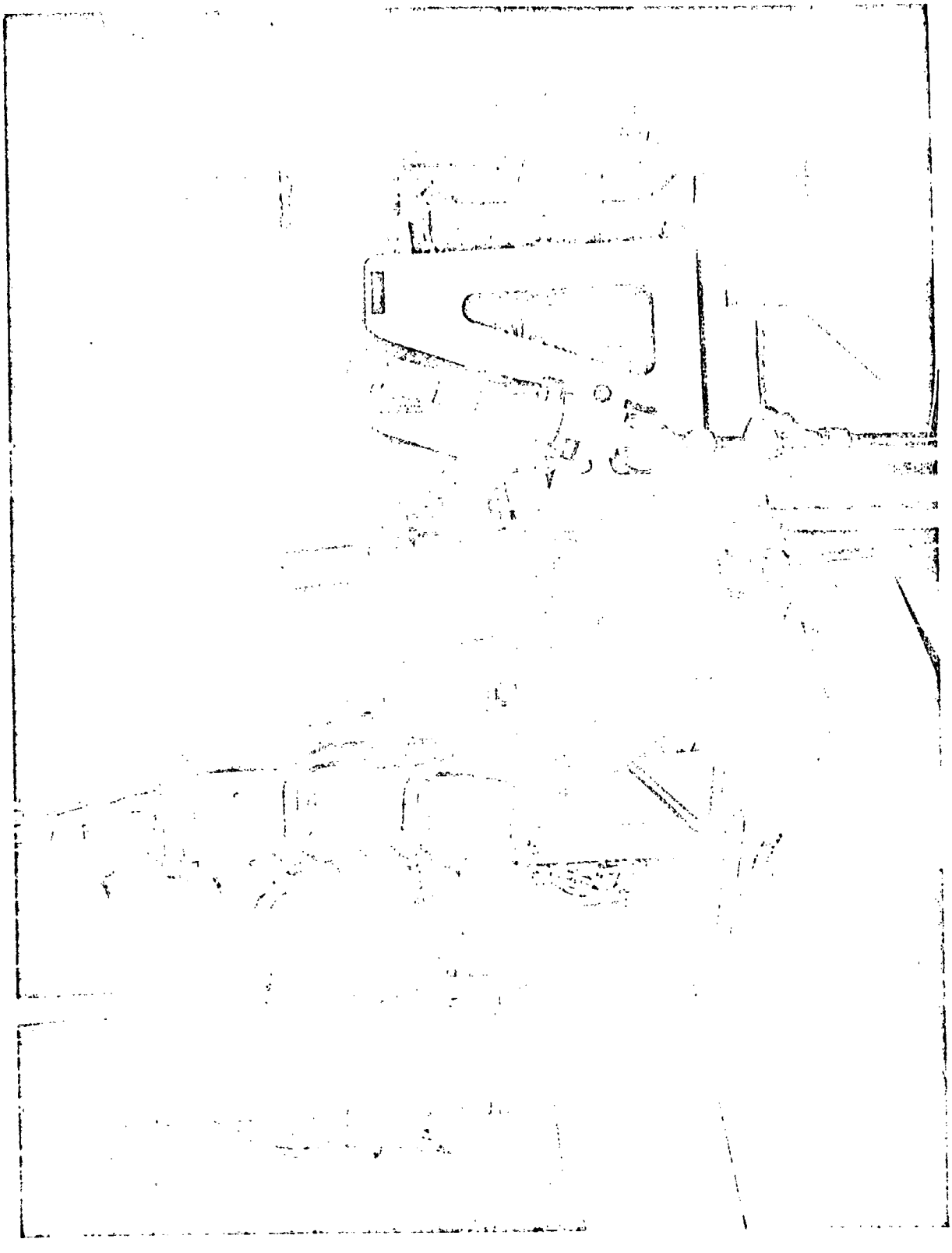

NEG. T6033-6

LM RCS DVT System - Engine Cluster Number 1

Figure 7

TABLE II
CORRELATION OF CHAMBER PRESSURE
WITH THRUST & SPECIFIC IMPULSE

	SINGLE ENGINE ALTITUDE TESTING	SEA LEVEL SYSTEM TESTING
• THRUST STEADY STATE	$C_{F_{VAC}} = \frac{F_{VAC}}{P_C A_T} = \frac{F_M + P_{CELL} A_E}{(P_{CM} + P_{CELL}) A_T}$	$F_{VAC} = C_{F_{VAC}} (P_{CM} + P_{SL}) A_T$
PULSE	$C_{VAC} = \frac{\int F dt}{\int P_C dt} = \frac{I_{T_M} + P_{CELL} A_E \Delta t}{\int P_{CM} dt + P_{CELL} \Delta t}$	$I_{T_{VAC}} = C_{VAC} \left[\int P_{CM} dt + P_{SL} \Delta t \right]$
• SPECIFIC IMPULSE STEADY STATE	$I_{SP_{VAC}} = \frac{F_{VAC}}{\dot{W}_P} = \frac{F_M + P_{CELL} A_E}{\dot{W}_P}$	$I_{SP_{VAC}} = \frac{C_{F_{VAC}} (P_{CM} + P_{SL}) A_T}{\dot{W}_P}$
PULSE	$I_{SP_{VAC}} = \frac{I_T}{W_P} = \frac{\int F dt}{\int \dot{W}_P dt}$	$I_{SP_{VAC}} = \frac{C_{VAC} \left[\int P_{CM} dt + P_{SL} \Delta t \right]}{\dot{W}_P dt}$

SYMBOL

A_E = EXIT AREA (INCHES^2)
A_T = THROAT AREA (INCHES^2)
C_F = THRUST COEFFICIENT
C = PULSE CORRELATION FACTOR(INCHES^2)
F = THRUST (POUNDS)
I_T = IMPULSE (POUND-SECOND)
I_{SP} = SPECIFIC IMPULSE (SECONDS)
W_P = PROPELLANT MASS (POUNDS)
$\dot{W}_P$ = TOTAL PROPELLANT FLOW (POUNDS)
Δt = MEASURED PULSE WIDTH (SECONDS)
P_C = CHAMBER PRESSURE (PSIA)
P_{CELL} = MEASURED CELL PRESSURE (PSIA)
P_{SL} = MEASURED SEA LEVEL PRESSURE (PSIA)

SUBSCRIPT

M = MEASURED
VAC = VACUUM OR SPACE CONDITION

NEG. T6020-26

LM RCS Engine Cluster Assembly

Figure 8

TABLE III

LUNAR MODULE RCS SYSTEM TEST SUMMARY

I. PROPELLANT EXPOSURE TIME

TEST	SYSTEM EXPOSED TO PROPELLANTS	SYSTEM PRESSURIZED (182 PSIA)
PRODUCTION SYSTEM	78 DAYS	35 DAYS
DVT SYSTEM	33 DAYS	24 DAYS

II. ENGINE FIRINGS

TEST	TOTAL NUMBER OF STARTS	TOTAL ENGINE FIRING TIME (SEC.)	MAXIMUM SINGLE ENGINE FIRING	
			NUMBER OF STARTS	FIRING TIME (SEC.)
PRE-PRODUCTION	18,618	8,903.21	4,353	1,407.92
PRODUCTION	56,667	8,255.68	11,860	1,591.73
DVT	23,176	3,764.15	5,324	607.37

TABLE IV

SUMMARY OF APOLLO LUNAR MODULE REACTION CONTROL SYSTEM TESTS

TEST TITLE	TEST OBJECTIVE/TASKS	REMARKS
1. System Checkout	Verify system cleanliness and leakage check functional check of valves and transducers calibration	Cleanliness evaluation entailed flushing complete system with Freon until particulate count was within specified limits.
2. System Operating Procedures	Helium fill and vent, propellant fill and vent, system securing between tests	
3. System Actuation	System prime - baseline engine performance firing	Measured pressure transients during system prime. Each engine fired in both steady state and pulse mode to establish individual baseline performance
4. Control Events	Firing of engine couples, translation maneuvers and engine pair firings	Evaluation of multiple engine firing performance
5. Duty Cycle Tests	Complete mission duty cycle firing including pressurized 48 hour hold period (simulating lunar stay). Ambient test provided basis of comparison for subsequent high and low temperature test	Propellant consumption and expulsion efficiencies were measured and computed
6. Off Design Operation	Verify system performance at high and low mixture ratio and high and low regulated pressure	Effect of valve response, ignition delay and chamber pressure levels were examined!
7. Crossfeed and Ascent Interconnect	Verify system performance by opening crossfeed valve, ascent interconnected valve and utilizing propellant from either all A or B system	
8. Failure Mode Operation	Nondestructive test simulating engine valve failures. Operation of system by manual control	Cluster isolation valve of simulated failed engine were closed, thereby closing off propellant supply to engine.
9. Decontamination and Examination	Decontaminate system and remove system assemblies/components for evaluation of contamination, wear or deterioration	Freon TF and Isopropyl alcohol were used as decontaminates of oxidizer and fuel system, respectively. After flushing less than ten parts per million of propellant concentration was found in flushing fluids

Figure 9 presents typical chamber pressure transients for one of the engines during pulse firing. Figure 10 presents the integrated chamber pressure and total impulse for the same engine plotted versus pulse width. During all pulse runs the first and third pulse was analyzed since the first pulse of a given pulse train is less efficient. This inefficiency is primarily due to the fact that the first pulse of a pulse train must fill the cavity of the injector between the engine valve and point of injection (this cavity is usually referred to as dribble volume) and energy transfer in the combustion chamber. It is evident that the third pulse is considerably sharper than the first and the rise time to nominal chamber pressure is approximately five milliseconds faster for the third pulse than the first.

Figures 11 through 14 present typical time histories of measured propellant manifold pressure during engine start up and shut down for single engines fired in the A system. Referring to the schematic of Figure 4, the transducers that measure these manifold pressures are approximately 30 inches upstream from the engine valve. As expected, the manifold pressure closest to the engine being fired experiences the largest transients and the oxidizer, owing to its higher density and weight flow, experiences larger pressure fluctuations. From a nominal pressure of about 175 psia the start transient, as measured at the manifold of the engine being fired, is characterized by a fall in pressure down to approximately 100 psia in 5 milliseconds followed by a rise to 200 to 250 psia, 10 milliseconds later. The engine shut off is characterized by a water hammer pressure maximum of about 300 psia which occurs within 5 milliseconds after engine shut down.

It can be noted in Figures 11 through 14 that after the initial opening/closing transient has subsided a fundamental frequency is imposed on the system, which is the system natural frequency discussed in Part 1-B. The frequency of this oscillation is highly dependent on the degree of pressurant saturation in the propellant and temperature of the propellant. The lower the frequency the "softer" the system. For the system tested, the calculated frequency for a "hard" or degassed system was 23.5 cps for the fuel and 17.1 cps for the oxidizer. Measured values of frequency were in excellent agreement with those calculated and it was observed that as the system remained pressurized the system tended to become softer and reached frequency values of approximately 21 cps and 10 cps for the fuel and oxidizer respectively. The change in frequency was gradual and System A's change did not necessarily follow System B's. No attempt was made to measure the amount of saturation, but monitoring of the manifold pressure oscillograph traces indicated a gradual change in frequency.

F. Control Events Tests

Control events tests were conducted to determine system performance during normal mode of engine operation that simulate firing conditions anticipated in vehicle control maneuvers. Engines were fired in couples in both the steady state and pulse mode. Engine pairs (engines located in the same cluster, fed by a common propellant source) were also fired during this test sequence.

CHAMBER PRESSURE TIME HISTORY SINGLE ENGINE OPERATIONS

Time Zero is Electrical ON, 200 Milliseconds OFF Time

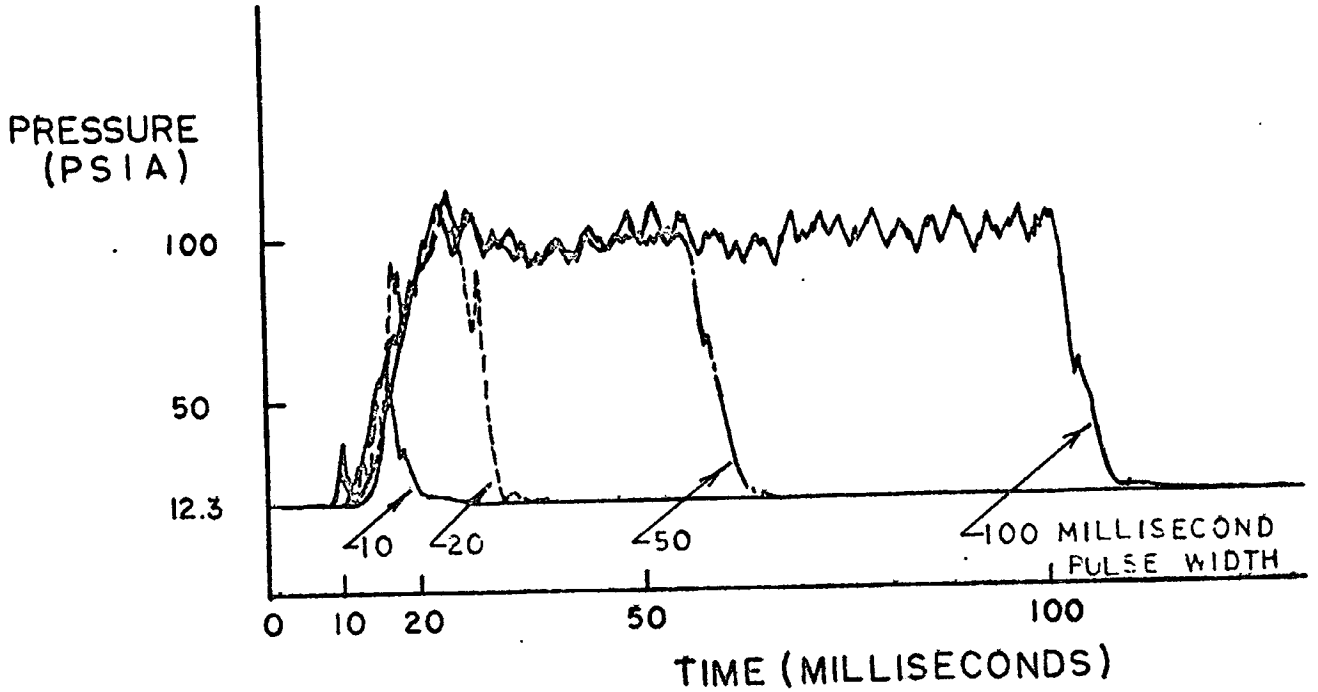

ENGINE 1F - PULSE NO. 1

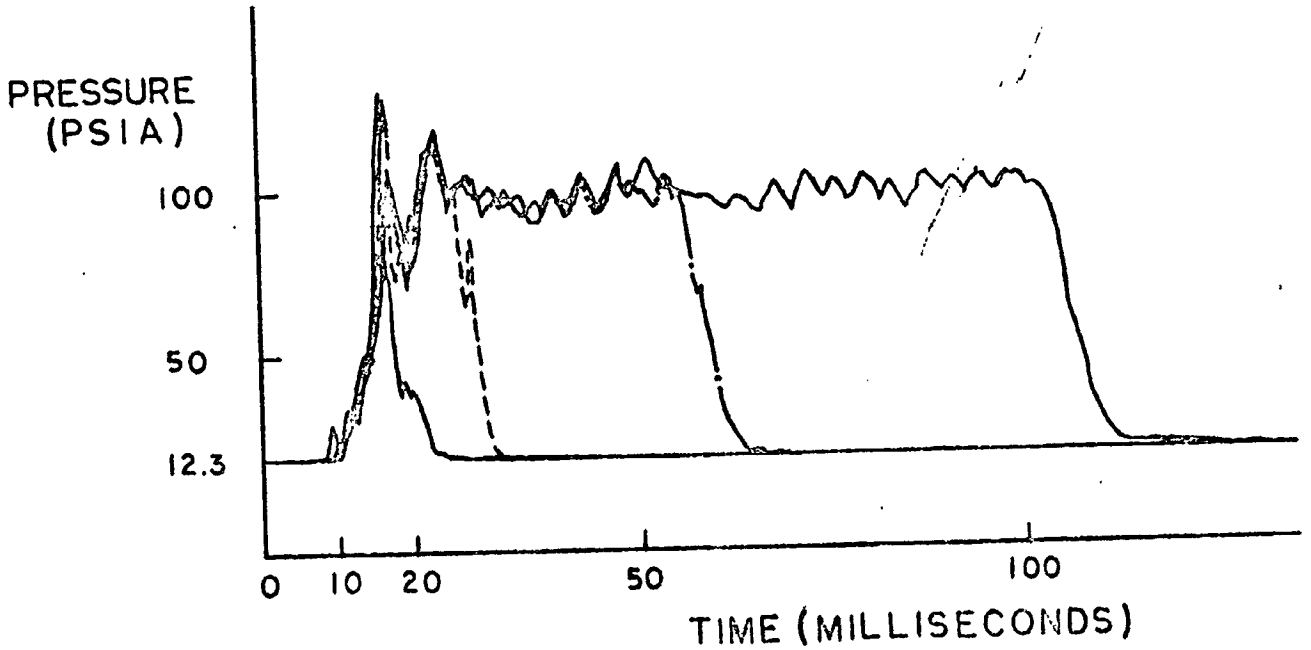

ENGINE 1F - PULSE NO. 3

Figure 9

ENGINE PERFORMANCE

ENGINE IF, OFF TIME = 0.020 SECONDS

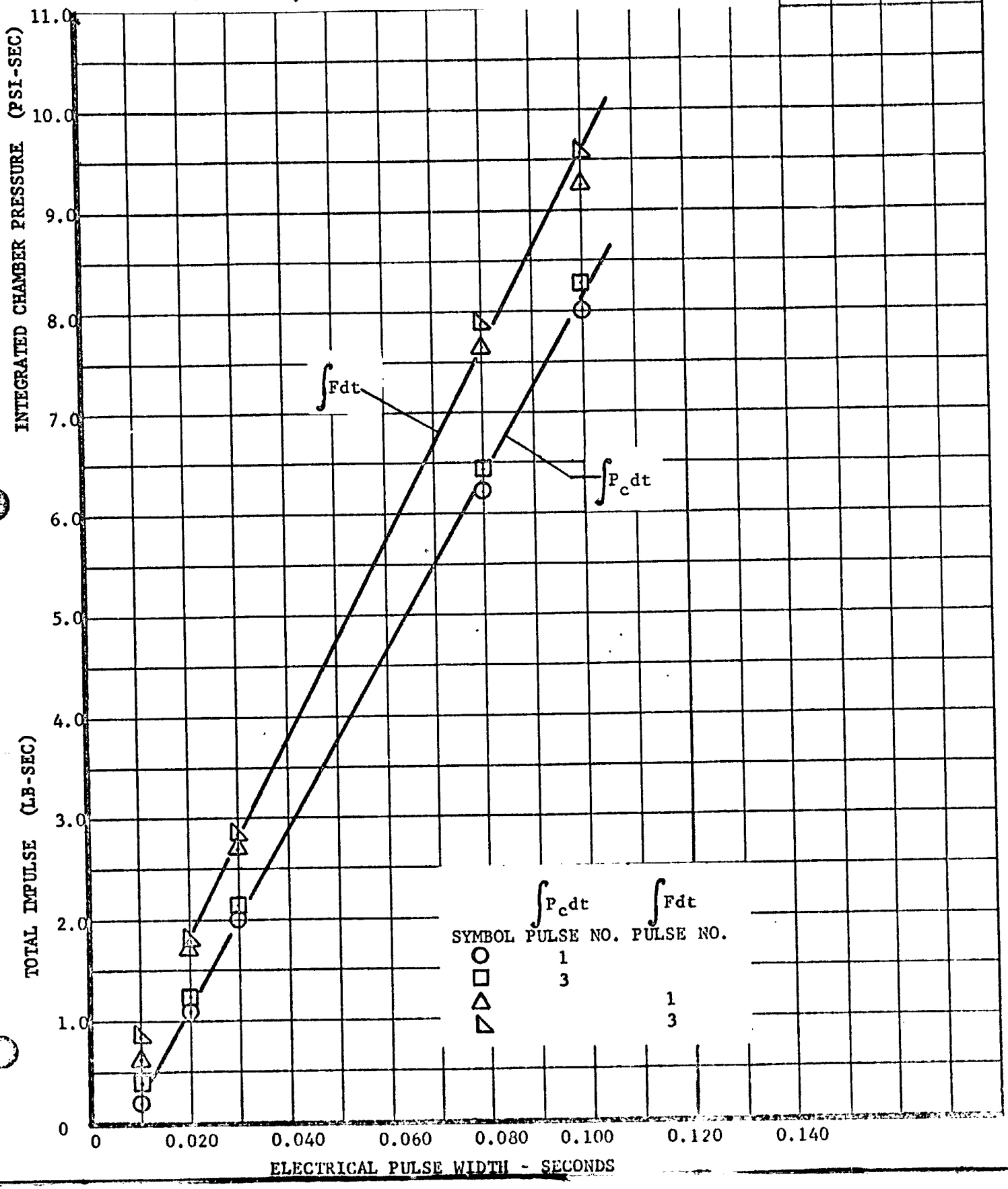

PROPELLANT SYSTEM MANIFOLD PRESSURE TIME HISTORY

SYSTEM A, ENGINE IF FIRING

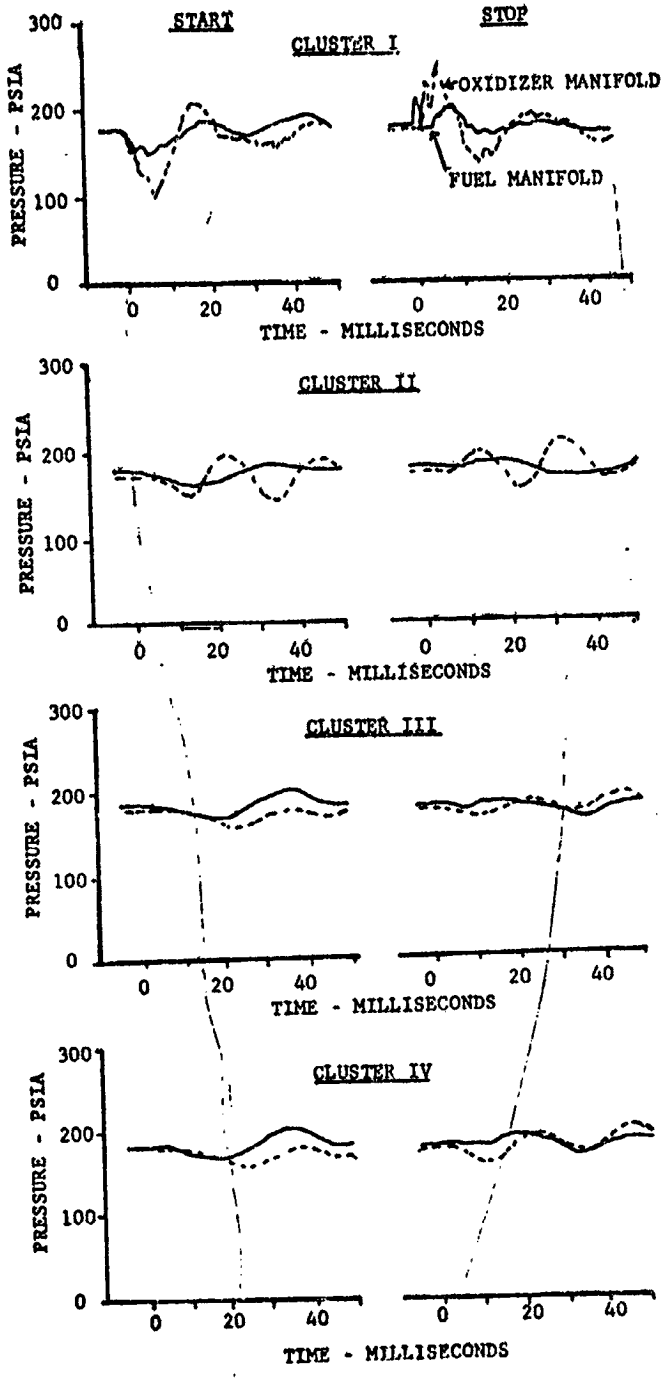

Figure 11

PROPELLANT SYSTEM MANIFOLD PRESSURE TIME HISTORY

SYSTEM A, ENGINE IID FIRING

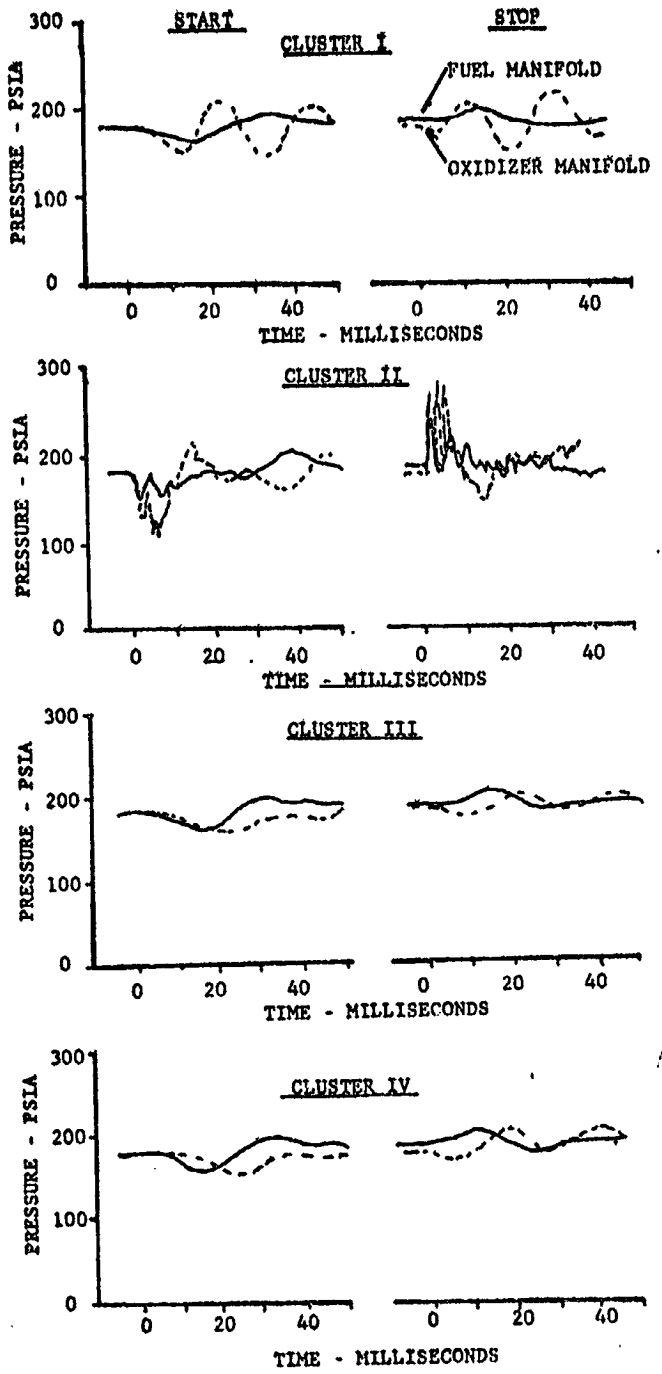

Figure 12

PROPELLANT SYSTEM MANIFOLD PRESSURE TIME HISTORY

SYSTEM A, ENGINE IIIS FIRING

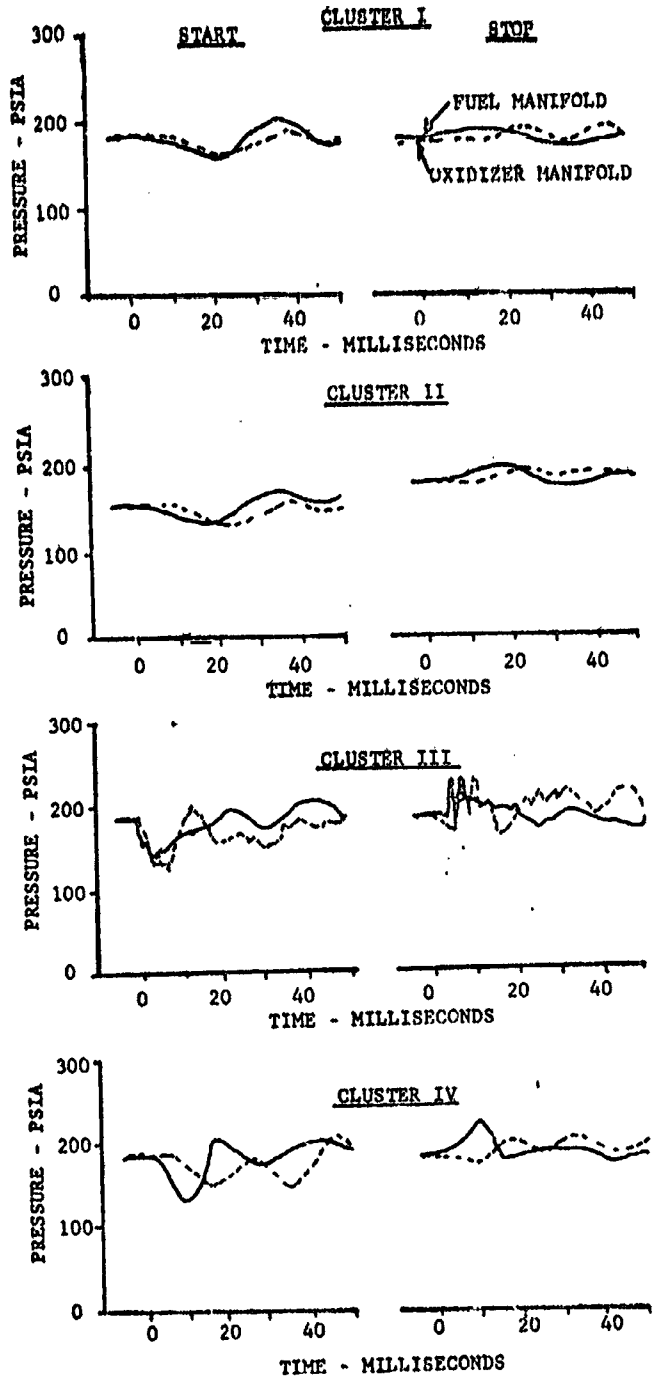

Figure 13

PROPELLANT SYSTEM MANIFOLD PRESSURE TIME HISTORY

SYSTEM A, ENGINE IVD FIRING

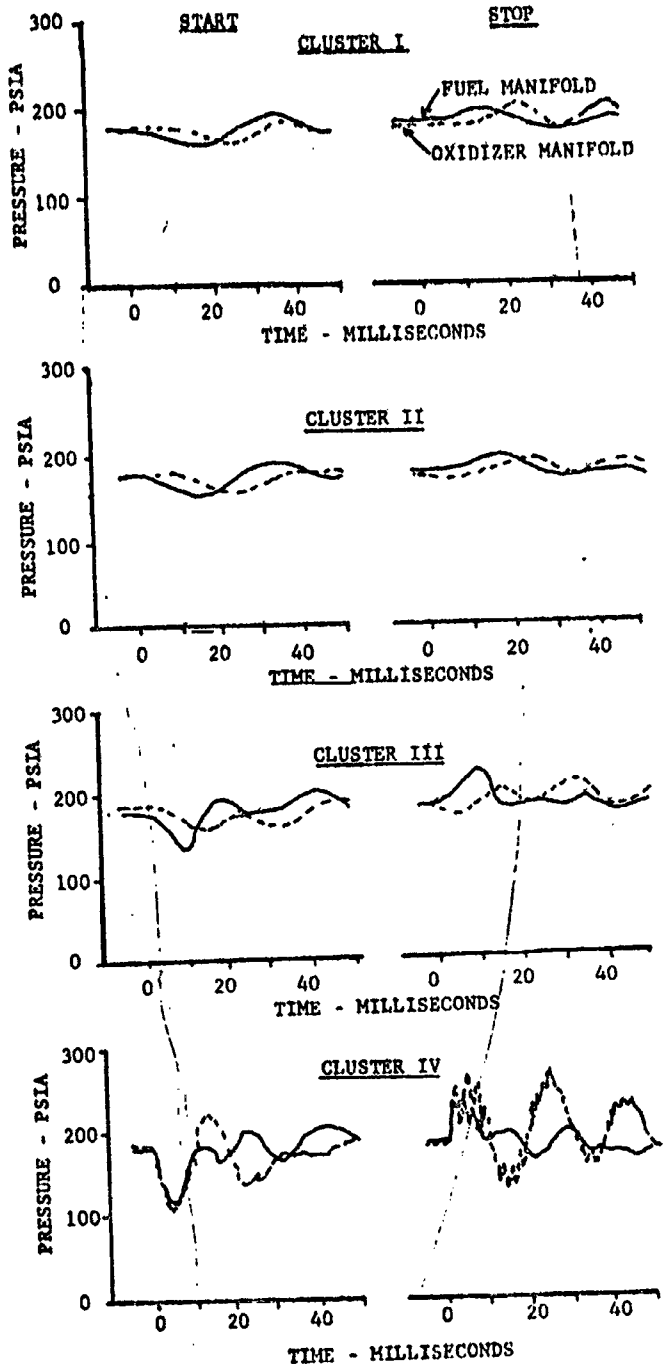

Figure 14

The firing of engine couples indicated that the initial transient of chamber pressure is affected by the location of the supply tankage. If the tankage to a particular engine is located far from the engine the initial chamber pressure rise is followed by a lower drop in pressure before recovery to its steady state value. Table V presents typical integrated chamber pressure data for engines of System A when fired as a couple at different pulse width. Also shown on the table, for comparison purposes, is the integrated chamber pressure of the engine when fired as a single engine in the system. The loss of impulse for engines located furthest from the supply tankage (Engines 3S and 4D) may be noted in Table V. The decrease in impulse is primarily attributed to the behavior of the initial transients; as the engine couples are fired for longer periods of time (as in the case of vehicle translation maneuvers) the percentage change in impulse is less.

Figure 15 presents the chamber pressure time history of an engine pair firing. Both engines are fired simultaneously with one engine shutting down after a one second on time while the other engine continues to fire. The start transient of both engines are identical; upon shut down of one of the engines a slight rise in the second engine's impulse is noted. Figure 16 illustrates two engines firing steady state, one engine starting and stopping during the operation of the second. The drop off and rises in chamber pressure as the second engine is fired and shut down is clearly indicated in this figure, both transients are damped out within 10 milliseconds. Figure 17 illustrates the behavior of the same set of engines when the second engine is pulsed for 20 milliseconds, rather than fired at steady state.

Figure 18A illustrates the behavior of an engine pair when a pulsing engine leads an engine firing steady state. Figure 18B illustrates a case where the same two engines are fired simultaneously with one engine pulsing and the second engine firing steady state. For the same pulse width the affect of imposing a transient during the pulse on time is clearly evident in the chamber pressure trace of Figures 18A and 18B.

Figure 19 illustrates the affect of pulsing a second engine for 50 milliseconds, 25 milliseconds after the first engine has fired. The expected decay and rise in the first engine's chamber pressure can be noted in the figure. Of particular interest is the fact that the impulse (chamber pressure) of the first engine is increased during the entire period that the second engine is fired. Phenomena of this type are extremely difficult to predict analytically and often difficult to repeat experimentally. The time phasing of the second engine's "on" command coupled with oscillations that are present in the propellant feed system will provide a different value of impulse response for the same pulse width. In some instances both engines will reach the same pressure level; in other cases one engine may partially starve the other. Through experimental verification these phenomena should be categorized to establish a tolerance band on pulse repetition rate and mode of operation.

TABLE V

COMPARISON OF INTEGRATED CHAMBER PRESSURE
WHERE ENGINES ARE FIRED SINGLY AND IN COUPLES

ENGINE		1F			2D			3S			4D		
PULSE WIDTH m-sec.	ENGINES FIRED	$\int P_c dt$ psi-sec.	COUPL. WITH ENG.	ROTAT. ABOUT	$\int P_c dt$ psi-sec.	COUPL. WITH ENG.	ROTAT. ABOUT	$\int P_c dt$ psi-sec.	COUPL. WITH ENG.	ROTAT. ABOUT	$\int P_c dt$ psi-sec.	COUPL. WITH ENG.	ROTAT. ABOUT
13	SINGLE	0.65			0.54			0.65			0.54		
	COUPLE 1	0.458	2D	-Y	0.340	1F	-Y	0.300	4D	+Y	0.314	3S	+Y
	COUPLE 2	0.617	4D	-Z	0.567	3S	+Z	0.470	2D	+Z	0.486	1F	-Z
25	SINGLE	1.68			1.61			1.66			1.57		
	COUPLE 1	1.597	2D	-Y	1.456	1F	-Y	1.372	4D	+Y	1.356	3S	+Y
	COUPLE 2	1.614	4D	-Z	1.521	3S	+Z	1.459	2D	+Z	1.394	1F	-Z
53	SINGLE	4.14			4.07			4.01			3.98		
	COUPLE 1	3.909	2D	-Y	3.804	1F	-Y	3.567	4D	+Y	3.603	3S	+Y
	COUPLE 2	4.070	4D	-Z	3.919	3S	+Z	3.772	2D	+Z	3.692	1F	-Z
93	SINGLE	7.66			7.63			7.37			7.48		
	COUPLE 1	7.617	2D	-Y	7.466	1F	-Y	7.297	4D	+Y	7.245	3S	+Y
	COUPLE 2	7.783	4D	-Z	7.575	3S	+Z	7.444	2D	+Z	7.391	1F	-Z

CHAMBER PRESSURE TIME HISTORY

(SIMULTANEOUS START OF TWO ENGINES AND SHUTDOWN OF ONE ENGINE)

	ENGINE	ON TIME
- - - - -	IVS	8.0 SEC.
———	IVD	1.0 SEC.

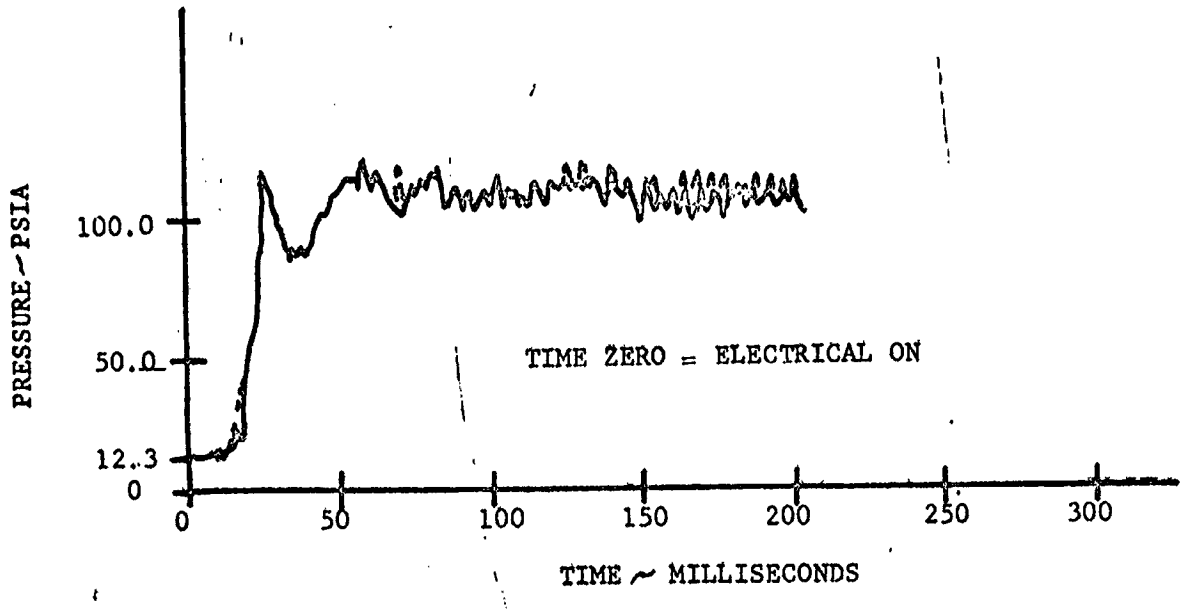

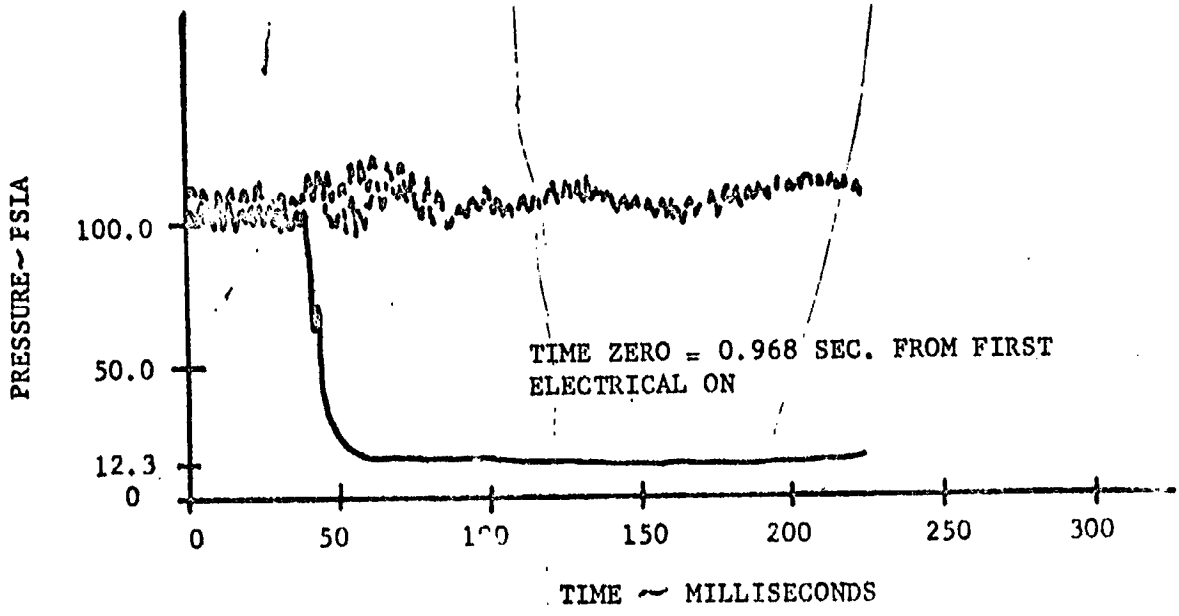

Figure 15

CHAMBER PRESSURE TIME HISTORY

(START AND SHUTDOWN DURING STEADY STATE OPERATION OF A SECOND ENGINE)

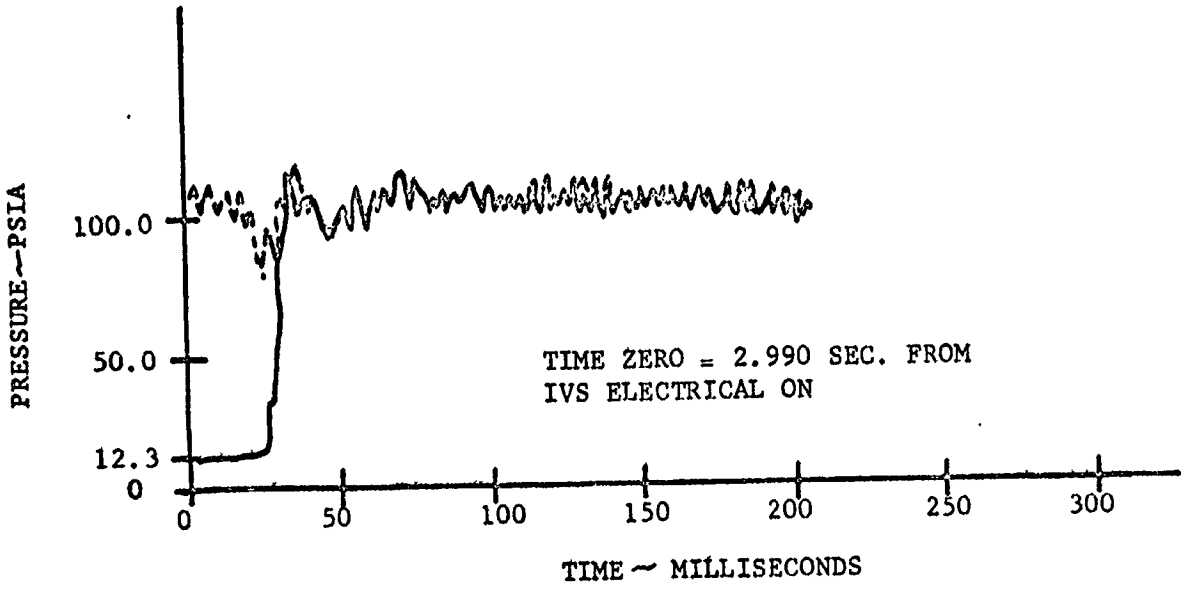

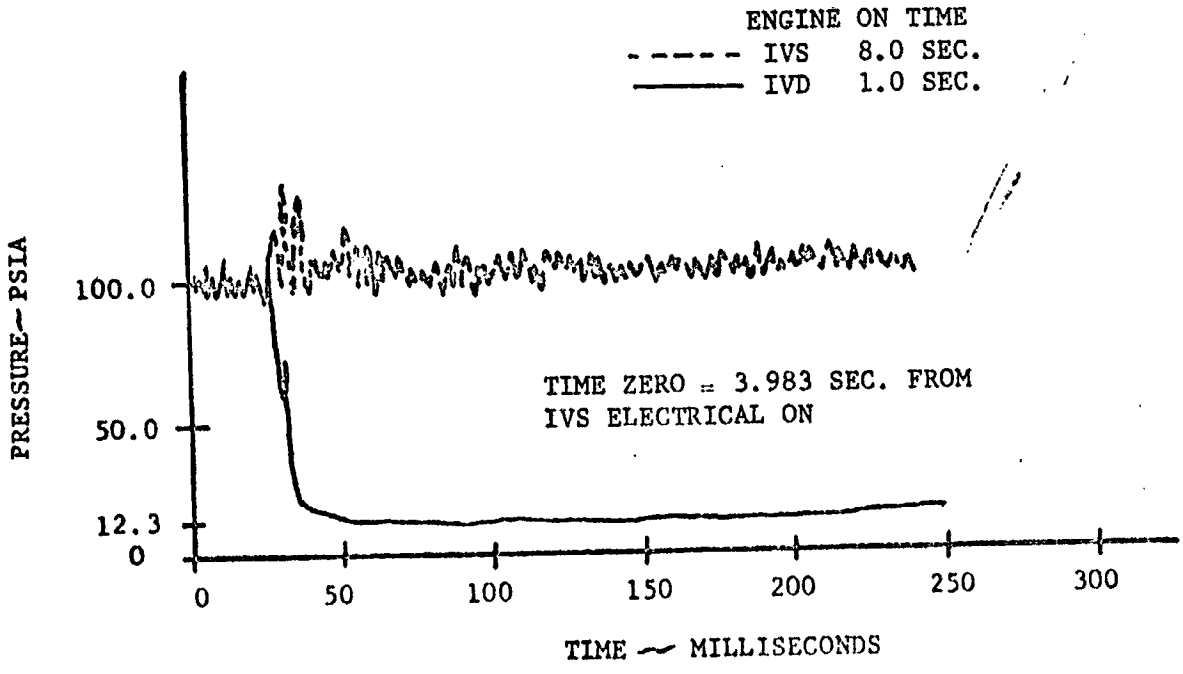

Figure 16

CHAMBER PRESSURE TIME HISTORY

(ONE ENGINE PULSED DURING THE OPERATION OF A SECOND)

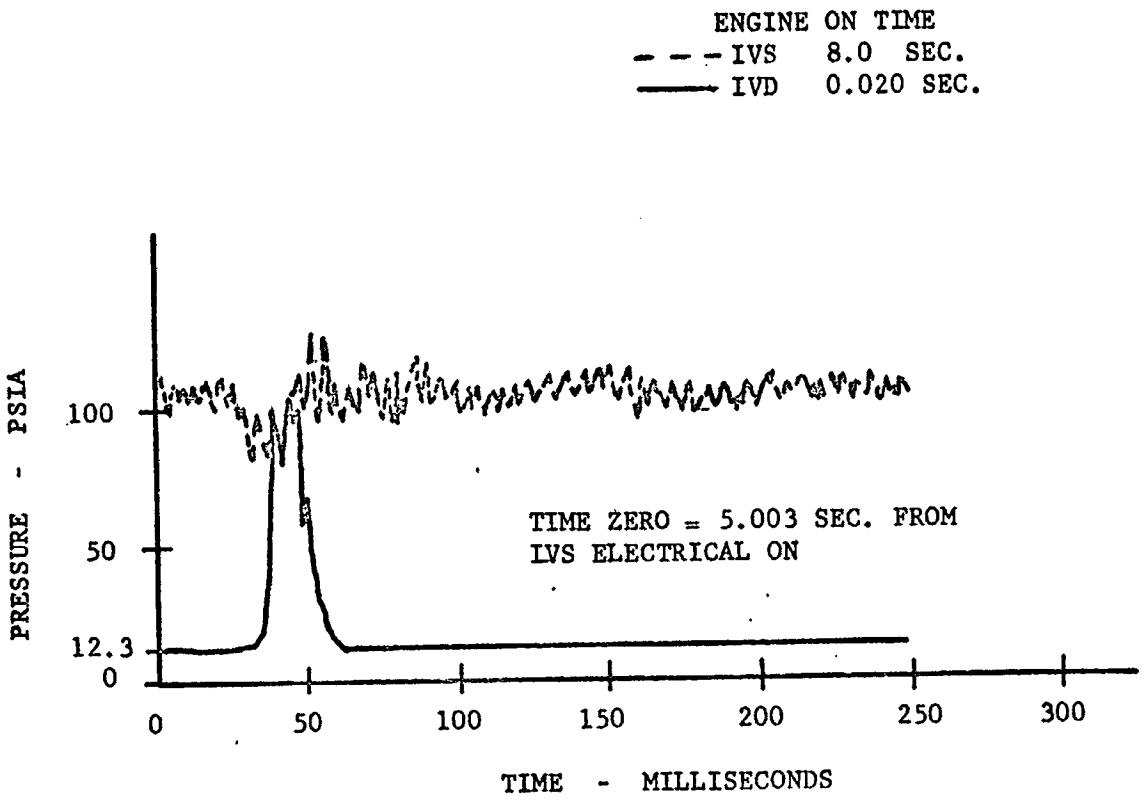

Figure 17

CHAMBER PRESSURE TIME HISTORY

ENGINE ON TIME
---- IVS 0.050 SEC.
——— IVD 1.0 SEC.

FIGURE 18a- PULSED ENGINE LEADING ENGINE FIRED STEADY STATE

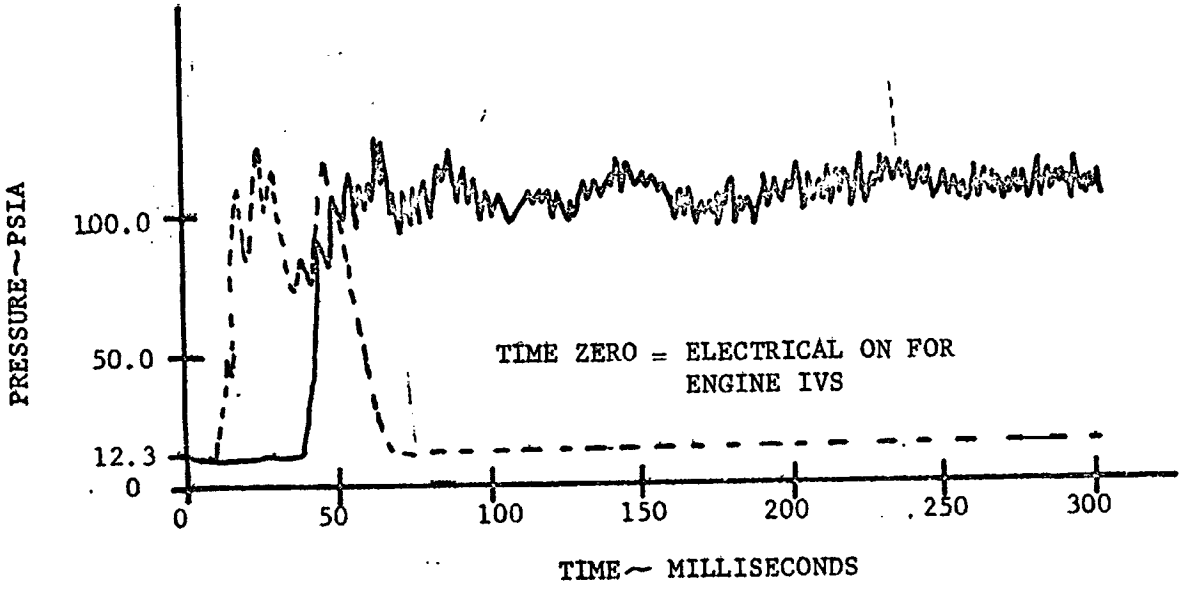

FIGURE 18b- SIMULTANEOUS START OF PULSE AND STEADY STATE

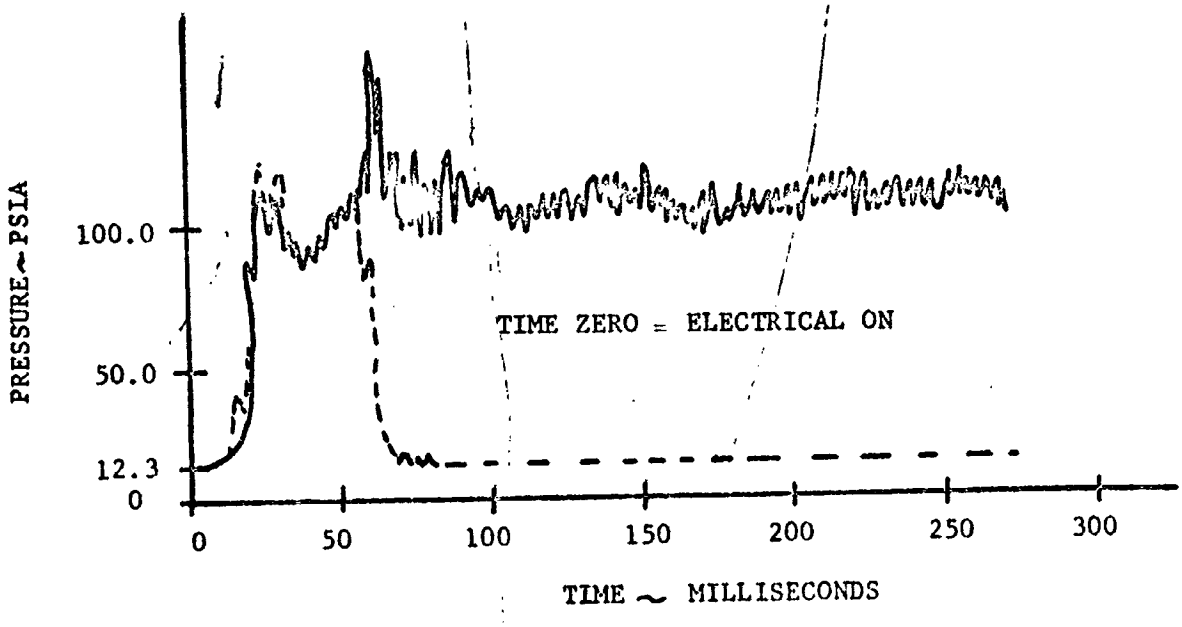

Figure 18

CHAMBER PRESSURE TIME HISTORY

(SECOND ENGINE PULSED 0.025 SECONDS AFTER FIRST)

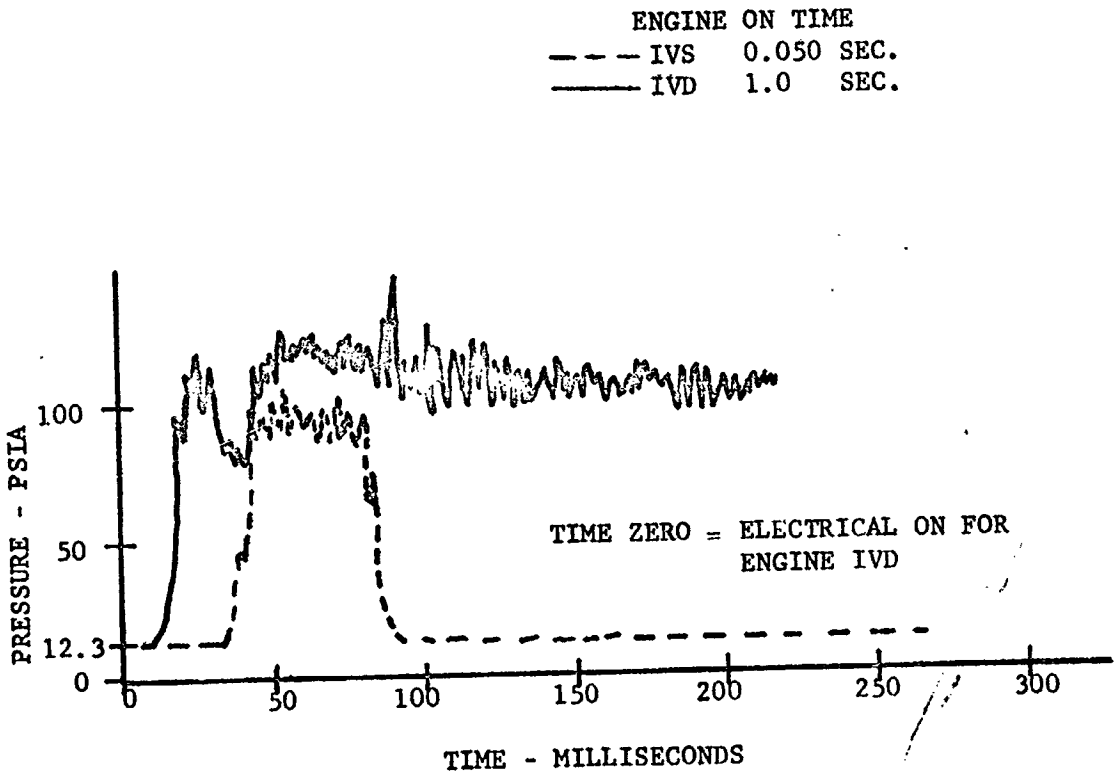

Figure 19

G. Duty Cycle Tests

A duty cycle test was conducted to verify proper operation of the reaction control system during a complete mission simulation. The duty cycle tests were conducted at ambient hardware and propellant temperatures. These tests also provided a basis of comparison for subsequent high and low temperature tests in the measurement of propellant consumption. The duty cycle test was conducted in two phases: the initial portion consumed approximately one-fourth of the system's propellant and the second portion, which was preceded by a 48 hour hold period (simulating lunar stay), consumed approximately one-half of the system's propellant.

The Design Verification Test (DVT) duty cycle test consisted of 13,299 firings and an accumulated firing time of 1,289.522 seconds. The duty cycle consisted of engine firings of 59 different pulse widths ranging from 0.013 to 4.980 seconds duration.

Propellant consumption for the duty cycle tests were computed by three different methods. They were:

1. The propellants were loaded into the system by filling tanks of known volume, temperature and ullage. After the completion of the test, the remaining propellants were drained from the tanks and weighed and substracted from the loaded amount to yield a "measured" consumption.
2. The propellant consumption was computed from the known duty cycle. By utilizing the average specific impulse and total impulse of the R-4D engine, as shown in Figures 20 and 21, the pulse width and number of firings were summed to yield the propellant consumed.
3. By monitoring and measuring the initial and final helium supply pressure and temperature and relating the change to an equivalent volumetric change in the propellant tanks, the propellant consumption can be computed (PVT method).

Ideally, the use of any of the above methods should yield propellant consumption with reasonable accuracy. Figure 22 represents a plot of method (1) and (2) for various duty cycle tests conducted during the DVT test. The data show reasonable agreement, with a maximum data point discrepancy of 4.0 lbm of fuel. Figure 23 shows the comparison between method (1) and (3). Data scatter of a maximum of 15.9 lbm of oxidizer less than the "measured" is evident in this plot. The PVT method is subject to a number of built-in errors. These consist of measurement accuracy of pressures at 3000 psia, helium leakage from the system, behavior of the gas as "non-ideal" and variable pressurant tank volume as a function of pressure decay. The data presented in Figure 23 assumed that the propellants were saturated with helium prior to the start of the test (if helium saturation did not occur, an error of 2% would be introduced in the final computation). The data was also corrected for leakage (when known), temperature, compressibility and volume distribution into the propellant tanks (based on O/F determined from "measured" data).

DVT SYSTEM IMPULSE, PULSE WIDTH CORRELATION

DUTY CYCLE DATA FOR SYSTEMS A AND B

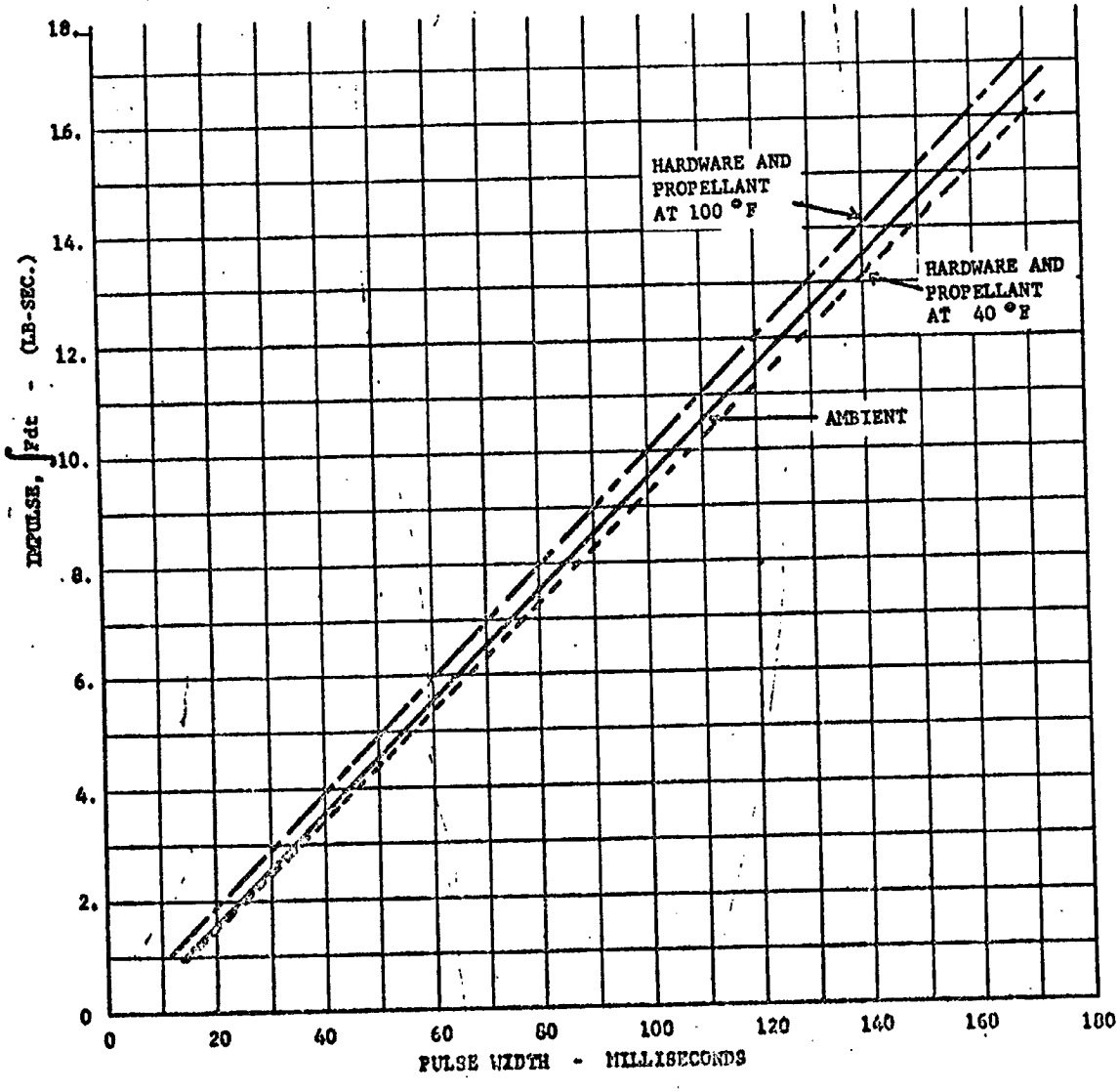

Figure 20

SPECIFIC IMPULSE, PULSE WIDTH CORRELATION

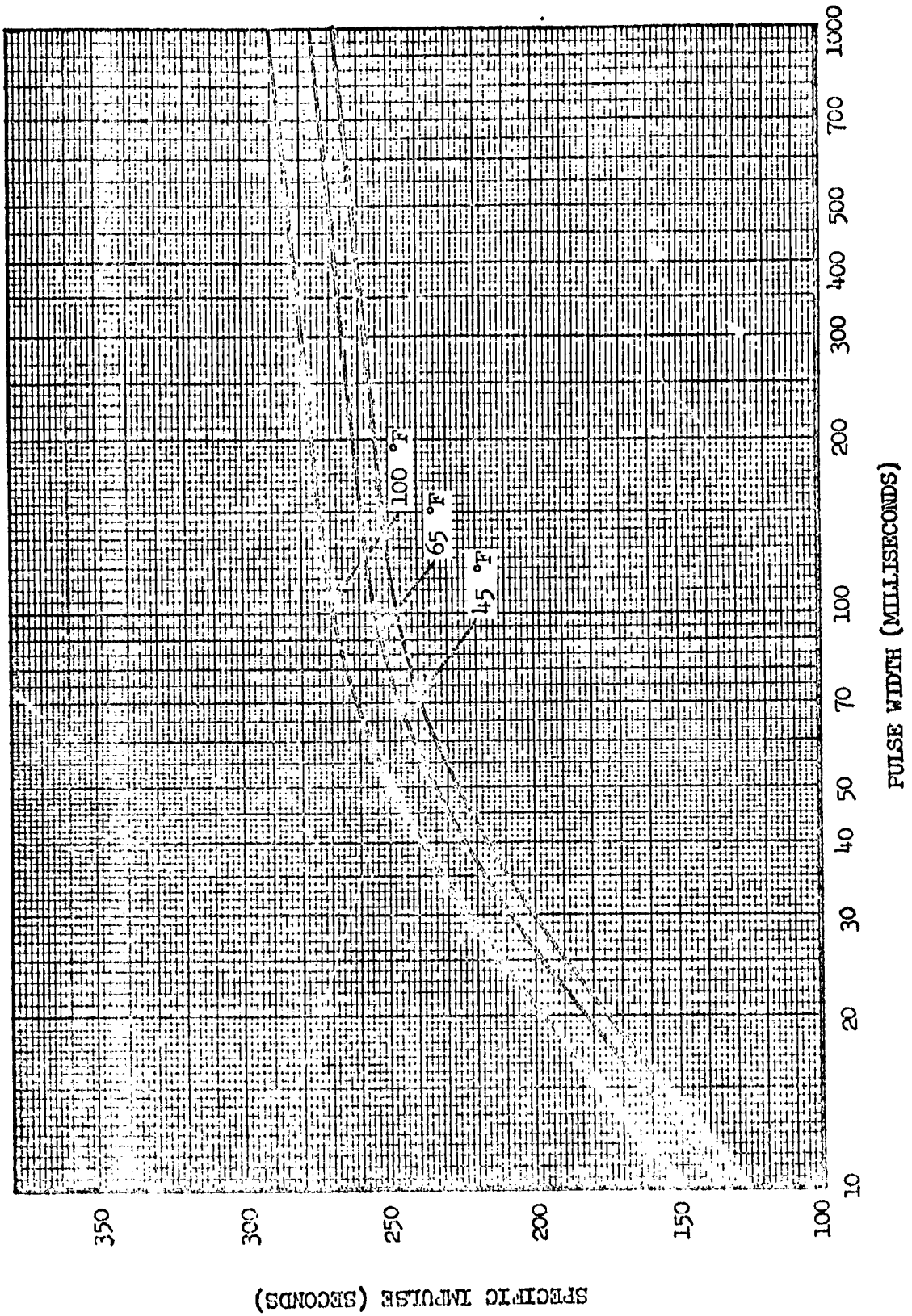

FIGURE 21

PROPELLANT CONSUMPTION CORRELATION
(PULSE WIDTH, IMPULSE, SPECIFIC IMPULSE)

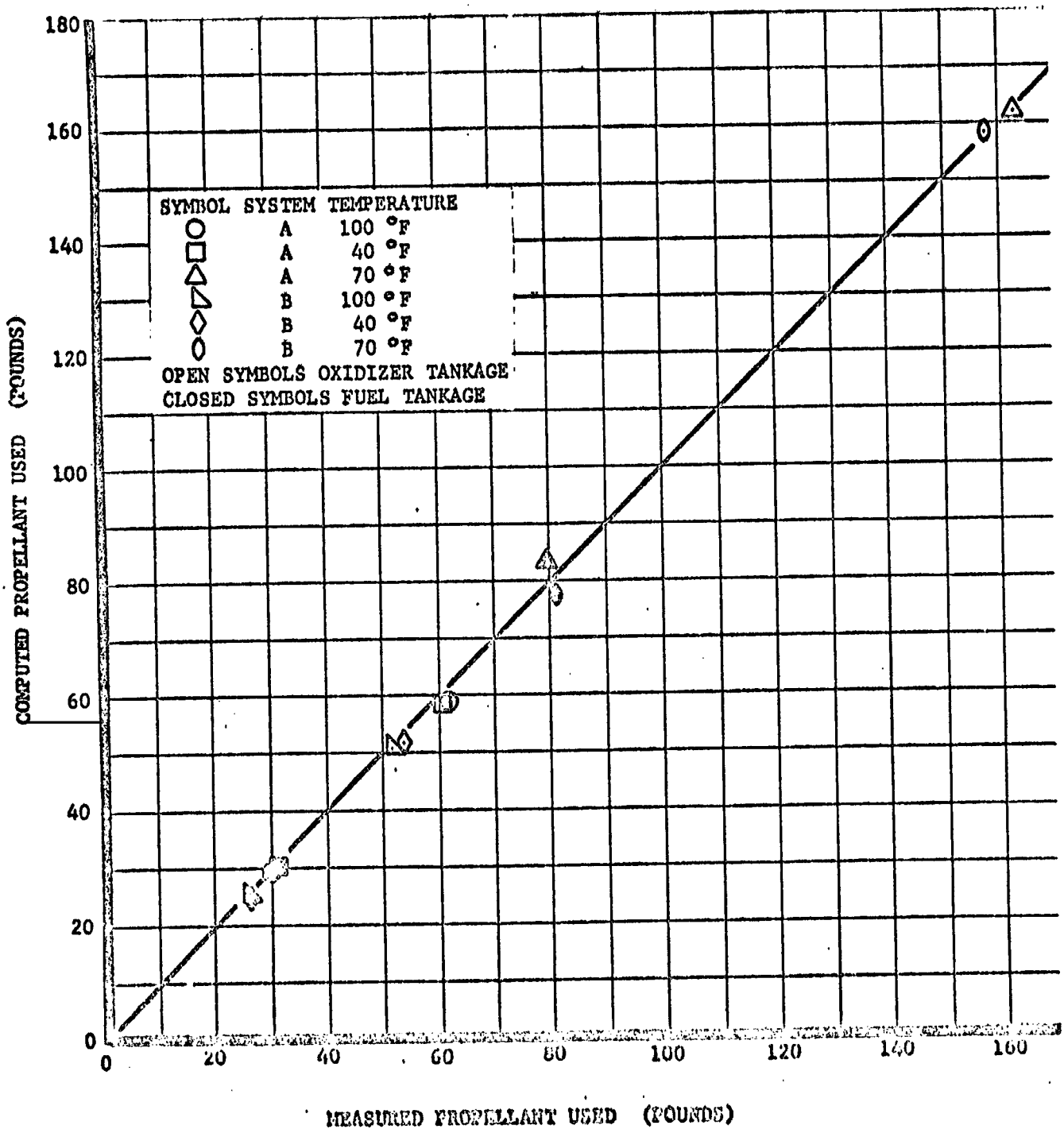

Figure 22

PROPELLANT CONSUMPTION CORRELATION

(HELIUM PRESSURE, TEMPERATURE, AND VOLUME)

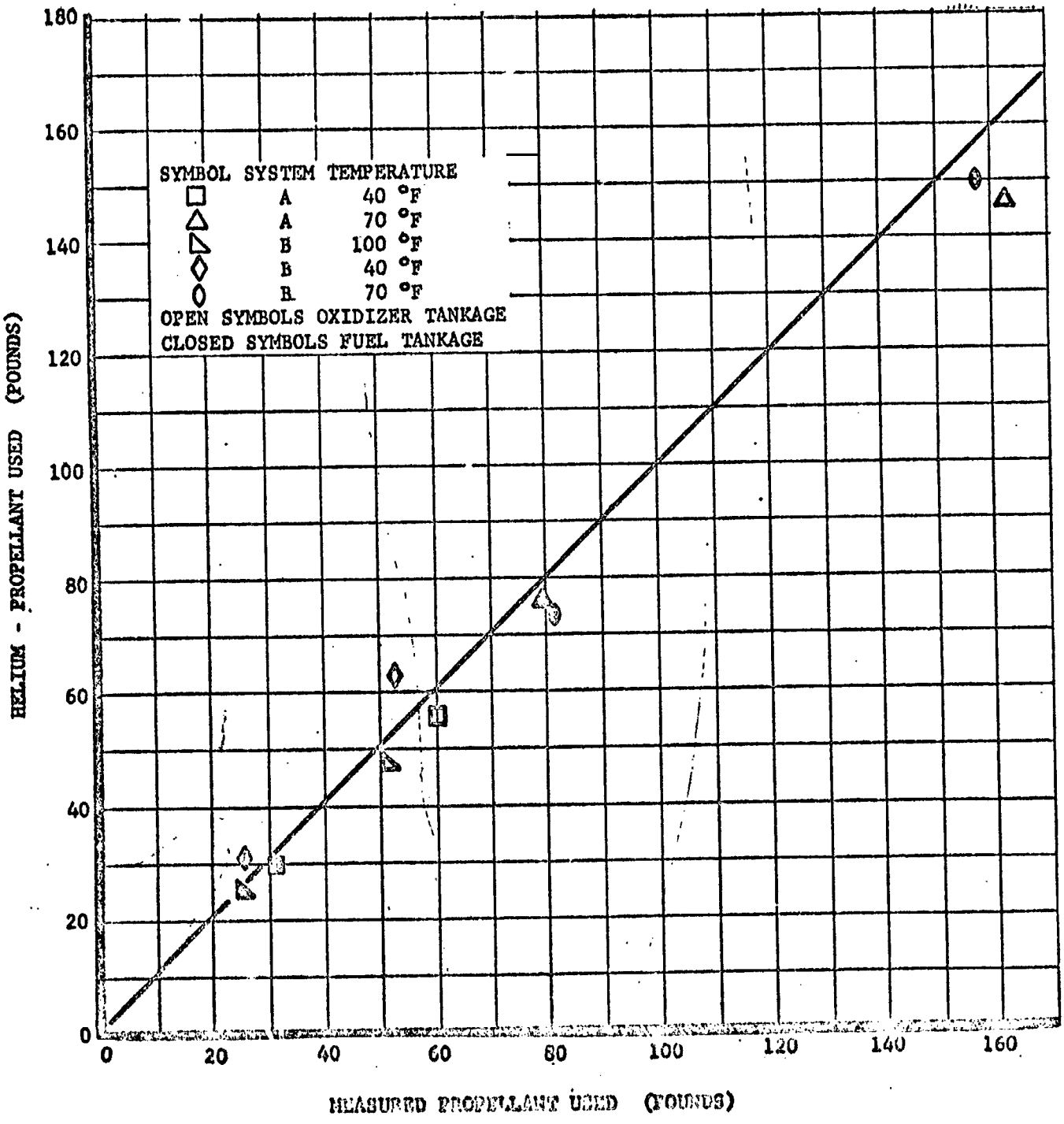

Figure 23

Throughout the entire test program the RCS propellant tank module, valves and lines were enclosed in a plastic tent to maintain a clean environment for all components. For the high and low temperature system tests the entire tent temperature was maintained at an equilibrium temperature of 100°F and 40°F respectively. Propellant consumption data obtained from the high and low temperature are included in the plot of Figures 22 and 23 and show excellent agreement with theoretical density change.

H. Off Design Operation

The objective of this series of tests was to investigate the performance of the LM RCS when off design conditions were imposed. The tests included operation at:

1. High (32 V d-c) and low (20 V d-c) engine solenoid valve voltage
2. High and low mixture ratio. The propellant tank pressures were purposely changed to yield an O/F ratio of 1.8 and 2.2.
3. High and low regulated inlet pressures. Fuel and oxidizer tanks were pressurized at 150, 180, and 240 psia.

Engine valve response and ignition delays were thoroughly documented during the high and low voltage tests. At low voltage the engine valves characteristically opened slower and closed faster and at high voltage the reverse was true. At a voltage level of 20 V d-c and a 10 millisecond pulse essentially no impulse was derived.

Results of the high and low mixture ratio tests corresponded to the theoretical performance of 50-50 UDMH-N_2H_4/N_2O_4. An approximately 5.5% decrease in integrated chamber pressure was noted over the 1.8 to 2.2 O/F mixture ratio range for a 100 millisecond pulse.

Figure 24 represents typical third pulse results of the high and low regulated pressure tests. A decrease in impulse is evident by lowering the system pressure. Figure 25 illustrates the magnitude of the steady state chamber pressure at the three supply pressure levels.

I. Crossfeed and Ascent Interconnect Tests

System crossfeed tests were conducted by operating all of the system engines from a single propellant source (A or B). The crossfeed was accomplished by closing the main line shutoff valve (just downstream of the propellant tank) of the system (A or B) which is deactivated and opening the crossfeed valves. Ascent interconnect tests were similarly conducted by opening the ascent interconnect valve.

ENGINE PERFORMANCE, MANIFOLD PRESSURE CORRELATION

THIRD PULSE DATA

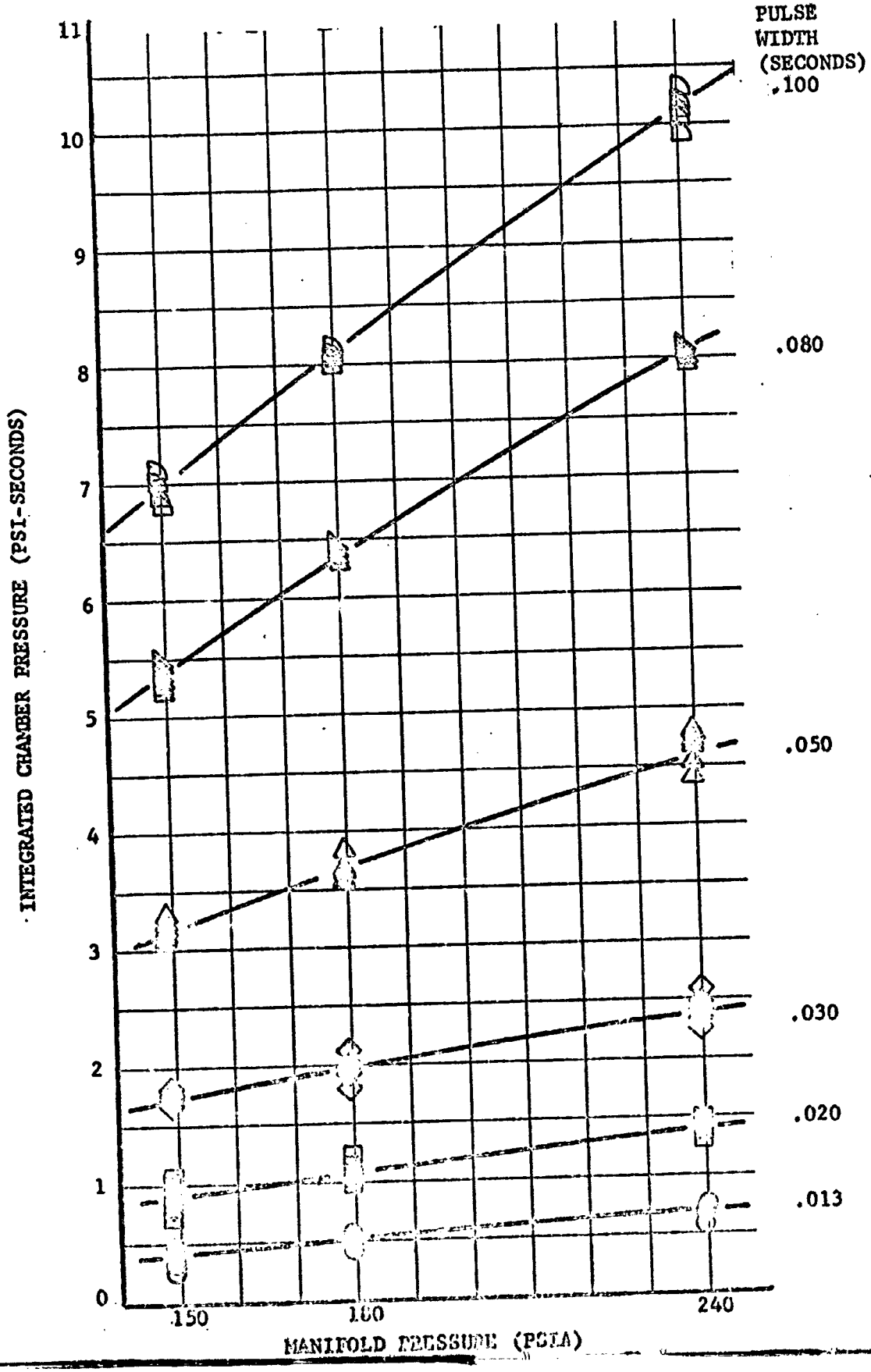

CHAMBER PRESSURE, MANIFOLD PRESSURE CORRELATION

BASELINE AND HIGH AND LOW TANK PRESSURE
SYSTEM B ENGINES ON TIME 5.0 SECONDS

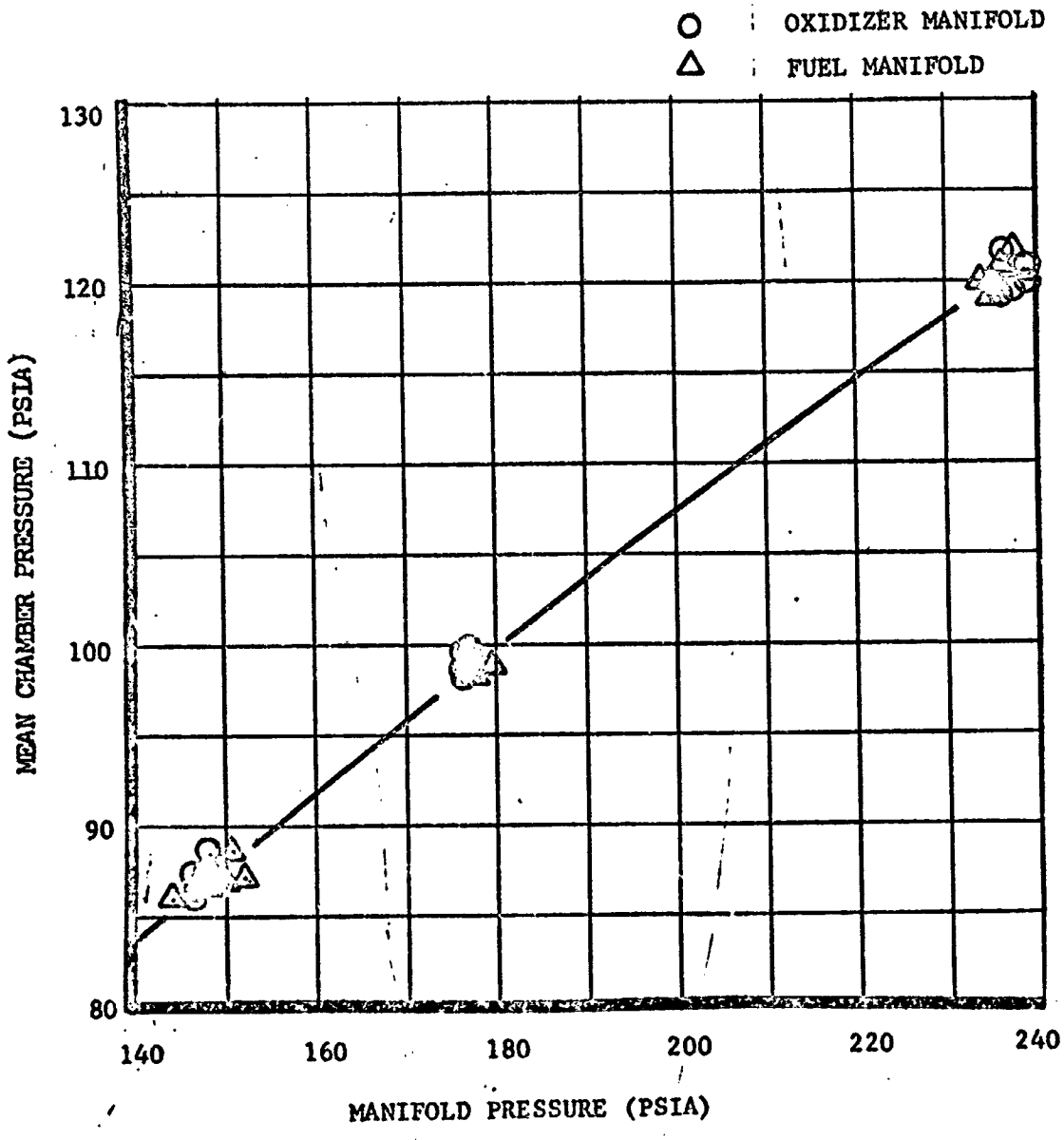

FIGURE 25

Throughout the crossfeed and interconnect tests various combinations of engine couples, translation maneuvers and engine pairs were fired to simulate worst case propellants manifold pressure dynamics. Multiple combination of leads and lags were also imposed on the engine by varying pulse frequency and pulse width. The documented data exhibited no adverse results.

J. Failure Mode Operation

These tests were designed to investigate the system performance during failure mode events. The areas investigated were:

1. The engine fails to shut off and the oxidizer and fuel cluster isolation valve are closed to the malfunctioning engine pair.
2. The engine oxidizer valve fails to shut off when an engine run is terminated and the oxidizer cluster isolation valve is closed to the malfunctioning engine.
3. Manual switching of the engine to obtain "short-as-possible-on-time".

All of the above tests were successfully accomplished. When the engines are shut off by the cluster isolation valve, the chamber pressure reaches ambient in approximately one second. Because little fuel is available for reaction, the closing of the oxidizer isolation valve (Item 2 above) produces a chamber pressure which decays within 0.06 seconds.

The manual operation of the engines was accomplished by two different circuitry. One method required a single depression of a switch using the engines automatic coil. The "on-off" time of the pulse in this instance was a function of the electronic switching circuit. On times of .064 to .102 seconds were obtained by this method. Another method by which the engines were operated manually was through the engine's secondary (or manual) coil. The operation in this mode requires the operator to depress the switch twice, once for "on" and another for "off". The response of this method is a function of the operator's reaction time and switching circuitry. On-times of 0.197 to 0.350 seconds were obtained by this method.

K. Decontamination and Examination

Upon completion of the firing tests the RCS was flushed with decontamination fluid to make the system safe for subsequent disassembly and examination. The decontamination fluids used were Freon TF for the oxidizer and isopropyl alcohol for the fuel system. Briefly, the decontamination procedure consisted of:

1. Purging the propellant tank and system lines of residual propellants by purging them through the engines with helium gas. Propellants were purged individually.
2. Loading the propellant tanks and lines with decontamination fluid and allowing the fluid to remain in the system for at least 30 minutes.

3. The decontamination fluid in the tank was drained and the tanks were purged with helium. The fluid in the lines was purged through the engine.
4. The propellant lines downstream of the tank were vacuum dried.

The above procedure was repeated three times. On the second and third cycles the helium side of the tank bladder was pressure purged after loading the decontamination fluid in the propellant side of the bladder by alternately pressurizing and venting the helium side of the bladders.

The final step in the decontamination procedure was a hot (200°F) purge of the propellant lines, followed by a vacuum dry.

During the third and final cycle of the decontamination procedure, samples of the fluid were taken and analyzed. By titration (Freon TF) and spectrophotometric (isopropyl alcohol) process, the concentration of propellant in the flushing fluid was found to be less than 10 ppm.

Aside from slight discoloration in certain parts and faint odors of the propellant, the disassembly of the system indicated no wear or deterioration from the system tests. Post calibration and performance checks of the valves and engine indicated no performance change.

IV. CONCLUSION

The testing of the LM Reaction Control System has indicated the importance of the coupling of the engine to the feed system. The dynamic behavior of the feed system pressure as affected by the engine's duty cycle demand, the degree of pressurant ingested in the propellant and location of the propellant source (tanks) with respect to the engine, all play a dominant role in the performance of the system.

As a result of good design, the actual testing of the LM RCS uncovered no significant problem areas. However, the variables of system pressure, temperature and voltage that were tested provides the confidence and realizable performance margins that can be achieved from the system.

The successful flight on January 23, 1968 of the first Lunar Module in earth orbit attest, in part, to the successful ground test of the reaction control system discussed herein. During this flight the RCS consumed all of its propellants (610 lbs) and an additional 230 pounds of propellant from the ascent propulsion system (through the interconnect valve) was consumed. The RCS engines were fired for a total of 2,719 seconds consisting of 16,277 pulses.

V. REFERENCES

1. Bergeron, Louis, "Water Hammer in Hydraulics and Wave Surges in Electricity", John Wiley and Sons, Inc., New York, 1961.

2. Parmakian, John, "Water Hammer Analysis", Prentice-Hall, Inc., New York, 1955.

3. "Pressurization Systems Design Guide", Volume II-B, Report No. 2736, Aerojet-General Corporation, Azusa, California, July 1966 (Revised).